WRPS-66391
Revision 0

FY 2019 ILAW Glass Ion Exchange Rate Testing

Prepared for the U.S. Department of Energy
Assistant Secretary for Environmental Management

Contractor for the U.S. Department of Energy
Office of River Protection under Contract DE-AC27-08RV14800

washingtonriver protectionsolutions

P.O. Box 850
Richland, Washington 99352

WRPS-66391
Revision 0

FY 2019 ILAW Glass Ion Exchange Rate Testing

I. L. Pegg
The Catholic University of America

C. Viragh
The Catholic University of America

I. S. Muller
The Catholic University of America

K. Gilbo
The Catholic University of America

Date Published
August 2019

DOE ORP

Prepared for the U.S. Department of Energy
Assistant Secretary for Environmental Management

Contractor for the U.S. Department of Energy
Office of River Protection under Contract DE-AC27-08RV14800

washingtonriver protectionsolutions

P.O. Box 850
Richland, Washington 99352

APPROVED
By Julia Raymer at 9:36 am, Jun 21, 2021

Release Approval | Date

Printed in the United States of America

VSL-19R4620-2

Final Report

FY 2019 ILAW Glass Ion Exchange Rate Testing

prepared by

Isabelle S. Muller, Charles Viragh, Konstantin Gilbo, and Ian L. Pegg

Vitreous State Laboratory
The Catholic University of America
Washington, DC 20064

for

Atkins Energy Federal EPC, Inc.
Columbia, MD 21046

and

Washington River Protection *Solutions*, LLC
Richland, WA

August 13, 2019

Rev. 0, 4/27/20

Completeness of Testing:

This report describes the results of work and testing specified by WRPS. The work and any associated testing followed established quality assurance requirements. The descriptions provided in this test report are an accurate account of both the conduct of the work and the data collected. Results required by the test program are reported. Also reported are any unusual or anomalous occurrences that are different from the starting hypotheses. The test results and this report have been reviewed and verified.

I. L. Pegg: ______________________ **Date:** 4/27/20
VSL Program Director/Principal Investigator

I. Joseph: Innocent Joseph ______________________ **Date:** 4/27/2020
Atkins Sub-Contract Manager

TABLE OF CONTENTS

List of Tables

List of Figures

List of Abbreviations

ANL-LRM	Argonne National Laboratory – Low-Activity Waste Reference Material
ASME	American Society of Mechanical Engineers
ASTM	American Society for Testing and Materials
CCC	Canister Centerline Cooling
CERCLA	Comprehensive Environmental Response, Compensation, and Liability Act
CUA	The Catholic University of America
CV	Check Valve
DCP-AES	Direct Current Plasma Atomic Emission Spectroscopy
DOE	Department of Energy
EDS	Energy Dispersive X-ray Spectroscopy
FEP	Fluorinated Ethylene Propylene Co-polymer
HDPE	High-Density Polyethylene
HLW	High Level Waste
ICP-AES	Inductively Coupled Plasma-Atomic Emission Spectroscopy
ICP-OES	Inductively Coupled Plasma-Optical Emission Spectroscopy
IDF	Integrated Disposal Facility
ILAW	Immobilized Low Activity Waste
IHLW	Immobilized High Level Waste
LAW	Low Activity Waste
LFRG	Low-Level Waste Disposal Facility Federal Review Group
NDR	Normalized Dissolution Rate
NIST	National Institute of Standards and Technology
ORP	Office of River Protection
PA	Performance Assessment
PCT	Product Consistency Test
PEEK	Polyetheretherketone
PFA	Perfluoroalkoxy Polymer
PFT	Pulsed-Flow Test
PNNL	Pacific Northwest National Laboratory
PP	Polypropylene
PUF	Pressurized Unsaturated Flow
QA	Quality Assurance
QARD	Quality Assurance Requirements and Description
RCRA	Resource Conservation and Recovery Act
ROD	Record of Decision
S/V	Ratio of Surface Area to Solution Volume
SEM	Scanning Electron Microscopy
SPFT	Single-Pass Flow-Through
SRL-EA	Savannah River Laboratory-Environmental Assessment Glass
TC&WM EIS	Tank Closure & Waste Management Environmental Impact Statement
TST	Transition State Theory

US	United States
VHT	Vapor Hydration Test
VSL	Vitreous State Laboratory
WRPS	Washington River Protection *Solutions*, LLC
WTP	Hanford Tank Waste Treatment and Immobilization Plant
XRD	X-Ray Diffraction
XRF	X-Ray Fluorescence Spectroscopy

SECTION 1.0
INTRODUCTION

1.1 Background

About 50 million gallons of high-level mixed waste is currently stored in underground tanks at The United States Department of Energy's (DOE's) Hanford site in the State of Washington. The Hanford Tank Waste Treatment and Immobilization Plant (WTP) will provide DOE's Office of River Protection (ORP) with a means of treating this waste by vitrification for subsequent disposal. The tank waste will be separated into low- and high-activity waste fractions, which will then be vitrified respectively into Immobilized Low Activity Waste (ILAW) and Immobilized High-Level Waste (IHLW) products. The ILAW product will be disposed of in an engineered facility – the Integrated Disposal Facility (IDF) – on the Hanford site, while the IHLW product is designed for acceptance into a national deep geological disposal facility for high-level nuclear waste. The ILAW and IHLW products must meet a variety of requirements with respect to protection of the environment before they can be accepted for disposal.

The Record of Decision (ROD) from the Tank Closure & Waste Management Environmental Impact Statement (TC&WM EIS) establishes the current waste streams to be disposed of at the IDF to be located in the 200 East Area, which include ILAW, secondary waste associated with ILAW production, and other on-site Hanford non-Comprehensive Environmental Response, Compensation, and Liability Act (CERCLA) waste. In accordance with the DOE order on radioactive waste management (DOE Order 435.1), the IDF performance assessment (PA) is intended to analyze the long-term impacts on human health and the environment of the disposition of waste placed into the facility. Evaluation of the impact of disposed waste requires the ability to predict the long-term release of key radionuclides from the engineered system. In the case of the IDF, the engineered system includes a number of components including the proposed Resource Conservation and Recovery Act (RCRA) cap, back fill material, ILAW glass, leachate collection system, etc.

Since 1998, the IDF PA (formerly the ILAW PA) has been supported by a PA maintenance plan focused on collecting the critical data needed to predict long-term performance: site geology, recharge, hydrology, geochemistry (measurement of site specific K_d values for key contaminants of concern), and waste form release. The purpose of the PA maintenance plan is to allow PA revisions to reflect new scientific information that reduces the technical uncertainty associated with critical aspects of the PA. Although many of the components contained in the engineered system and addressed in previous IDF PAs are important in minimizing radionuclide release, arguably the most important, protective, and uncertain aspect of the engineered system is the long-term performance of the ILAW glass. The ILAW glass serves as a primary barrier that minimizes radionuclide release. Therefore, developing robust, scientifically defensible predictions of long-term glass performance for the IDF PA is critical. The technical approach that is currently used to predict long-term release from ILAW glass for the IDF PA has gained acceptance from the Low-Level Waste Disposal Facility Federal Review Group (LFRG) and the international community evaluating the long-term corrosion of waste glass. It has also been peer reviewed and approved by a panel of independent experts during development of the 1998 IDF PA.

In the early IDF PAs, three prototypic glasses that spanned the range of glass compositions expected to be produced at the WTP were selected based upon specific processing constraints and composition projections that were current at the time. However, subsequent work has expanded the range of glass compositions that may be produced at the WTP and this type of composition range expansion is likely to continue through the life of the project. Thus, while the basic technical approach is well developed, there is a need to expand the range of glasses tested in order to span the composition range expected to be disposed of in the IDF and to develop an understanding of the dependence of the underlying model parameters and reaction network on the ILAW glass composition. Consequently, more recent testing has been directed towards addressing that need. Results from that work have identified a number of areas for potential improvement of the glass corrosion model that has been developed to support the ILAW PA, one of which is the way in which ion exchange is included in the model. Washington River Protection *Solutions*, LLC (WRPS) has contracted with Atkins and the Vitreous State Laboratory (VSL) of The Catholic University of America (CUA) to provide scientific and technical support for the ILAW PA and, in particular, testing to assess potential alternative approaches for addressing ion exchange, which is the subject of the present report. The work described herein was performed according to a Test Plan [1] that is responsive to the corresponding WRPS scope of work [2].

The following sections provide a brief review of the current approach for modeling ILAW release; the alternative ion exchange modeling approach that was evaluated in the present work; and an overview of the testing approach. Details and results are provided in the subsequent sections of this report.

1.2 ILAW Release Approach for the IDF PA

The technical approach that is currently used to predict long-term release from ILAW glass for the IDF PA has been developed, refined, and updated over the past decade or so. The approach and the supporting test data for ILAW glasses have been extensively documented [3 - 19]. A brief summary is presented in this section.

The underlying premise of the IDF PA is that the source term for radionuclide release is controlled by the long-term weathering of the glass matrix. This engineering-based approach has been used in previous PAs to provide the defense-in-depth required to defend the above premise and demonstrate through computer simulations that the proposed glass waste form will meet the regulatory requirements put forth by the LFRG. The focus of this engineering-based approach is on estimating the model parameters and chemical reaction network needed to provide a robust simulation of glass weathering and the corresponding release of radionuclides over the period of performance (~10,000 years). The overall model incorporates the effects of chemical affinity and ion exchange as discussed below. The model parameters $\vec{k}_o, \eta, E_a,$ and K_g are used to populate a chemical affinity-based kinetic rate law that is based upon Transition State Theory (TST) [20]:

$$r = \vec{k}_0 10^{\eta pH} \exp\left(\frac{-E_a}{RT}\right)\left[1-\left(\frac{Q}{K_g}\right)\right]^{\sigma} \tag{1.1}$$

where
- r is the dissolution rate of the glass [g/(m^2 d)],.
- $\vec{k}_o$ is the forward rate constant [g /(m^2 d)],
- pH is the negative of the logarithm to base 10 of the hydrogen ion activity,
- η is the power law coefficient,
- E_a is the apparent activation energy (kJ/mol),
- R is the gas constant [8.314 . 10^{-3} kJ/(mo1 K)],
- T is the temperature (K),
- Q is the ion activity product (unitless), K_g is the pseudo-equilibrium constant for the rate controlling phase or phases (unitless)[1], and σ is the Temkin coefficient, which has been theoretically shown to equal one.

Equation (1.1) relates the effects of: (1) pH, (2) temperature, and (3) the activities of species that affect the rate of glass dissolution via Q. Equation (1.1) is based on the kinetic rate equation developed by Åagaard and Helgeson [21], as applied to glass by Grambow [22] wherein orthosilicic acid (H_4SiO_4) is the only rate controlling species in Q.

In addition to the dissolution rate equation (1.1), a term is included in the IDF PA calculations to predict the ion-exchange rate (r_{IEX}) between sodium in the glass and hydrogen ions in the aqueous phase, as the glass-water reaction proceeds. In general, the ion exchange rate is thought to be a function of temperature, glass composition, and reaction progress (stage of the glass-water reaction). The potential importance of the contribution from ion exchange in the long-term corrosion mechanism had been emphasized previously by Feng and Pegg [23 - 25]. In previous glass testing work in support of the IDF PA, the standard approach to estimate this parameter has been that of McGrail et al. [5] and Pierce et al. [9] whereby r_{IEX} is obtained by

[1] Although these are unitless, their magnitudes depend on the units used and therefore the units must be specified; typically mol L^{-1}.

subtraction of the boron dissolution rate from the sodium dissolution rate; measurement of its temperature dependence also permits estimation of the activation energy of the Na ion exchange reaction E_{IEX}. More recently, various issues with this approach have been identified [26, 27] including: (i) the reliability of this subtraction approach in view of the apparent diffusive release of boron [13, 15]; (ii) an error in the calculation r_{IEX} that has been propagated through previous work [27]; and (iii) the use of an r_{IEX} that is independent of time and solution composition [26, 27]. In view of these issues, WRPS has commissioned studies of potential alternative approaches for incorporation of ion exchange into the rate law [26, 27]; the results from testing to address these issues are the subject of the present report.

The use of Equation (1.1) with suitably estimated parameters, together with provisions for solution speciation and secondary phase formation (as is typically performed with geochemical model codes with appropriate secondary phase data), allows for the source-term to be determined within a reactive chemical transport modeling framework that takes into account the coupled effects of fluid flow and glass-water reactions on the chemistry of fluids percolating through the disposal facility. Coupling the fluid chemistry with a kinetic rate equation allows the simulations to describe the response of the glass corrosion rate to changes in fluid composition as a function of time and space.

In previous work, the model parameters for Equation (1.1) have been obtained from the analysis of data produced using a variety of experimental techniques. The single-pass flow through (SPFT) test has been the primary technique used to estimate the coefficients of Equation (1.1). The results of the present work show that pulsed flow tests can also be used to obtain the parameters of Equation (1.1). Other tests used to evaluate glass durability are long-term high surface to volume ratio (S/V) product consistency test (PCT-B), vapor hydration test (VHT), and pressurized unsaturated flow (PUF) test. This suite of tests evaluates different aspects of the glass-water reaction over the course of the various regimes of glass weathering: the initial forward rate regime; the decreasing rate regime; the residual rate regime; and the alteration rate renewal regime. These regimes are described below.

The initial forward rate consists of both ion-exchange and hydrolysis reactions. In dilute to near-saturated solutions, the TST-based model (without the ion-exchange term) successfully accounts for silicate dissolution in terms of temperature, pH, and reactive surface area because hydrolysis is the controlling reaction. However, as the glass-water reaction proceeds and the concentrations of glass components (particularly the dissolved silicic acid concentration) increase in solution, the rate of dissolution decreases. For ILAW glasses tested under alkaline conditions, it has been observed that ion exchange becomes the dominant process controlling glass weathering under these near-saturated conditions [8]. The data collected from SPFT experiments conducted as a function of pH, temperature, and silicic acid concentration are used to study these processes and to obtain the model parameters $\bar{k}_o, \eta, E_a, \text{and} K_g$.

As the glass continues to dissolve, the aqueous concentration of dissolved components approaches saturation with respect to the formation of a hydrated surface layer. The hydrated surface layer forms when relatively insoluble glass components (e.g., Al, Fe, and Si) accumulate in the bulk solution and condense at the glass-water interface. The rate of dissolution then continues at a relatively constant residual rate consistent with a process controlled by diffusion through the hydrated surface layer. The key alteration phase is often a clay mineral, such as a smectite or chlorite [13, 28]. The precipitation kinetics associated with these phases can be complex, but in general the rate of secondary phase growth increases in response to an increase in the magnitude of supersaturation [29, 30]. In cases where an appreciable level of ion-exchange is present, the data collected from SPFT experiments conducted as a function of silicic acid concentration can be used to obtain the model parameter r_{IEX}. Variable temperature experiments can also permit the determination of the activation energy for r_{IEX} and extrapolation of r_{IEX} to a specific repository temperature.

Finally, depending on the type of alteration phases that form, the glass-water reaction can increase from the residual rate and return to an elevated rate. This type of behavior has been observed in accelerated testing with high temperatures and high solid surface area to volume ratios for various glasses including US HLW glasses [31-36], other HLW glasses [37-47], as well as Hanford low-activity waste (LAW) glasses [13, 28, 34, 48, 49].

The combined H^+/Na^+ ion exchange and hydrolysis of the silicate network lead to the formation of a multi-layered reaction zone including a hydrated layer, a porous gel layer, and crystalline phases that precipitate on the surface. Increasing the S/V (PCT-B) is one method to explore higher reaction progresses and identify the secondary phases that are associated with resumption.

The data collected from VHT [13, 50], PCT-B [28, 34, 35, 47, 49, 50], and PUF experiments [9] along with geochemical modeling and solid-phase characterization are used to identify the key alteration phases formed as the glass weathers. The results from these tests provide the additional information needed to identify and constrain the appropriate chemical reaction network required for model simulations.

The above elements of the glass-water interactions are incorporated into the conceptual model that is used in the IDF PA to model glass dissolution, as described in more detail elsewhere [51].

1.3 Alternative Ion Exchange Approach

As described above, the current approach for modeling the release of contaminants from glass dissolution in the IDF PA employs a chemical affinity-based kinetic rate law that is used in combination with a term (r_{IEX}) that is intended to represent H^+/Na^+ ion exchange, together with the formation of secondary solid phases. Historically, the ion-exchange term has been assumed to be a constant for any given glass and depends only on temperature. The present work addresses the need for an improved methodology for including ion exchange and for measuring the relevant H^+/alkali ion exchange parameters. The approach follows the recommendations provided in reference [26], which are in turn based on the findings of Feng and Pegg [25]. Thus, specific features of the present approach include:

- Recognition that ion exchange is a diffusive process and therefore the rate is expected to decrease as the square root of time;
- Recognition that ion exchange involves the exchange of an alkali ion by a hydronium ion or a proton and therefore the rate is expected to depend on the concentration of those species in solution. In other words, the ion exchange rate is expected to depend on the solution pH and to decrease as the pH increases;
- Recognition that ion exchange involves an activation energy and the rate is therefore expected to show an Arrhenius dependence on temperature;
- Recognition that all alkalis are subject to ion exchange, not just sodium. While sodium is the major alkali in LAW glasses, lithium becomes increasingly important as the sulfur content in the waste increases since lithium (and other species such as vanadium and calcium) is added in increasing amounts to the glass formulations. Significant amounts of potassium are present in some LAW streams.

As stated earlier, in comparison, the present approach used in the IDF PA employs an ion exchange rate that is constant with respect to time and solution composition, and for sodium only.

The approach of Feng and Pegg [25] addresses all of the above issues and provides a rational basis for improvement of the manner in which ion exchange is incorporated into the IDF PA modeling. In this approach, the release of alkalis by ion exchange is governed by the following rate equation [25]:

$$\frac{d[R^+]}{dt} = \frac{1}{2} k_d \frac{S}{V} \left(\frac{[H^+]}{[H^+]_0} \right)^{\alpha} t^{-1/2} \quad , \tag{1.2}$$

where $[R^+]$ is the solution concentration of alkali R, k_d is a rate constant, S is the glass surface area, V is the solution volume, $[H^+]$ is the H^+ concentration, $[H^+]_0$ is a scaling factor, t is time, and α is a constant (set equal to one half in [25] based on consistency with the data set). It should be noted that this provides a separate release mechanism for alkali above and beyond that provided by Equation (1.1).

Mathematically, both the time dependence and the pH dependence in Equation (1.2) are equivalent to those later described by Ojovan et al. [52] and subsequently implemented in the GRAAL model [53, 54], which together provide further underpinning of the basis for this approach. However, the interpretation is somewhat different in the GRAAL model (diffusion of all species through a protective layer in the GRAAL model [53, 54] versus diffusion-controlled release of alkali via ion exchange in [25] and [52]).

The temperature dependence is included by replacing k_d by $k_d(T)$ and writing:

$$k_d(T) = k_{d0} \exp\left(-\frac{E_{ad}}{RT}\right) \tag{1.3}$$

where $k_d(T)$ is the temperature dependent rate constant, k_{d0} is a constant, E_{ad} is an effective activation energy for ion exchange, R is the gas constant, and T is the absolute temperature. As noted previously [26], if the ion exchange process is further interpreted in terms of the Doremus interdiffusion model [55], the rate constants are interpreted as diffusion constants and the term RT is replaced by $2RT$ in Equation (1.3); we adopt the rate constant approach and effective activation energy shown in Equation (1.3) in the present work.

As noted above, in the present IDF PA, sodium ion exchange is incorporated via an ion exchange rate that is assumed to be a constant (though sometimes temperature dependent) for any given glass. That rate, r_{IEX}, is expressed as moles of sodium released from the glass per unit time per unit glass surface area (typically mol m^{-2} s^{-1}). Clearly, that quantity can be obtained from Equation (1.2) by simply dividing by S/V. Thus, combining all of these results, the proposed new ion exchange rate is given by:

$$r_{IEX} = \frac{1}{2} k_{d0} exp\left(-\frac{E_{ad}}{RT}\right)\left(\frac{[H^+]}{[H^+]_0}\right)^{\alpha} t^{-1/2} \tag{1.4}$$

Setting $[H^+]_0$ = 1 mol per liter and using pH = -log $[H^+]$, where "log" denotes the logarithm to base ten, we obtain:

$$r_{IEX} = \frac{1}{2} k_{d0} \exp\left(-\frac{E_{ad}}{RT}\right) 10^{-\alpha pH} t^{-\frac{1}{2}} \tag{1.5}$$

and therefore:

$$\log r_{IEX} = A + \frac{B}{T} + CpH - \frac{1}{2}\log t \tag{1.6}$$

where $A = \log(k_{d0}/2)$, $B = -(E_{ad}/R)\log e$, and $C = -\alpha$.

We can also generalize Equation (1.4) to allow for deviation from square-root-of-time behavior by writing:

$$r_{IEX} = \frac{1}{2} k_{d0} exp\left(-\frac{E_{ad}}{RT}\right)\left(\frac{[H^+]}{[H^+]_0}\right)^{\alpha} t^{-\gamma} \quad (1.7)$$

which yields:

$$\log r_{IEX} = A + \frac{B}{T} + CpH + D \log t \quad (1.8)$$

where D = - γ.

Equations (1.6) and (1.8) were used for the regression analysis of the PFT data, as described in Section 6.

The above approach could potentially address many of the shortcomings in the present IDF PA rate law and should be relatively simple to implement. However, any such approach requires a supporting test program that is designed to determine, over the range of ILAW glass compositions of interest, the new model parameters that are introduced. The work described herein provides a first step in such a program.

It should be noted that ion exchange and matrix dissolution do not occur independently but are coupled processes that occur simultaneously, as described previously [25]. Thus, while in isolation, Equation (1.2) indicates that the ion exchange rate goes to zero as time goes to infinity, that is not the case when that process is coupled with matrix dissolution, described, for example, by Equation (1.1). Essentially, the velocity with which the diffusive alkali depletion front propagates into the glass is proportional to Equation (1.2) and that velocity decreases as that depletion layer increases in thickness. However, the glass is also being dissolved at the outer surface (the surface in contact with the solution) via matrix dissolution and, therefore, that surface propagates inwards at a velocity proportional to Equation (1.1); this process tends to thin the alkali depletion layer. This is a classic moving boundary problem, which has a steady-state solution wherein the two velocities become equal and the depletion layer moves inwards but with a constant thickness [25]. As a result, the time dependence will change from that typical for a diffusive system ($t^{-1/2}$) to a time independent system (t^0). Finally, other processes, such as the evolution of the solution composition and secondary phase formation, also modify the overall reaction trajectory. Thus, in implementation, Equations (1.1) and (1.5) (or the corresponding version of (1.7)) are coupled through the solution chemistry and speciation and precipitation reactions, which are typically handled in a geochemical code that forms part of the overall model. In the original work of Feng and Pegg [25], this coupling of the solution chemistry (but not secondary phase formation) was performed explicitly for silicon species only. Furthermore, the moving boundary aspects of the problem were handled in an approximate fashion by noting that, within this model, the velocity of the ion exchange front cannot fall below the velocity of the matrix dissolution front; therefore, if the calculated velocity of the ion exchange front does fall below the velocity of the matrix dissolution front, the former should be replaced by the latter, which leads to a corresponding criteria for the ion exchange rate and matrix dissolution rate. Feng and Pegg [25] describe the various regimes in this overall process as these two rates approach each other and, ultimately, become equal.

1.4 Test Overview

The present work addresses the need for:

1) An improved ion exchange model for ILAW corrosion; and

2) Improved methods for measuring the parameters in the new ion exchange model that are ideally more reliable, and more efficient and cost effective than the present approach that employs the SPFT.

Thus, per the Test Plan [1] and WRPS work scope [2], this work focused on the alternative ion exchange modeling approach described in Section 1.3 and the use of the pulsed-flow test (PFT) as a potential alternative to the SPFT for determining ion exchange rate parameters. Ion exchange rates for selected LAW glasses were measured using the SPFT approach and compared with those obtained using the PFT. The test conditions included variations in temperature, pH, and time in order to test the potential alternative ion exchange model described in Section 1.3.

The glasses selected for this work are LAWC22 [12], IDF1B2 [13], and ORLEC28 [18]. Amongst the baseline glasses that have previously been subjected to SPFT testing, LAWC22 was selected for tests using both the SPFT and the PFT methods because it has the highest measured ion exchange rate so far and contains both sodium and lithium. Amongst the enhanced high waste loading glasses that have previously been subjected to SPFT testing, IDF1B2 was selected because it has a high measured ion exchange rate and the highest sodium content; it has no lithium and very low potassium. Finally, ORLEC28 was selected because it contains high sodium and relatively high potassium and has an intermediate sodium ion exchange rate [18].

The work included fabrication, heat treatment, and confirmation of the composition of the selected glasses followed by testing to determine ion exchange rates using the SPFT and the pulsed flow methods. The data were analyzed to test the applicability of the ion exchange model form proposed by Feng and Pegg [25], as described in Section 1.3. The scope of the present work included both SPFT and pulsed-flow testing on glass LAWC22 and pulsed-flow testing on glasses IDF1B2 and ORLEC28. Tests were conducted at three temperatures (70°C, 40°C and 23°C) and five different buffer compositions covering a pH range from 7 to 11 (at room temperature) with a minimum of ten sampling times for each experiment. The leachants were spiked with silicic acid in order to decrease the rate of matrix dissolution so that the relative ion exchange contribution to the overall glass dissolution rate was enhanced.

In parallel with the above mentioned SPFT tests, the LAWC22 glass was also subjected to SPFT tests in non-saturated solutions in order to provide further comparison with the results from previous work [12]. The temperatures (70°C, 40°C and 23°C) and the pH range (from 7 to 11 at room temperature) were the same, as were the leachant compositions except that they were not spiked with silicic acid.

SECTION 2.0
GLASS SELECTION AND FABRICATION

2.1 Glass Selection

The glasses that were considered candidates for this work are LAW glasses for which SPFT testing has been conducted previously and for which estimates of the ion exchange rate have been made. A summary of the kinetic parameters previously determined from SPFT testing on LAW glasses [19] is provided in Table 2.1.

Amongst the baseline glasses, LAWC22 was selected because it has the highest measured ion exchange rate and contains both sodium and lithium. Glass LAWB45 shows no measurable ion exchange rate and glass LAWA44 does not contain lithium (LAWABP1 is a derivative of LAWA44 that was not intended as a production glass and its composition lies outside of the WTP baseline LAW glass composition space).

Amongst the high waste loading glasses, IDF1B2 was selected because it has a high measured ion exchange rate and the highest sodium content; it contains no lithium and very low potassium. Finally, ORLEC28 was selected because it has high sodium and relatively high potassium contents. Table 2.2 provides a description of the glass compositions highlighting the species used to monitor matrix dissolution and the alkalis for which ion exchange rates were determined.

These glass compositions include spikes of rhenium and molybdenum as potential indicators of matrix dissolution (as potential alternatives to boron, as suggested previously [15, 17, 19]) and cesium, which together with sodium, lithium, and potassium, allows for assessment and comparison of the behavior of all of the alkalis in LAW glasses. Rhenium is also a non-radioactive surrogate for Tc and its dissolution behavior, therefore, provides information regarding the long-term immobilization of Tc in LAW glasses.

The recommendations of the above glass compositions for testing [56] were reviewed and approved by WRPS before preparation, characterization, and testing of these glasses.

2.2 Glass Preparation

The three glass compositions selected were prepared from reagent grade or higher purity chemicals according to VSL standard operating procedures. Briefly, an appropriate combination of well-mixed chemicals was melted at 1200ºC for 75 minutes in a platinum-gold crucible. Mixing of the melt was accomplished with a platinum stirrer beginning 15 minutes after the start of melting and continuing for the next 60 minutes, until the end of melting. The melt batch included a rhenium spike targeted at 0.1 wt% Re_2O_7, if all of it were retained in the glass. Since rhenium is subject to significant volatile loss from the glass during melting, excess Re_2O_7 was added to compensate, assuming an average retention of 53.5% based on extensive past testing [57]. This results in the addition of 0.93 g, instead of 0.50 g of Re_2O_7, to each batch targeting 500 g of glass. Spikes of Cs_2O and MoO_3, targeted at 0.15 wt% and 0.10 wt%, respectively, were not over-batched since any volatile losses, which are expected to be smaller than for rhenium, have not been as well quantified as that for rhenium.

The as-melted glass samples (before heat treatment) generally showed no visible sulfate layer. Glasses IDF1B2IX[2] and ORLEC28IX were emerald green in color and LAWC22IX was dark brown due to its high Fe_2O_3 content. A portion (~50 to 60 g) of the as-melted glass was set aside and the remainder was subjected to canister centerline cooling (CCC) heat treatment according to the WTP LAW container cooling profile [58] shown in Figure 2.1. After CCC heat treatment, the sample was about 11 cm in diameter at the surface and about 2 cm thick. Glasses LAWC22IXCCC and ORLEC28IXCCC remained translucent throughout (brown and dark emerald green respectively). Glass IDF1B2IXCCC included a crystallization layer of about 8 mm in thickness at the platinum crucible wall. This lighter-colored crystallized section (near crucible wall) was easily separated from the rest of the glass allowing separate evaluation of the two sections, as described in Section 2.4.

2.3 Glass Compositional Analysis

The primary method used for glass composition analysis was X-ray fluorescence spectroscopy (XRF) on powdered glass samples. A PANalytical Axios^{mAX}-Advanced XRF spectrometer was used for this purpose. The XRF is calibrated over a range of glass compositions using standard reference materials traceable to the National Institute of Standards and Technology (NIST), as well as waste glasses such as the Argonne National Laboratory – Low-Activity Waste Reference Material (ANL-LRM) [59] and the Defense Waste Processing Facility (DWPF) – Environmental Assessment Glass (SRL-EA) [60]. Since boron and lithium are not determined by this procedure, it is supplemented by acid digestion followed by solution analysis, as described below.

Glass samples for analysis by direct current plasma atomic emission spectroscopy (DCP-AES) or inductively coupled plasma atomic emission spectroscopy (ICP-AES) analysis are first subjected to microwave-assisted total acid dissolution in Teflon vessels according to VSL standard operating procedures. Twenty milliliters of a 1:5 mixture of concentrated $HF:HNO_3$ is diluted to 50 ml and used for the dissolution. This procedure is similar to the

[2] "IX" is appended to the parent glass names to distinguish the specific composition used for the present work.

American Society for Testing and Materials (ASTM) Test Method C1412-99, which also employs a mixture of concentrated HF and HNO_3 in microwave digestion of pulverized glass samples; supplemental use of HCl/H_3BO_3 is not included in the VSL procedure since boron is normally one of the analytes. The solutions resulting from the acid digestion are analyzed by DCP-AES or ICP-AES.

The glass composition analyses were performed on replicate samples, including the as-melted glasses and the core section of the sample subjected to CCC, which were both analyzed separately for composition by XRF and DCP-AES after total acid digestion. The samples are typically rejected when major oxides, with target concentrations of 3 wt% or more, show relative deviations from the target composition of greater than 10% (or 0.2 wt% absolute for SO_3). The results provided in Table 2.3 show that the glasses are on target for all of the major glass constituents. SO_3 is also found to be slightly below target, with a minimum loss of 0.01 to 0.04 wt% SO_3 from target and no significant differences are observed between the as-melted glass and the sample subjected to CCC.

Rhenium was one of three spikes that were added for the specific purpose of estimating ion-exchange in glass leaching. Rhenium was over-batched to compensate for volatile loss during melting; evaluation of 363 earlier crucible melts at a target Re_2O_7 concentration of 0.1 wt% showed an average retention of 53.5% [57]. With this compensation, the rhenium content in the three glass samples subjected to CCC varies from 0.12 to 0.14 wt% Re_2O_7. Batching did not include any compensation for volatility of the other two spikes, cesium and molybdenum. The spike of 0.15 wt% Cs_2O in all measured glass samples was found to be on target, with minor analytical variability. Molybdenum was batched at 0.1 wt% and was measured at 0.08 wt% MoO_3 in all three samples subjected to CCC, indicating a relatively small volatile loss during melting. The measured rhenium, cesium, and molybdenum concentrations were used in normalization of the leaching data in Sections 4 and 5.

2.4 Glass Evaluation and Preparation for Pulse-Flow and SPFT Testing

In addition to composition analysis, evaluation of the glass samples included scanning electron microscopy (SEM) imaging of cross-sectioned, polished and carbon-coated grains with energy dispersive X-ray spectroscopy (EDS) analysis. These methods were used to verify that samples LAWC22IXCCC and ORLEC28IXCCC were free of crystallization and, in the case of IDF1B2IXCCC, to identify the crystalline phases observed in the layer of glass near the crucible wall and to verify that the glass in the center of the crucible was free of secondary phases. Contact with platinum likely catalyzed crystal formation in the laboratory CCC heat treatment but similar crystallization at the full-scale WTP container-melt interface, if present, is expected to be a very small fraction of the total volume of glass in the LAW container. The crystalline layer was, therefore, cut away with a diamond saw.

The glass sample IDF1B2IXCCC from near the crucible wall contained lazurite, a sodium sulfate aluminosilicate phase estimated at about 13 vol% by SEM in the first few millimeters of glass sample that was in contact with the crucible wall. The morphology and main constituents identified by EDS indicate the sulfate sodalite lazurite, as was identified in earlier preparation of this glass [18]. Composition analysis by EDS of glass free of crystallization at the center of the crucible showed results consistent with the XRF analysis and the target glass composition.

Glass ground from segments from the center area of each CCC heat treated sample were used for SPFT and Pulsed-Flow tests. Prior to their use in the leach tests, the glass samples were crushed and sieved to 100-200 mesh (75-149 μm). The ground glass was washed (2 minutes in deionized water and 2 minutes in 99% absolute ethanol) and air-dried to remove fines, which tend to dissolve faster than glass grains during alteration experiments and, thus, interfere with test results.

To simplify discussion in subsequent sections of this report, the three glasses are referred to as LAWC22, ORLEC28, and IDF1B2 with the understanding that all of the samples that were tested were collected from the above described batches, CCC heat treated, and free of any crucible-contact crystallized material.

SECTION 3.0
ION-EXCHANGE RATE TESTING

3.1 Pulsed-Flow and SPFT Test Matrix

LAWC22 glass was subjected to both Pulsed-Flow and SPFT tests as a function of pH, temperature, and time at silicic acid saturation. This permits: (i) Direct comparison of the results from the two methods to provide an assessment of the Pulsed-Flow test for determination of ion exchange rates; and (ii) Estimation of the parameters in the alternative ion exchange model (Section 1.3) from the data. Pulsed-Flow tests were also conducted on glasses IDF1B2 and ORLEC28 and the results were compared to previous SPFT data on these two glasses.

The standard SPFT test matrix on a single glass includes 48 tests that vary temperature, pH, silicic acid concentration, and test time. In the present work, which was focused on the determination of ion exchange rates, only the highest silicic acid concentrations (at each test condition) was used. In previous SPFT testing, the tests at pH 11 and 12 have employed LiOH/LiCl "buffers." These solutions are not very effective at holding the pH but, more important for the present purpose, they introduce large (and artificial) concentrations of lithium, which can ion exchange with other alkalis (notably sodium) in the glass, thereby complicating data interpretation. Therefore, alkali-containing buffers were avoided in the present work. Instead the amine buffer piperidine was used for pH 11; testing at pH 12 was not performed. In addition to the deletion of the pH 12 tests, it was necessary to reduce the number of temperature conditions from four to three due to funding limitations. In this manner, the ion exchange test matrix on a single glass could be completed with 15 tests, according to the matrix described in Table 3.1, which includes:

- Five values of pH (7, 8, 9, 10, 11)
- Three values of temperature (23, 40, 70°C)
- All tests at silicic acid saturation
- All tests measure B, all alkali species, Al, Re, Mo, and Cs in solution
- All tests run for sufficient time to adequately define the time dependence (10 to 30 days) and a minimum of 10 samples for each experiment.

Although, the focus of the present work is on ion exchange rates, LAWC22 glass was also subjected to a series of SPFT tests in leachant solutions without a silica spike for further comparison to previous work. The matrix for these tests is presented in Table 3.2. These tests were run in parallel with those described above in silica saturated buffers, at the same temperatures (23, 40, 70°C), same durations, and same buffers, pH (7, 8, 9, 10, 11), except without the silicic acid spikes.

3.2 Solution Preparation

Glass leaching experiments at a pH_{RT}[3] range from 7 to 10 were performed in 0.05 M tris(hydroxymethyl)aminomethane (Tris) solutions buffered to the target pH using concentrated HNO_3. Glass leaching experiments at pH_{RT} 11 were performed in piperidine. Piperidine was also used for the pH 10 solutions. For a 0.05 M piperidine buffer, 4.26 g piperidine (Aldrich, >99.5%, d= 0.862 g/mL, pKa 11.22) was removed with a syringe from the sealed bottle, added dropwise to a tared plastic bottle containing deionized water and diluted to one liter. The pH of this piperidine-base 0.05 M stock solution was about 11.9. Concentrated nitric acid (~1900 µL) was added to adjust the pH to 11 for one liter of buffer that does not contain silica. The pH_T[4] values of the buffer solutions, heated to the test temperature, were measured using a temperature-compensated pH meter. Determination of pH_T was necessary for the calculation of dissolution rates using Equation (1.1). The pH values are compared in Table 3.3. The temperature variation of the pH for the LiOH buffers used previously and that of the present piperidine buffers were not significantly different.

Leaching solutions containing varying amounts of Si were prepared by dissolving analytical grade silicic acid powder ($SiO_2.H_2O$) in 0.05 M Tris or piperidine. Due to the low solubility of amorphous silica in aqueous solutions, stock solutions containing at least 140 ppm [Si] were prepared, heated at 90°C for a period of time, decanted carefully into fresh bottles to avoid transfer of precipitated solids, and analyzed by ICP-AES or DCP-AES in order to determine the concentration of Si. As necessary, the stock solutions were diluted to the target [Si] and buffered to pH_{RT} 7, 8, 9, or 10, as previously described. For the piperidine stock solution, the 2.5 g of silicic acid powder added to one liter of 0.05 M piperidine solution could not be completely dissolved even after a week at 90 °C. After careful decantation and analysis (~800 ppm Si) the solution was diluted with 0.05 M piperidine to the target [Si] and the pH was adjusted from about 11.5 to 11.0 using concentrated nitric acid. The silicic acid (pKa ~ 9.9) brings down the pH of the piperidine solution, so less HNO_3 is needed to adjust the pH to 11. Silicic acid brings down the pH of the 0.05 M Tris solution also to about 9.6, so that about 15 drops of piperidine are needed to adjust the pH to 10.0.

3.3 Summary of SPFT Method

In a SPFT experiment, a solution flows at constant temperature and rate through a reaction cell (leaching reactor) containing the sample. The system is open-ended, hence operating in a "single-pass" mode. The reactor employs diffusive mixing facilitated by a very long residence time (of the order of tens of hours) of the mobile phase in the reactor. In the SPFT

[3] Subscript indicates pH values obtained from measurements at room temperature (RT).
[4] Subscript indicates pH values measured at the test temperature *T*.

test, the dissolution kinetics of a glass specimen of a specific composition is quantified over a range of pH values (typically 7 to 12), temperatures (typically 23 to 90 °C), and solution compositions (typically Si doped). Dissolution rate parameters are obtained following establishment of steady-state conditions between the glass and the aqueous solution. At steady-state conditions, the pH and concentrations of elements in the leaching solution are invariant with respect to time and the chemical affinity of the system remains constant (pseudo-equilibrium conditions). By conducting a matrix of tests in which the pH, temperature, and leachant composition are varied in turn while holding the other test variables fixed, it is possible to generate a set of data from which each of the parameters in the rate equation (Equation (1.1)) can be determined.

3.4 Description of the SPFT Experimental Setup

The SPFT apparatus used in the present work follows recommendations provided in a corresponding ASTM standard practice [61] and is functionally equivalent to one previously employed for LAW glass testing [13]. Figure 3.1 shows a single specimen test train marked by an index "*i*" along the diagram. There were several such trains running simultaneously at the same constant temperature for the duration of the given test set. The only wetted materials throughout the system are plastics. These include high-density polyethylene (HDPE), polypropylene (PP), polyetheretherketone (PEEK), perfluoroalkoxy polymer (PFA), and fluorinated ethylene propylene co-polymer (FEP). These materials are known not to leach out any components that are relevant to the glass leaching process. However, since leaching solutions have elevated pH values and all tests have long durations, protection from ingress of atmospheric CO_2 is an issue, as all plastics are somewhat permeable to carbon dioxide. To address this, all reservoirs and enclosures are continuously purged with CO_2-free air (<1 ppm CO_2 from a dedicated Balston model 75-52NA "zero" gas generator). A short length of interconnecting PEEK tubing (less than 1 m of 1.59 mm OD x 0.51 mm ID) was exposed to ambient atmosphere – an insignificant exposure considering PEEK's carbon dioxide permeability constant [62] of $6.1 \cdot 10^{-9}$ $cm^3_{(STP)} \cdot cm/cm^2 \cdot s \cdot atm$ at 25 °C, which is an order of magnitude lower than the one for commonly used FEP and PFA materials [63] ($7.0 \cdot 10^{-8}$ and $9.4 \cdot 10^{-8}$ $cm^3_{(STP)} \cdot cm/cm^2 \cdot s \cdot atm$ at 25 °C, respectively).

The leaching solution is prepared ahead of time in a quantity sufficient for the entire test duration. The solution is contained in a continuously purged reservoir *R* from which it is drawn into a pump *P* and discharged through the reaction cell (LC in Figure 3.1). The pump operation is computer controlled. Upon entering the constant temperature oven, the leaching solution passes through a 50 cm long thermal equilibration coil (TEC in Figure 3.1) before reaching the reaction cell. The solution leaves the reactor and analytical samples are collected downstream in a series of bottles. Samples are collected periodically throughout the test at predetermined times. Within a given run (temperature) all analytical samples (*S*) were indexed according to train number (index $1<i<12$) and order of collection (index $1<j<N$).

3.5 Description of Pulsed-Flow Experimental Setup

The rationale for flow-through tests such as the SPFT is to achieve steady state with respect to species in solution in order to control the affinity term in the rate law. Frequently, that steady state corresponds to essentially very dilute conditions wherein the affinity term is equal to one. This condition is favored by higher flow rate, but then the concentrations in solution become very small and therefore a practical compromise must be reached. Typical volumetric flow rates employed in SPFT tests on LAW glasses have been in the range of about 7 to 50 µL/min, which corresponds to about 10 to 72 mL/day.

An often simpler approach to flow-through testing than employing continuous flow is to employ pulsed flow, wherein a portion of the leachate solution is replaced by fresh leachant at regular intervals to achieve the same average flow rate. This type of partial replenishment test was developed and employed extensively by VSL beginning in the 1980s for the HLW glass development and testing program and was called the “Pulsed-Flow Test.” VSL has many hundreds of such tests still in progress that have been running for many decades.

The present tests were designed with a periodic replacement of 50% of the leachate with fresh leachant in a 50 ml stainless steel (304L) vessel. The replacements were set at intervals of 1-day at 70 °C and 3-days at 40 °C and 23 °C. The quantity of glass was adjusted so that its surface area would approach the linear flow rate[5], q/S, and residence time values employed in the standard SPFT tests, as described in Table 3.1. From each of the 25 ml samples collected, an aliquot of 5 ml was pipetted and reserved for pH measurement and the remaining 20 ml was sampled for analysis after acidification.

3.6 Sample Analysis

pH was measured on each sample collected from the flow-tests and pH values were found to remain at the target buffer selected with less than 1% relative deviation. Each SPFT test also included a collection of samples that were designated for pH measurements in order to ensure that solution pH was maintained constant throughout a specific test.

Collected samples designated for solution analysis were acidified with a small amount of concentrated HNO_3 and analyzed by ICP-AES for B, Al, Li, K, Na, and Re. Additional analyses of Mo, Re, and Cs were conducted by inductively coupled plasma – mass spectroscopy (ICP-MS).

A total of 45 pulsed-flow tests and 30 SPFT tests were performed yielding nearly 900

---

[5] The linear flow rate is calculated as the volumetric flow rate divided by the total surface area of glass in the test vessel.

individual samples analyzed for solution chemistry. For SPFT tests, a sample was accepted for analysis only if its flow rate deviated from the average flow rate of its specific train by ≤5%. The average flow rate for all tests was within 10% of the corresponding target flow rate. At the end of the experiment, the altered glasses were collected, water-washed gently, and air dried. Altered glass samples were archived for potential future characterization.

3.7 Data Reduction

The reduction of the SPFT data follows the guidelines in the ASTM standard [61]; modifications for reduction of the Pulsed-Flow data are described in Section 3.8.

If a glass specimen having a known surface area is contacted by a solution that flows continuously at a known flow rate and at a constant temperature, the concentration of the i-th soluble glass component in the effluent solution exiting the reactor vessel can be used to calculate the amount of glass that has dissolved. The flow rate is determined by dividing the mass of solution that is collected for analysis by the duration over which it was collected. The dissolution rate of the glass (g m^{-2} day^{-1}) is then calculated as:

$$(rate) = \frac{\left[C_i - C_i^o\right] \cdot \left(\frac{F}{S^o}\right)}{f_i} \tag{3.1}$$

where:

C_i - is the steady-state concentration of component i measured in the effluent solution (g/L)
$C_i°$ - is the background concentration of component i in the influent solution as measured in a blank test (g/L)
F - is the solution flow rate (L/day)
$S°$ - is the initial surface area of the glass sample that is exposed to solution (m^2), and
f_i - is the mass fraction of component i in the glass (g/g).

Several samples of the effluent solution are collected during the test to determine the steady-state concentrations of dissolved glass components at a particular solution flow rate.

When testing a crushed glass sample, its surface area ($S°$) is calculated as the product of the specific surface area and the mass of glass (m_g) used in the test. The specific surface area is approximated based on the mesh size of the fraction used in the test and the density of the glass. The particles of glass are presumed to be spherical with diameter (d) equal to the arithmetic average of the openings of the sieves used to prepare the material. The specific surface area (S_p) of a glass having a density ρ is [61]:

$$S_p = {}^{6}\!/_{\rho \cdot d} \tag{3.2}$$

thus,
$$S^o = S_p \cdot m_g \tag{3.3}$$

The volumetric flow rate (*F*) is calculated by dividing the mass of solution that is collected by the time for its collection and its density (which can be assumed to be 1 g/cm^3 in most cases).

During glass dissolution, the mass and surface area of the glass sample are expected to change over time as material is dissolved. The surface area S_j at time *j* during a SPFT test is calculated from the following expression [61]:

$$S_j = \frac{3}{\rho r_o} m_0^{1/3} m_j^{2/3} \tag{3.4}$$

where r_o is the radius of the glass particle and m_j is the sample mass at time *j*. The parameter m_j is estimated by the equation [64]:

$$m_i = m_o - \frac{1}{f_i}\left[\sum_{n=1}^{j-1} F_n C_{n,i} \Delta t_n + F_j C_{j,i} \frac{\Delta t_j}{2}\right], \text{j} \geq 1 \tag{3.5}$$

where *i* is an element representative of glass dissolution such as B. Here it should be noted that Equation (3.5) inherently assumes uniform dissolution during SPFT testing and the absence of any surface alterations such as cracking.

To determine the steady-state concentration (C_i), the measured concentration of the *i*-th component is plotted as a function of time in order to visually identify the data to be used. Data that precede the attainment of steady-state conditions are excluded before calculating mean and standard deviation of the remainder. The relative standard deviation (the standard deviation divided by the mean) of the calculated steady state concentration must be less than 0.15 for the test results to be valid [61]. Soluble components monitored in this fashion typically include silicon, aluminum, sodium, and boron. The parameters of Equation (1.1) are typically estimated using normalized dissolution rate (NDR) of boron.

Calculation of Parameters η, E_a, and k_0. The test data obtained under dilute conditions are used to determine the dependence of glass dissolution rate on pH (the parameter η in Equation (1.1)), the activation energy of the dissolution, and the rate constant. As described previously [12-19], log NDR is plotted as a function of pH_T at a specific temperature and linear regression of the data is performed for pH_T >7. Because the parameter η is assumed to be independent of temperature, the power law coefficient for a particular glass is considered to be the average value obtained at various temperatures. Once the parameter η is determined in this way, the activation energy E_a and rate constant k_0 of the glass are determined by performing a nonlinear regression on all data obtained under dilute conditions ($[Si]_{in}=0$)) using Equation (1.1) [8].

Estimation of K_g. K_g is estimated from the NDR values obtained at steady state when the glass is leached in the presence of different concentrations of Si and at specific pH and T. To determine the parameter K_g at a given T, NDR values are plotted as a function of the activity of orthosilicic acid ($a[H_4SiO_4]$) present in the effluent solutions at steady state (Equation (1.1)) and a linear regression on the data is performed. Values of $a[H_4SiO_4]$ are determined from the corresponding solution chemistry using the geochemical code PHREEQC. According to Equation (1.1), K_g is given by the value of $a[H_4SiO_4]$ at NDR = 0 [8]. To determine the K_g value at the presumed repository temperature of 15°C, the natural logarithm of the measured K_g values is plotted against the reciprocal of the absolute temperature and a linear regression is performed on the data [8].

Estimation of ion exchange parameters. r_{IEX} and E_{ad} for Na, Li, K, and Cs: Alkali ion exchange rates were obtained by subtracting the normalized dissolution rates of either Mo, Re, or B from the normalized dissolution rate of the alkali and converting the result to moles of the specific alkali per unit glass surface area per unit time (*not* moles of *glass* per unit area per unit time). The activation energy E_{ad} of each alkali evaluated was determined by performing a linear regression of the natural logarithm of the measured r_{IEX} values versus the reciprocal of the absolute temperature. The slope of each regression provides $-E_{ad}/R$ according to Equation (1.3). The results from the regression were then used to extrapolate the r_{IEX} values of each alkali to the presumed repository temperature of 15°C.

3.8 Pulsed-Flow Test Data Reduction

Extraction of leach rates from the pulsed flow data requires a different approach from that used for the SPFT data per ASTM C1662 described in Section 3.7. The leachant flow in the SPFT is continuous whereas in the PFT it is pulsed and therefore discrete. It is instructive to describe first the derivation of the rate equation for the continuous case.

3.8.1 Continuous Flow Case

We consider a sample of glass with surface area S in a reactor of volume V that is filled with leachant that flows through the reactor continuously at a constant volumetric flow rate F. The rate of release of species i from the glass at time t is $r_i(t)$ (mass of species i released into the leachant per unit surface are of glass per unit time). The mass of species i in solution in the reactor at time t is $m_i(t)$ and the concentration is $c_i(t) = m_i(t)/V$. That mass increases as a result of release from the glass and decreases as a result of the leachant flow, such that its rate of change is given by:

$$\frac{dm_i(t)}{dt} = r_i(t)S - c_i(t)F \tag{3.6}$$

and therefore:

$$\frac{dc_i(t)}{dt} = r_i(t)\frac{S}{V} - c_i(t)\frac{F}{V} \tag{3.7}$$

At steady state, $dc_i(t)/dt = 0$, so:

$$r_i = c_i(t)\frac{F}{S} \tag{3.8}$$

To obtain the rate of glass dissolution, r_g, we normalize by dividing by f_i, the mass fraction of species i in the glass to obtain:

$$r_g = c_i(t)\frac{F}{Sf_i}\ , \tag{3.9}$$

which, except for blank subtraction, is exactly the result given in Eq. 3.1 for analysis of SPFT data.

3.8.2 Pulsed-Flow Case

In the PFT, after each time interval Δt, a sample of the leachate of volume ΔV is withdrawn from the vessel for analysis and a volume ΔV of fresh leachant is added to the vessel. Considering the n^{th} and $(n+1)^{\text{th}}$ samplings, we denote the concentrations of species i at each point in this process as follows:

$c_{i,n}$ = the concentration of species i at the n^{th} sampling <u>before</u> replacement

$c_{i,n,s}$ = the concentration of species i at the n^{th} sampling <u>after</u> replacement (i.e., at the start of the next leaching interval)

$c_{i,n+1}$ = the concentration of species i at the $(n+1)^{\text{th}}$ sampling <u>before</u> replacement (i.e., at the end of that leaching interval).

The mass of species *i* in the leachant in the vessel after sampling is equal to the mass before sampling minus the mass removed; this quantity divided by the volume gives the concentration at the start of the interval:

$$c_{i,n,s} = (c_{i,n}V - c_{i,n}\Delta V)/V = c_{i,n}\left(1 - \frac{\Delta V}{V}\right) \tag{3.10}$$

Over the interval Δt, the mass of species *i* added to the solution in the reactor is $r_i S \Delta t$; it is also equal to the change in the concentration multiplied by the leachate volume:

$$(c_{i,n+1} - c_{i,n,s})V = \left\lfloor c_{i,n+1} - c_{i,n}\left(1 - \frac{\Delta V}{V}\right)\right\rfloor V \tag{3.11}$$

Setting these equal we obtain:

$$r_i(t) = \frac{c_{i,n+1} - c_{i,n}\left\lfloor 1 - \frac{\Delta V}{V}\right\rfloor}{\Delta t \frac{S}{V}} \tag{3.12}$$

As before, the rate of glass dissolution, $r_g(t)$, is obtained by normalizing by dividing by f_i, the mass fraction of species *i* in the glass:

$$r_g(t) = \frac{c_{i,n+1} - c_{i,n}\left\lfloor 1 - \frac{\Delta V}{V}\right\rfloor}{\Delta t \frac{S}{V} f_i} \tag{3.13}$$

This is identical to the equation used previously at VSL to extract normalized glass dissolution rates from Pulsed-Flow test data (see, for example [65]).

At steady state, $c_{i,n+1} = c_{i,n}$ and therefore:

$$r_g = c_{i,n}\frac{\Delta V}{\Delta t}\frac{1}{Sf_i} = c_{i,n}\frac{F}{Sf_i}\ , \tag{3.14}$$

which agrees with the continuous case above (Equation (3.9)).

In the present work, Equation (3.13) was applied to PFT data for each of the alkalis (Li, Na, K, and Cs) and also to the data for the species used to measure release via matrix dissolution (B, Mo, and Re). Alkali ion exchange rates were then obtained by subtracting the normalized dissolution rates of either Mo, Re, or B from the normalized dissolution rate of the alkali and converting the result to moles of the specific alkali per unit glass surface area per unit time (*not* moles of *glass* per unit area per unit time). Thus, for alkali R (R = Li, Na, K, Cs) and matrix dissolution indicator M (M = B, Mo, Re), r_{IEX} is given by:

$$r_{IEX,R} = (r_{g,R} - r_{g,M})\frac{f_R}{W_R}, \tag{3.15}$$

where W_R is the atomic mass of R. Since r_g is typically stated in units of g m^{-2} d^{-1} whereas r_{IEX} is typically stated in units of mol m^{-2} s^{-1}, the result in Equation (3.15) is then further divided by the number of seconds per day.

SECTION 4.0
SPFT TEST RESULTS

4.1 SPFT Tests in Dilute Solutions

As described in Section 3, LAWC22 was subjected to a number of tests in dilute conditions. The steady state dissolution rates were determined as described above and the parameters η, E_a, and k_0 were calculated. The K_g value was also estimated. Data obtained from the elemental analysis of collected effluent samples at three temperatures are listed in Appendix A, Tables A1, A3, A5 (lines A1-E1), which also show the corresponding normalized[6] dissolution rates for each analyzed element as calculated from Equation (3.1); these transient rates converge over time to the steady state dissolution rates of glass alteration for a specific set of test conditions. Subsequently, normalized dissolution rates for each element (NDR_i) were plotted against time and steady state was determined for each analyzed element. Normally, the last three samples were considered; the exceptions are shown in bold. Plots of the data from all tests are provided in Appendix B, where the *y*-axes of the graphs show NDR_i, where *i* is one of the following elements: B, Al, Na, Li, K, Si, Re, Cs, or Mo. The glass dissolution rate is denoted as *NDR*; since boron is used as the conventional indicator of glass dissolution, this term refers to the dissolution rate of B (NDR_B) at steady state.

In general, the rates decrease monotonously toward the steady state value at low pH, they are roughly constant at intermediate pH, and show a maximum at higher pH, before decreasing slowly toward the steady state value.

4.1.1 Dynamic Dissolution of LAWC22 Under Dilute Conditions

At acidic or circumneutral pH_T Na, Li and B are released faster than Si and Al, resulting in incongruent dissolution. As the pH of influent solution increases to slightly or moderately alkaline values (pH_T 8-10), congruent or near-congruent dissolution is observed. As in prior studies, the concentration of Al released into the effluent solutions was apparently controlled by the solubility of the element at the specific pH. Mo and Re are released roughly congruently with Na, Li, and B.

[6] Normalized with respect to the content of the element *i* in the glass composition.

4.1.2 Estimation of Kinetic Parameters η, E_a, and k_0

Steady-state glass dissolution rates at a specific set of alteration conditions measured for glass LAWC22 are shown in Table 4.1. The evolution of these forward dissolution rates as a function of pH_{RT} at a specific temperature is depicted in the plots of Figure 4.1. The NDR_B at 40°C and pH_T 7.61 appears to be an outlier that is responsible for the greater slope at 40°C than the for the other two experiments. Eliminating this inconsistent data point yields a comparable slope to that for the other temperatures (dotted linear trend line).

The kinetic parameters η, E_a, and k_0 were calculated from the steady-state dissolution rates selected from those listed in Table 4.1, as described in Section 3.7. Figure 4.2 shows the plots of log *NDR* vs. pH_T used to determine the value of coefficient η at each temperature. Table 4.2a summarizes the obtained η estimates shown in the individual plots of Figures 4.2 and provides the mean of the values determined at various temperatures. This assumes that the parameter η is independent of temperature. The calculated η value for LAWC22 is 0.46±0.03, which is within the expected range for nuclear waste glasses and is very close to the value of 0.42 reported previously [9, 12] based on measurements at four different temperatures instead of three.

A non-linear regression performed using the JMP data analysis software on all data obtained at pH_T >7, gave an apparent E_a value of 69±11 kJ mol^{-1} and an estimated value for the kinetic rate constant (k_0) of 2.0 x 10^5 gm^{-2}d^{-1}, as shown in Table 4.2b. These values have somewhat larger errors than those reported previously likely because they were determined from data at just three temperatures instead of four in the earlier work [9]. Nevertheless, the values are within the expected range for the dissolution of silicate glasses under dilute conditions and are very similar to the values of 64 kJ mol^{-1} (E_a) and 1.0 x 10^5 gm^{-2}d^{-1}(k_0), reported previously for LAWC22 [9, 19].

4.2 SPFT Tests in Saturated Solutions

Simultaneously with the above described tests in dilute solutions, the same LAWC22 glass was also subjected to 15 tests (five pH values at three temperatures) in silicic acid saturated buffers. The main purpose of these tests was to measure the ion-exchange rates and to collect data to compare the SPFT and pulsed-flow test results. As is apparent from Table 3.1, the test matrices were designed in such a way that the conditions for the two types of tests were as close as possible. The temperatures, buffers, and the average linear flow rates were exactly the same, with only the residence times and the average volumetric flow rates sometimes differing.

4.2.1 Dynamic Dissolution of LAWC22 under Saturated Conditions

The data obtained from the elemental analysis of collected effluent samples at the three temperatures are listed in Appendix A, Tables A2, A4, A6 (lines A2-E2) together with the corresponding normalized dissolution rates for each analyzed element as calculated from Equation (3.1) and the steady state values obtained as described in Section 4.1. Similarly, the plots of NDR for B, Na, Li, K, Al, Re, Mo, Cs versus time are presented in Appendix B. Additional data for the elements relevant to ion-exchange and the corresponding ion-exchange rates are presented in Appendix A, Tables A7-9.

The dissolution rates for all elements relevant to ion-exchange rate calculation are presented in Table 4.3. The ion-exchange rates for Na calculated based on the three elements (B, Mo, and Re) against time are presented in Appendix C. In general, the results for Mo and Re tracked very closely and rates based on the average of the two are therefore also employed. In addition to data for Na, data for three other alkalis, Li, K, and Cs were also analyzed. However, for LAWC22, the low potassium concentration in the glass meant that the K data were too noisy to be evaluated. Although also present at low concentrations, Cs could be analyzed with higher sensitivity by ICP-MS and therefore the Cs results are presented together with the data for Na and Li.

4.2.2 Time Dependence of Ion Exchange

Ion-exchange rates are plotted as functions of the reciprocal of the square root of time ($t^{-1/2}$) for each pH value in Figures 4.3, 4.4, and 4.5 for 70 °C, 40 °C, and 23 °C, respectively. In all cases, the Na data show linear relationship with positive slope, as would be expected for a diffusion controlled process. That is also the case for Li except for the data at $pH_{RT} = 7$ at 70 ºC, which shows the opposite slope. The Cs data also show a negative slope in the acidic range; this may be an artifact of the very low rates that are being measured.

Figure 4.6 shows an alternative presentation of the data for Li at 40 ºC as a plot of $\log(r_{IEX})$ versus $\log(t)$. Linear relationships are evident with slopes in the range of -0.4 to -0.9, in reasonable agreement with the expected value of -0.5 from the diffusion equation. Furthermore, there is a systematic variation with pH, as discussed below.

4.2.3 pH Dependence of Ion Exchange

Plots of $\log(r_{IEX})$ versus pH_T (pH measured at the test temperature) are presented in Figure 4.7. The results are generally similar to the more extensive data obtained from the pulsed-flow tests, with which they are compared and discussed in more detail in Section 5.

4.2.4 Temperature Dependence of Ion Exchange

The temperature dependence of r_{IEX} was evaluated from plots of ln(r_{IEX}) versus 1/T, as shown in Figure 4.8. Similar analysis of data from the Pulsed-Flow tests is described in Section 5.0. The activation energy for ion-exchange, E_{ad}, was estimated from these plots, and the extrapolated value of r_{IEX} at 15 °C was calculated. The calculated r_{IEX} values using either B or Mo and Re as matrix dissolution tracers are presented in Table 4.4. The E_{ad} and r_{IEX} values for Na presented in Table 4.5 are in good agreement with the previously reported values of 45 kJ/mol and r_{IEX} at 15 °C of 1.28×10^{-11} mol m^{-2} s^{-1} [9, 18], respectively; the results are also in good agreement with those from the Pulsed-Flow tests, discussed in Section 5.5.

4.2.5 Estimation of K_g

Determination of K_g was not an objective of the present work and the test matrix was focused instead on ion exchange. However, by combining the data collected in dilute solutions at pH 9 with some of the data collected under saturated conditions, it proved possible to estimate the K_g parameter from these test results. To determine the parameter K_g at a given T, as described in Section 3.7, NDR values are plotted as a function of the activity of orthosilicic acid ($a[H_4SiO_4]$) dissolved in the effluent solutions at steady state and a linear regression on the data is performed. Values of $a[H_4SiO_4]$ are determined from the corresponding solution chemistry using the geochemical code PHREEQC. According to Equation (1.1), K_g is given by the value of $a[H_4SiO_4]$ at NDR = 0 [8]. To determine the K_g value at the presumed repository temperature of 15 °C, the natural logarithm of the measured K_g value is plotted against the reciprocal of the absolute temperature and a linear regression is performed on the data [18].

Reasonable trends are observed for the measurement at pH 9 in dilute conditions and the measurements at pH 8, 9, and 10 in saturated solutions. The plots for K_g determination at three different temperatures, based on both B and Re as matrix dissolution tracers, are presented in Figure 4.9; the Arrhenius plot to estimate K_g at 15 °C is presented in Figure 4.10. The values of K_g obtained using B (1.74×10^{-3} mol L^{-1}) and Re (1.69×10^{-3} mol L^{-1}) are very close and also close to those measured by the Pulsed-Flow technique (see Section 5.0) and published for other glasses [19].

SECTION 5.0
PULSED-FLOW TEST RESULTS

This section provides a discussion of the results from the Pulsed-Flow tests. The results from regression analysis of the data in terms of the model described in Section 1.3 are presented in Section 6.

5.1 General Observations

Effluent solution analytical results for ten successive samples (daily at 70 °C and every 3 days at 40 °C and 23 °C) are provided in Appendix D. The steady-state concentrations of dissolved glass components were calculated as the average of the concentrations of the last few samples in each experiment, and collected in Tables 5.1 to 5.3 for LAWC22, ORLEC28, and IDF1B2, respectively. The steady-state concentrations were identified visually (see Appendix E) with attention to minimizing the percent relative standard deviation (%RSD) of the dataset averaged. The normalized dissolution rate values were calculated according to the data analysis methods described in Section 3.8 and accounting for the surface area correction based on boron concentration in the leachates.

Sodium dissolution rates are nearly congruent with those of boron in the acidic range (pH_{RT} of 7 and 8 at 70 °C are 5.96 and 6.91 respectively, pH_{RT} of 7 is 6.63 at 40 °C). Potassium and lithium dissolution rates generally remain lower than that of sodium, and in many cases, their dissolution rates fall below that of boron. Consequently, subtracting the boron dissolution rate from that of the alkali is clearly not a viable method to determine the ion-exchange rate. It is only when pH and silica content increase that the overall dissolution rates decrease and boron behaves less like the alkalis in the present tests. This is generally attributed to the increased concentration of H_3O^+ available for inward diffusion into the glass in acidic pH conditions, which promotes the dissociation of boron-oxygen bonds in B-O-B or B-O-Si units; as stated in reference [66], the presence of protons (acidic conditions) decreases considerably the hydrolysis reaction barriers (18-60 kJ/mol vs. 98-102 kJ/mol in neutral conditions). This results in lower or unmeasurable alkali ion exchange rates estimated by difference between boron and alkali dissolution rates in the acidic range, contrary to the expectation that ion exchange rates should increase as the pH decreases.

The present data show clearly that rhenium and molybdenum are valuable, and perhaps preferable, markers of glass matrix dissolution and for that reason, were used throughout this data analysis in preference to boron in the estimation of ion-exchange rates (though all are reported). The Na ion-exchange rate was estimated by subtracting from the sodium dissolution rate the dissolution rate of Re or Mo (or an average), in a manner similar to previous data analysis [12-19]. The Na ion-exchange rate was also estimated based on boron dissolution rate but, as noted above, was frequently not measurable because the boron dissolution rate is high at low pH and equal to or greater than the dissolution rates for alkalis. The ion-exchange rate values obtained from subtracting the dissolution rate for Re and Mo from those for the alkali components are in excellent agreement with each other. In the rest of the discussion below, the ion-exchange rate values are the average ion exchange rates calculated based on Re and Mo dissolution rates, and in the few instances where values based on either one could not be estimated, the value based on only the other is used in the evaluations below.

Plots of Na ion exchange rates calculated using Mo, Re, and B as tracers for bulk glass dissolution as functions of time are presented in Appendix F. From the plots it can be seen that ion exchange rates are highest at the early times and reach steady value at longer times. These steady values of the ion exchange rates (average of the last three to five points) calculated from the average of rates calculated using Mo and Re as tracers are listed in Table 5.4.

Ion exchange rates for two other alkalis, Li and K, are also evaluated and reported here. Lithium is a significant glass modifier added in LAWC22 where it represents about one-third of the total alkali in the glass; potassium is relatively high in the waste composition on which ORLEC28 is based and represent about one-tenth of the total alkali content in the glass. Ion exchange rates for both Li and K were evaluated by difference of their normalized dissolution rates from those for Mo and Re and, when possible, from the normalized dissolution rate of B. Li and K ion exchange rates (average of the last three to five points, as for Na described above) calculated from the average of the rates calculated from Mo and Re as tracers are provided in Table 5.4.

The third spike included in the present study is cesium, which was added to evaluate its leach rate in comparison to the other alkalis. As expected, its leach rate is generally higher than that of Mo and Re and clearly higher in the acidic range where the ion exchange rate is higher. As, discussed below, cesium shows an ion exchange rate that is about two to three times lower than that of sodium, which in agreement with previous observations [67].

5.2 LAWC22 Pulsed-Flow Test Results

LAWC22 contains four alkalis (Li, Na, K, and a Cs spike of 0.1 wt%) with sodium representing more than two-thirds of the total glass alkali content (14.88 mol% Na_2O), lithium most of the rest (5.36 mol% Li_2O), plus a small amount of K (0.05 mol% K_2O) and Cs (0.03 mol% Cs_2O). The cesium concentration in the leachate was analyzed by ICP-MS along with Mo and Re. K was analyzed by ICP-OES along with all other main glass constituents in the leachate but the K concentration was too low to yield meaningful ion-exchange data for this glass; instead, ORLEC28 was used for that purpose, as described below.

Effluent solution analytical results for LAWC22 Pulsed-Flow tests at 70 °C, 40 °C, and 23 °C are provided in Appendix D, Tables D1, D2, and D3 respectively, for analyses conducted by ICP-OES, and Tables D10 to D12, respectively, for analyses conducted by ICP-MS. The steady-state dissolution rates of dissolved glass components are collected in Table 5.1 and illustrated in Appendix E, Figures E1 to E3, for the three test temperatures.

5.2.1 Time Dependence of Ion-Exchange in LAWC22

The time dependence of the sodium ion exchange rates estimated from fourteen of fifteen experiments with glass LAWC22 fit well to the $t^{-1/2}$ relationship, as shown in the plots of Figure 5.1. The only experiment that did not show a good fit (R^2 of 0.47) was at 70 °C and pH_T of 5.96; these data were frequently excluded from later analyses (e.g., extrapolation to 15 °C). The fitted data follow the inverse square root of time dependence given in Equation (1.2), with slopes of the linear fit decreasing as the pH increases.

Lithium ion exchange rates show a similar trend, as shown in Figure 5.2; the calculated ion exchange rates for lithium in the figure are based on Re as the tracer for glass matrix dissolution. In all cases except the most acidic one (70°C and pH_T of 5.96), the decrease of ion exchange rate over time fits well to the $t^{-1/2}$ time dependence.

The cesium leaching rate is two to three orders of magnitude lower than that of sodium (see Table 5.3) and in most cases lower than the normalized rate for boron. Therefore, the cesium ion exchange rate could not be estimated based on boron but could be estimated using either Re or Mo as the tracer for matrix dissolution by using results from the late samplings (7 to 10 days at 70 °C, beyond 20 days at 40 °C and 23 °C). The paucity of data did not permit generation of a time dependence plot but were sufficient to compare Cs ion exchange rate values to the rates for other alkalis (Table 5.4).

5.2.2 pH Dependence of Ion Exchange in LAWC22

The logarithm of the sodium, lithium, and cesium ion exchange rates (average steady values) are plotted as a function of pH_T in Figure 5.3. Unless noted, the ion exchange rate values are based on dissolution rates of Mo and Re; in some of the plots, the dotted lines show the trend if boron is used as the basis, demonstrating how the acidic region biases the ion exchange rate estimation based on boron.

As shown in Figure 5.3, the logarithms of the ion exchange rates of the three alkalis decrease linearly as the pH increases (with reasonable fit R^2 values ranging from 0.53 to 0.98), in general accord with the model described in Section 1.3.

It is known that Li^+ diffuses at a slower rate than Na^+ through the glass because, although smaller in size, it possesses a larger field strength [8, 68]. A comparison of the respective Na^+ and Li^+ ion exchange rates for all temperatures and pH conditions used in Pulsed-Flow tests shows on average a factor of 9 difference between the two rates (Figure 5.4). Since lithium content in glass LAWC22 is 2.8 times lower than the Na content, lithium ion exchange rate is about a third that of sodium once adjusted for the respective molar fractions in the glass.

Cs^+ has been reported to exhibit a diffusion coefficient that is 10 times lower than that for Na^+ and to possess a diffusion activation energy that is higher than that of Na^+ by a factor of 2 [16] because heavier cations such as Cs^+ favor stabilization of terminal NBOs [69]. As with Li^+ above, ion exchange rates for Na^+ and Cs^+ were compared for all temperatures and pH conditions tested in PFT. As shown in the lower part of Figure 5.4, there is on average a factor of 1000 difference between the two rates; since the cesium content in glass LAWC22 is 440 times lower than the Na content, the Cs^+ ion exchange rate is about two times lower than the rate for Na^+ once adjusted for the respective molar fractions in the glass.

5.3 IDF1B2 and ORLEC28 Pulsed-Flow Test Results

The two other glass compositions subjected to Pulsed-Flow testing were selected to represent the high alkali region of LAW formulations: IDF1B2 with the highest sodium (27.35 mol% Na_2O) with a trace amount of potassium (0.09 mol% K_2O), and ORLEC28 with combined high limit of sodium plus potassium (24.52 mol% Na_2O and 2.46 mol% K_2O). Neither contain lithium and both include the same spike of 0.04 mol% Cs_2O as in LAWC22. Effluent solution analytical results for ORLEC28 and IDF1B2 Pulsed-Flow tests at 70 °C, 40 °C, and 23 °C are collected in Appendix D, Tables D4 to D9 for analyses conducted by ICP-OES and Tables D13 to D18 for analyses conducted by ICP-MS. The steady-state concentrations of dissolved glass components are collected in Tables 5.2 and 5.3 for ORLEC28 and IDF1B2, respectively, and illustrated in Appendix E for the three test temperatures.

As expected, and in agreement with earlier SPFT test results [13, 18], the normalized leach rates for boron and sodium are higher than for LAWC22, particularly in the acidic and near-neutral conditions. As pH increases and temperature decreases, the difference lessens considerably. Furthermore, the normalized leach rates for Mo and Re remain comparable between all three glasses, indicating similar level of matrix dissolution in the three glasses.

5.3.1 Time Dependence of Ion Exchange in IDF1B2 and ORLEC28

The time dependence of the Na ion exchange rate from thirty experiments with glasses ORLEC28 and IDF1B2 generally fit well the expected $t^{-1/2}$ relationship (Figures 5.5 and 5.6 for ORLEC28 and IDF1B2, respectively), as was observed with LAWC22. At long times, the values tend to stabilize and these limiting values are collected in Table 5.4 for all three glasses.

The potassium concentration is low in IDF1B2 and showed dissolution rates that are much lower than those for Na and, in most cases, lower than those for boron. Therefore, further evaluation of the K data for this glass was not conducted.

5.3.2 pH Dependence of Ion Exchange in IDF1B2 and ORLEC28

As shown in Figure 5.7, the logarithms of the ion exchange rates of sodium, potassium, and cesium for ORLEC28 show similar trends, decreasing linearly as the pH increases, in general accord with the model described in Section 1.3. As can be seen in the figure, the K ion exchange rate is about one order of magnitude lower than that for sodium (between 10 to 50 times lower, with larger differences at higher pH and lower temperature). Because of its larger size, K^+ is expected to diffuse through the glass at a slower rate than Na^+. A comparison of respective Na^+ and K^+ ion exchange rates for all temperatures and pH conditions used in Pulsed-Flow tests shows on average a factor of 20 between the two rates (Figure 5.8). Since the potassium content in glass ORLEC28 is 10 times lower than the Na content, the sodium ion exchange rate is about two times higher than the potassium ion-exchange rate once adjusted for the respective molar fractions in the glass.

For IDF1B2, as shown in Figure 5.9, the logarithms of the ion exchange rates of sodium and cesium for IDF1B2 show similar trends, decreasing linearly as the pH increases, in general accord with the model described in Section 1.3. However, because of the lower K concentration in the glass, there are too few data to display for potassium for this glass.

As observed for LAWC22, the cesium ion exchange rate is two to three orders of magnitude lower than that of sodium in both glasses. Comparison of the respective Na and Cs ion exchange rates in ORLEC28 and IDF1B2 for all temperature and pH conditions tested in PFT (Figures 5.10) shows that the average difference between the two rates is larger in IDF1B2 than in ORLEC28. The sodium ion exchange rate in ORLEC28 is a factor of about 3000 larger than the Cs ion exchange rate; since the cesium content in ORLEC28 glass is 670 times lower than the Na content in this glass, the Cs ion-exchange rate is about five times lower than the Na ion exchange rate, once adjusted for the respective molar fractions in the glass. This result is similar to that for glass LAWC22. In IDF1B2, the ratio of ion exchange rates (Na/Cs) is around 15,000 and the cesium content is 758 times lower than the sodium content in this glass, indicating a much lower cesium ion exchange rate in comparison to sodium in this glass. This is discussed further in the next section, along with the temperature dependence of the ion exchange rates in the three glasses.

5.4 Temperature Dependence of Ion Exchange for LAWC22, ORLEC28, and IDF1B2

As reflected in Equation (1.3), the ion exchange rate is expected to show an Arrhenius dependence on temperature. Therefore, the activation energy for alkali ion exchange, E_{ad}, and the rate of ion exchange at the presumed repository temperature of 15 ºC are calculated by plotting the natural logarithm of r_{IEX} as a function of the reciprocal of the absolute temperature and performing a linear regression on the data. The ion exchanges rates for Na, Li, K, and Cs collected in Table 5.4 were used for this purpose. The results are summarized below.

r_{IEX} *Na* (15 °C): Plots of natural logarithm of sodium ion exchange rate as a function of 1/T are presented in Figure 5.11 for all three glasses using all of the ion exchange rates calculated from the Pulsed-Flow tests. A linear regression was performed on the data to determine the activation energy (E_{ad}) and to estimate the r_{IEX} value at 15 °C. These linear regressions are shown in Figure 5.11 for the three glasses. The results for the three glasses are:

E_{ad} Na = 52.6±6.8 kJ mol^{-1} for LAWC22,
E_{ad} Na = 73.2±8.0 kJ mol^{-1} for ORLEC28, and
E_{ad} Na = 54.7±5.9 kJ mol^{-1} for IDF1B2.

The r_{IEX} (15 °C) values are calculated by extrapolation to be the following[7]:

r_{IEX} Na (15°C) = 1.16×10^{-11} mol m^{-2} s^{-1} for LAWC22
r_{IEX} Na (15°C) = 4.56×10^{-11} mol m^{-2} s^{-1} for ORLEC28
r_{IEX} Na (15°C) = 1.11×10^{-10} mol m^{-2} s^{-1} for IDF1B2.

r_{IEX} *Li* (15 °C): The lithium ion exchange rate regression plot is presented in Figure 5.12 for LAWC22 only, since this is the only glass that contains lithium. The plot shows ion exchange rates calculated from Pulsed-Flow test data at saturating conditions at 70 °C, 40 °C, and 23 °C. From the linear regressions shown in Figure 5.12, we obtain:

E_{ad} Li = 37.2 ± 11.8 kJ mol^{-1} in LAWC22, and
r_{IEX} Li (15 °C) = 3.72×10^{-12} mol m^{-2} s^{-1} for LAWC22.

r_{IEX} *K* (15 °C): The potassium ion exchange rate regression plot is presented in Figure 5.13 for ORLEC28 only, since this is the glass that contains the largest concentration of K. Using all ion exchange rates calculated from Pulsed-Flow tests at saturating conditions at 70 °C, 40 °C

[7] Using boron as the tracer for matrix dissolution, slightly higher values are calculated. The following values were obtained: 1.71×10^{-11} mol m^{-2} s^{-1} for LAWC22, 4.76×10^{-11} mol m^{-2} s^{-1} for ORLEC28, and 1.67×10^{-10} mol m^{-2} s^{-1} for IDF1B2. Using only the results of the three experiments per glass conducted at pH_{RT} 9 (using Mo/Re as tracers for matrix dissolution) also returns excellent correlations (R^2 0.86 to 0.98), and provides calculated r_{IEX} (15 °C) values that are in good agreement with the results obtained from all 15 experiments: 1.12×10^{-11} mol m^{-2} s^{-1} for LAWC22, 3.86×10^{-11} mol m^{-2} s^{-1} for ORLEC28, and 1.05×10^{-10} mol m^{-2} s^{-1} for IDF1B2.

and 23°C, the linear regressions shown in Figure 5.13, yield:

E_{ad} K = 78.0 ±8.7 kJ mol^{-1} in ORLEC28, and
r_{IEX} K (15 °C) = 2.25×10^{-12} mol m^{-2} s^{-1} for ORLEC28.

***r_{IEX}* *Cs* (15 °C):** Cesium ion-exchange rate regression plots are presented in Figure 5.14 for the three glasses using available ion exchange rates collected from Pulsed-Flow tests at 70 °C, 40 °C, and 23 °C. Unfortunately, a few values were not usable, particularly for IDF1B2, and the linear fits were generally not as good as for the other alkalis (lower R^2). Results of the linear regressions shown in Figure 5.14 gave the following:

E_{ad} Cs = 50.2±11.8 kJ mol^{-1} for LAWC22,
E_{ad} Cs = 71.4±9.4 kJ mol^{-1} for ORLEC28, and
E_{ad} Cs = 61.8±7.9 kJ mol^{-1} for IDF1B2.

The r_{IEX} values at 15 °C were calculated by extrapolation to be the following:

r_{IEX} Cs (15 °C) = 5.39×10^{-15} mol m^{-2} s^{-1} for LAWC22
r_{IEX} Cs (15 °C) = 1.67×10^{-14} mol m^{-2} s^{-1} for ORLEC28, and
r_{IEX} Cs (15 °C) = 6.26×10^{-15} mol m^{-2} s^{-1} for IDF1B2.

5.4.1 Comparison of Ion Exchange Rates for Na, Li, K, Cs

The observed variation in r_{IEX} (15 °C) in units of mol m^{-2} s^{-1} includes the effect of variations of the concentrations of the various alkalis in the three glasses, which differ significantly. In order to compare the intrinsic ion exchanges rates for each alkali for each glass, it is therefore useful to first normalize r_{IEX} for a given alkali by the molar concentration of that alkali in the glass. It is convenient to then consider the ratio of the normalized r_{IEX} for sodium to the normalized r_{IEX} for any other alkali. Doing so, we obtain the following ratios:

Li for LAWC22:	1.1
K for ORLEC28:	2.0
Cs for LAWC22:	4.9
Cs for ORLEC28:	4.1
Cs for IDF1B2:	27.0

These trends for the ratios of normalized r_{IEX} (15 °C) values are in general agreement with the results from analysis of data at all temperatures and pH values shown in Figures 5.4, 5.8, and 5.10, discussed above. For example, the dissolution rate plots in Figure E2 (Appendix E) demonstrate close congruency between Na and Li, which is in agreement with close ion exchange rates normalized to the glass composition. They are also in qualitative agreement with expectations based on the increasing size of K and Cs compared to Na and effects of the higher field strength of Li compared to Na.

5.4.2 Ion Exchange Activation Energies

The results from comparison of the ion exchange activation energies obtained from evaluating individually each alkali ion are presented in Figure 5.15. Within the experimental errors, E_{ad} values are very comparable for each glass composition and appear to depend more on the glass composition than the type of alkali, with the following average values:

E_{ad} LAWC22 = 47 ±8 kJ mol^{-1} for LAWC22,
E_{ad} ORLEC28 = 74±3 kJ mol^{-1} for ORLEC28, and
E_{ad} IDF1B2 = 58±6 kJ mol^{-1} for IDF1B2.

It is not clear based on a comparison of the glass compositions why the value of E_{ad} is higher for ORLEC28 than for the other two glasses. Experimental results indicate that ORLEC28 is a more leach resistant glass and in long term leach tests [28] it is also the glass showing the least alteration to date.

5.5 Estimation of K_g for LAWC22, ORLEC28, and IDF1B2

As noted above, determination of K_g was not an objective of the present work and the test matrix was focused instead on ion exchange. However, the available data from the Pulsed-Flow tests were assessed to determine whether it was possible to estimate the K_g parameter from such test results. If so, this could provide a potential alternative test method for determination of this parameter. As described in Section 4.2.5, estimation of the K_g value requires a linear regression of the steady state NDR vs. $a[H_4SiO_4]$. This regression is conducted here using two parallel approaches: using NDR_B and using NDR_{Re}. In view of the limitation in using boron as a matrix dissolution indicator in the acidic region (discussed above), the NDR_B regressions systematically excluded the data at pH_T = 5.96 (pH_{RT} 7 at 70 °C). $[H_4SiO_4]$ activities were estimated using the code PHREEQC with solution input descriptions corresponding to the leachates from the tests. As observed with the SPFT test results, the data at pH_{RT} 11 did not comport to the trends expected according to Equation (1.1) and were therefore excluded from this analysis.

The results of regressions at the three experimental temperatures for both NDR_B and NDR_{Re} are given in Figures 5.16, 5.17 and 5.18 for LAWC22, ORLEC28, and IDF1B2, respectively. Plots of the NDR values for boron and rhenium as functions of orthosilicic acid activity and the various fitted equations are given in each figure.

K_g is the value of $a[H_4SiO_4]$ at a dissolution rate of zero (NDR = 0 for Q/K_g equal to one in Equation (1.1)). From the linear fits, six K_g values were calculated for each glass: at three temperatures, using NDR_B and NDR_{Re}.

Results of the above analysis, given in Table 5.5 and Figure 5.19, provide the data necessary to plot these estimated K_g values as a function of 1/T (K^{-1}) to estimate the value of K_g at the presumed repository temperature of 15ºC. As is evident from the Table 5.5, the various K_g values are very similar; a representative K_g value for all three glasses could be set at the average value of $K_g = (1.98 \pm 0.03) \times 10^{-3}$ mol L^{-1}. Since K_g reflects the variation of the reaction affinity with silicic acid activity, it is perhaps not unreasonable that the K_g values for relatively similar silicate glasses should be similar.

SECTION 6.0
MODELING OF PULSED-FLOW TEST DATA

The alkali ion exchange rate data obtained from Pulsed-Flow tests for all three glasses were analyzed according to the model described in Section 1.3. It should be noted that whereas the results described in Section 5 were obtained by assessing the variation of the ion exchange rates separately with respect to each of the independent variables (time, temperature, and pH), the results in this section were obtained by instead performing regression analysis of the entire data set against the models described in Section 1.3.

The analysis was performed using JMP Pro Version 15.0. For each alkali for each glass, the test matrix (10 time intervals, 5 pH values, and 3 temperatures) provides up to 150 data points for each case. However, this number was reduced somewhat by cases in which the rate subtraction yielded negative values or where the statistical analysis identified points as outliers. Whenever possible, which was the vast majority of the cases, the average of the ion exchange rates obtained by differences from Re and from Mo were used in the fit; in other cases only one or the other was used.

Two forms of the model described in Section 1.3 were used: one in which a square root of time dependence was used and another in which a power law in time was used in which the exponent was a fitted parameter (as opposed to being fixed at a value of -½). Thus, the data were analyzed according to Equation (1.6) and also according to Equation (1.8).

Data for three alkalis (Na, Li, Cs) were analyzed for LAWC22, three alkalis for ORLEC28 (Na, K, Cs), and two alkalis for IDF1B2 (Na, Cs). Thus, a total of 16 models were developed.

Table 6.1 presents the regression statistics, fitted parameters, and uncertainties in the fitted parameters for all alkalis and all three glasses for the square-root-of-time model in Equation (1.6). Predicted versus measured plots for each case are shown in Figures 6.1 – 6.8. Overall, these three-parameter fits of data sets containing between 103 and 145 points are very good. For sodium, the R^2 values are between 0.825 and 0.948; values for cesium are between 0.596 and 0.782, while the potassium and lithium values are 0.897 and 0.614, respectively. The lower values for cesium likely reflect the greater uncertainty in the data as a result of the very low cesium concentrations in the glass and therefore the leachates. The activation energies are consistent with the general range found in previous measurements on LAW glasses. However, the values are uniformly lower than the corresponding values obtained in Section 5 from analysis of the temperature dependence of the ion exchange rates at long times. The pH exponent α is reasonably consistent across all of the fits. The mean value across all fits is 0.205; the mean value for sodium is 0.194 and the mean value for cesium is 0.204; the values for potassium and lithium are 0.240 and 0.205, respectively.

Table 6.2 presents the regression statistics, fitted parameters, and uncertainties in the fitted parameters for all alkalis and all three glasses for the power-of-time model in Equation (1.8), where the time exponent is now a fitted parameter instead of being fixed at a value of ½. Predicted versus measured plots for each case are shown in Figures 6.9 – 6.16. Again, overall, these four-parameter fits of data sets containing between 103 and 145 points are very good. For sodium, the R^2 values are between 0.897 and 0.972; values for cesium are between 0.690 and 0.845, while the potassium and lithium values are 0.922 and 0.819, respectively. Again, the lower values for cesium likely reflect the greater uncertainty in the data as a result of the very low cesium concentrations in the glass and therefore the leachates. All of the fits with Equation (1.8) are slightly better than those obtained using Equation (1.6); this is still true when comparing the R^2_{adj} which is intended to account for the effect of the difference in the number of fitting parameters. However, the difference is not great. The activations energies are very close to those determined from the fits to Equation (1.6) and are consistent with the general range found in previous measurements on LAW glasses; the one exception is the value for lithium, which was low in the fit to Equation (1.6) and is lower by about a factor of two in the fit to Equation (1.8). The pH exponent α is reasonably consistent across all of the fits and in good agreement with the results from the fits to Equation (1.6). The mean value across all fits is 0.201; the mean value for sodium is 0.181 and the mean value for cesium is 0.202; the values for potassium and lithium are 0.238 and 0.219, respectively. The additional parameter γ is reasonably consistent across all of the fits. The mean value across all fits is 0.694; the mean value for sodium is 0.662 and the mean value for cesium is 0.620; the values for potassium and lithium are 0.596 and 1.110, respectively. Overall, therefore, the present data set suggest that the parameter γ may be slightly larger than ½, perhaps closer to 0.7. This deviation could be a reflection of departures from simple diffusion behavior such as the effects of concentration- and spatially dependent diffusion coefficients, which would not be unlikely in the altered glass reaction zone.

The results for lithium for LAWC22 are somewhat aberrant in that the activation energy is atypically low and the value of γ is higher than the values obtained for all the other cases. The reason for this is not yet clear.

Figures 6.17 and 6.18 show predicted versus measured plots for sodium for all three glasses for the fits to Equation (1.6) and (1.8), respectively. Figure 6.19 compares the predicted effects of temperature and pH on the sodium ion exchanges rates at 15 °C calculated from the fits to Equation (1.6).

SECTION 7.0
COMPARISON OF RESULTS, SUMMARY, AND CONCLUSIONS

The present work addressed the need for:

1) An improved methodology for including ion exchange in the model for ILAW corrosion; and

2) An improved method for measuring the relevant ion exchange parameters that is ideally more reliable, efficient, and cost effective than the present approach that employs the SPFT test.

Thus, this work focused on the alternative ion exchange modeling approach described in Section 1.3 and the use of the Pulsed-Flow test as a potential alternative to the SPFT test for determining ion exchange rate parameters. Ion exchange rates for selected LAW glasses were measured using the SPFT approach and compared with those obtained using the Pulsed-Flow test. The test conditions included variations in temperature, pH, and time in order to test the proposed alternative ion exchange model.

The glasses selected for this work were LAWC22, IDF1B2, and ORLEC28. Amongst the baseline glasses that have previously been subjected to SPFT testing, LAWC22 was selected for tests using both the SPFT test and the PFT methods because it has the highest measured ion exchange rate so far and contains both sodium and lithium. No sodium ion exchange rate could be measured on two other lithium containing glasses previously evaluated in SPFT (LAWB45, IDF7-E12). Amongst the enhanced high waste loading glasses that have previously been subjected to SPFT testing, IDF1B2 was selected because it has a high measured ion exchange rate and the highest sodium content; it has no lithium and very low potassium. Finally, ORLEC28 was selected because it contains high sodium and relatively high potassium.

The three selected glasses were fabricated to also include three spikes: Mo and Re as potential alternatives to boron as indicators of glass matrix dissolution and Cs to evaluate its ion exchange rate in comparison to other alkalis. An extensive set of leaching data was collected using two techniques:

1) The conventional SPFT experimental setup was used with a different set of test conditions that focused on determining the ion exchange rate as a function of time, temperature, and pH.

2) The Pulsed-Flow test method, which provides a simpler means of performing flow-through testing. The Pulsed-Flow tests used an identical set of pH and

silica saturation conditions as in those used in the SPFT tests and matches as closely as possible the average flow rate conditions.

The data that were collected were analyzed to extract the various model parameters with particular emphasis on ion exchange. In addition, the results from the two test methods were compared with each other and, where possible, with the results from previous work.

LAWC22 was tested using both the SPFT reduced matrix and the Pulsed-Flow test, and data are also available from previous standard SPFT testing. Table 7.1 shows that the SPFT results for k_0, E_a, and η compare very well to those obtained in previous work. Similarly, Table 7.2 shows that there is good agreement between the K_g values at 15 °C obtained from SPFT and Pulsed-Flow tests in the present work and the value from previous work. As shown in Table 7.3, for the ion exchange parameters r_{IEX} (15 °C) and E_{ad} for sodium, there is good agreement between the values obtained from SPFT and Pulsed-Flow tests in the present work and the values from previous work.

ORLEC28 and IDF1B2 were subjected to testing using only the Pulsed-Flow method. Table 7.4 shows that the K_g values at 15 °C for IDF1B2 obtained in the present work are in good agreement with the value from previous work. Conversely, for ORLEC28, the value from previous work is about an order of magnitude lower than the values obtained in the present work; it is worth noting, however, that the previously reported value was not well-determined by the data set [18]. Tables 7.5 and 7.6 show, for ORLEC28 and IDF1B2, respectively, the values of the ion exchange parameters r_{IEX} (15 °C) and E_{ad} for sodium obtained from Pulsed-Flow tests in the present work and the values from previous work. Again, there is good agreement between the respective values.

Table 7.7 compares the values of the ion exchange parameters r_{IEX} (15 °C) and E_{ad} for Na, Li, K, and Cs obtained from Pulsed-Flow tests and SPFT tests in the present work.

It is striking that the values of K_g values at 15 °C for all three glasses obtained from the Pulsed-Flow tests are very similar, as can be seen in Table 5.5; a representative K_g value for all three glasses could be set at the average value of $K_g = (2.0 \pm 0.03) \times 10^{-3}$ mol L^{-1}.

Overall, these results lead to the following key conclusions:

- The Pulsed-Flow test method provides results that are in good agreement with those from SPFT tests for all of the glasses tested. This method therefore provides a viable and more cost effective alternative to the SPFT method for deriving model parameters for ion exchange.

- The Pulsed-Flow method also provides values for K_g that agree well with those from SPFT testing. This is important in view of the fact that K_g is one of the more influential model parameters and a parameter that has previously been challenging to determine reliably by SPFT testing.

- The modified SPFT test matrix provides a reasonable basis for determination of the ion exchange rate parameters. This matrix is about half the size of the standard SPFT test matrix and should be considerably cheaper to execute. The present results show that the derived data are also useful for estimation of other model parameters (K_g, for example) .

The data are also in general accord with expectations based on the proposed ion exchange model described in Section 1.3:

- The measured ion exchanges rates follow the predicted linear dependence on the reciprocal of the square root of time reasonably well.
- The measured ion exchanges rates follow the predicted dependence on pH, with the logarithms of the ion exchange rates decreasing linearly as the pH increases.
- The measured ion exchanges rates follow the predicted Arrhenius dependence on temperature, with the logarithms of the ion exchange rates decreasing linearly with the reciprocal of the absolute temperature.
- Na, Li, K, and Cs all follow the above behavior reasonably well but with rate constants that depend on the alkali in the order Na > Li > K > Cs.

Based on these findings, the alkali ion exchange rate data obtained from Pulsed-Flow tests were subjected to regression analysis to extract the parameters of the model described in Section 1.3. It should be noted that whereas the results described above were obtained by assessing the variation of the ion exchange rates separately with respect to each of the independent variables (time, temperature, and pH), the following results were obtained by instead performing regression analysis of the entire data set against the models described in Section 1.3. The analysis was performed using JMP Pro Version 15.0.

Two forms of the model described in Section 1.3 were used: one in which a square root of time dependence was used and another in which a power law in time was used in which the exponent was a fitted parameter (as opposed to being fixed at a value of -½). Thus, the data were analyzed according to Equation (1.6) and also according to Equation (1.8). Data for three alkalis (Na, Li, Cs) were analyzed for LAWC22, three alkalis for ORLEC28 (Na, K, Cs), and two alkalis for IDF1B2 (Na, Cs). Thus, a total of 16 models were developed.

Overall, the three-parameter fits of Equation (1.6) to data sets containing between 103 and 145 points are very good. For sodium, the R^2 values are between 0.825 and 0.948; values for cesium are between 0.596 and 0.782, while the potassium and lithium values are 0.897 and 0.614, respectively. The lower values for cesium likely reflect the greater uncertainty in the data as a result of the very low cesium concentrations in the glass and therefore the leachates. The activations energies are consistent with the general range found in previous measurements on LAW glasses. However, the values are uniformly lower than the corresponding values obtained in Section 5 from analysis of the temperature dependence of the ion exchange rates at long times. The pH exponent α is reasonably consistent across all of the fits. The mean value across all fits is 0.205; the mean value for sodium is 0.194 and the mean value for cesium is 0.204; the values for potassium and lithium are 0.240 and 0.205, respectively.

Similarly, four-parameter fits of Equation (1.8) to the same data sets are also very good. For sodium, the R^2 values are between 0.897 and 0.972; values for cesium are between 0.690 and 0.845, while the potassium and lithium values are 0.922 and 0.819, respectively. Again, the lower values for cesium likely reflect the greater uncertainty in the data as a result of the very low cesium concentrations in the glass and therefore the leachates. All of the fits with Equation (1.8) are slightly better than those obtained using Equation (1.6); this is still true when comparing the R^2_{adj} which is intended to account for the effect of the difference in the number of fitting parameters. However, the difference is not great. The activation energies are very close to those determined from the fits to Equation (1.6) and are consistent with the general range found in previous measurements on LAW glasses; the one exception is the value for lithium, which was low in the fit to Equation (1.6) and is lower by about a factor of two in the fit to Equation (1.8). The pH exponent α is reasonably consistent across all of the fits and in good agreement with the results from the fits to Equation (1.6). The mean value across all fits is 0.201; the mean value for sodium is 0.181 and the mean value for cesium is 0.202; the values for potassium and lithium are 0.238 and 0.219, respectively. The additional parameter γ is reasonably consistent across all of the fits. The mean value across all fits is 0.694; the mean value for sodium is 0.662 and the mean value for cesium is 0.620; the values for potassium and lithium are 0.596 and 1.110, respectively. Overall, therefore, the present data set suggest that the parameter γ may be slightly larger than ½, perhaps closer to 0.7. This deviation could be a reflection of departures from simple diffusion behavior such as the effects of concentration- and spatially dependent diffusion coefficients, which would not be unlikely in the altered glass reaction zone.

The results for lithium for LAWC22 are somewhat aberrant in that the activation energy is atypically low and the value of γ is higher than the values obtained for all the other cases. The reason for this is not yet clear.

As in previous work, attempts were made to estimate the ion exchange rate by subtraction of the normalized boron dissolution rate from that of each of the alkalis; however, positive values were obtained only for sodium. As noted above, this approach assumes that boron is released solely by matrix dissolution whereas its release appears to follow diffusive kinetics. This issue was resolved by including spikes of rhenium and molybdenum, which provided excellent alternative indicators of matrix dissolution with results that were generally in very close agreement with each other. Similar observation in this regard were found in both the Pulse-Flow test data and the SPFT test data. Thus, while parameters were extracted using the conventional boron-based approach wherever possible as well as using the Mo- and Re-based approaches, the data indicate that the Mo/Re approach is to be preferred. Unlike boron, molybdate and perrhenate, which are the dominant Mo and Re species in the glass and which are isomorphous (and also isomorphous with sulfate and chromate), are insignificant participants in the glass matrix, instead residing interstitially [70-74]. They are relatively large and therefore diffusive release should be insignificant. Thus, their release relies upon the dissolution of the surrounding glass matrix. Both species form very soluble anions and can be spiked and analyzed reliably at low concentrations such that they do not participate significantly in secondary phase formation, particularly in the case of rhenium. Overall, therefore, we consider these species to be good candidates for alternative markers of matrix dissolution.

SECTION 8.0
QUALITY ASSURANCE

This work was conducted under a quality assurance (QA) program compliant with the applicable criteria of 10 CFR 830.120; the American Society of Mechanical Engineers (ASME) NQA-1-2008 including NQA-1a-2009 addenda; and DOE Order 414.1D, Quality Assurance. These QA requirements are implemented through a Quality Assurance Project Plan for WRPS work [75] that is conducted at VSL. Test and procedure requirements by which the testing activities are planned and controlled are also defined in that plan. The program is supported by VSL standard operating procedures were used for this work [76]. This is LAW work and is not subject to the requirements of DOE/RW-0333P, Office of Civilian Waste Management Quality Assurance Requirements and Description (QARD).

SECTION 9.0
REFERENCES

[1] "FY 2019 ILAW Glass Ion Exchange Rate Testing", C. Viragh, I.S. Muller, and I.L. Pegg, VSL-18T4620-1, Rev. 0, Vitreous State Laboratory, The Catholic University of America, Washington DC, 2/11/19.

[2] Request for Off-Site Services (Technical) Statement of Work, "ILAW Glass Durability Testing to Support IDF PA," Rev. 0, Requisition #314744, Washington River Protection Solutions, LLC (WRPS), 10/17/18.

[3] "Experimentally Determined Dissolution Kinetics of Na-rich Borosilicate Glasses at Far-From-Equilibrium Conditions: Implications for Transition State Theory," J.P. Icenhower, B.P. McGrail, W.J. Shaw, E.M. Pierce, P. Nachimuthu, D.K. Shuh, E.A. Rodriguez, and J.L. Steele, *Geochimica Cosmochimica Acta,* 72, 2767-2788 (2008).

[4] "Measurement of Kinetic Rate Law Parameters on a Na-Ca-Al Borosilicate Glass for Low-Activity Waste," B.P. McGrail, W.L. Ebert, A.J. Bakel, and D.K. Peeler, *J. Nucl. Mater.* 249, 175-189 (1997).

[5] "Low-Activity Waste Glass Studies: FY 2000 Summary Report," B.P. McGrail, J.P. Icenhower, P.F. Martin, D.R. Rector, H.T. Schaef, E.A. Rodriguez, and J.L. Steele, PNNL-13381, Pacific Northwest National Laboratory, Richland, WA (2000).

[6] "Waste Form Release Data Package for the 2001 Immobilized Low-Activity Waste Performance Assessment," B.P. McGrail, J.P. Icenhower, P.F. Martin, H.T. Schaef, M.J. O'Hara, E.A. Rodriguez, and J.L. Steele, PNNL-13043, Rev. 2, Pacific Northwest National Laboratory, Richland, WA (2001).

[7] "Laboratory Testing of Bulk Vitrified Low-Activity Waste Forms to Support the 2005 Integrated Disposal Facility Performance Assessment," E.M. Pierce, B.P. McGrail, L.M. Bagaasen, E.A. Rodriguez, D.M. Wellman, K.N. Geiszler, S.R. Baum, L.R. Reed, J.V. Crum, and H.T. Schaef, PNNL-15126, Rev. 2, Pacific Northwest National Laboratory, Richland, WA (2005).

[8] "Kinetic Rate Law Parameter Measurements on Borosilicate Waste Glass: Effect of Temperature, pH, and Solution Composition on Alkali Ion Exchange," E.M. Pierce, B.P. McGrail, J.P. Icenhower, E.A. Rodriguez, J.L. Steele, and S.R. Baum, *American Chemical Society Division of Environmental Chemistry*. American Chemical Society, Philadelphia, PA (2004).

[9] "Waste Form Release Data Package for the 2005 Integrated Disposal Facility Performance Assessment," E.M. Pierce, B.P. McGrail, E.A. Rodriguez, H.T. Schaef, K.P. Saripalli, R.J. Serne, K.M. Krupka, P.F. Martin, S.R. Baum, K.N. Geiszler, L.R. Reed, and W.J. Shaw, PNNL-14805, Pacific Northwest National Laboratory, Richland, WA (2004).

[10] "An Experimental Study of the Dissolution Rates of Simulated Aluminoborosilicate Waste Glasses as a Function of pH and Temperature under Dilute Conditions," E.M. Pierce, E.A. Rodriguez, L.J. Calligan, W.J. Shaw, and B.P. McGrail, *Applied Geochemistry,* 23, 2559-2573 (2008).

[11] "A Strategy to Conduct an Analysis of the Long-Term Performance of Low-Activity Waste Glass in a Shallow Subsurface Disposal System at Hanford," J.J. Neeway, E.M. Pierce, V.L. Freedman, J.V. Ryan, and N.P. Qafoku, PNNL-23503, Rev. 0, Pacific Northwest National Laboratory, Richland, WA (2014).

[12] "Immobilized Low-Activity Waste Glass Release Data Package for the Integrated Disposal Facility Performance Assessment," V.L. Freedman, J.V. Ryan, and D.H. Bacon, PNNL-24615, Draft, Pacific Northwest National Laboratory, Richland, WA, August 2015.

[13] "ILAW Glass Testing for Disposal at IDF: Phase 1 Testing," A.E. Papathanassiu, I.S. Muller, M. Brandys, K. Gilbo, A. Barkatt, I. Joseph and I.L. Pegg, Final Report, VSL-11R2270-1, Rev. 0, Vitreous State Laboratory, The Catholic University of America, Washington, DC, 6/6/11.

[14] "A Strategy to Conduct an Analysis of the Long-Term Performance of Low-Activity Waste Glass in a Shallow Subsurface Disposal System at Hanford," B.P. McGrail, W.L. Ebert, D.H. Bacon, and D.M. Strachan, PNNL-11834, Pacific Northwest National Laboratory, Richland, Washington, February 1998.

[15] "FY2016 ILAW Glass Testing for Disposal at IDF" A.E. Papathanassiu, C. Viragh, I.S. Muller, and I.L. Pegg, Final Report, VSL-17R3860-1, Rev. 0, Vitreous State Laboratory, The Catholic University of America, Washington, DC, 7/12/17.

[16] "FY2016 ILAW Glass Corrosion Testing with the Single-Pass Flow-Through Method," J.J. Neeway, B.D. Williams, R.M. Asmussen, I.I. Leavy, B.P. Parruzot, J.R. Stephenson, E.A. Cordova, E.M. McElroy, Final Report, PNNL-26169, RPT-IGTP-013, Rev. 0, Pacific Northwest Laboratory, Richland, WA, April 2017.

[17] "FY2017 ILAW Glass SPFT Testing for Disposal at IDF: Glass IDF21-EC14," C. Viragh, H. Abramowitz, I.S. Muller, A.E. Papathanassiu, and I.L. Pegg, Final Report, VSL-17R4320-1, Rev. 0, Vitreous State Laboratory, The Catholic University of America, Washington DC, 2/27/18.

[18] "FY2017 ILAW Glass Corrosion Testing with the Single-Pass Flow-Through Method," J.J. Neeway et al., Final Report, PNNL-27098, RPT-IGTP-015, Rev. 0.0, Pacific Northwest Laboratory, Richland, WA, February 2018.

[19] "FY2018 ILAW Glass SPFT Testing for Disposal at IDF: Glasses ORLEC46 and ORLEC52," C. Viragh, H. Abramowitz, I.S. Muller, A.E. Papathanassiu, and I.L. Pegg, Final Report, VSL-18R4510-2, Rev. 0, Vitreous State Laboratory, The Catholic University of America, Washington DC, 12/26/18.

[20] "The Activated Complex in Chemical Reactions," H. Eyring, *J. Chem. Phys.* **3**, 107-114 (1935).

[21] "Thermodynamic and Kinetic Constraints on Reaction Rates among Minerals and Aqueous Solutions. I. Theoretical Considerations," P. Åagaard and H.C. Helgeson, *Am. J. Sci.,* 282, 237-285 (1982).

[22] "A General Rate Equation for Nuclear Waste Glass Corrosion," B. Grambow, *Material Research Symposium Proceedings,* 44, 15-27 (1985).

[23] "Kinetic Ion Exchange Salt Effects on Glass Leaching," X. Feng and I.L. Pegg, *Energy, Environment and Information Management*, Eds. H. Wang, S. Chang, and H. Lee, Argonne, IL, p. 7-9, (1992).

[24] "Effects of Salt Solutions on Glass Dissolution," X. Feng and I.L. Pegg, *Phys. Chem. Glasses*, 35, 1 (1994).

[25] "A Glass Dissolution Model for the Effects of S/V on Leachate pH," X. Feng and I.L. Pegg, J. *Non-Cryst. Solids*, 175, 281 (1994).

[26] "Survey of Literature on the Role of Ion Exchange in Glass Corrosion," A.E. Papathanassiu, W. Gong, W. Lutze, and I.L. Pegg, Final Report, VSL-17L4320-1, Rev. 0, Vitreous State Laboratory, The Catholic University of America, Washington DC, 8/2/17.

[27] "A Critical Review of Ion Exchange in Nuclear Waste Glasses to Support the Immobilized Low-Activity Waste Integrated Disposal Facility Rate Model," C.E. Lonergan, PNNL-26594, RPT-IGTP-018, Rev 0.0, Pacific Northwest Laboratory, Richland, WA, August 2017.

[28] "FY2019 Long-Term PCT of ILAW Glasses", I.S. Muller, and I.L. Pegg, VSL-19R4620-1, Rev. 0, Vitreous State Laboratory, The Catholic University of America, Washington, DC, 9/30/19.

[29] "Dissolution and Precipitation Kinetics of Sheet Silicates," K.L. Nagy, *Silicate Mineral Dissolution*. Mineralogical Society of America, Washington, DC (2001).

[30] "Letter: Simultaneous Precipitation Kinetics of Kaolinite and Gibbsite at 80°C and pH 3," K.L. Nagy, and A.C. Lasaga, Geochimica et Cosmochimica Acta, 57, 4329 – 4335 (1993).

[31] "Preliminary Results of Durability Testing with Borosilicate Glass Compositions," M. Adel-Hadadi, R. Adiga, Aa. Barkatt, X. Feng, I.L. Pegg, et al., Tech. Info. Center, Office of Sci. and Tech. Info., USDOE, DOE/NE/44139-34, (1988).

[32] "Compositional Effects on Chemical Durability and Viscosity of Nuclear Waste Glasses – Systematic Studies and Structural Thermodynamic Models," X. Feng, Ph.D. Thesis, The Catholic University of America (1988).

[33] "Leach Rate Excursions in Borosilicate Glasses: Effects of Glass and Leachant Composition," Aa. Barkatt, S.A. Olszowka, W. Sousanpour, M.A. Adel-Hadadi, R. Adiga, Al. Barkatt, G.S. Marbury, and S. Li, Mat. Res. Soc. Symp. Proc., 212, 65 (1991).

[34] "Alteration Layers on Glasses After Long-Term Leaching," A.C. Buechele, S.T.- Lai, and I.L. Pegg, *Ceramic Transactions*, Eds. D.K. Peeler and J.C. Marra, vol. 87, p. 423, American Ceramic Society (1998).

[35] "Compositional Effects on the Long-Term Durability of Nuclear Waste Glasses: A Statistical Approach," S. Ribet, I.S. Muller, I.L. Pegg, S. Gin, and P. Frugier, Mat. Res. Soc. Symp. Proc. Vol. 824 (2004).

[36] "Characterization of Alteration Phases on HLW Glasses after 15 Years of PCT Leaching," I.S. Muller, S. Ribet, I.L. Pegg, S. Gin, and P. Frugier, *Ceramic Transactions*, Vol. 176 (2005).

[37] "The Long-Term Corrosion and Modeling of Two Simulated Belgian Reference High-Level Waste Glasses – Part II," J. Patyn, P. Van Iseghem, and W. Timmermans, Mat. Res. Symp. Soc. Proc., 176, 299 (1990).

[38] "New Insight into the Residual Rate of Borosilicate Glasses: Effect of S/V and Glass Composition", S. Gin, P. Frugier, P. Jollivet, F. Bruguier, E. Curti, Int. J. Appl. Glass Sci., 4 (4), 371-382 (2013).

[39] "Nuclear Glass Durability: New Insight into Alteration Layer Properties," S. Gin, C. Guittonneau, N. Godon, D. Neff, D. Rebiscoul, M. CabieS. Mostefaoui, J. Phys. Chem. C 115 (38), 18696-18706, (2011).

[40] "An International Initiative on Long-Term Behavior of High-Level Nuclear Waste Glass," S. Gin, A. Abdelouas, L.J. Criscenti, W.L. Ebert, K. Ferrand, T. Geisler, M.T. Harrison, *et al.*, Mater. Today 16, 243–248 (2013).

[41] "Origin and Consequences of Silicate Glass Passivation by Surface Layers", S. Gin, P. Jollivet, M. Fournier, F. Angeli, P. Frugier, T. Charpentier, Nat. Commun., 6 (2015).

[42] "The Fate of Silicon During Glass Corrosion Under Alkaline Conditions: A Mechanistic and Kinetic Study with the International Simple Glass," S. Gin, P. Jollivet, M. Fournier, C. Berthon, Z. Wang, A. Mitroshkov, Z. Zhu, J. V. Ryan, Geochim. Cosmochim. Acta, 151, 68–85 (2015).

[43] "Resumption of Nuclear Glass Alteration: State of the art," M. Fournier, S. Gin, P. Frugier, J. Nucl. Mater., 448, 348–363 (2014).

[44] "Open Scientific Questions About Nuclear Glass Corrosion," S. Gin, Procedia Materials Science, 163-171 (2014).

[45] "Current Understanding and Remaining Challenges in Modeling Long-Term Degradation of Borosilicate Nuclear Waste Glasses," J.D. Vienna, J.V. Ryan, S. Gin, and Y. Inagaki, Int. J. Appl. Glass Sci., 4, 283–294 (2013).

[46] "Contribution of Atom-Probe Tomography to a Better Understanding of Glass Alteration Mechanisms: Application to a Nuclear Glass Specimen Altered 25 years in a Granitic Environment," S. Gin, J.V. Ryan, D.K. Schreiber, J. Neeway, and M. Cabie, Chem. Geol. 349, 99–109 (2013).

[47] "Effect of Composition on the Short-Term and Long-Term Dissolution Rates of Ten Borosilicate Glasses of Increasing Complexity from 3 to 30 oxides", S. Gin, X. Beaudoux, F. Angeli, C. Jegou, N. Godon, J. Non-Cryst. Solids, 358, 2559–2570 (2012).

[48] "Development of the Vitrification Compositional Envelope to Support Complex-Wide Application of MAWS Technology," I.S. Muller, H. Gan, A.C. Buechele, S.T. Lai, and I.L. Pegg, DOE/CH-9601, September 1996.

[49] "Alteration Phases on High Sodium Waste Glasses after Short- and Long-Term Hydration," A.C. Buechele, S.-T. Lai, and I.L. Pegg, *Ceramic Transactions*, vol. 107, p. 251 (2000).

[50] "FY15 ILAW Glass Testing for Disposal at IDF", I.S. Muller, and I.L. Pegg, VSL-15R3790-1, Rev. 0, Vitreous State Laboratory, The Catholic University of America, Washington, DC, 4/15/16.

[51] "Low-Activity Waste Glass Release Calculations for the Integrated Disposal Facility Performance Assessment," R. Arthur, C. Cheng, B. Paris, RPP-CALC-61031, Rev. 0, Intera, Inc. for Washington River Protection Solutions, LLC, Richland, WA, May 2, 2017.

[52] "The Ion Exchange Phase in Corrosion of Nuclear Waste Glasses," M.I. Ojovan, A. Pankov, and W.E. Lee, J. Nucl. Mater., 358, 57-68 (2006).

[53] "SON 68 Nuclear Glass Dissolution Kinetics: Current State of Knowledge and Basis of the New GRAAL Model," P. Frugier, S. Gin, Y. Minet, T. Chave, B. Bonin, N. Godon, J.E. Lartigue, P. Jollivet, A. Ayral, L. De Windt, and G. Santarini, J. Nucl. Materials, 380, 8-21 (2008).

[54] "Application of the GRAAL Model to Leaching Experiments with SON 68 Nuclear Glass in Initially Pure Water," P. Frugier, T. Chave, S. Gin, and J.E. Lartigue, J. Nucl. Materials, 392, 552-567 (2009).

[55] "Interdiffusion of Alkali and Hydronium Ions in Glass: Partial Ionization," R.H. Doremus, J. Non-Cryst. Solids, 48, 431 (1982).

[56] "Selection of ILAW Glasses for FY 2019 Ion Exchange Testing," Vitreous State Laboratory, The Catholic University of America, Washington, DC, 12/4/18.

[57] "FY2018 Long-Perm PCT of ILAW Glasses", I.S. Muller, and I.L. Pegg, VSL-18R4510-1, Rev. 0, Vitreous State Laboratory, The Catholic University of America, Washington, DC, 12/19/18.

[58] "LAW Container Centerline Cooling Data" RPP-WTP Memorandum, L. Petkus to C. Musick, CCN# 074181, 10/16/03.

[59] "Round Robin Testing of a Reference Glass for Low-Activity Waste Forms," W.L. Ebert and S.F. Wolf, Department of Energy Report ANL-99/22, Argonne National Laboratory, Argonne, IL (1999).

[60] "Characterization of the Defense Waste Processing Facility (DWPF) Environmental Assessment (EA) Glass Standard Reference Material," C.M. Jantzen, N.E. Bibler, D.C. Beam, C.L. Crawford, and M.A. Pickett, WSRC-TR-92-346, Westinghouse Savannah River Company, Aiken, SC, June, 1993.

[61] "Standard Practice for Measurement of the Glass Dissolution Rate Using the Single-Pass Flow-Through Test Method," ASTM Standard C 1662-10.

[62] "Permeability of PEEK to Carbon Dioxide," Journal of Applied Polymer Science, F. De Candia and V. Vittoria, 51, 2103 (1994).

[63] Data from IDX Health and Science (formerly Upchurch Scientific) 2009-2010 Catalogue, p. 75.

[64] "Evaluation of the Single-Pass Flow Through Test to Support a Low-Activity Waste Specification," B.P. McGrail and D.K. Peeler, Final Report, PNNL-10746, Pacific Northwest Laboratory, Richland, WA, 1995.

[65] "Leach Rate Excursions in Borosilicate Glasses: Effects of Glass and Leachant Composition," Aa. Barkatt, S.A. Olszowka, W. Sousanpour, M.A. Adel-Hadadi, R. Adiga, Al. Barkatt, G.S. Marbury, and S. Li, Mat. Res. Soc. Symp. Proc, 65, vol. 212 (1991).

[66] Material Recovery & Waste Form Development, 2015 Accomplishments Report, FCRD-MRWFD-2016-000001, INL/EXT-15-37053, p.113 (2015).

[67] "Self Diffusion of ^{22}Na and ^{137}Cs in Simulated Nuclear Waste Glass," K. Nonaka. H. Nakajima, S. Mitsui, and J. Echigoya, Mater. Trans, 43, 654-659 (2002).

[68] "Low-Temperature Lithium Diffusion in Simulated High-Level Boroaluminosilicate Nuclear Waste Glasses," J.J. Neeway, S. Kerisit, S. Gin, Z. Wang, Z. Zhu, and J.V. Ryan, J. Non-Cryst. Solids, 405, 83-90 (2014).

[69] ''Probing Alkali Coordination Environments in Alkali Borate Glasses by Multinuclear Magnetic Resonance", V. K. Michaelis, P. M. Aguiar, and S. Kroeker, J. Non-Cryst. Solids, 353, 2582–90 (2007).

[70] "Dissimilar Behavior of Technetium and Rhenium in Borosilicate Waste Glass as Determined by X-Ray Absorption Spectroscopy," W.W. Lukens, D.A. McKeown, A.C. Buechele, I.S. Muller, D.K. Shuh, and I.L. Pegg, Chem. Mater., 19, 559 (2007).

[71] "Tc and Re Behavior in Waste Glass Vapor Hydration Tests," D.A. McKeown, A.C. Buechele, W.W. Lukens, D.K. Shuh, and I.L. Pegg, Environ. Sci. Technol., 41, 431 (2007).

[72] "Raman Studies of Technetium in Borosilicate Waste Glass," D.A. McKeown, A.C. Buechele, W.W. Lukens, I.S. Muller, D.K. Shuh, and I.L. Pegg, Radiochimica Acta, 95, 275 (2007).

[73] "Tc and Re Behavior in Borosilicate Waste Glass Vapor Hydration Tests II," A.C. Buechele, D.A. McKeown, W.W. Lukens, D.K. Shuh, and I.L. Pegg, J. Nuclear Materials, 429, 159 (2012).

[74] "X-ray Absorption and Raman Spectroscopy Studies of Molybdenum Environments in Borosilicate Waste Glasses," D.A. McKeown, H. Gan, and I.L. Pegg, J. Nucl. Mater., 488, 143 (2017).

[75] "Quality Assurance Project Plan for WRPS Support Activities Conducted by VSL," VSL-QAPP-WRPS, Rev. 5, Vitreous State Laboratory, The Catholic University of America, Washington, DC, 9/30/19.

[76] "Master List of Controlled VSL Manuals and Standard Operating Procedures in Use," QA-MLCP, Rev. 171, Vitreous State Laboratory, The Catholic University of America, Washington, DC, 12/13/19.

Table 2.1. Summary of Kinetic Parameters Determined from SPFT Testing on LAW Glasses [19].

Glass Name	k_0 g-glass m^{-2} d^{-1}	η	Eα kJ mol^{-1}	K_g (15°C)[a] mol L^{-1}	r_{IEX} (15°C)* mol m^{-2} s^{-1}	Source
ORLEC46	$2.9x10^4$	0.39±0.06	58±3	(1.2×10^{-3})	1.4×10^{-10} **	VSL-18R4510-2
ORLEC52	$2.0x10^6$	0.43±0.04	72±4	(5.7×10^{-4})	2.6×10^{-11} **	VSL-18R4510-2
ORLEC28	$2.7x10^6$	0.55±0.02	79±2	(1.3×10^{-4})	2.7×10^{-11} **	PNNL-27098, Rev 0
ORLEC33	$3.8x10^6$	0.56±0.02	81±2	(1.1×10^{-4})	3.3×10^{-11} **	PNNL-27098, Rev 0
ORLEC14	$2.7x10^6$	0.48±0.04	76±2	(6.75×10^{-4})	7.4×10^{-11} **	VSL-17R4320-1, Rev. 0
IDF18-A161	$5.9x10^6$	0.28±0.06	61±6	(2.3×10^{-4})	7.6×10^{-11}	PNNL-26169, Rev 0
ORPLG9	$2.5x10^8$	0.36±0.07	81±7	(log K_g = 100)	5.3×10^{-11}	PNNL-26169, Rev. 0
IDF7-E12	$5.7x10^4$	0.32±0.03	55±5	$1.87x10^{-3}$	$<1x10^{-10}$	VSL-17R3860-1, Rev. 0
LAWA44	$1.3x10^4$	0.49±0.08	60±7	$1.87x10^{-3}$ ***	$5.3x10^{-11}$	PNNL-24615, Rev. 0
LAWB45	$1.6x10^4$	0.34±0.03	53±3	$1.79x10^{-3}$ ***	0	PNNL-24615, Rev. 0
LAWC22	$1.0x10^5$	0.42±0.02	64±2	$1.80x10^{-3}$ ***	1.2×10^{-10}	PNNL-24615, , Rev. 0
					1.28×10^{-11} **	Corrected value
IDF1B2	$4.6x10^4$	0.49±0.05	64±4	$1.70x10^{-3}$	3.4×10^{-10}	VSL-11R2270-1, Rev. 0
					6.21×10^{-11} **	Corrected value
LAWABP1	$3.4x10^6$	0.35±0.03	68±3	$4.90x10^{-4}$	$3.4x10^{-11}$	PNNL-24615, Rev. 0

* As-reported values; uncorrected except where indicated (see [27]).
** Corrected value, see [27].
*** Corrected value, see [13].
[a] Questionable values are shown in parentheses - Glass dissolution data do not agree with the kinetic rate law.

Table 2.2. Alkali Content and Species Used to Monitor Matrix Dissolution in Three LAW Glasses.

	Glass ID, wt%	**LAWC22**	**ORLEC28**	**IDF1B2**	**Notes**
Composition (wt%)	Na_2O	14.40	22.11	25.00	Alkali species undergoing ion exchange
	K_2O	0.08	3.36	0.12	
	Li_2O	2.50	0	0	
	Cs_2O	0.15	0.15	0.15	
	B_2O_3	10.05	10.00	7.30	Species used to monitor matrix dissolution
	MoO_3	0.10	0.10	0.10	
	Re_2O_7	0.10	0.10	0.10	
Composition (mol%)	Na_2O	14.88	24.52	27.35	Alkali species undergoing ion exchange
	K_2O	0.05	2.46	0.09	
	Li_2O	5.36	0	0	
	Cs_2O	0.04	0.04	0.04	
	B_2O_3	9.25	9.87	7.11	Species used to monitor matrix dissolution
	MoO_3	0.04	0.04	0.04	
	Re_2O_7	0.02	0.02	0.02	
IX Measurements	**Na IX (mol m^{-2} s^{-1})**	1.28×10^{-11}	2.70×10^{-11}	6.31×10^{-11}	Only "corrected" basis [27] is used herein
	Reference	PNNL-14805, 2004 [9]	PNNL-27098, 2018 [18]	VSL-11R2270-1, 2011 [13]	-
	Technique Used in this report	Pulsed Flow Test and SPFT Test	Pulsed Flow Test	Pulsed Flow Test	-

Table 2.3. Target and Analyzed Compositions (wt%) of Glasses Selected for Ion-Exchange Testing.

Glass ID	**LAWC22**	**LAWC22IX**	**LAWC22IX CCC**	**IDF1B2**	**IDF1B2IX**	**IDF1B2IX CCC**	**ORLEC28**	**ORLEC28IX**	**ORLEC28IX CCC**
	Target	Analyzed*	Analyzed*	Target	Analyzed*	Analyzed*	Target	Analyzed*	Analyzed*
Al_2O_3	6.07	6.02	6.08	10.00	10.05	9.89	10.00	10.00	9.99
B_2O_3	10.05	9.77	9.78	7.30	7.44	6.84	10.00	9.59	9.64
CaO	5.11	5.18	5.25	1.10	1.13	1.14	1.95	1.98	1.97
Cr_2O_3	0.01	0.02	0.02	0.52	0.59	0.66	0.44	0.40	0.43
Cs_2O	0.15	0.15	0.16	0.15	0.15	0.17	0.15	0.14	**0.15**
Fe_2O_3	5.42	5.74	5.83	1.10	1.18	1.30	0.60	0.71	0.69
K_2O	0.08	0.10	0.10	0.12	0.11	0.12	3.36	3.17	3.24
Li_2O	2.50	2.54	2.57	0.00	0.00	0.00	0.00	0.03	0.03
MgO	1.51	1.52	1.51	1.10	1.15	1.13	1.00	1.02	1.06
MoO_3	0.10	0.09	0.08	0.10	0.07	0.08	0.10	0.07	0.08
Na_2O	14.40	13.56	13.70	25.00	25.47	24.65	22.11	21.96	22.03
NiO	0.03	0.04	0.03	0.04	0.05	0.05	0.01	0.01	0.01
PbO	0.01	0.01	0.01	0.00	0.00	0.00	0.01	0.01	0.01
SiO_2	46.64	47.15	46.74	39.85	39.79	39.92	37.41	38.09	37.66
SnO_2	0.00	0.00	0.00	1.08	0.93	1.02	2.33	1.89	2.13
TiO_2	1.14	1.28	1.26	0.00	0.04	0.04	0.60	0.67	0.63
V_2O_5	0.00	0.00	0.00	2.00	2.06	2.12	0.00	0.00	0.00
ZnO	3.07	2.96	3.04	3.65	3.51	3.67	3.00	2.93	2.87
ZrO_2	3.03	2.96	3.05	5.44	5.30	5.59	6.03	5.97	6.01
Cl	0.05	0.05	0.05	0.11	0.09	0.10	0.20	0.16	0.16
F	0.14	0.14$	0.14$	0.49	0.49$	0.49$	0.08	0.08$	0.08$
P_2O_5	0.07	0.07	0.08	0.23	0.24	0.24	0.12	0.14	0.13
SO_3	0.32	0.32	0.28	0.52	0.47	0.49	0.40	0.41	0.39
Re_2O_7	0.10	0.14	**0.12**	0.10	0.14	**0.14**	0.10	0.13	**0.12**
Total	100.0	99.8	99.9	100.0	100.5	99.9	100.0	99.6	99.5

*Analyzed by XRF except for boron and lithium, which were measured by DCP-AES
$ Target concentration

Table 3.1. Comparison of SPFT and Pulsed-Flow Test Matrix.

Temperature [°C]	Single Pass Flow-Through Test (cell volume 61 ml)									Pulsed-Flow Test (cell volume 50 ml)						
	$[Si]_{in}$	F	pH	m_g	S	S/V	RT	Flow	q/S	m_g	S	S/V	RT	Sampling Interval	Flow	q/S
	[*ppm*]	[*µl/min*]		[*g*]	m^2	m^{-1}	(days)	cc/day	10^{-8} m/sec	[*g*]	m^2	m^{-1}	(days)	(days)	cc/day	10^{-8} m/sec
23	35	7	7	4.0	0.080	1311	6.1	10	0.15	3.278	0.066	1311	6.0	3	8.3	0.15
	40	7	8	4.0	0.080	1311	6.1	10	0.15	3.278	0.066	1311	6.0	3	8.3	0.15
	52.5	7	9	4.0	0.080	1311	6.1	10	0.15	3.278	0.066	1311	6.0	3	8.3	0.15
	90	7	10	2.0	0.040	656	6.1	10	0.29	1.639	0.033	656	6.0	3	8.3	0.29
	230	7	11	2.0	0.040	656	6.1	10	0.29	1.639	0.033	656	6.0	3	8.3	0.29
40	40	7	7	2.0	0.040	656	6.1	10	0.292	1.650	0.033	660	6.0	3	8.3	0.292
	45	7	8	2.0	0.040	656	6.1	10	0.292	1.650	0.033	660	6.0	3	8.3	0.292
	60	7	9	2.0	0.040	656	6.1	10	0.292	1.650	0.033	660	6.0	3	8.3	0.292
	105	7	10	1.0	0.020	328	6.1	10	0.583	0.826	0.017	330	6.0	3	8.3	0.584
	270	7	11	1.0	0.020	328	6.1	10	0.583	0.826	0.017	330	6.0	3	8.3	0.584
70	55	35	7	1.55	0.031	508	1.2	50	1.88	0.770	0.015	308	2.0	1	25.0	1.88
	60	35	8	1.55	0.031	508	1.2	50	1.88	0.770	0.015	308	2.0	1	25.0	1.88
	80	35	9	1.55	0.031	508	1.2	50	1.88	0.770	0.015	308	2.0	1	25.0	1.88
	140	35	10	1.00	0.020	328	1.2	50	2.92	0.495	0.010	198	2.0	1	25.0	2.92
	360	35	11	1.00	0.020	328	1.2	50	2.92	0.495	0.010	198	2.0	1	25.0	2.92

Table 3.2. Baseline Matrix for SPFT Testing in Dilute Solutions.

Temp [°C]	Train # "*i*"	Duration [*d*]	Dt_{samp} [*d*]	# Samples "*N*"	$[Si]_{in}$ [*ppm*]	F [*μl/min*]	pH	m_g [*g*]
1	*2*	*3*	*4*	*5*	*6*	*7*	*8*	*9*
23	1	30	3.0	10	0	7.0	7	1.00
	2	30	3.0	10	0	7.0	8	1.00
	3	30	3.0	10	0	7.0	9	1.00
	4	30	3.0	10	0	7.0	10	0.50
	5	30	3.0	10	0	7.0	11	0.50
40	1	20	2.0	10	0	28.0	7	1.00
	2	20	2.0	10	0	28.0	8	1.00
	3	20	2.0	10	0	28.0	9	1.00
	4	20	2.0	10	0	28.0	10	0.50
	5	20	2.0	10	0	28.0	11	0.50
70	1	10	1	10	0	35	7	1.00
	2	10	1	10	0	35	8	1.00
	3	10	1	10	0	35	9	1.00
	4	10	1	10	0	35	10	0.50
	5	10	1	10	0	35	11	0.50

Table 3.3. Measured *in Situ* pH (pH_T) of Influent Solutions.

Buffer	**$pH_{23°C}$**	**$pH_{40°C}$**	**$pH_{70°C}$**
Tris – HNO_3	**7.0**	6.6	6.0
Tris – HNO_3	**8.0**	7.6	6.9
Tris – HNO_3	**9.0**	8.6	8.0
Piperidine	**10.0**	9.6	9.0
Piperidine	**11.0**	10.7	10.0
LiOH/LiCl	**10.0**	9.6	9.0
LiOH/LiCl	**11.0**	10.7	10.0

Table 4.1. Measured SPFT Glass Dissolution Rates for LAWC22 Glass Alteration Under Dilute Conditions.

Target pH_{RT}	T (°C)	Rate ($g\text{-}glass\ m^{-2}\ d^{-1}$)
7	70	0.0524±0.002
8	70	0.0124±0.0003
9	**70**	**0.0466±0.0012**[a]
10	70	0.1334±0.0022
11	70	0.2454±0.0102
7	40	0.00181±0.00025
8	40	0.00054±0.00005
9	**40**	**0.00593±0.00012**
10	40	0.02437±0.00021
11	40	0.05287±0.0044
7	23	0.00038±0.00005
8	23	0.00033±0.00003
9	**23**	**0.0013±0.00002**
10	23	0.00532±0.00004
11	23	0.00905±0.00098

[a]In bold: Dissolution rates at pH_{RT} 9.

Table 4.2a. Value of the Kinetic Parameter η for Glass LAWC22 from SPFT Tests.

Temperature (°C)	η
70	0.4293
40	0.4649
23	0.4933
Average	0.463
Standard Deviation	0.032

Table 4.2b. Values of the Kinetic Parameters E_a and k_0 for Glass LAWC22 from SPFT Tests.

Parameter	Value
k_0	2.0 x 10^5 g-glass $m^{-2}d^{-1}$
E_a	69±11 kJ mol^{-1}

Table 4.3. Dissolution Rates[(a)] (average at steady-state) of the glass based on B, Li, K, Na, Cs, Mo, and Re from SPFT Tests with LAWC22 at 70 °C, 40 °C, and 23 °C, and standard deviation[(b)].

Temperature	$[Si]_{in}$	pH_T	NDR_B, g-glass m^{-2} d^{-1}	NDR_{Li}, g-glass m^{-2} d^{-1}	NDR_{Na}, g-glass m^{-2} d^{-1}	NDR_K, g-glass m^{-2} d^{-1}	NDR_{Mo}, g-glass m^{-2} d^{-1}	NDR_{Cs}, g-glass m^{-2} d^{-1}	NDR_{Re}, g-glass m^{-2} d^{-1}
70°C	55	5.96	0.0546±0.0022	0.0284±0.0011	0.0528±0.0019	0.0327±0.0015	0.0567±0.0495	0.0465±0.009	0.0115±0.0027
	60	6.91	0.0154±0.0008	0.0144±0.0008	0.0159±0.001	0.0123±0.0009	0.0236±0.0021	0.0146±0.0008	0.0061±0.0006
	80	7.98	0.0068±0.0001	0.0086±0.0002	0.0096±0.0002	0.023±0.0035	0.013±0.0001	0.0073±0.0003	0.0073±0.0002
	140	8.98	0.0030±0.0004	0.0063±0.0008	0.0074±0.0009	-0.0152±0.002	0.0041±0.0005	0.003±0.0002	0.0029±0.0002
	360	9.96	0±0	0.0015±0.0002	0.0048±0.0002	-0.1172±0.0029	0.001±0.00005	0.00099±0.00009	0.00054±0.00007
40°C	40	6.63	0.0022±0.00008	0.00199±0.00014	0.00259±0.00014	0.00215±0.00035	0.0004±0.00009	0.00136±0.0002	0.00103±0.00018
	45	7.61	0.00095±0.00007	0.00141±0.00013	0.00159±0.00014	0.0011±0.00095	0.00063±0.00006	0.00073±0.00005	0.00075±0.00008
	60	8.63	0.00078±0.00007	0.00122±0.0001	0.00139±0.00011	0.00217±0.00049	0.00054±0.00005	0.00046±0.00003	0.00052±0.00004
	105	9.63	0.00079±0.00012	0.00139±0.00016	0.00159±0.0002	0.00206±0.00142	0.00092±0.00008	0.00072±0.00005	0.00079±0.00008
	270	10.67	0.0021±0.00025	0.00239±0.00024	0.00298±0.00027	0.0036±0.00244	0.00227±0.0003	0.00145±0.00015	0.00178±0.00026
23°C	35	7	0.00046±0.00004	0.00069±0.00006	0.00068±0.00006	0.00159±0.0003	0.00014±0.00001	0.00029±0.00001	0.00027±0.00003
	40	8	0.00029±0.00003	0.00050±0.00005	0.00054±0.00006	0.000336±0.0003	0.00017±0.00002	0.00021±0.00001	0.00027±0.00002
	52.5	9	0.00023±0.00002	0.00040±0.00004	0.00047±0.00004	0.00107±0.0004	0.00019±0.00001	0.00017±0.00001	0.00019±0.00002
	90	10	0.00029±0.00003	0.00045±0.00004	0.00056±0.00005	0.00037±0.00022	0.00031±0.00002	0.00022±0.00001	0.00026±0.00002
	230	11	0.0010±0.00002	0.00108±0.00002	0.00130±0.00005	0.00274±0.00211	0.00114±0.00003	0.00066±0.00003	0.0009±0.000005

(a) In the rate unit, "g" represents the mass of glass dissolved based on the indicated species as described in section 3.7.

(b) The standard deviation of average calculated at steady-date. Data that precede the attainment of steady-state conditions are excluded before calculating mean and standard deviation of the remainder. The relative standard deviation (the standard deviation divided by the mean) of the calculated steady state concentration must be less than 0.15 for the test results to be valid.

Table 4.4. Alkali Ion Exchange Rates (in mol m^{-2} s^{-1})[(a)] from SPFT Tests Performed on LAWC22.

Method			Boron Based			Mo&Re Based		
pH_{RT}	pH_T	$[Si]_{in}$	$r_{IEX\ Na\text{-}B}$, mol m^{-2} s^{-1}	$r_{IEX\ Li\text{-}B}$, mol m^{-2} s^{-1}	$r_{IEX\ Cs\text{-}B}$, mol m^{-2} s^{-1}	$r_{IEX\ Na\text{-}Mo\&Re}$, mol m^{-2} s^{-1}	$r_{IEX\ Li\text{-}Mo\&Re}$, mol m^{-2} s^{-1}	$r_{IEX\ Cs\text{-}Mo\&Re}$, mol m^{-2} s^{-1}
70°C Experiments								
7	5.96	55	Not reportable	Not reportable	Not reportable	2.221E-09	3.262E-10	4.318E-12
8	6.91	60	2.731E-11	Not reportable	Not reportable	5.227E-10	1.592E-10	1.037E-12
9	7.98	80	1.503E-10	3.318E-11	7.279E-14	1.277E-10	2.510E-11	2.187E-14
10	8.98	140	2.340E-10	6.256E-11	1.795E-14	2.409E-10	5.288E-11	1.441E-14
11	9.96	360	2.555E-10	2.880E-11	1.216E-13	2.267E-10	1.230E-11	5.548E-14
40°C Experiments								
7	6.63	40	2.213E-11	Not reportable	Not reportable	1.005E-10	2.455E-11	7.860E-14
8	7.61	45	3.426E-11	8.734E-12	Not reportable	4.830E-11	1.377E-11	1.247E-14
9	8.63	60	3.309E-11	8.498E-12	Not reportable	4.646E-11	1.329E-11	Not reportable
10	9.63	105	4.300E-11	1.156E-11	Not reportable	3.981E-11	1.042E-11	Not reportable
11	10.67	270	4.836E-11	5.989E-12	Not reportable	5.151E-11	7.118E-12	Not reportable
23°C Experiments								
7	7	35	1.171E-11	4.470E-12	Not reportable	2.534E-11	9.359E-12	1.062E-14
8	8	40	1.337E-11	4.025E-12	Not reportable	1.897E-11	6.033E-12	4.950E-15
9	9	52.5	1.270E-11	3.319E-12	Not reportable	1.488E-11	4.100E-12	Not reportable
10	10	90	1.457E-11	3.051E-12	Not reportable	1.495E-11	3.189E-12	Not reportable
11	11	230	1.635E-11	1.476E-12	Not reportable	1.489E-11	2.771E-12	Not reportable

[(a)] "mol" in the r_{iex} units means moles of the indicated alkali metal released by ion exchange.

Table 4.5. Ion Exchange Activation Energies and Extrapolated Rate Constants Determined for LAWC22 by SPFT Test.

Method	E_{ad}, kJ/mol		r_{IEX} (15 °C), mol m^{-2} s^{-1}	
	All pH	pH 9	All pH	pH 9
Na-Mo&Re	56 ±7 (47)*	38 ± 6	8.7×10^{-12}	1.1×10^{-11}
Na-B	40 ± 7	44 ± 1	8.9×10^{-12}	7.6×10^{-12}
Li-Mo&Re	46 ± 10	31 ± 10	2.7×10^{-12}	3.5×10^{-12}
Li-B	46 ± 5	41 ± 1	1.8×10^{-12}	2.1×10^{-12}
Cs-Mo&Re	56 ± 28	Not reportable	3.6×10^{-15}	Not reportable

* For the value given in parentheses the lowest pH measurement at 70 °C has been omitted.

Table 5.1. Dissolution Rates[(a)] of the glass based on B, Li, K, Na, Cs, Mo, and Re from Pulsed-Flow Tests with LAWC22 at 70 °C, 40 °C, and 23 °C.

Temperature	$[Si]_{in}$	pH_T	NDR_B, g-glass m^{-2} d^{-1}	NDR_{Li}, g-glass m^{-2} d^{-1}	NDR_{Na}, g-glass m^{-2} d^{-1}	NDR_K, g-glass m^{-2} d^{-1}	NDR_{Mo}, g-glass m^{-2} d^{-1}	NDR_{Cs}, g-glass m^{-2} d^{-1}	NDR_{Re}, g-glass m^{-2} d^{-1}
70°C	55	5.96	0.0509±0.0036[(b)]	0.0287±0.0025	0.0484±0.0043	0.0044±0.0022	0.0023±0.0002	0.03±0.0041	0.0082±0.0013
	60	6.91	0.015±0.0008	0.0133±0.0006	0.0152±0.001	<DL	0.0042±0.0005	0.0136±0.0007	0.0059±0.0005
	80	7.98	0.0069±0.0003	0.0081±0.0003	0.0092±0.0004	<DL	0.0069±0.0013	0.0068±0.0014	0.0068±0.0017
	140	8.98	0.0015±0.0002	0.0045±0.001	0.011±0.0015	<DL	0.0027±0.0009	0.0028±0.0007	0.0018±0.0002
	360	9.96	-0.0015±0.0002	0.0009±0.0003	0.0043±0.0006	0.0566±0.006	0.0010±0.0001	0.0012±0.0001	0.0006±0.0001
40°C	40	6.63	0.00305±0.00009	0.0023±0.00007	0.00314±0.00016	0.00426±0.00072	0.00037±0.00003	0.00216±0.00074	0.00102±0.00007
	45	7.61	0.00096±0.00007	0.00081±0.0001	0.0014±0.00011	0.00119±0.001	0.00061±0.00008	0.0008±0.00006	0.00083±0.00024
	60	8.63	0.00074±0.00003	0.00072±0.00009	0.00115±0.00012	0.0017±0.00057	0.00070±0.00006	0.00070±0.00004	0.00079±0.00025
	105	9.63	0.00053±0.00011	0.00027±0.00016	0.0018±0.0002	<DL	0.00126±0.00065	0.00082±0.00013	0.00077±0.00031
	270	10.67	0.00159±0.00008	0.00106±0.00013	0.00056±0.00015	0.01468±0.0108	0.00224±0.00011	0.00182±0.00018	0.00207±0.00064
23°C	35	7	0.00134±0.00141	0.00172±0.00139	0.0016±0.00126	0.00746±0.00495	0.00100±0.00015	0.00061±0.0002	0.00114±0.00122
	40	8	0.00031±0.00011	0.00073±0.00015	0.00073±0.00013	<DL	0.00017±0.00006	0.00037±0.00009	0.00035±0.00004
	52.5	9	0.00021±0.00008	0.00064±0.00011	0.00067±0.00009	0.00093±0.00057	0.00021±0.00008	0.0003±0.00004	0.0003±0.00006
	90	10	0.00022±0.00009	0.00064±0.00014	0.00073±0.0001	<DL	0.00024±0.00009	0.00037±0.00008	0.00035±0.00003
	230	11	0.00160±0.00136	0.00215±0.0013	0.00209±0.0015	0.01976±0.05874	0.00228±0.00171	0.00143±0.00126	0.00177±0.00104

(a) In the rate unit, "g-glass" represents the mass of glass dissolved based on the indicated species as described in Section 3.7.
(b) The average of the last two to four points is generally calculated with a standard deviation given.

Table 5.2. Dissolution Rates of B, Li, K, Na, Cs, Mo, and Re from Pulsed-Flow Tests with ORLEC28 at 70 °C, 40 °C, and 23 °C.

Temperature	$[Si]_{in}$	pH_T	NDR_B, g-glass m^{-2} d^{-1}	NDR_{Na}, g-glass m^{-2} d^{-1}	NDR_K, g-glass m^{-2} d^{-1}	NDR_{Mo}, g-glass m^{-2} d^{-1}	NDR_{Cs}, g-glass m^{-2} d^{-1}	NDR_{Re}, g-glass m^{-2} d^{-1}
70°C	55	5.96	0.3000±0.0070	0.2994±0.0145	0.2804±0.027	0.0045±0.0012	0.1135±0.0302	0.0099±0.0021
	60	6.91	0.1516±0.0070	0.1557±0.0147	0.1220±0.0115	0.0042±0.0006	0.0444±0.0083	0.0014±0.0062
	80	7.98	0.0865±0.0057	0.0935±0.0021	0.0537±0.0042	0.0040±0.0008	0.0171±0.0001	0.0037±0.0002
	140	8.98	0.0510±0.0035	0.0543±0.0024	0.0231±0.002	0.0013±0.0003	0.0084±0.0016	0.0011±0.0001
	360	9.96	0.0229±0.0019	0.0287±0.0028	0.0142±0.0016	0.0011±0.0002	0.0081±0.0018	0.0011±0.0004
40°C	40	6.63	0.02011±0.00062	0.02015±0.00087	0.01702±0.0008	0.00088±0.00004	0.00796±0.00051	0.00295±0.00016
	45	7.61	0.00871±0.00017	0.00881±0.00034	0.00682±0.00034	0.00064±0.00006	0.00278±0.00032	0.00123±0.00020
	60	8.63	0.00403±0.00020	0.00467±0.00031	0.00262±0.00009	0.00052±0.00003	0.0012±0.00008	0.00076±0.00005
	105	9.63	0.00257±0.00008	0.00392±0.00019	0.00146±0.00011	0.00033±0.00004	0.0008±0.00002	0.00049±0.00003
	270	10.67	0.00047±0.00008	0.00104±0.00013	0.00108±0.00002	0.00048±0.00010	0.00065±0.00008	0.00035±0.00008
23°C	35	7	0.00279±0.00087	0.00342±0.00083	0.00248±0.00061	0.00029±0.00013	0.00138±0.00034	0.0009±0.00031
	40	8	0.00108±0.00032	0.00213±0.00036	0.00026±0.00156	0.00009±0.00007	0.00065±0.00015	0.00035±0.00015
	52.5	9	0.00050±0.00018	0.00163±0.00026	0.00071±0.00004	0.00004±0.00005	0.00041±0.00008	0.00021±0.00009
	90	10	0.00011±0.00009	0.00146±0.00022	0.00064±0.0001	0.000004±0.00001	0.00046±0.0001	0.00014±0.00011
	230	11	<DL	0.00101±0.00017	0.00084±0.00004	0.00009±0.00011	0.00043±0.00014	0.00026±0.00006

*The average of the last two to four points is generally calculated with a standard deviation given.

Table 5.3. Dissolution Rates of B, Li, K, Na, Cs, Mo, and Re from Pulsed-Flow Tests with IDF1B2 at 70 °C, 40 °C, and 23 °C.

Temperature	$[Si]_{in}$	pH_T	NDR_B, g-glass m^{-2} d^{-1}	NDR_{Na}, g-glass m^{-2} d^{-1}	NDR_K, g-glass m^{-2} d^{-1}	NDR_{Mo}, g-glass m^{-2} d^{-1}	NDR_{Cs}, g-glass m^{-2} d^{-1}	NDR_{Re}, g-glass m^{-2} d^{-1}
70°C	55	5.96	0.1657±0.0124	0.1694±0.0085	0.1170±0.0248	0.0207±0.0031	0.0515±0.010	0.0212±0.0021
	60	6.91	0.0841±0.0064	0.1027±0.012	0.0225±0.0098	0.0171±0.0036	0.0177±0.0018	0.0135±0.0043
	80	7.98	0.0432±0.0041	0.0598±0.0059	<DL	0.0087±0.0010	0.0076±0.0008	0.0072±0.0011
	140	8.98	0.0270±0.0025	0.0388±0.0034	<DL	0.0019±0.0000	0.0039±0.0007	0.0017±0.0000
	360	9.96	0.0103±0.0010	0.0238±0.0033	<DL	0.0009±0.0003	0.0032±0.0004	0.0006±0.0001
40°C	40	6.63	0.00833±0.00032	0.01248±0.00087	0.00025±0.00002	0.00331±0.00045	0.00253±0.00020	0.0028±0.00029
	45	7.61	0.00397±0.00016	0.00861±0.00077	<BL	0.00158±0.00006	0.00113±0.00005	0.00132±0.00007
	60	8.63	0.00153±0.00010	0.00564±0.00007	<BL	0.00073±0.00002	0.00068±0.00001	0.00072±0.00001
	105	9.63	0.00109±0.0000	0.00471±0.00023	<BL	0.0005±0.00008	0.00051±0.00003	0.00042±0.00002
	270	10.67	<BL	0.00202±0.00012	<BL	0.00047±0.00005	0.00053±0.00002	0.00032±0.00002
23°C	35	7	0.00251±0.00124	0.00755±0.00087	0.00012±0.00005	0.00214±0.00146	0.00164±0.00097	0.00174±0.00104
	40	8	0.00081±0.00036	0.00408±0.00083	0.00001±0.00001	0.00020±0.00037	0.00046±0.00035	0.00036±0.00025
	52.5	9	0.00036±0.00015	0.00279±0.00027	0.00003±0.00002	0.00009±0.00005	0.00029±0.00005	0.00021±0.00005
	90	10	0.00022±0.00011	0.00264±0.00041	<BL	0.00005±0.00006	0.00037±0.00005	0.00019±0.00004
	230	11	<BL	0.0017±0.00029	<BL	0.00009±0.00008	0.00028±0.00005	0.00017±0.00005

*The average of the last two to four points is generally calculated with a standard deviation given.
DL – Detection limit

Table 5.4. Alkali Ion Exchange Rates at saturation (in mol m^{-2} s^{-1})[(a)] from All Pulse-Flow Tests Performed on LAWC22, ORLEC28, and IDF1B2.

Glass ID			LAWC22			ORLEC28			IDF1B2	
pH_{RT}	pH_T	$[Si]_{in}$	$r_{IEX\ Na}$, mol m^{-2} s^{-1}	$r_{IEX\ Li}$, mol m^{-2} s^{-1}	$r_{IEX\ Cs}$,* mol m^{-2} s^{-1}	$r_{IEX\ Na}$, mol m^{-2} s^{-1}	$r_{IEX\ K}$, mol m^{-2} s^{-1}	$r_{IEX\ Cs}$, * mol m^{-2} s^{-1}	$r_{IEX\ Na}$, mol m^{-2} s^{-1}	$r_{IEX\ Cs}$, [(b)] mol m^{-2} s^{-1}
70°C Experiments										
7	5.96	55	2.51E-09	4.81E-10	3.13E-12	2.37E-08	2.26E-09	1.29E-11	1.44E-08	3.78E-12
8	6.91	60	5.41E-10	1.57E-10	9.82E-13	1.27E-08	1.02E-09	1.41E-12	7.75E-09	2.88E-13
9	7.98	80	1.24E-10	2.36E-11	2.46E-13	7.15E-09	4.79E-10	1.75E-12	4.84E-09	1.56E-13
10	8.98	140	4.57E-10	3.84E-11	1.15E-13	4.32E-09	1.91E-10	7.28E-13	3.40E-09	2.26E-13
11	9.96	360	1.87E-10	6.56E-12	4.19E-14	2.20E-09	1.22E-10	6.89E-13	2.10E-09	3.16E-13
40°C Experiments										
7	6.63	40	1.32E-10	3.10E-11	5.47E-13	1.51E-09	1.27E-10	2.77E-12	9.30E-10	Non reportable
8	7.61	45	3.96E-11	3.49E-12	1.55E-13	6.57E-10	4.77E-11	8.66E-13	6.47E-10	Non reportable
9	8.63	60	2.49E-11	2.02E-12	1.98E-13	3.33E-10	1.62E-11	2.60E-13	4.49E-10	Non reportable
10	9.63	105	5.73E-11	Non reportable	1.54E-13	2.80E-10	8.91E-12	1.03E-13	3.90E-10	1.13E-14
11	10.67	270	Not reportable	Non reportable	9.42E-14	4.93E-11	5.35E-12	7.56E-14	1.47E-10	2.59E-14
23°C Experiments										
7	7	35	2.74E-11	1.24E-11	1.77E-13	2.33E-10	1.53E-11	1.63E-14	4.41E-10	Non reportable
8	8	40	2.56E-11	8.60E-12	7.52E-14	1.67E-10	7.85E-12	6.57E-14	3.73E-10	1.26E-14
9	9	52.5	2.22E-11	6.73E-12	8.95E-14	1.25E-10	4.30E-12	3.70E-14	2.55E-10	9.56E-15
10	10	90	2.33E-11	Non reportable	7.35E-14	1.20E-10	4.52E-12	6.69E-14	2.43E-10	2.28E-14
11	11	230	Non reportable	Non reportable	Non reportable	7.75E-11	5.76E-12	4.55E-14	1.50E-10	1.34E-14

(a) "mol" in the r_{iex} units means moles of the indicated alkali metal released by ion exchange.

(b) At 40°C, r_{IEX} Cs was calculated by difference to Re when Mo data was not reportable.

Table 5.5. Regressions Results to Evaluate K_g from Pulsed-Flow Test Data for LAWC22, ORLEC28, and IDF1B2.

	Temperature	NDR element	Slope	Intercept	K_g (mol L^{-1})
LAWC22	**70°C Linear fit**	B	-0.0109	0.0377	3.46 x 10^{-3}
		Re	-0.0037	0.0152	4.11 x 10^{-3}
	40°C Linear fit	B	-0.0008	0.0022	2.75 x 10^{-3}
		Re	-0.0004	0.0015	3.75 x 10^{-3}
	23°C Linear fit	B	-0.0015	0.0029	1.93 x 10^{-3}
		Re	-0.0012	0.0024	2.00 x 10^{-3}
	15°C extrapolation	LAWC22 K_g based on NDR_B			**1.81** x 10^{-3}
		LAWC22 K_g based on NDR_{Re}			**2.00** x 10^{-3}
LAWC22 average K_g = 1.90 x 10^{-3}					
ORLEC28	**70°C Linear fit**	B	-0.081	0.3181	**3.93** x 10^{-3}
		Re	-0.0039	0.0140	**3.59** x 10^{-3}
	40°C Linear fit	B	-0.0156	0.0330	**2.12** x 10^{-3}
		Re	-0.0042	0.0084	**2.00** x 10^{-3}
	23°C Linear fit	B	-0.0010	0.0031	**3.10** x 10^{-3}
		Re	-0.0012	0.0022	**1.83** x 10^{-3}
	15°C extrapolation	ORLEC28 K_g based on NDR_B			**2.42** x 10^{-3}
		ORLEC28 K_g based on NDR_{Re}			**1.48** x 10^{-3}
ORLEC28 average K_g = 1.95 x 10^{-3}					
IDF1B2	**70°C Linear fit**	B	-0.0458	0.1770	**3.86** x 10^{-3}
		Re	-0.0125	0.0428	**3.42** x 10^{-3}
	40°C Linear fit	B	-0.0078	0.0162	**2.08** x 10^{-3}
		Re	-0.0041	0.0083	**2.02** x 10^{-3}
	23°C Linear fit	B	-0.0008	0.0025	**3.13** x 10^{-3}
		Re	-0.0024	0.0045	**1.88** x 10^{-3}
	15°C extrapolation	IDF1B2 K_g based on NDR_B			**2.44** x 10^{-3}
		IDF1B2 K_g based on NDR_{Re}			**1.55** x 10^{-3}
IDF1B2 average K_g = 2.00 x 10^{-3}					

Table 6.1. Summary of Regression Statistics and Model Parameters; Uncertainties in Parentheses.

Glass ID	**ORLEC28**	**ORLEC28**	**ORLEC28**	**IDF1B2**	**IDF1B2**	**LAWC22**	**LAWC22**	**LAWC22**
Element	K	**Na**	Cs	Cs	**Na**	**Na**	Cs	Li
R^2	0.897	0.921	0.782	0.596	0.948	0.825	0.603	0.614
R^2_{Adj}	0.895	0.920	0.779	0.589	0.948	0.822	0.595	0.608
Root Mean Square Error	0.25	0.19	0.32	0.43	0.12	0.24	0.45	0.35
Mean of Response (Log_{10} $\boldsymbol{r_{IEX}}$)	-9.74	-8.49	-11.95	-12.61	-8.40	-9.40	-12.70	-10.03
Number of Observations	135	140	132	114	145	135	103	131
Model Terms: Log (r_{IEX}) = A + (B/T) + C× pH - (1/2)*log(t)								
A (Intercept)	0.916 (0.35)	1.31 (0.27)	-3.14 (0.46)	-4.90 (0.63)	-0.999 (0.16)	-1.72 (0.33)	-4.92 (0.72)	-4.56 (0.49)
B (1/Temp, K)	-2732 (117)	-2525 (89)	-2258 (152)	-2110 (214)	-1893 (52)	-2022 (108)	-1720 (223)	-1188 (162)
C (pH)	-0.240 (0.015)	-0.215 (0.012)	-0.197 (0.019)	-0.120 (0.029)	-0.168 (0.007)	-0.158 (0.015)	-0.296 (0.034)	-0.205 (0.022)
Parameters in Equation 1.6:								
Log (k_{d0}, mol m^{-2} $s^{-1/2}$)	3.69 (0.35)	4.08 (0.20)	-0.37 (0.46)	-2.13 (0.63)	1.77 (0.16)	1.07 (0.33)	-2.15 (0.72)	-1.79 (0.49)
E_{ad}, kJ	52.3 (2.2)	48.3 (1.7)	43.2 (2.9)	40.4 (4.1)	38.7 (1.0)	38.7 (2.1)	32.9 (4.3)	22.7 (3.1)
α	0.240 (0.015)	0.215 (0.012)	0.197 (0.019)	0.120 (0.029)	0.210 (0.007)	0.158 (0.015)	0.296 (0.034)	0.205 (0.022)

Table 6.2. Summary of Regression Statistics and Model Parameters; Uncertainties in Parentheses.

Glass ID	**ORLEC28**	**ORLEC28**	**ORLEC28**	**IDF1B2**	**IDF1B2**	**LAWC22**	**LAWC22**	**LAWC22**
Element	K	**Na**	Cs	Cs	**Na**	**Na**	Cs	Li
R^2	0.922	0.944	0.845	0.709	0.972	0.897	0.690	0.819
R^2_{Adj}	0.921	0.943	0.842	0.701	0.971	0.895	0.681	0.815
Root Mean Square Error	0.25	0.19	0.32	0.43	0.11	0.22	0.45	0.30
Mean of Response (Log_{10} $\boldsymbol{r_{IEX}}$)	-10.26	-8.99	-12.47	-13.11	-8.899	-9.890	-13.19	-10.50
Number of Observations	135	140	132	114	145	135	103	131
Model Terms: Log (r_{IEX}) = A + (B/T) + C× pH + D*log(t)								
A (Intercept)	0.654 (0.42)	1.063 (0.32)	-3.726 (0.55)	-5.749 (0.75)	-1.402 (0.17)	-2.466 (0.37)	-4.241 (0.88)	-6.065 (0.46)
B (1/Temp, K)	-2620 (153)	-2421 (116)	-2009 (198)	-1753 (274)	-1725 (62)	-1692 (312)	-1995 (300)	-494 (166)
C (pH)	-0.238 (0.015)	-0.215 (0.012)	-0.196 (0.019)	-0.110 (0.029)	-0.167 (0.006)	-0.162 (0.014)	-0.299 (0.034)	-0.219 (0.019)
D (log(t))	-0.596 (0.086)	-0.582 (0.059)	-0.711 (0.109)	-0.866 (0.180)	-0.641 (0.031)	-0.764 (0.067)	-0.283 (0.159)	-1.110 (0.083)
Parameters in Equation 1.8:								
Log (k_{d0}, mol m^{-2} $s^{-1/2}$)	3.42 (0.42)	3.83 (0.32)	-0.96 (0.55)	-2.98 (0.75)	1.37 (0.17)	0.30 (0.37)	-1.47 (0.88)	-3.30 (0.46)
E_{ad}, kJ	50.2 (2.9)	46.3 (2.2)	38.5 (3.8)	33.6 (5.2)	33.0 (1.2)	32.4 (2.5)	38.2 (5.8)	9.5 (3.2)
α	0.238 (0.015)	0.215 (0.012)	0.196 (0.019)	0.110 (0.029)	0.167 (0.006)	0.162 (0.014)	0.299 (0.034)	0.219 (0.019)
γ	0.596 (0.086)	0.582 (0.059)	0.711 (0.109)	0.866 (0.180)	0.641 (0.031)	0.764 (0.067)	0.283 (0.159)	1.110 (0.083)

Table 7.1. Values of the Kinetic Parameters k_0, E_a, and η for Glass LAWC22 from SPFT Tests and Comparison to Previous Work.

Parameter	This Work SPFT, Three Temperatures	Reference [9] SPFT, Four Temperatures
k_0	2.0×10^5 $gm^{-2}d^{-1}$	1.0×10^5 $gm^{-2}d^{-1}$
E_a	69±11 kJ mol^{-1}	64±2 kJ mol^{-1}
η	0.46±0.03	0.42±0.02

Table 7.2. Values of the Parameter K_g (mol L^{-1}) at 15 °C for Glass LAWC22 from SPFT Tests and Pulsed-Flow Tests and Comparison to Previous Work.

Basis	This Work		Reference [9], Corrected per [13] SPFT
	SPFT	Pulsed-Flow	
Based on NDR_B	1.74×10^{-3}	1.81×10^{-3}	1.8×10^{-3}
Based on NDR_{Re}	1.69×10^{-3}	2.00×10^{-3}	-

Table 7.3. Values of the Parameters r_{IEX} (mol m^{-2} s^{-1}) for Sodium at 15 °C and E_{ad} (kJ mol^{-1}) for Glass LAWC22 from SPFT Tests and Pulsed-Flow Tests and Comparison to Previous Work.

Parameter	This Work		Reference [9], Corrected per [27] SPFT
	SPFT	Pulsed-Flow	
$r_{IEX\ Na}$	8.7×10^{-12}	1.16×10^{-11}	1.28×10^{-11}
E_{ad}	56 ±7 (47)*	53 ± 7	45± 4

* For the value given in parenthesis the lowest pH measurement at 70 °C has been omitted.

Table 7.4. Values of the Parameter K_g (mol L^{-1}) at 15 °C for Glasses ORLEC28 and IDF1B2 from Pulsed-Flow Tests and Comparison to Previous SPFT Results.

Glass	This Work, Pulsed-Flow		Previous Work, SPFT Based on NDR_B
	Based on NDR_B	Based on NDR_{Re}	
ORLEC28	2.42 x 10^{-3}	1.48 x 10^{-3}	(1.3 x 10^{-4}) [18]
IDF1B2	2.44 x 10^{-3}	1.55 x 10^{-3}	1.7 x 10^{-3} [13]

Parentheses indicate a value that was not well determined by the data

Table 7.5. Values of the Parameters r_{IEX} (mol m^{-2} s^{-1}) for Sodium at 15 °C and E_{ad} (kJ mol^{-1}) for Glass OLEC28 from Pulsed-Flow Tests and Comparison to Previous Work.

Parameter	This Work, Pulsed-Flow	Reference [18], Corrected per [27] SPFT
r_{IEX}	4.6 × 10^{-11}	2.7 x 10^{-11}
E_{ad}	73 ±8	Not reported

Table 7.6. Values of the Parameters r_{IEX} (mol m^{-2} s^{-1}) for Sodium at 15 °C and E_{ad} (kJ mol^{-1}) for Glass IDF1B2 from Pulsed-Flow Tests and Comparison to Previous Work.

Parameter	This Work, Pulsed-Flow	Reference [13], Corrected per [27] SPFT
r_{IEX}	1.1 ×10^{-10}	6.2 x 10^{-11}
E_{ad}	55 ± 6	58 ± 3

Table 7.7. Comparison of Activation Energies and Extrapolated Ion Exchange Rates Determined for Three Glasses by SPFT Test and Pulsed-Flow Test.

Method	Element	Glass ID	E_{ad} kJ/mol	r_{IEX} (15 °C) mol m^{-2} s^{-1}
			All pH	All pH
SPFT (Mo&Re)	Na	LAWC22	56 ±7 (47)*	8.7×10^{-12}
PFT (Mo&Re)	Na	LAWC22	53 ± 7	1.2×10^{-11}
PFT (Mo&Re)	Na	ORLEC28	73 ± 8	4.6×10^{-11}
PFT (Mo&Re)	Na	IDF1B2	55 ± 6	1.1×10^{-10}
SPFT (Mo&Re and B)	Li	LAWC22	46 ± 10	2.7×10^{-12}
PFT (Mo&Re)	Li	LAWC22	37 ± 12	3.7×10^{-12}
PFT (Mo&Re)	K	ORLEC28	78 ± 9	2.5×10^{-12}
SPFT (Mo&Re)	Cs	LAWC22	56 ± 28	3.6×10^{-15}
PFT (Mo&Re)	Cs	LAWC22	50 ± 12	5.4×10^{-15}
PFT (Mo&Re)	Cs	ORLEC28	71 ± 9	1.7×10^{-14}
PFT (Mo&Re)	Cs	IDF1B2	62 ± 8	6.3×10^{-15}

*Lowest pH measurement at 70 °C has been omitted for this value in parentheses.

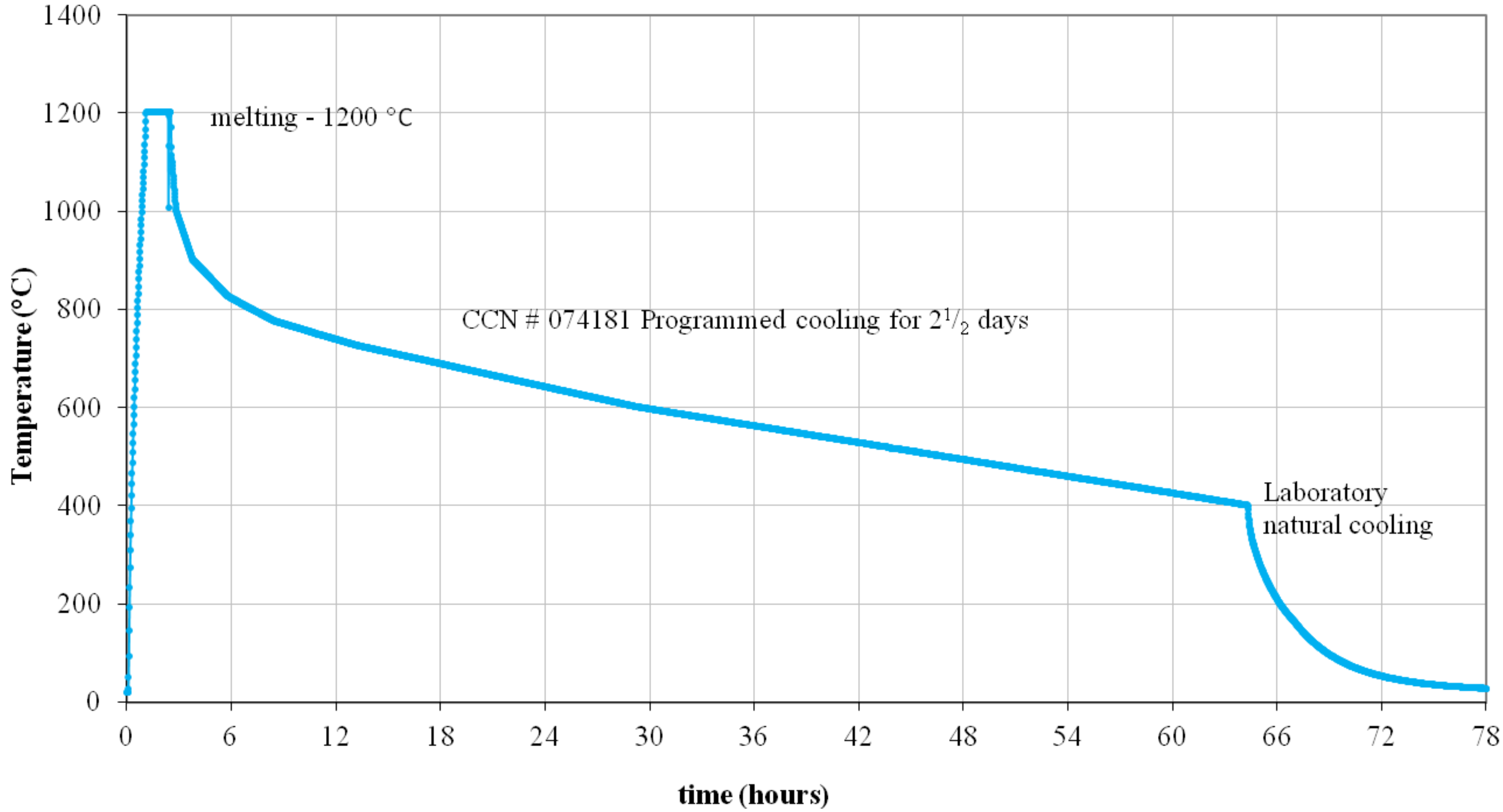

Figure 2.1. CCC profile recorded in the preparation of LAWC22IXCCC.

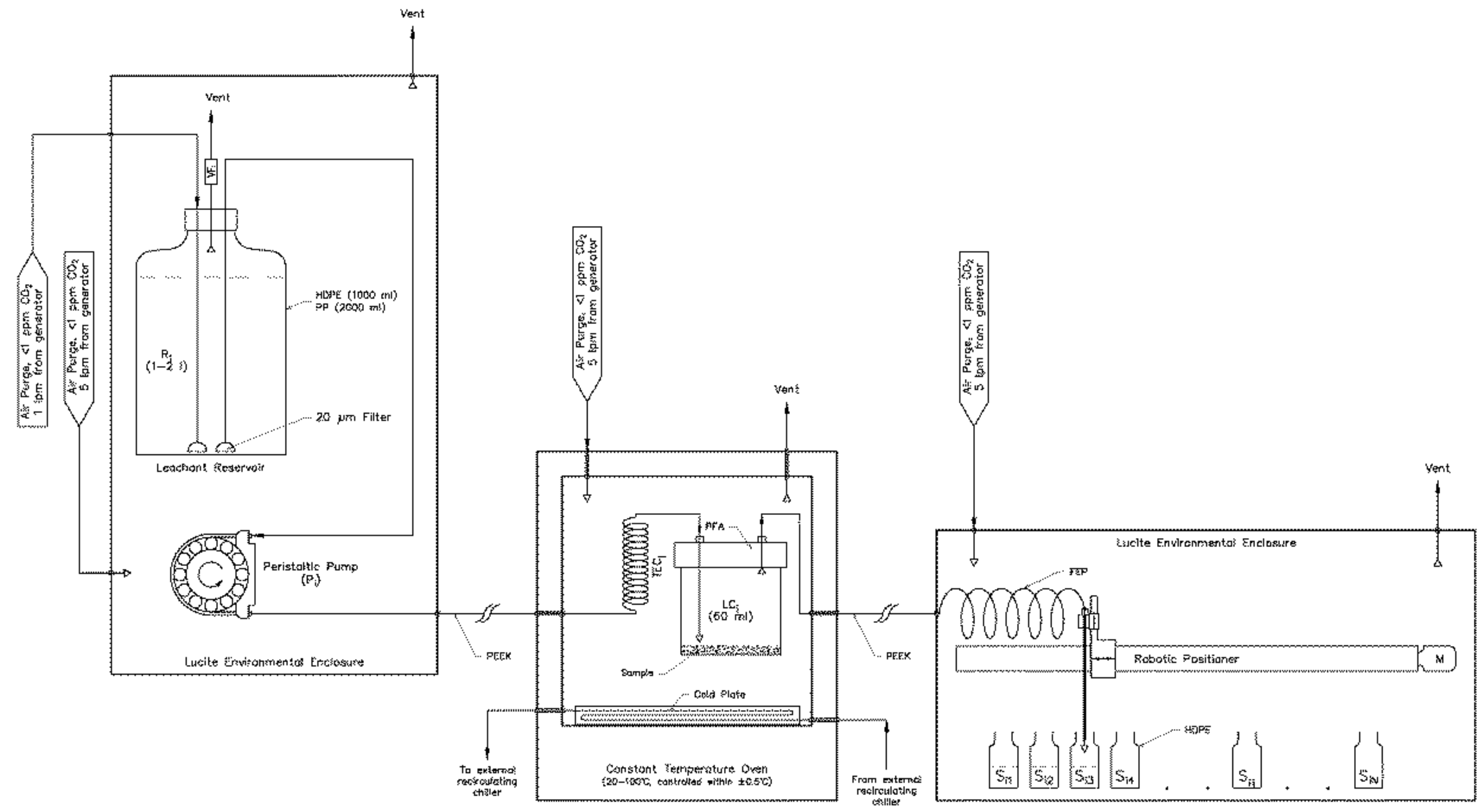

Figure 3.1. Schematic diagram showing a single testing train of the SPFT test setup. The actual setup consists of two 6-line peristaltic pumps enabling 12 testing trains to run simultaneously at one flow rate or 6 + 6 trains at two different flow rates. See text for description.

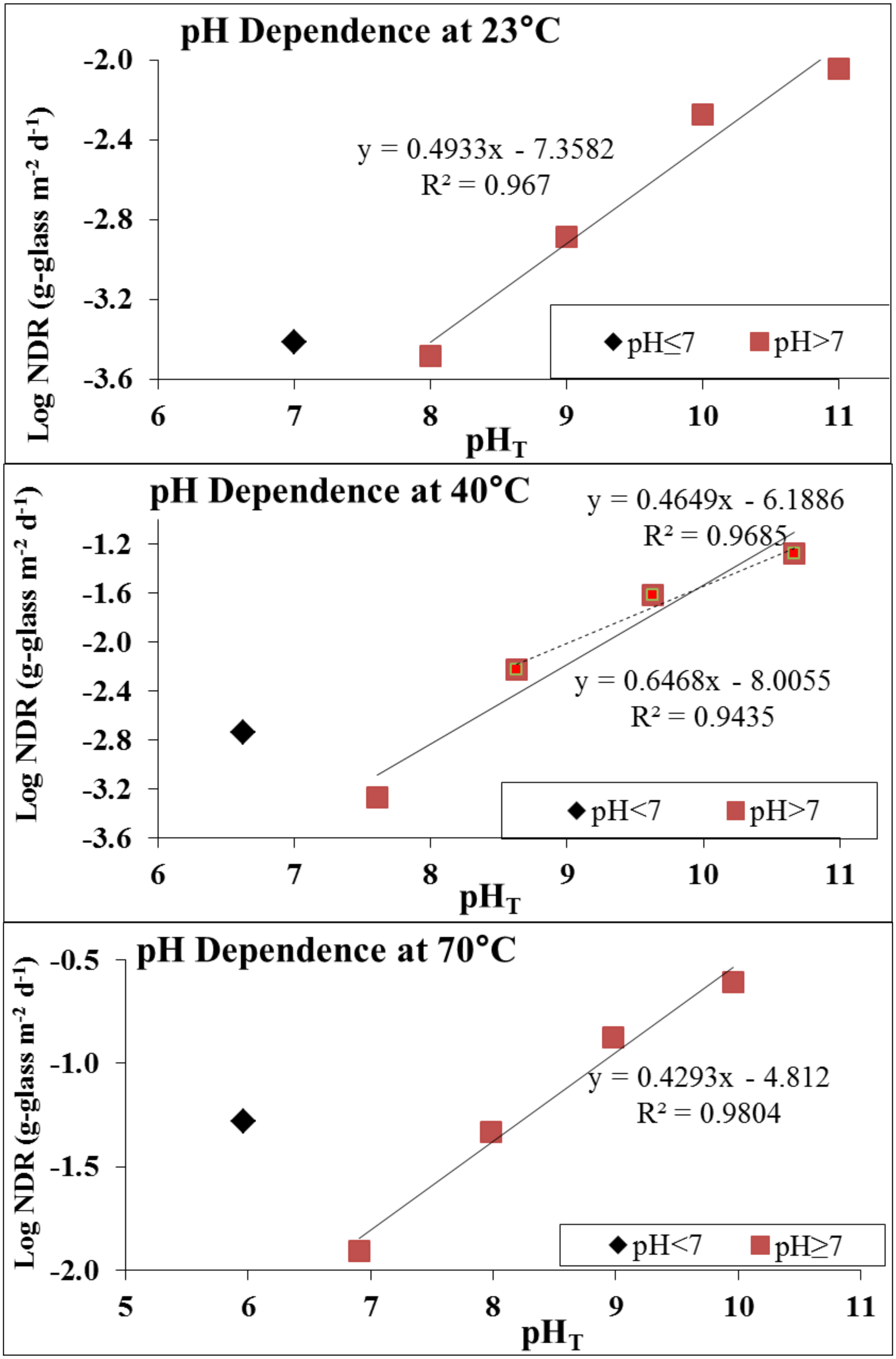

Figure 4.1. Plots of Log NDR_B vs. pH_T for LAWC22 used to determine the average value of the parameter η.

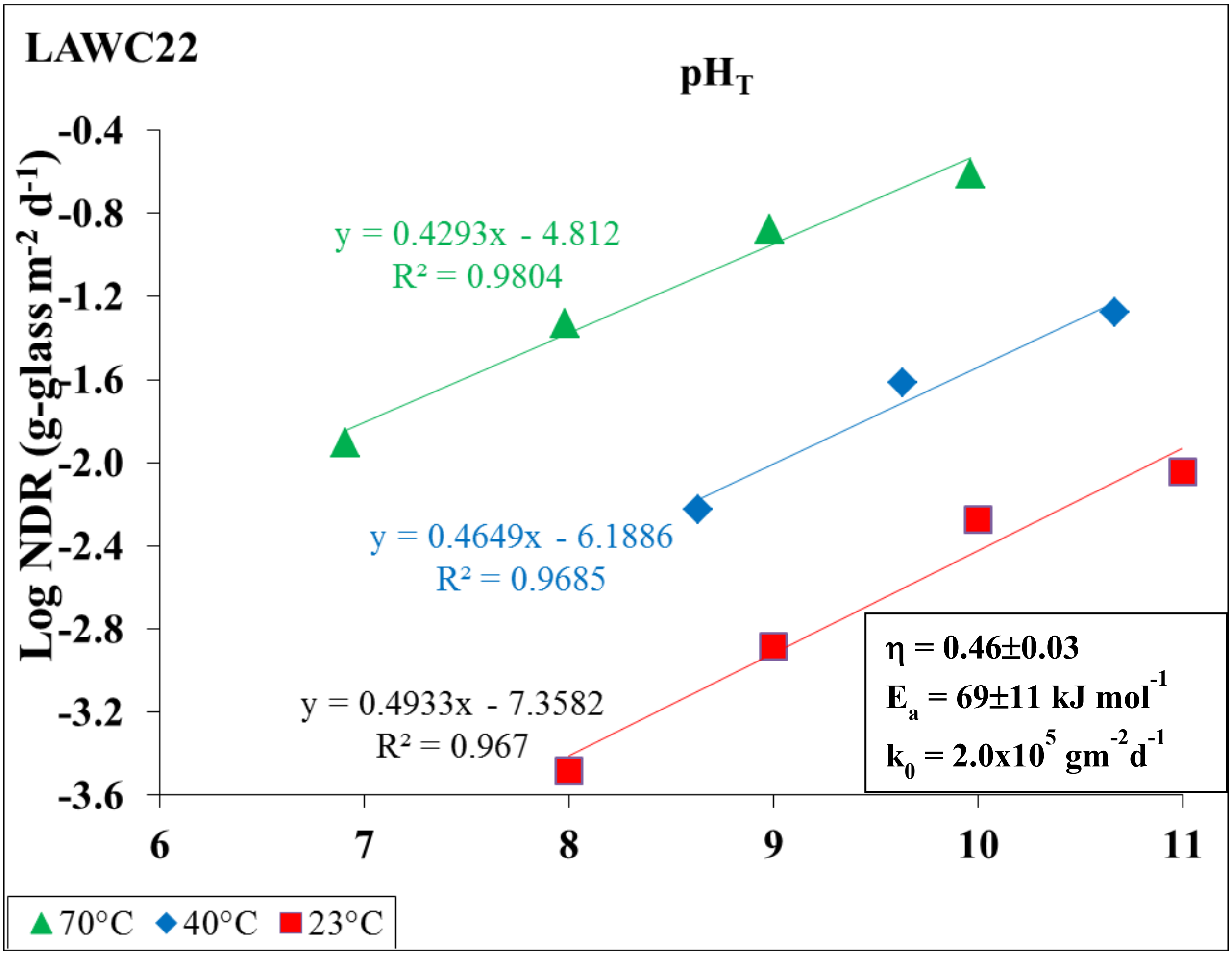

Figure 4.2. Plots of Log NDR_B vs. pH_T for LAWC22 and regression results to determine the parameters η, k_0 and E_a.

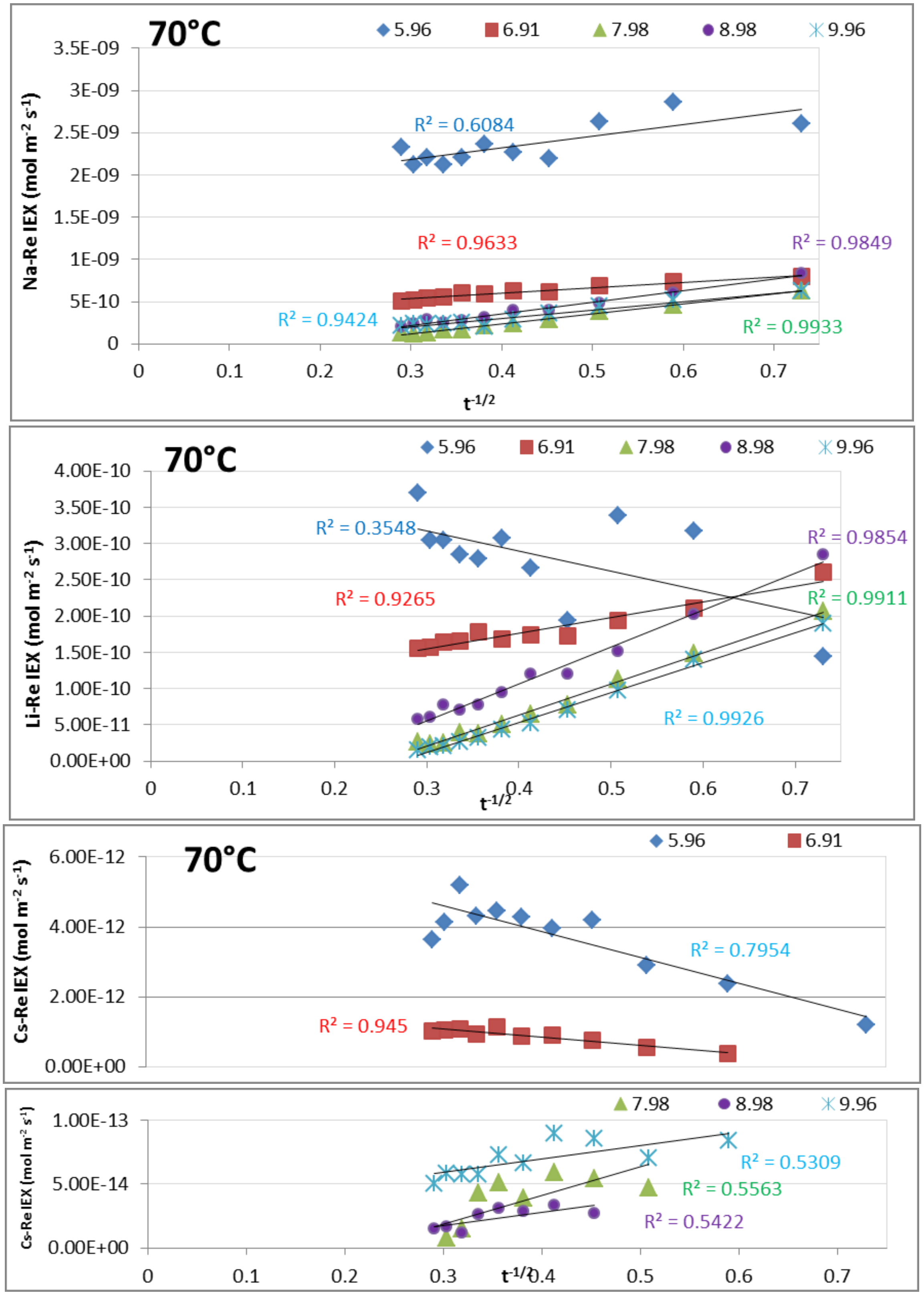

Figure 4.3. Time dependence of ion exchange rates for Na, Li and Cs in LAWC22 at 70°C. Legend shows pH_T values.

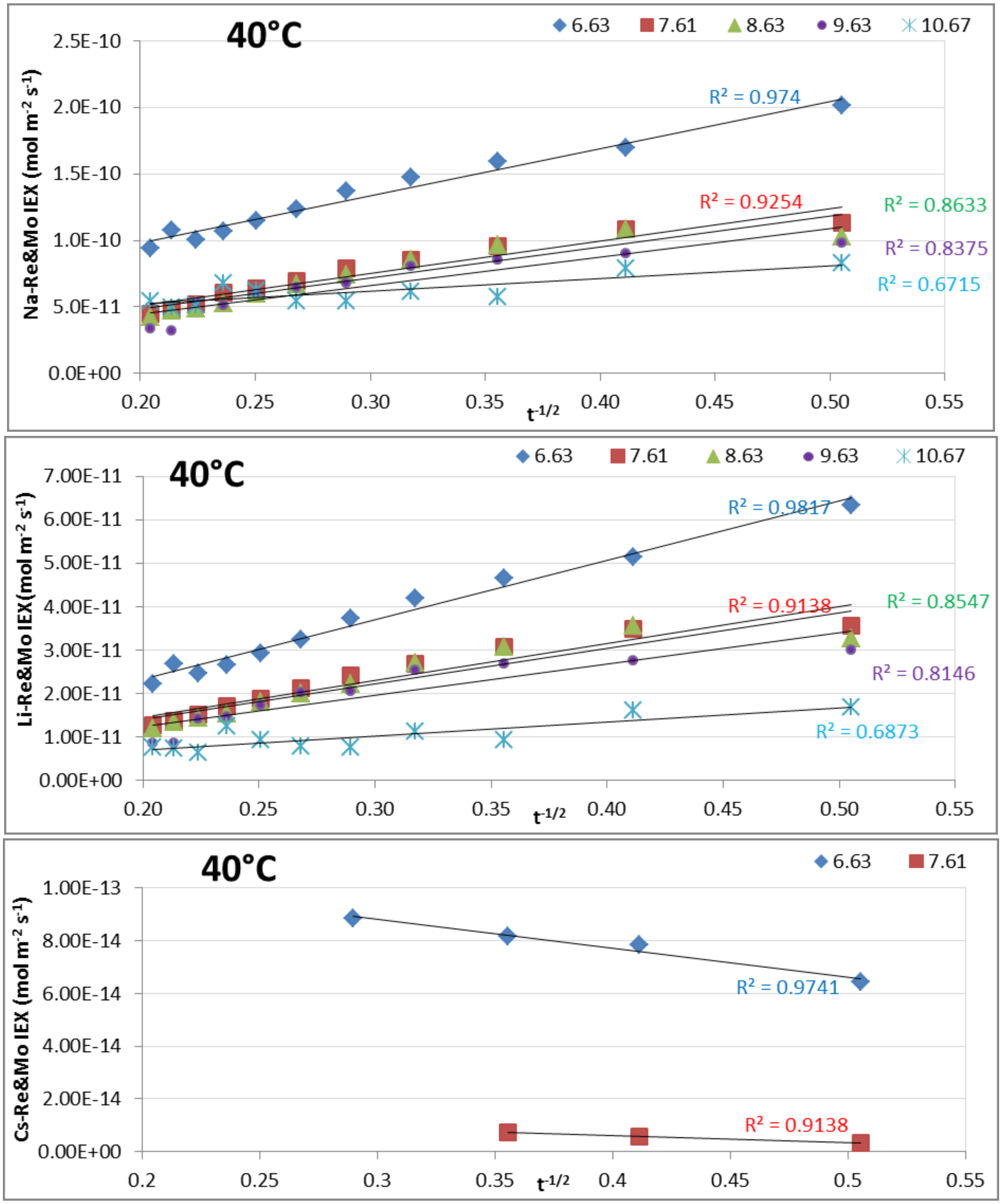

Figure 4.4. Time dependence of ion-exchange rate for Na, Li and Cs in LAWC22 at 40 °C. Legend shows pH_T values.

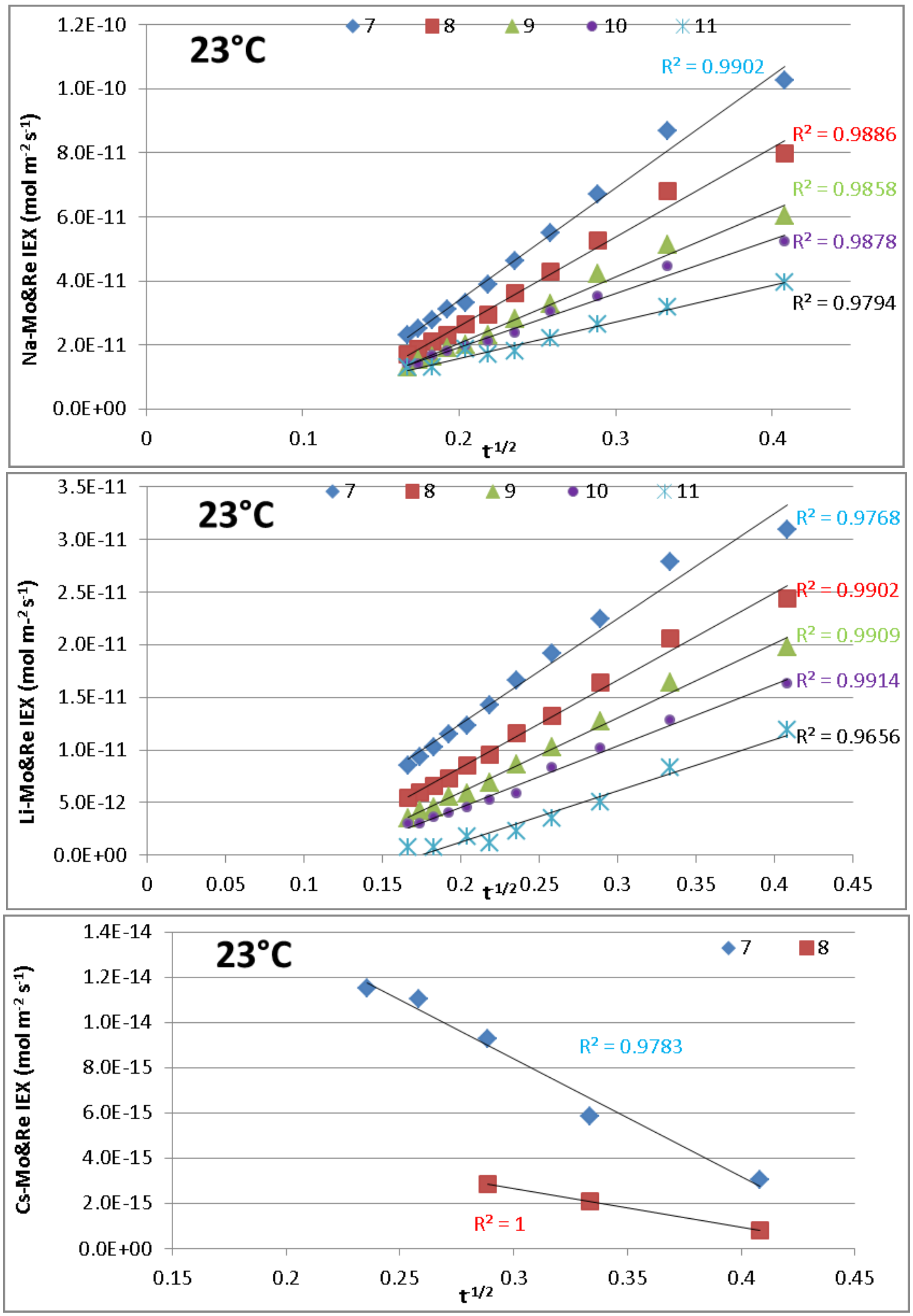

Figure 4.5. Time dependence of ion-exchange rate for Na, Li and Cs at 23 °C.

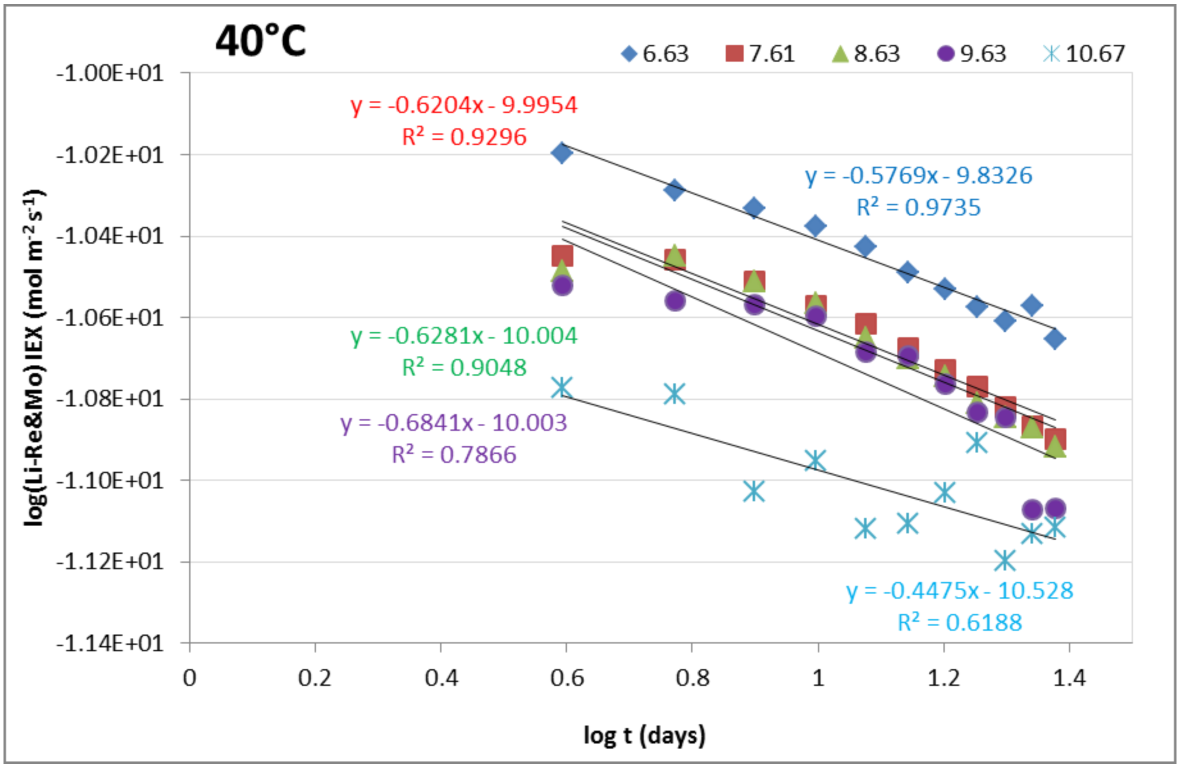

Figure 4.6. Log (r_{IEX}) versus log (*t*) plot for Li in LAWC22 at 40 °C. The average slope is about -0.6 ±0.09.

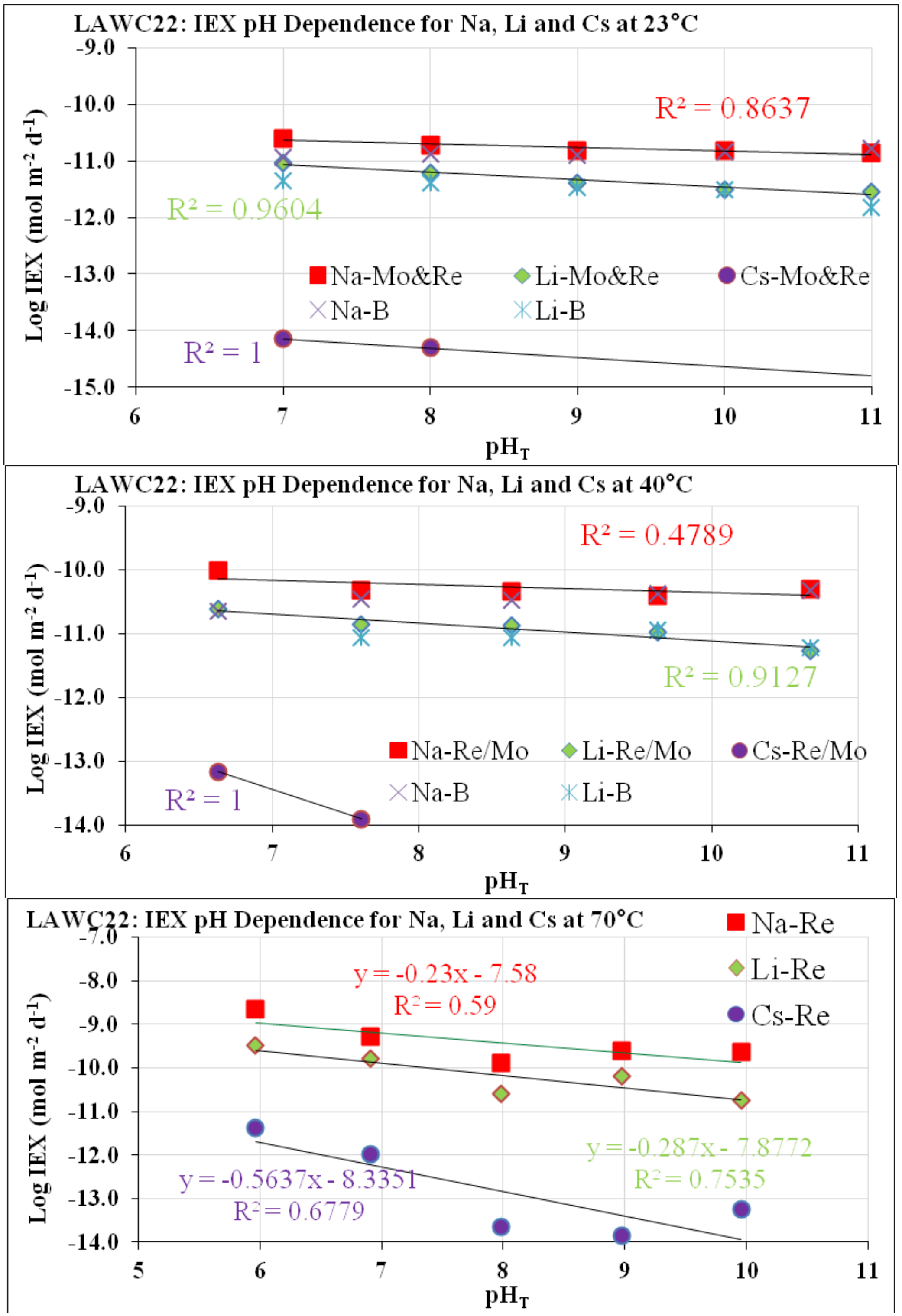

Figure 4.7. pH Dependence of ion exchange rates for Na, Li, and Cs.

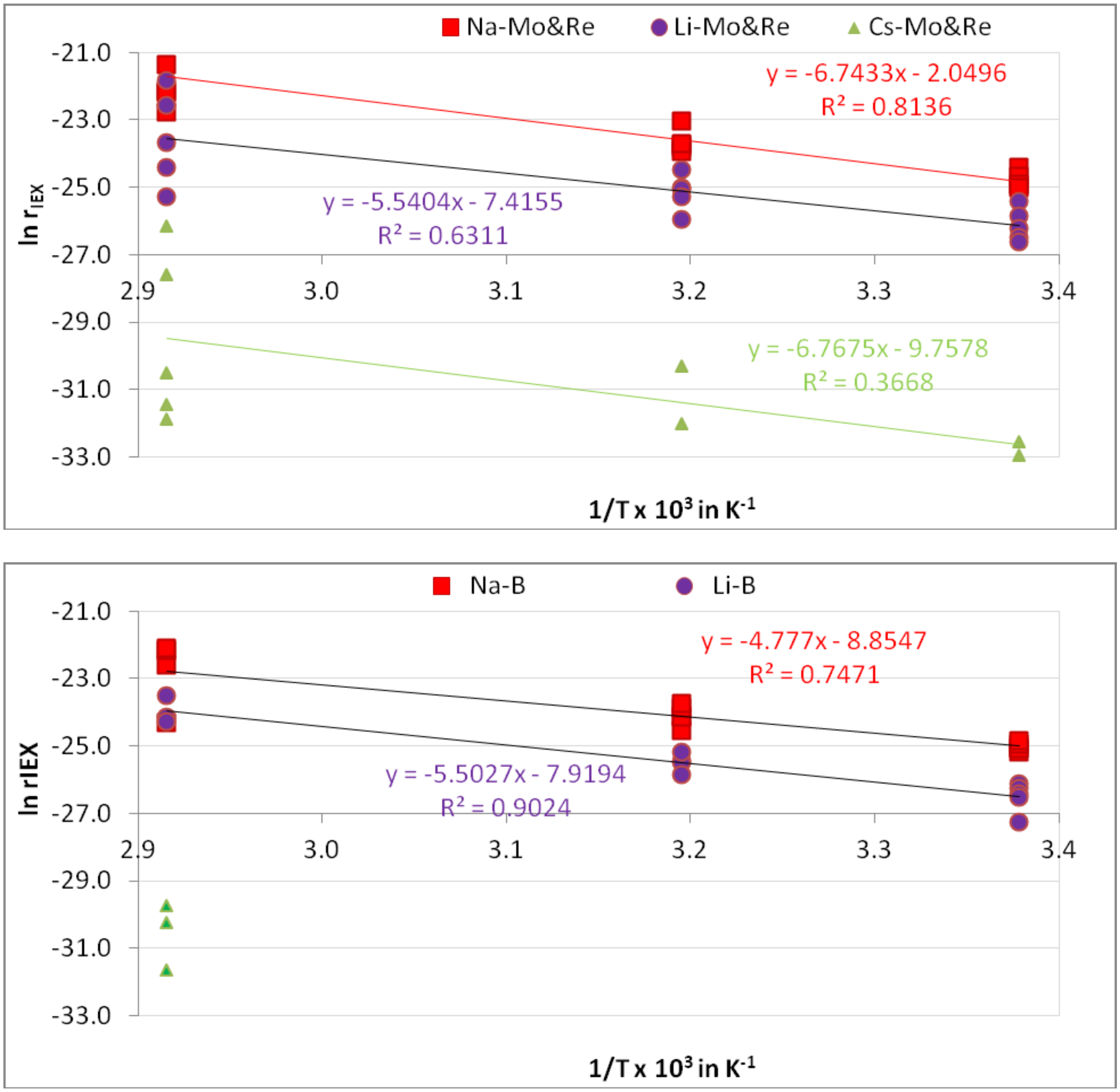

Figure 4.8. Plots of ln(r_{IEX}) as a function of 1/T (K^{-1}) for LAWC22 for Na, Li, and Cs based on dissolution of either Mo & Re, or B.

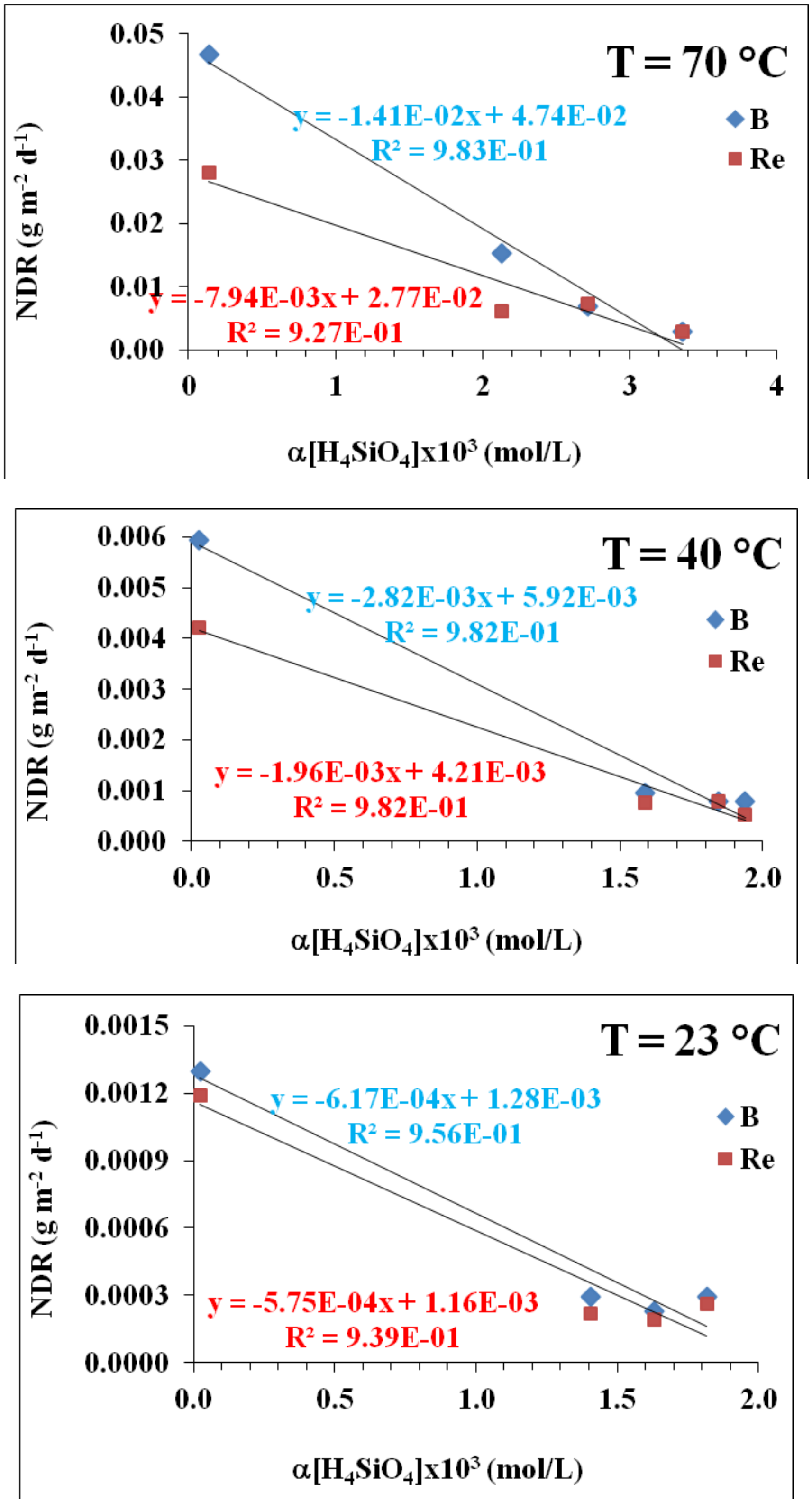

Figure 4.9. Linear regressions of boron and rhenium steady state NDR as a function of $[H_4SiO_4]$ to assess K_g for LAWC22 by SPFT test.

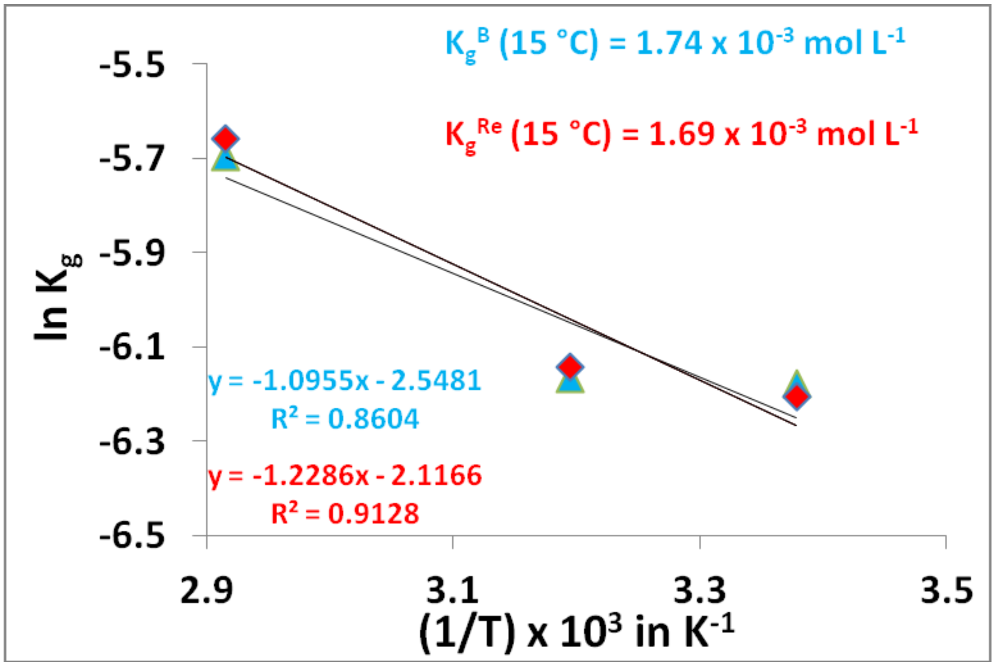

Figure 4.10. Arrhenius plots of K_g values for LAWC22 obtained from linear regression (Figure 4.9) as a function of 1/T (K^{-1}) to estimate K_g at 15 °C.

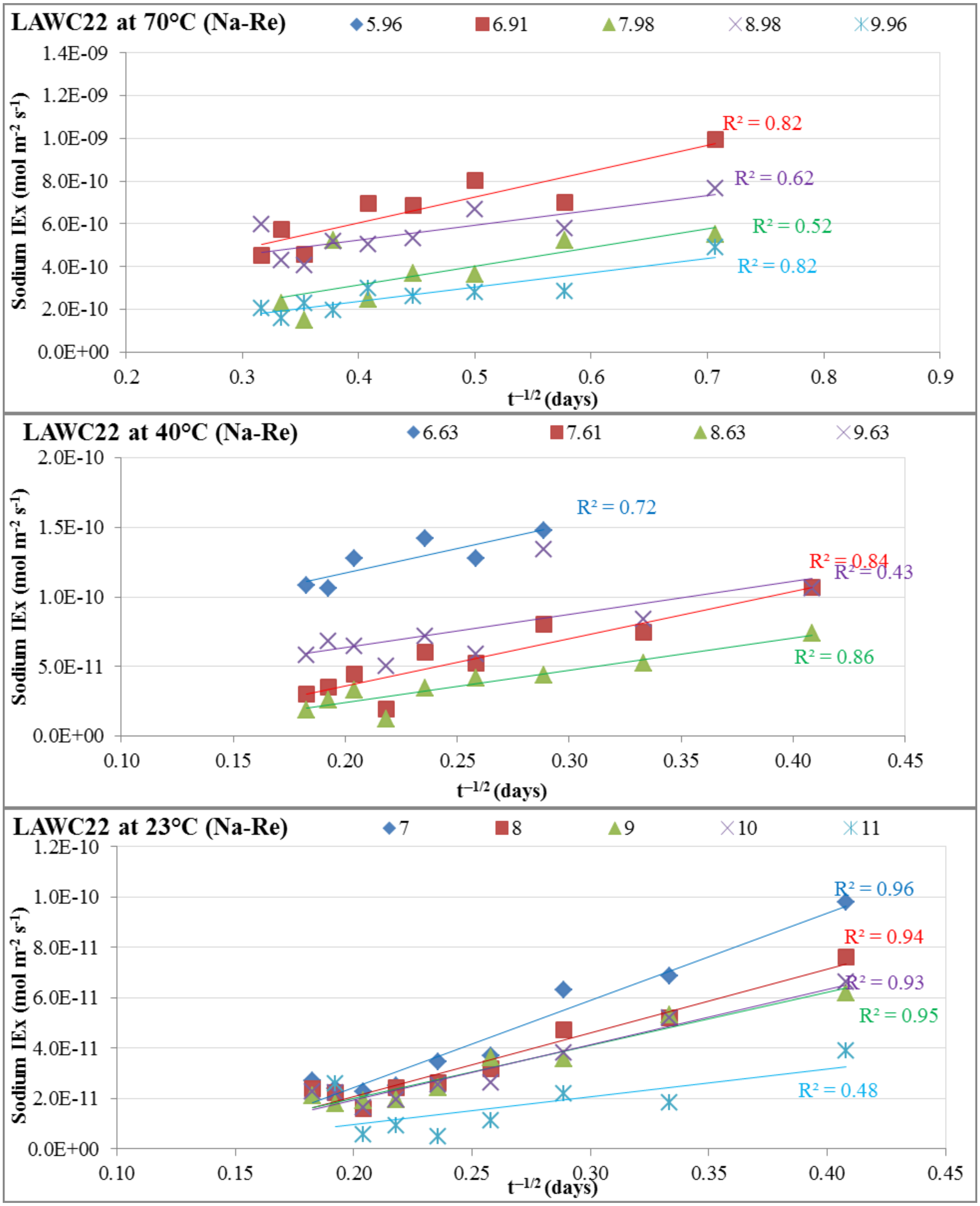

Figure 5.1. Plots of sodium ion exchange rate as a function of time (in days) from Pulsed-Flow tests conducted at 70 °C, 40 °C, and 23 °C with LAWC22.

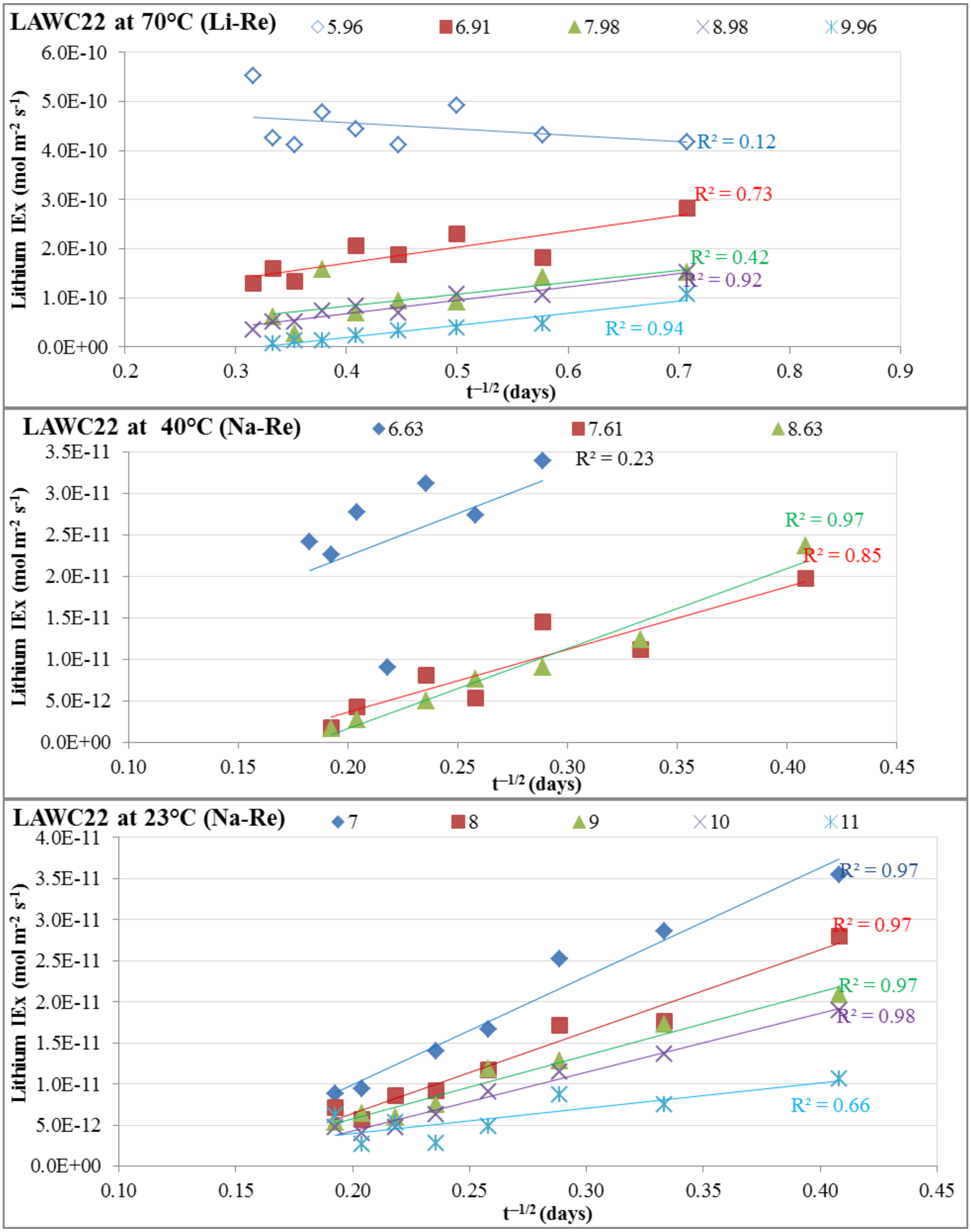

Figure 5.2. Plots of lithium ion exchange rate as a function of square root of time from Pulsed-Flow tests conducted at 70 °C, 40 °C, and 23 °C with LAWC22.

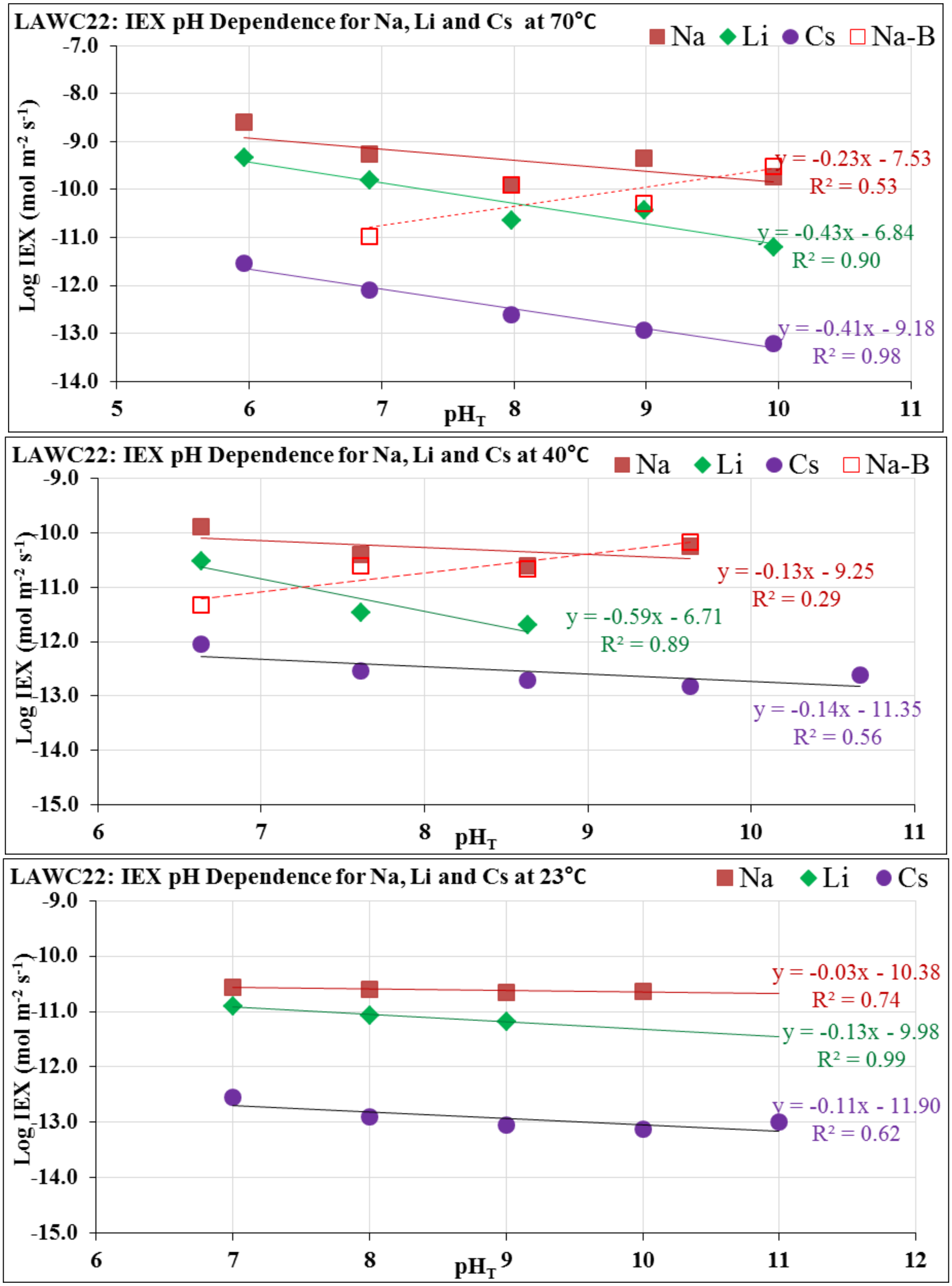

Figure 5.3. Plots of sodium, lithium, and cesium ion exchange rates as a function of pH for LAWC22.

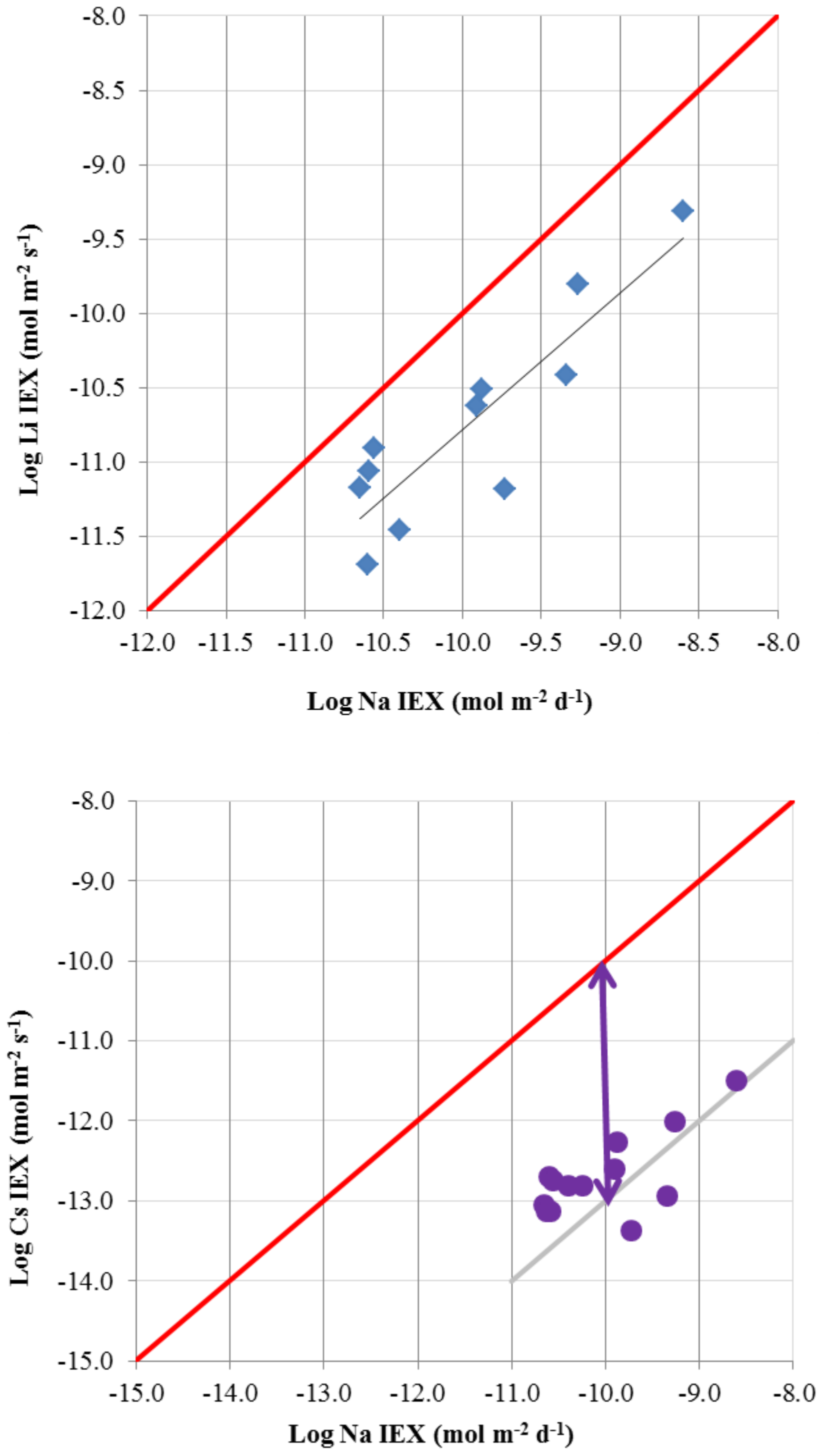

Figure 5.4. Plots of lithium (top) and cesium (bottom) ion exchange rates as a function of sodium ion exchange rate at all pH and temperature values for LAWC22. The red line denotes equality of the alkali ion exchange rates; the Li data fall ~0.7 log units below Na and the Cs data fall ~3 log units below Na.

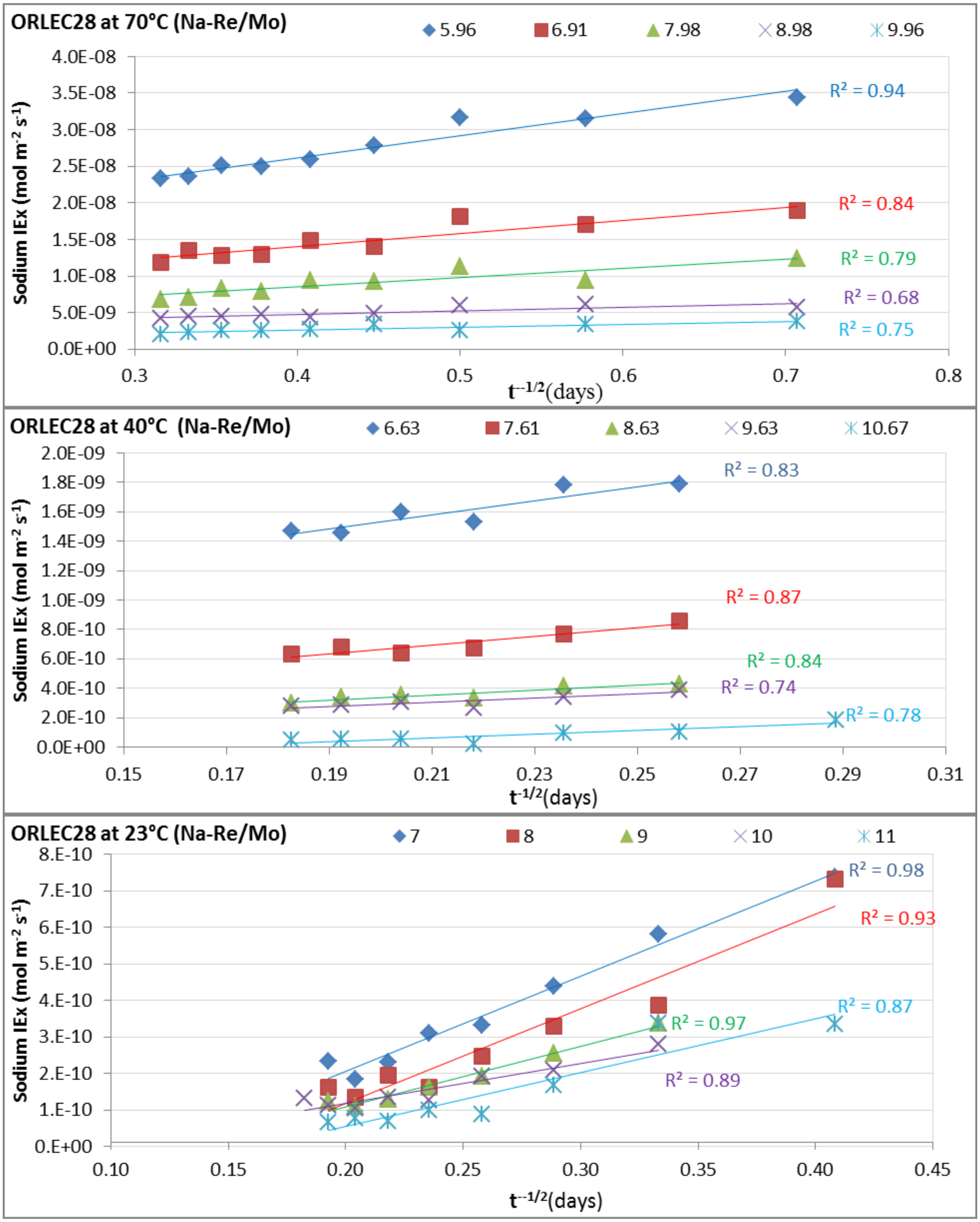

Figure 5.5. Plots of sodium ion exchange rates as a function of square root of time from Pulsed-Flow tests conducted at 70 °C, 40 °C, and 23 °C with ORLEC28.

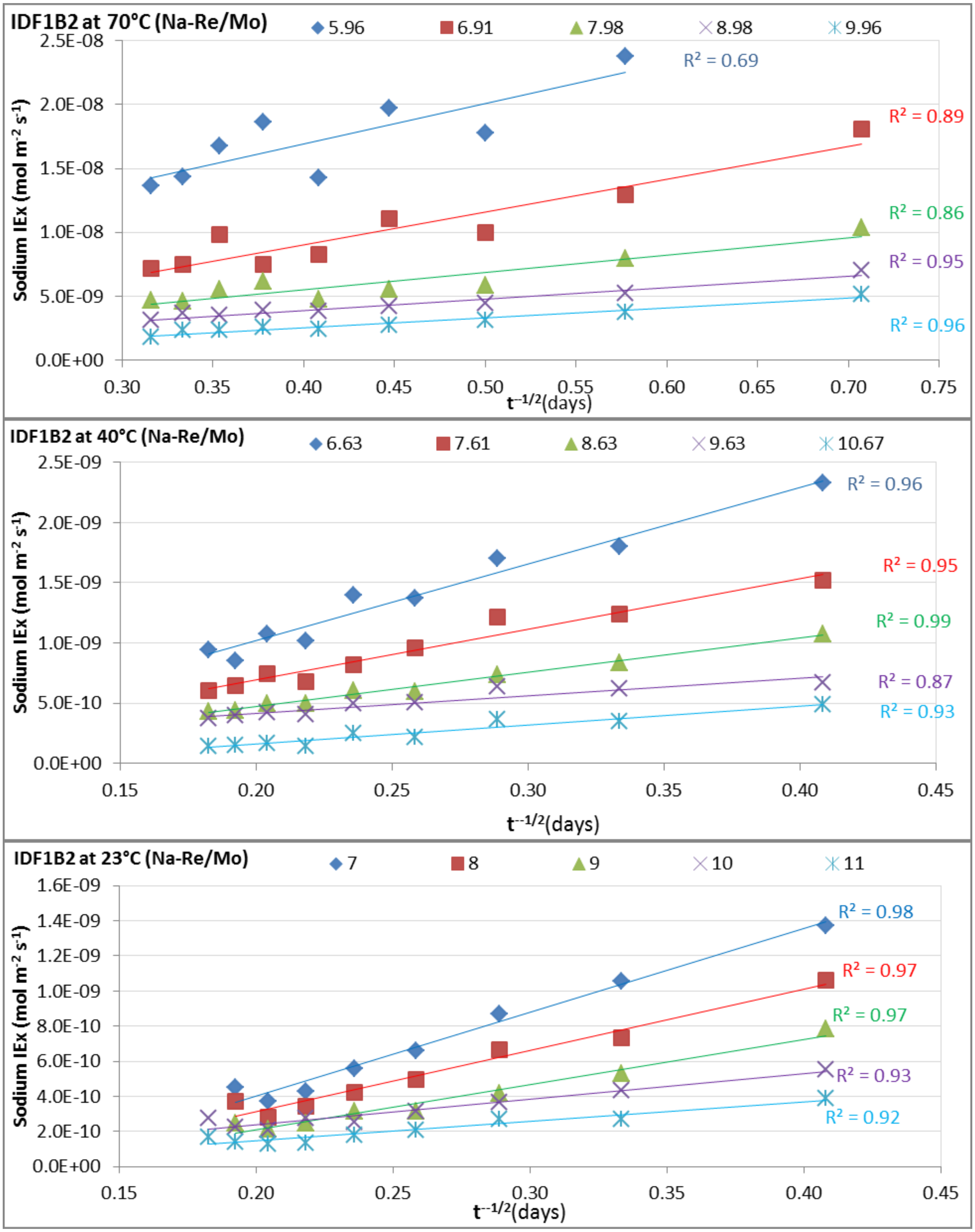

Figure 5.6. Plots of sodium ion exchange rates as a function of time from Pulsed-Flow tests conducted at 70 °C, 40 °C, and 23 °C with IDF1B2.

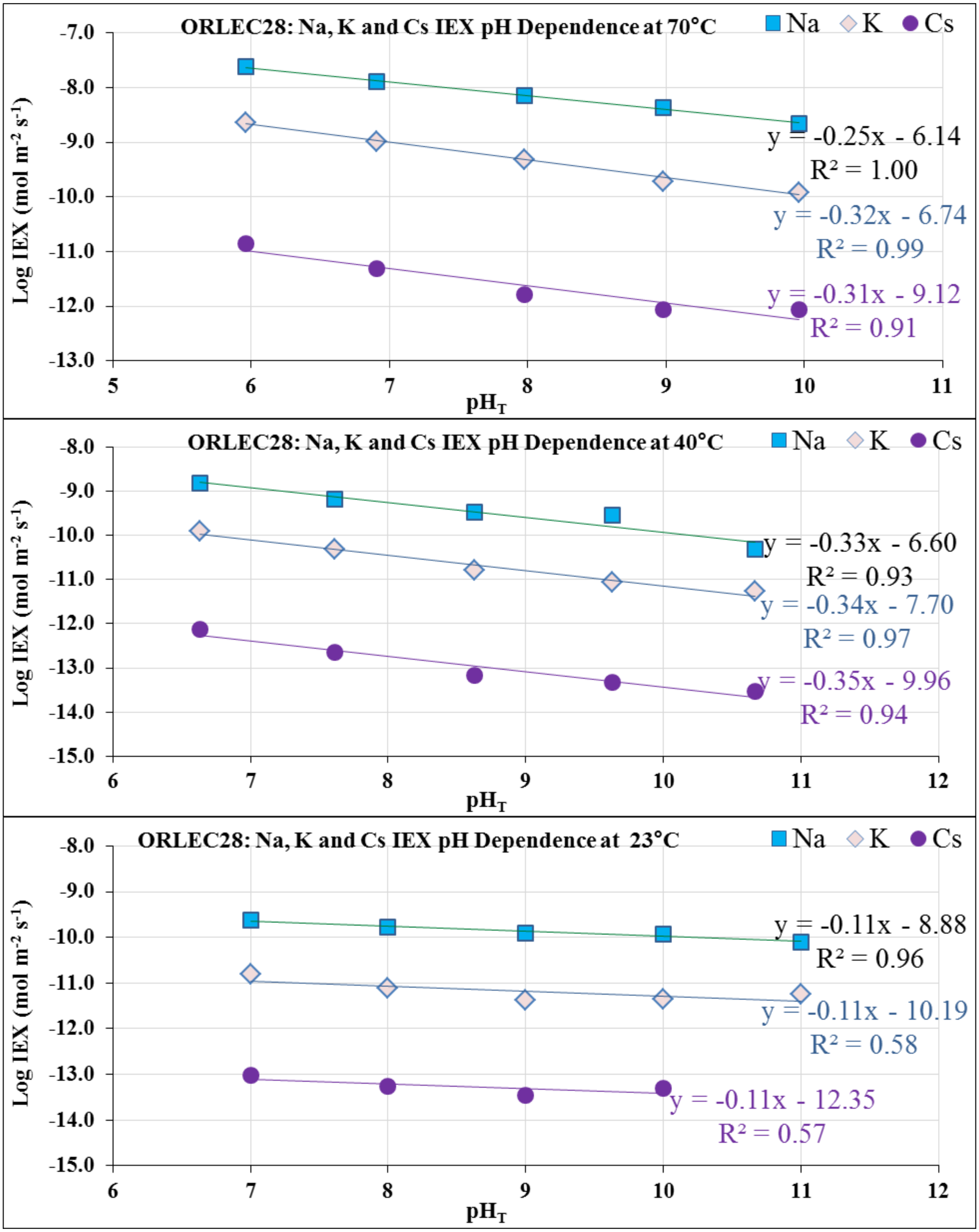

Figure 5.7. Plots of sodium, potassium, and cesium ion exchange rates as a function of pH for ORLEC28; note the equal slopes close to -0.3 at high temperature and -0.1 at 23°C.

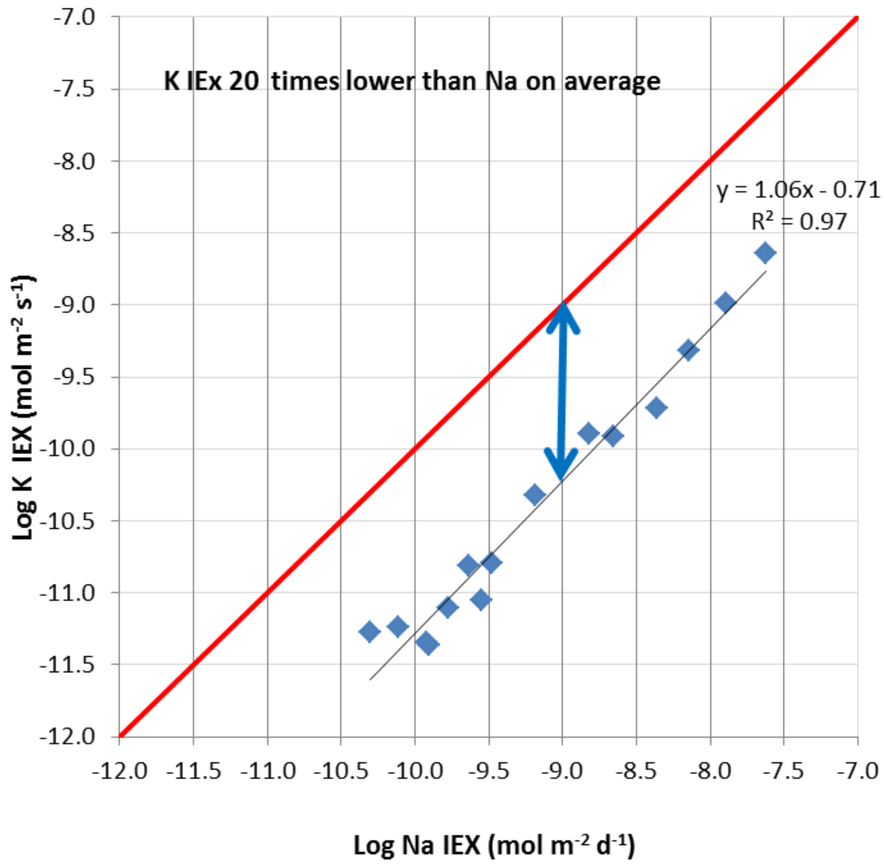

Figure 5.8. Plots of potassium ion exchange rate as a function of sodium ion exchange rate at all pH and temperature values for ORLEC28. The red line denotes equality of the alkali ion exchange rates; the K data fall ~1.2 log units below Na.

.

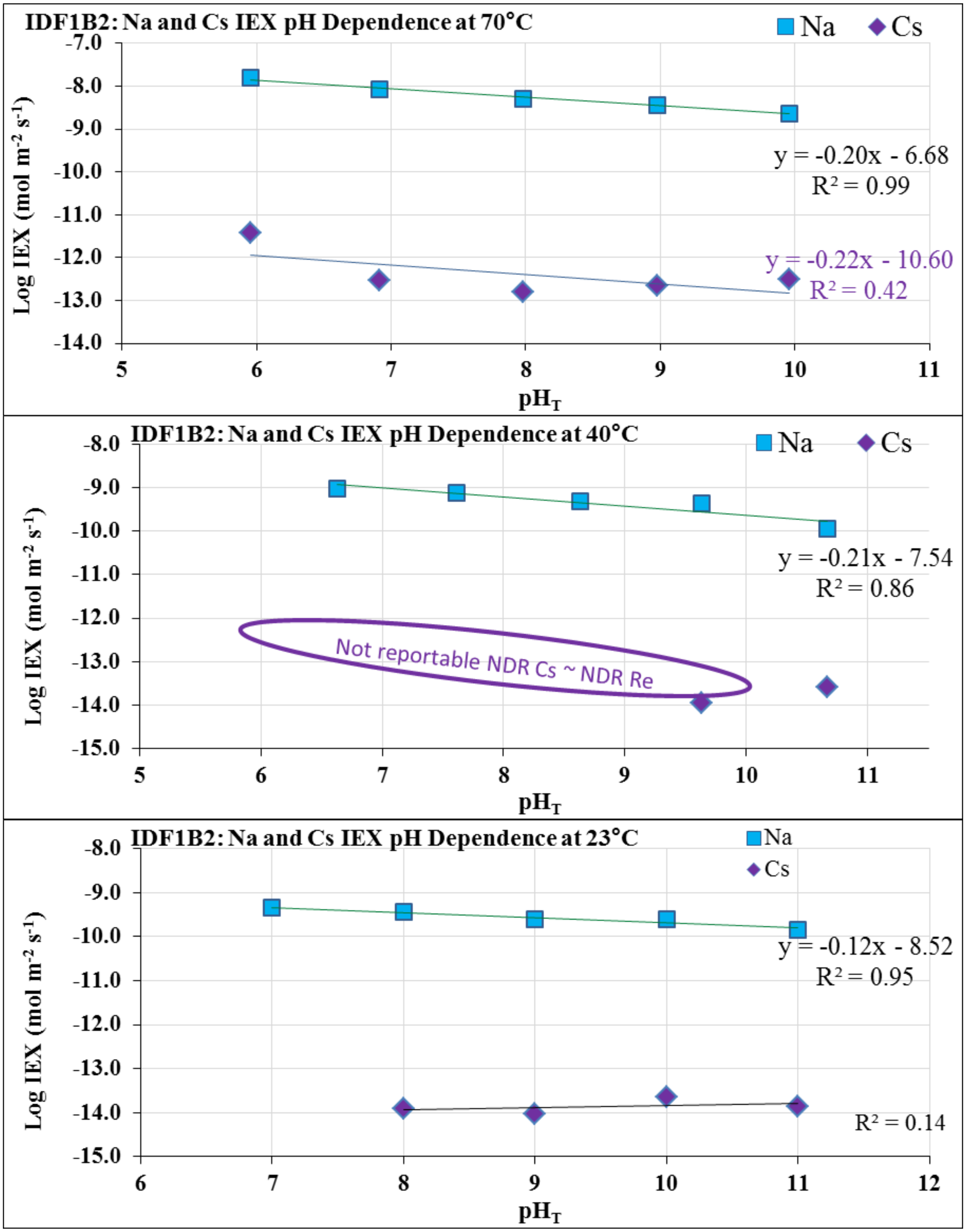

Figure 5.9. Plots of sodium and cesium ion exchange rates as a function of pH for IDF1B2.

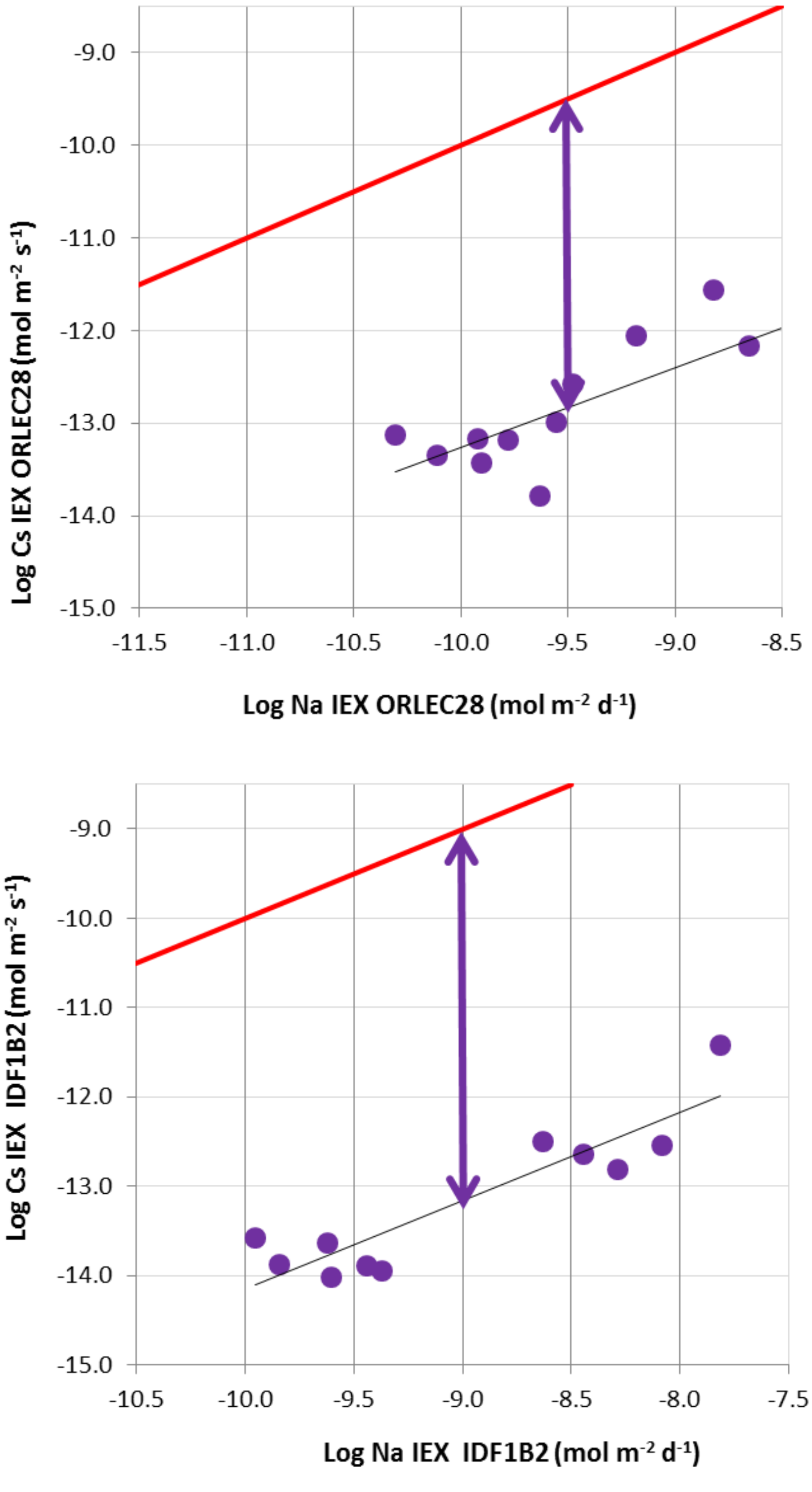

Figure 5.10. Plots of cesium ion exchange rate as a function of sodium ion exchange rate at all pH and temperature values for ORLEC28 (top) and IDF1B2 (bottom). The red line denotes equality of the alkali ion exchange rates; the Cs data fall ~3.5 to 4 log units below Na.

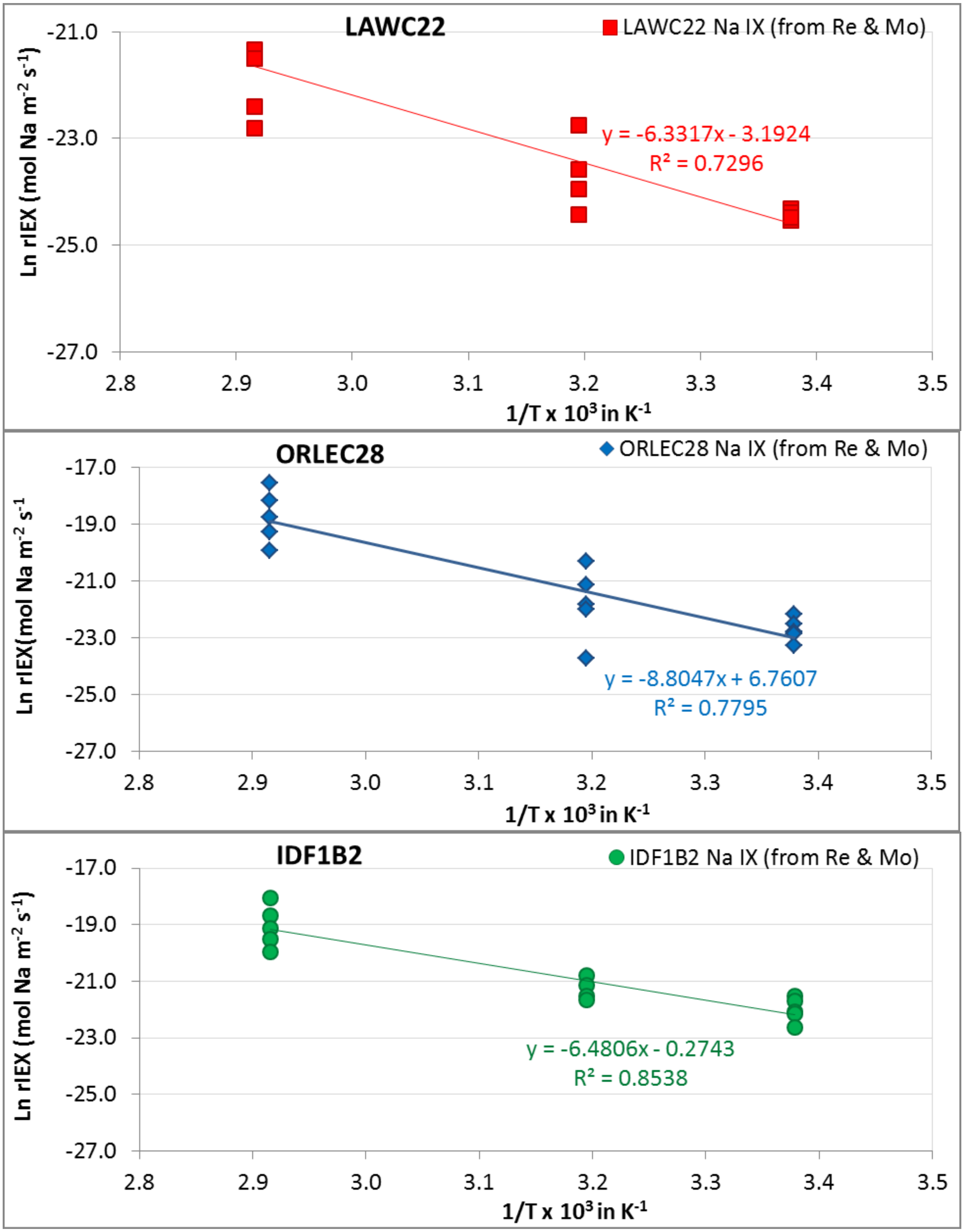

Figure 5.11. Plots of Ln($r_{IEX\ Na}$) as a function of 1/T (K^{-1}) for LAWC22, ORLEC28, and IDF1B2.

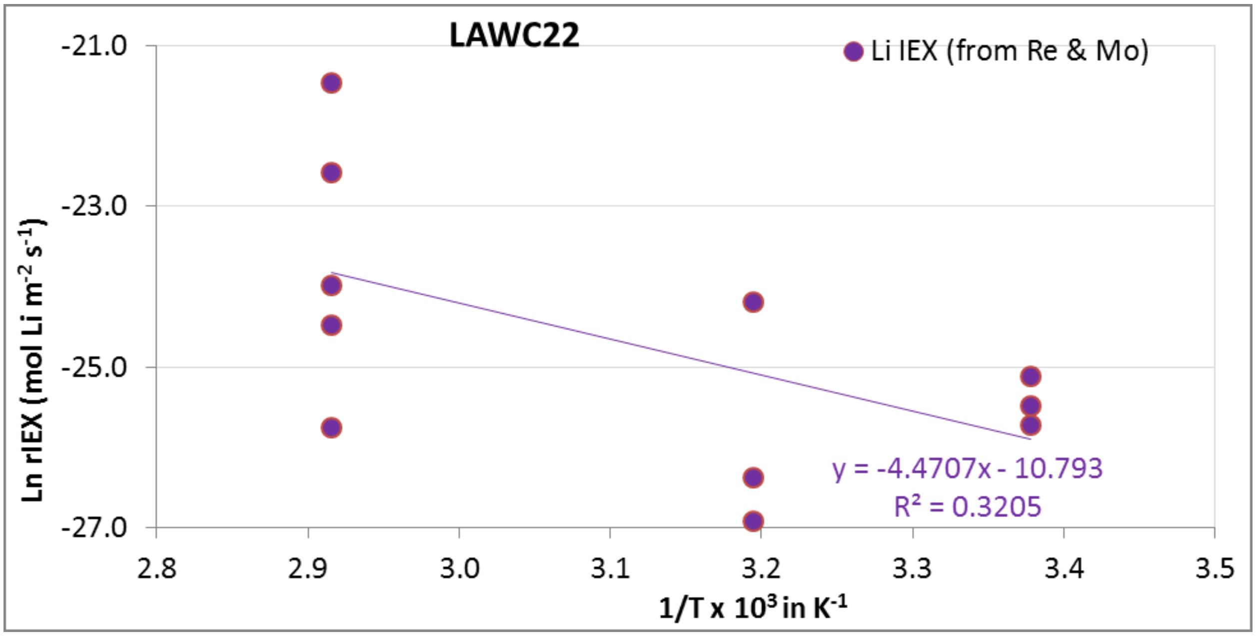

Figure 5.12. Plots of Ln($r_{IEX\ Li}$) as a function of 1/T (K^{-1}) for LAWC22.

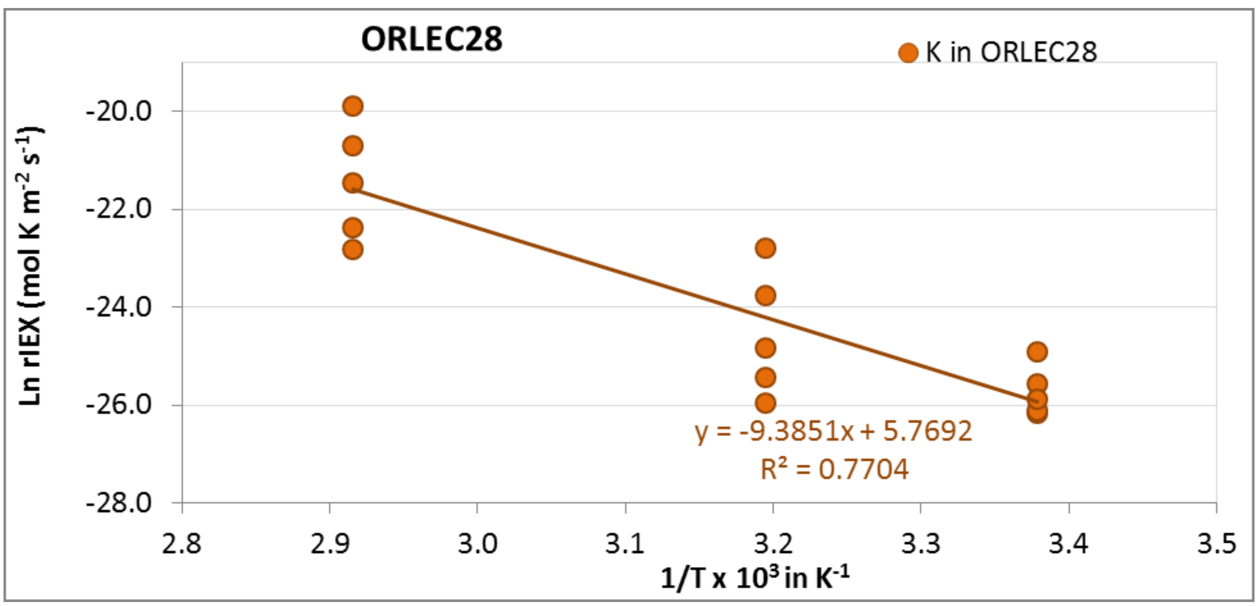

Figure 5.13. Plots of Ln($r_{IEX\ K}$) as a function of 1/T (K^{-1}) for ORLEC28.

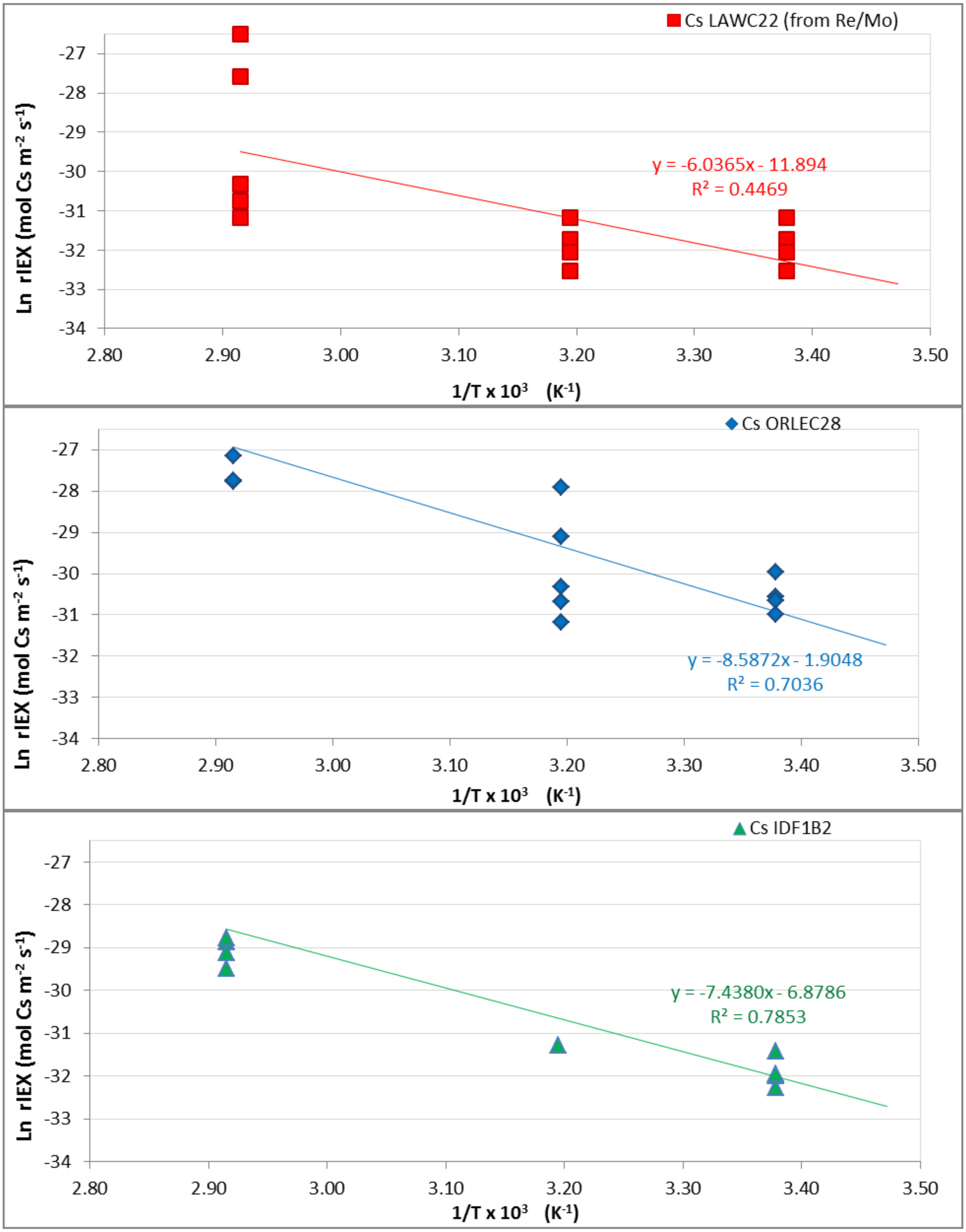

Figure 5.14. Plots of Ln($r_{IEX\ Cs}$) as a function of 1/T (K^{-1}) for LAWC22, ORLEC28, and IDF1B2.

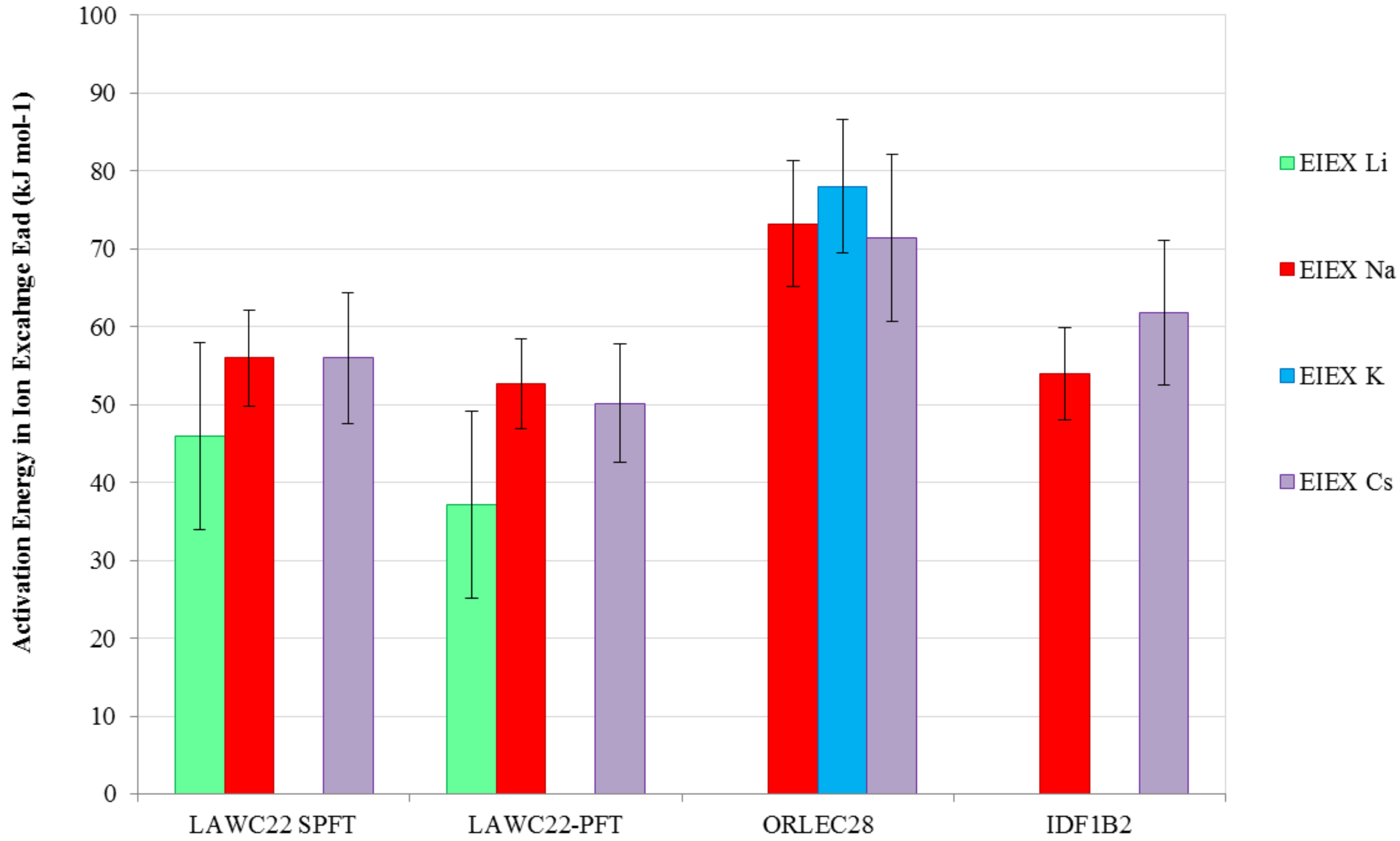

Figure 5.15. Plots of ion exchange activation energy E_{ad} for the various alkalis for LAWC22, ORLEC28, and IDF1B2 by SPFT and Pulsed-Flow tests.

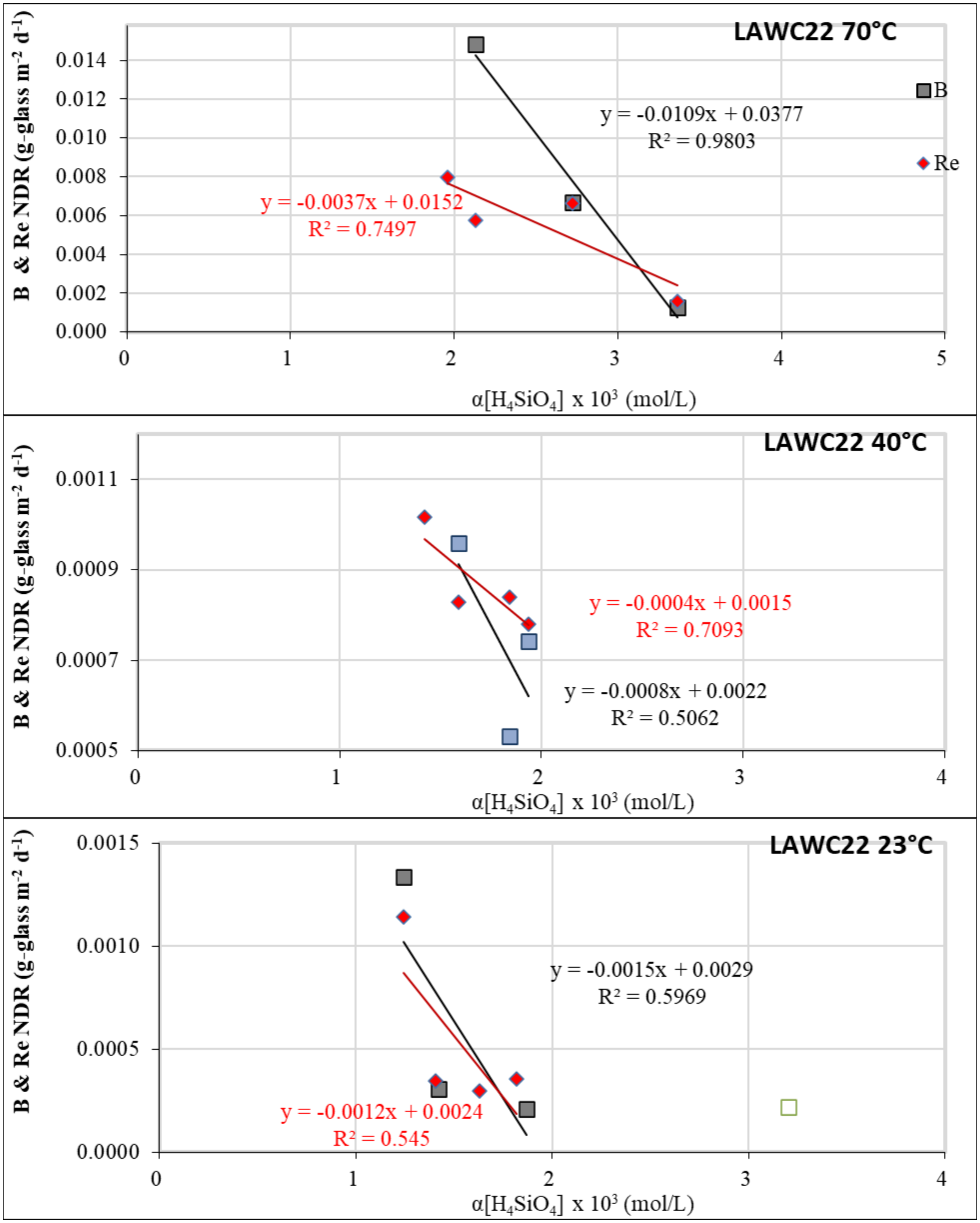

Figure 5.16. Linear regressions of boron and rhenium steady state NDR as a function of [H_4SiO_4] to assess K_g for LAWC22.

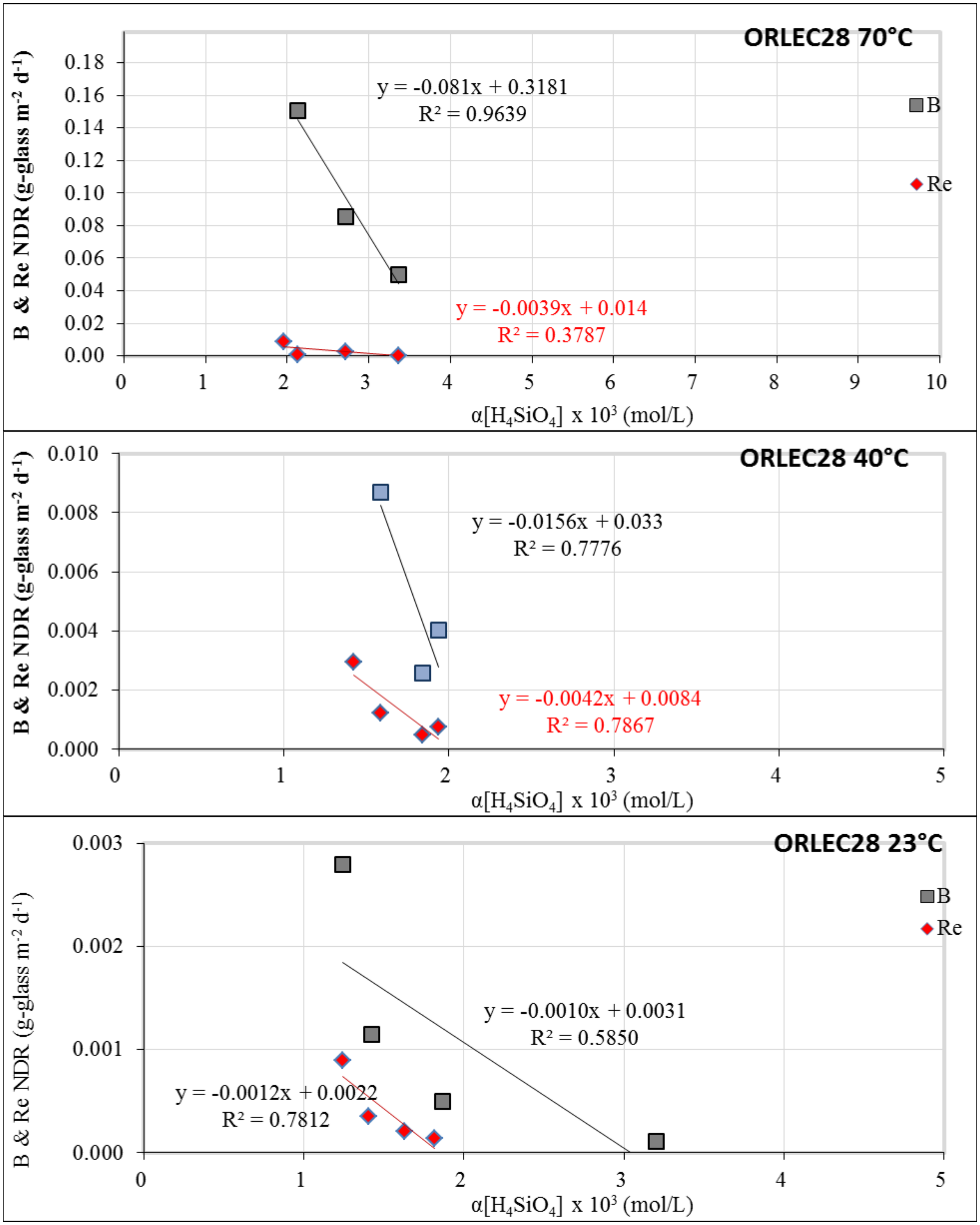

Figure 5.17. Linear regressions of boron and rhenium steady state NDR as a function of $[H_4SiO_4]$ to assess K_g for ORLEC28.

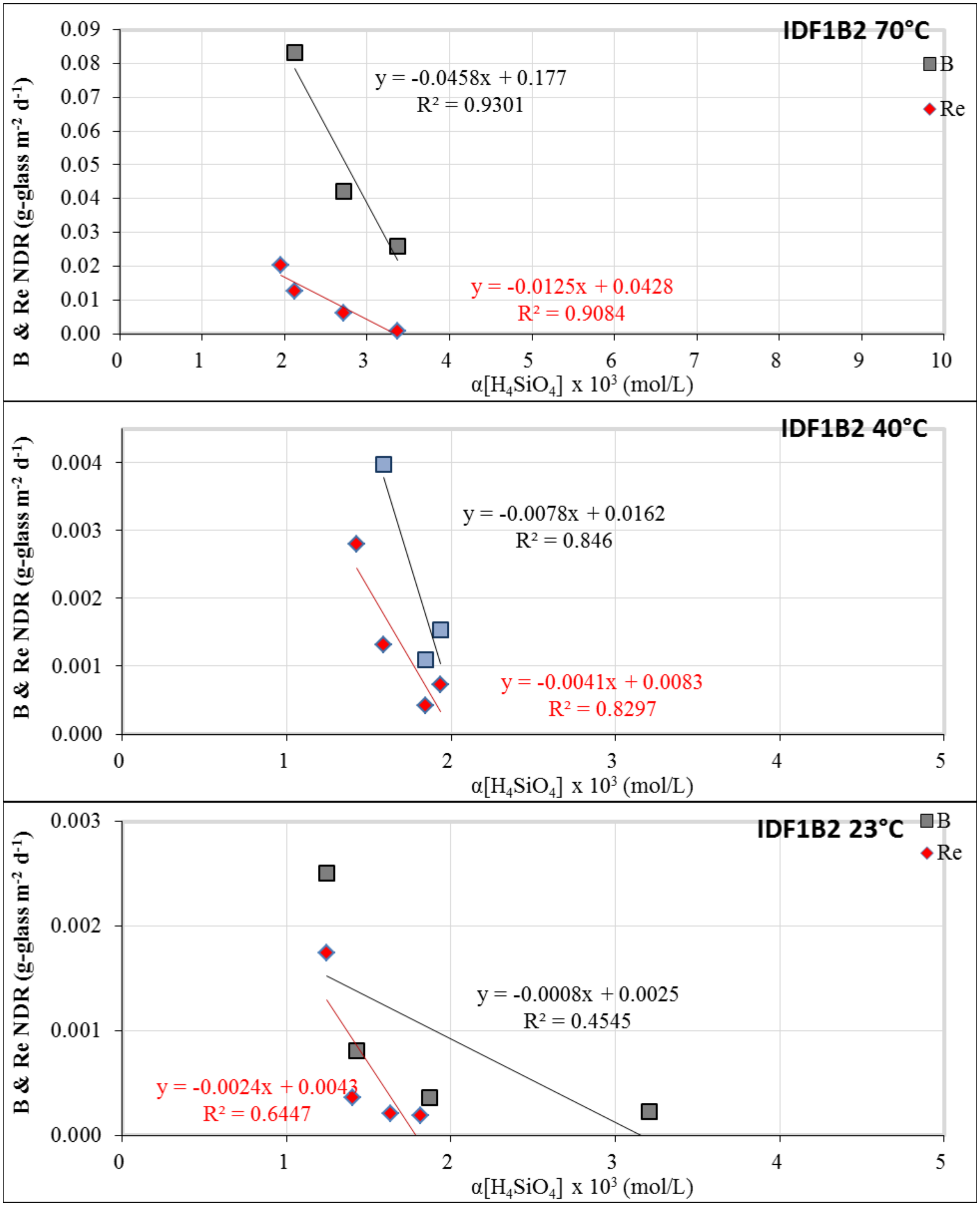

Figure 5.18. Linear regressions of boron and rhenium steady state NDR as a function of $[H_4SiO_4]$ to assess K_g for IDF1B2.

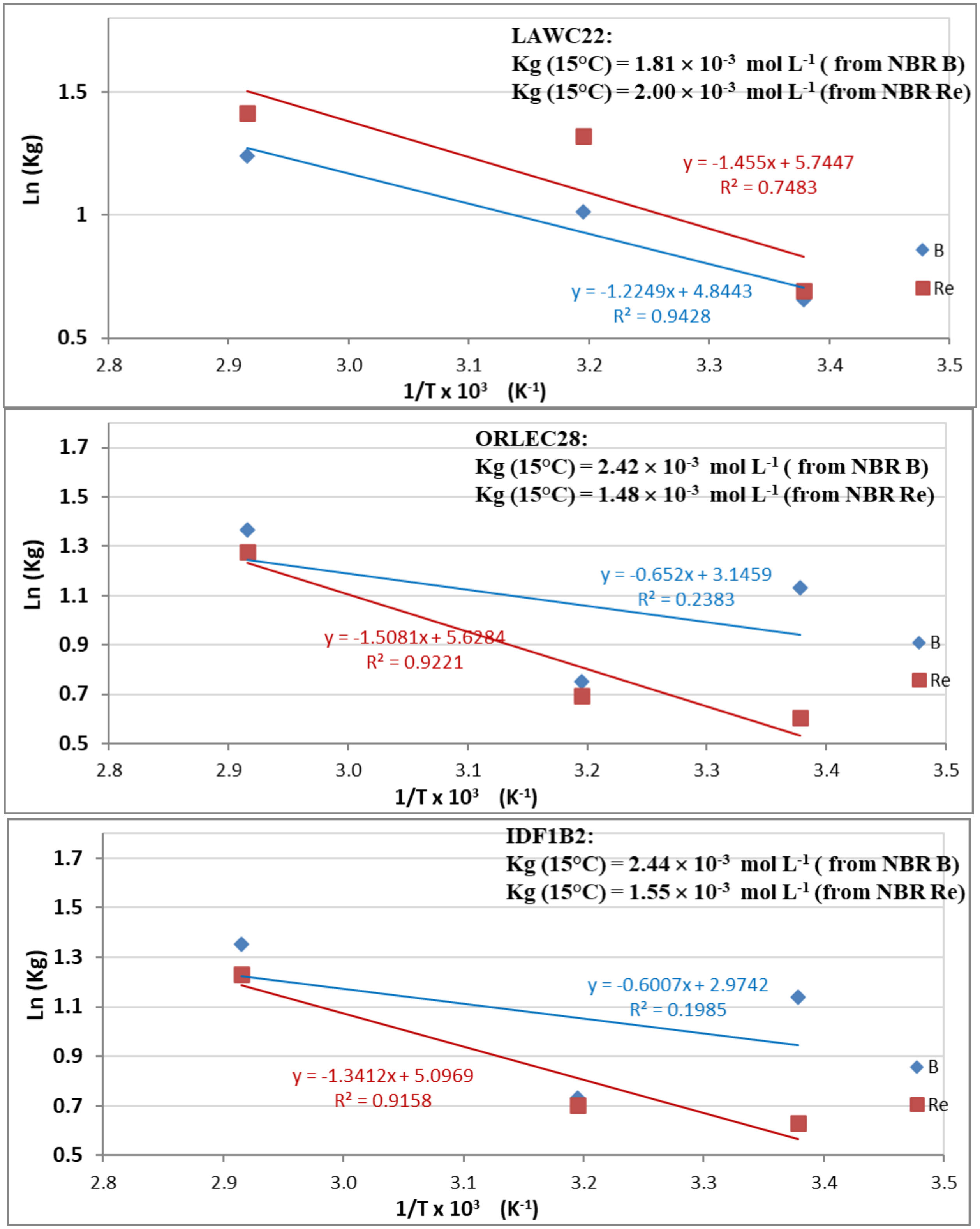

Figure 5.19. Ln K_g values for LAWC22, ORLEC28, and IDF1B2 obtained from linear regression (Figures 5.16 to 5.18) as a function of 1/T (K^{-1}) to estimate K_g at 15°C.

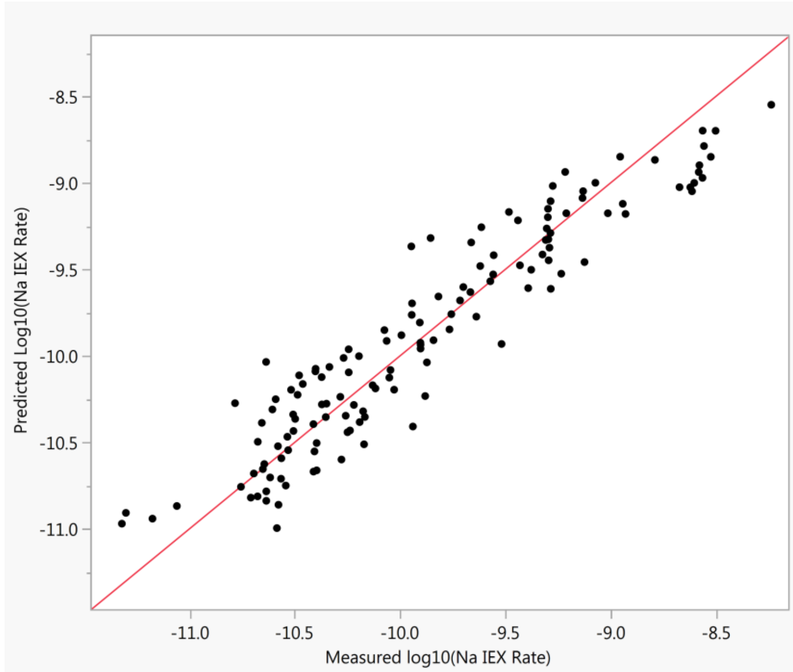

Figure 6.1. Predicted vs. measured plot for sodium ion exchange rate for LAWC22 (Equation 1.6).

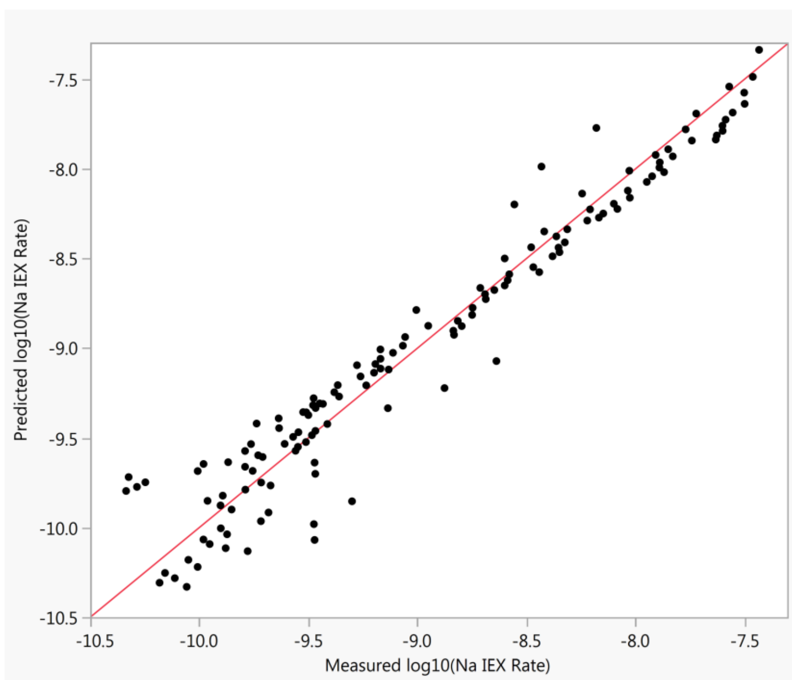

Figure 6.2. Predicted vs. measured plot for sodium ion exchange rate for ORLEC28 (Equation 1.6).

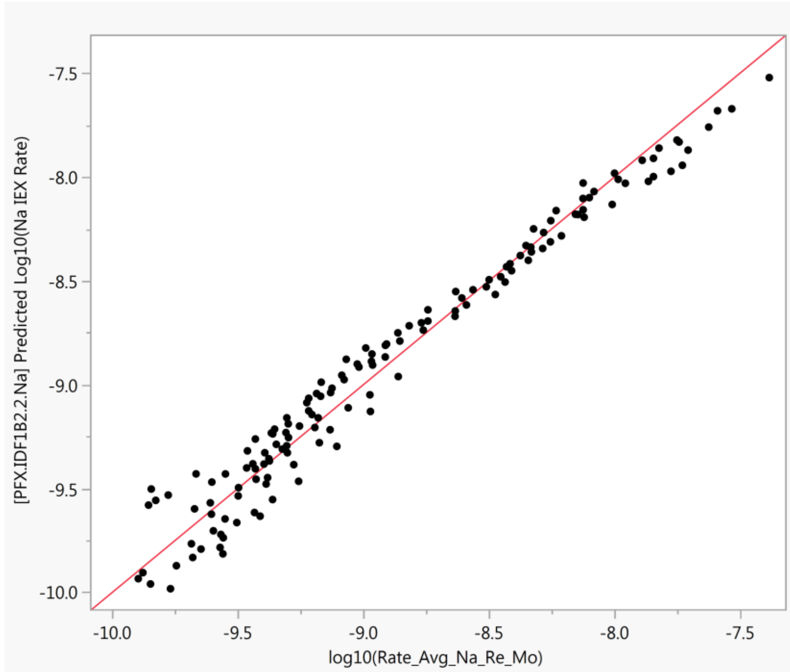

Figure 6.3. Predicted vs. measured plot for sodium ion exchange rate for IDF1B2 (Equation 1.6).

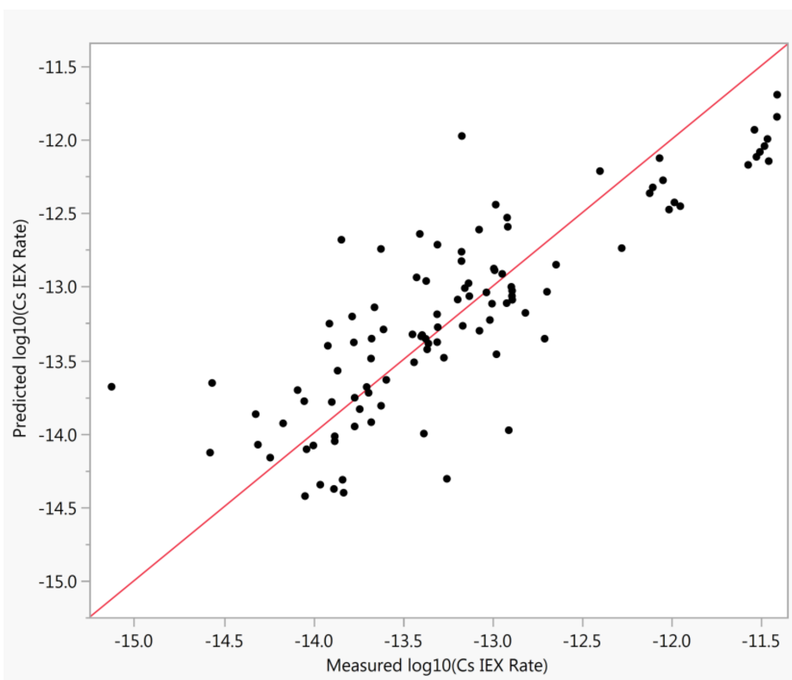

Figure 6.4. Predicted vs. measured plot for cesium ion exchange rate for LAWC22 (Equation 1.6).

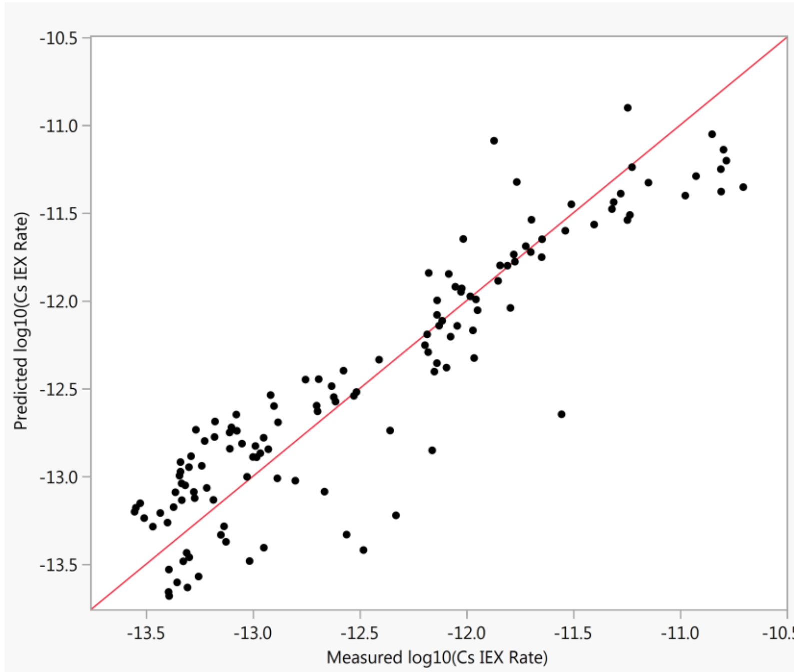

Figure 6.5. Predicted vs. measured plot for cesium ion exchange rate for ORLEC28 (Equation 1.6).

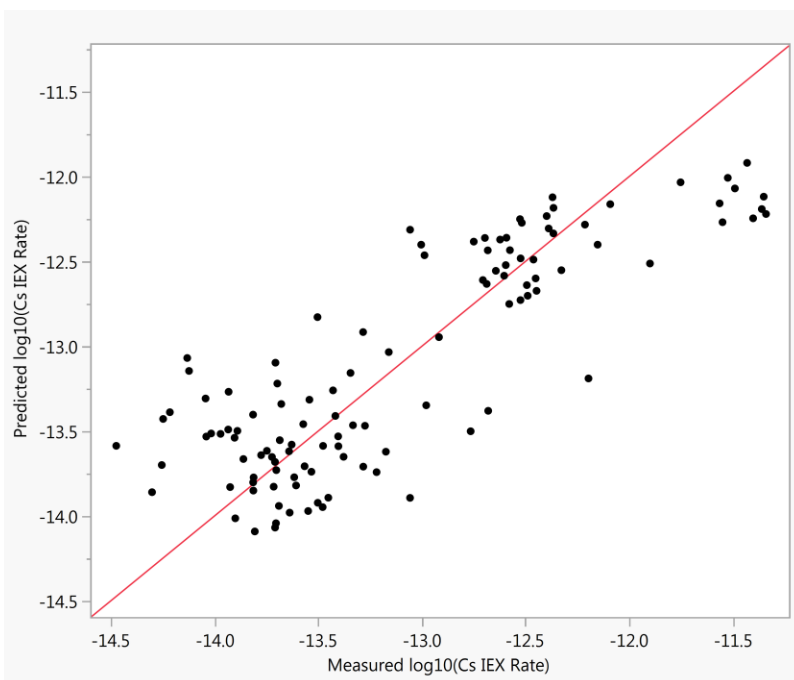

Figure 6.6. Predicted vs. measured plot for cesium ion exchange rate for IDF1B2 (Equation 1.6).

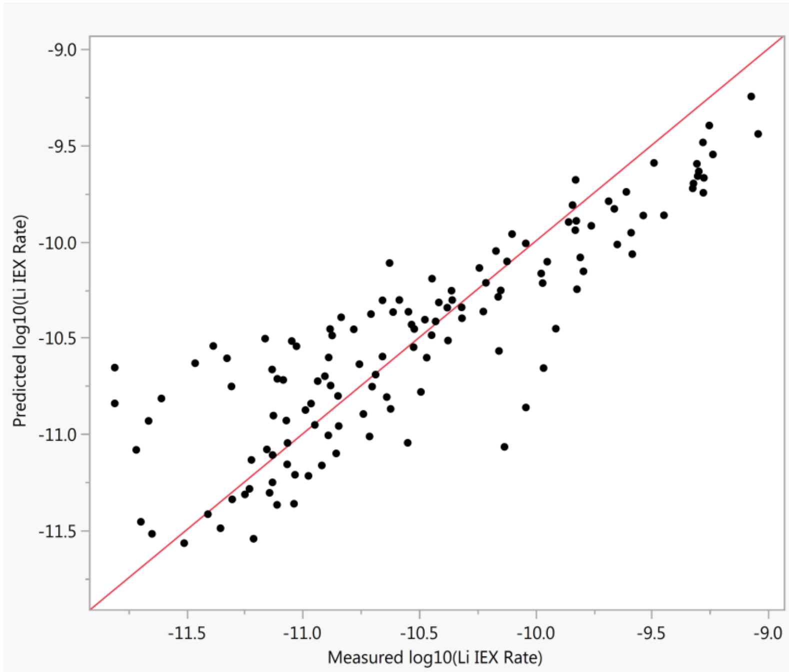

Figure 6.7. Predicted vs. measured plot for lithium ion exchange rate for LAWC22 (Equation 1.6).

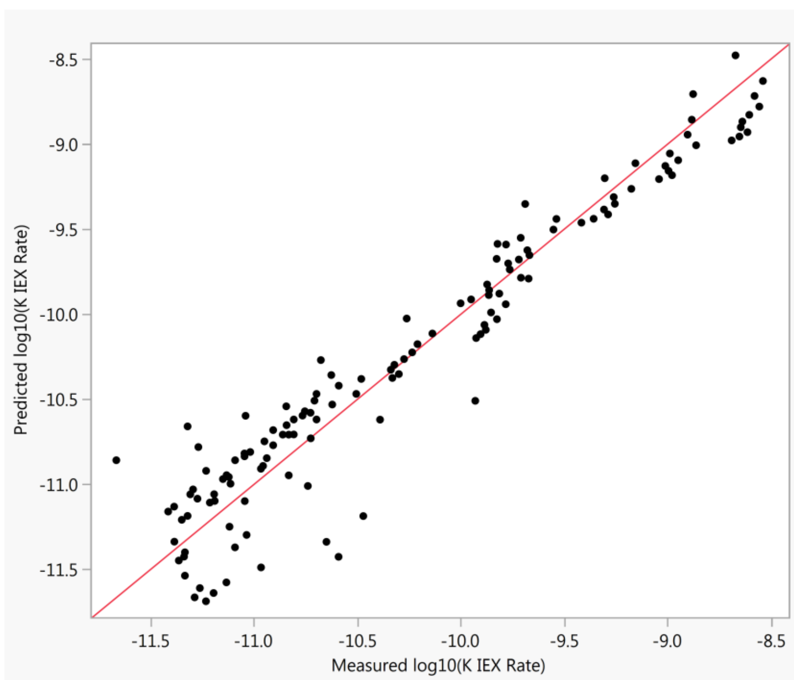

Figure 6.8. Predicted vs. measured plot for potassium ion exchange rate for ORLEC28 (Equation 1.6).

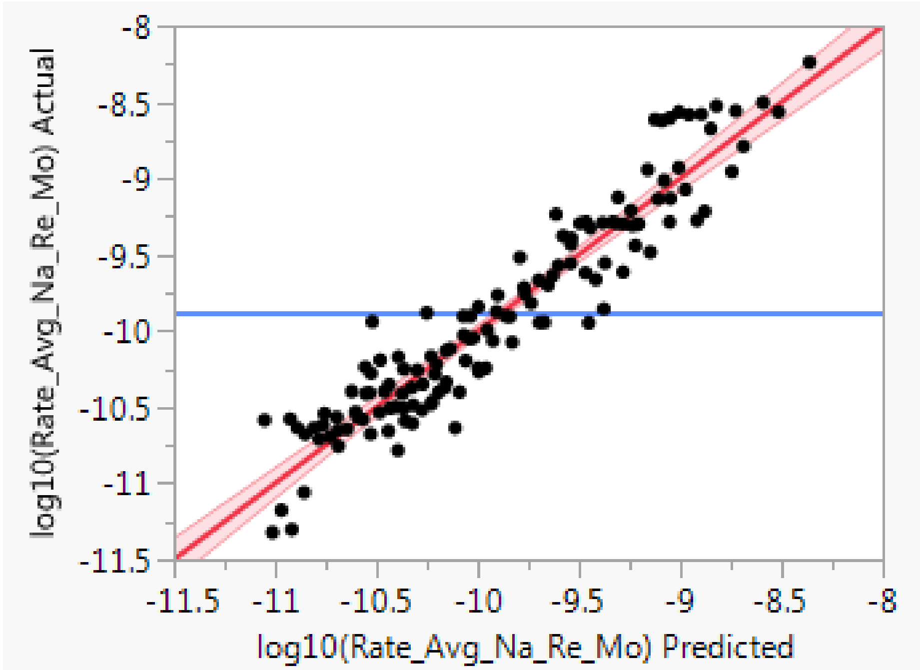

Figure 6.9. Predicted vs. measured plot for sodium ion exchange rate for LAWC22 (Equation 1.8).

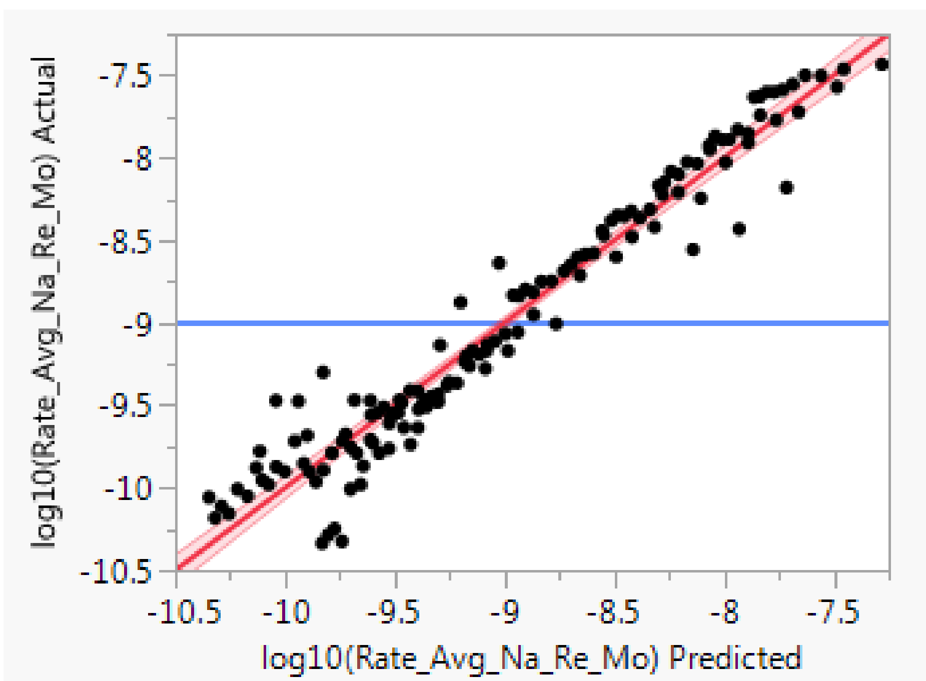

Figure 6.10. Predicted vs. measured plot for sodium ion exchange rate for ORLEC28 (Equation 1.8).

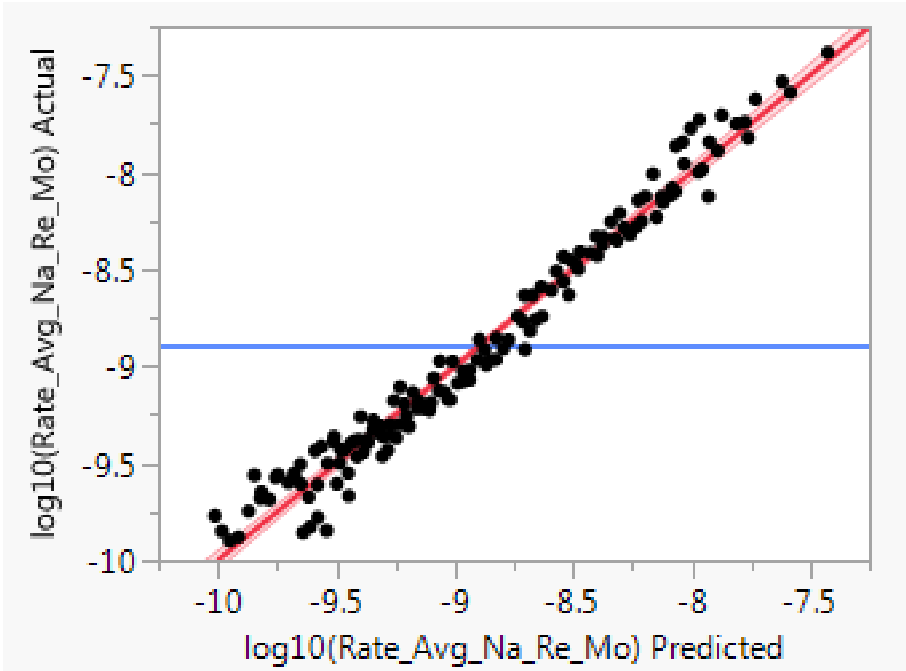

Figure 6.11. Predicted vs. measured plot for sodium ion exchange rate for IDF1B2 (Equation 1.8).

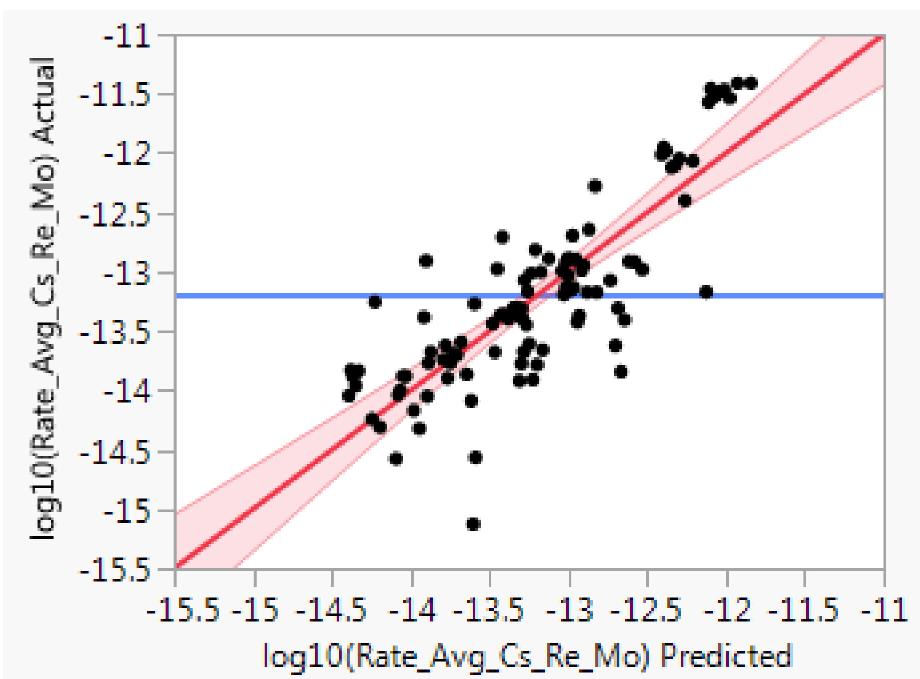

Figure 6.12. Predicted vs. measured plot for cesium ion exchange rate for LAWC22 (Equation 1.8).

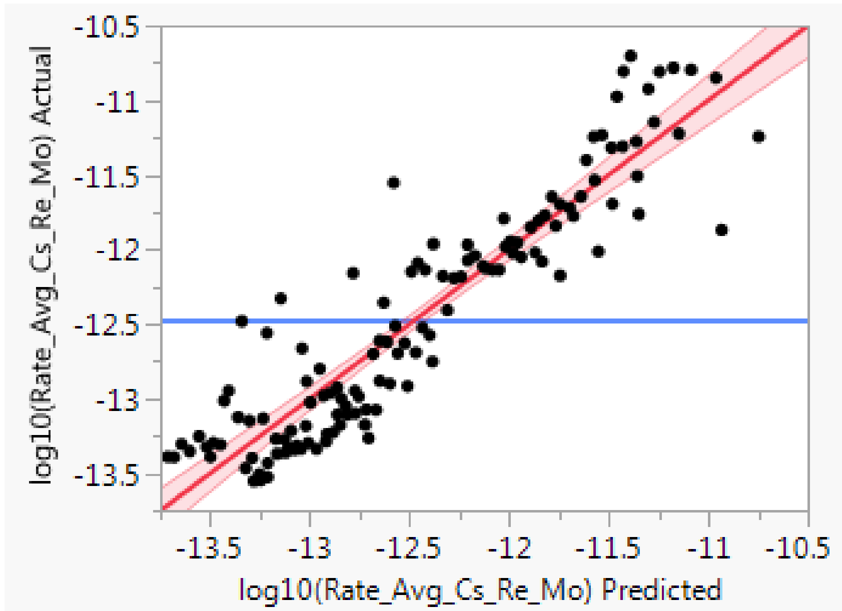

Figure 6.13. Predicted vs. measured plot for cesium ion exchange rate for ORLEC28 (Equation 1.8).

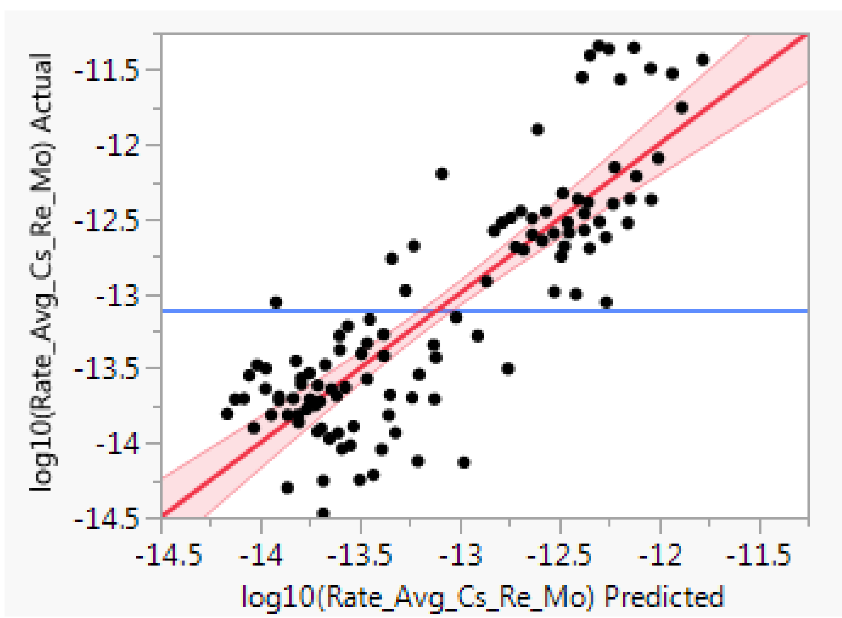

Figure 6.14. Predicted vs. measured plot for cesium ion exchange rate for IDF1B2 (Equation 1.8).

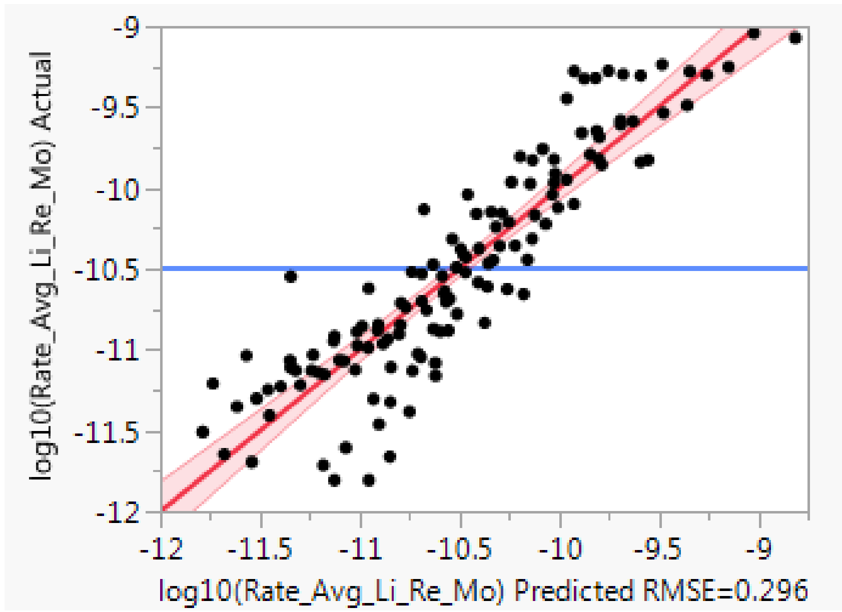

Figure 6.15. Predicted vs. measured plot for lithium ion exchange rate for LAWC22 (Equation 1.8).

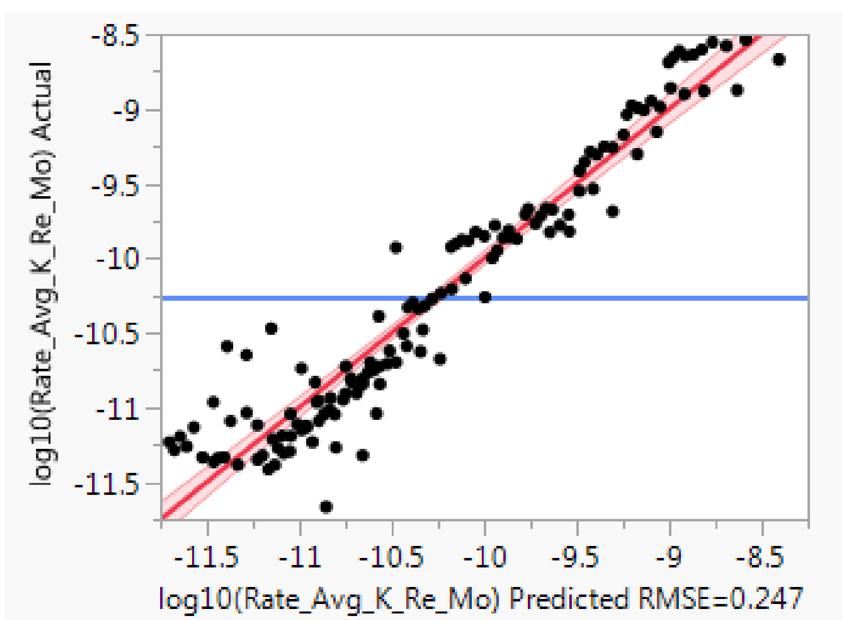

Figure 6.16. Predicted vs. measured plot for potassium ion exchange rate for ORLEC28 (Equation 1.8).

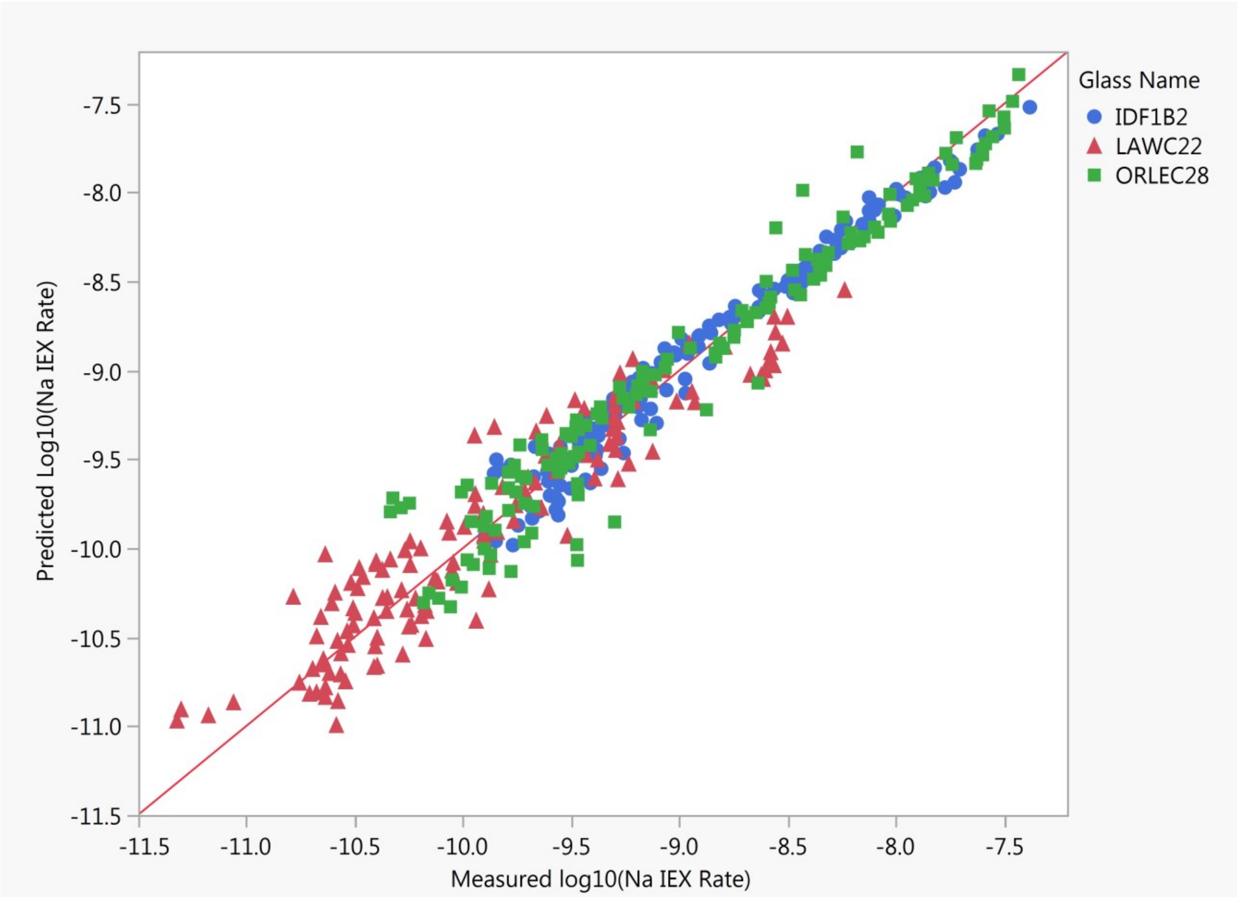

Figure 6.17. Predicted vs. measured plot for sodium ion exchange rate for all three glasses using model given by Equation 1.6.

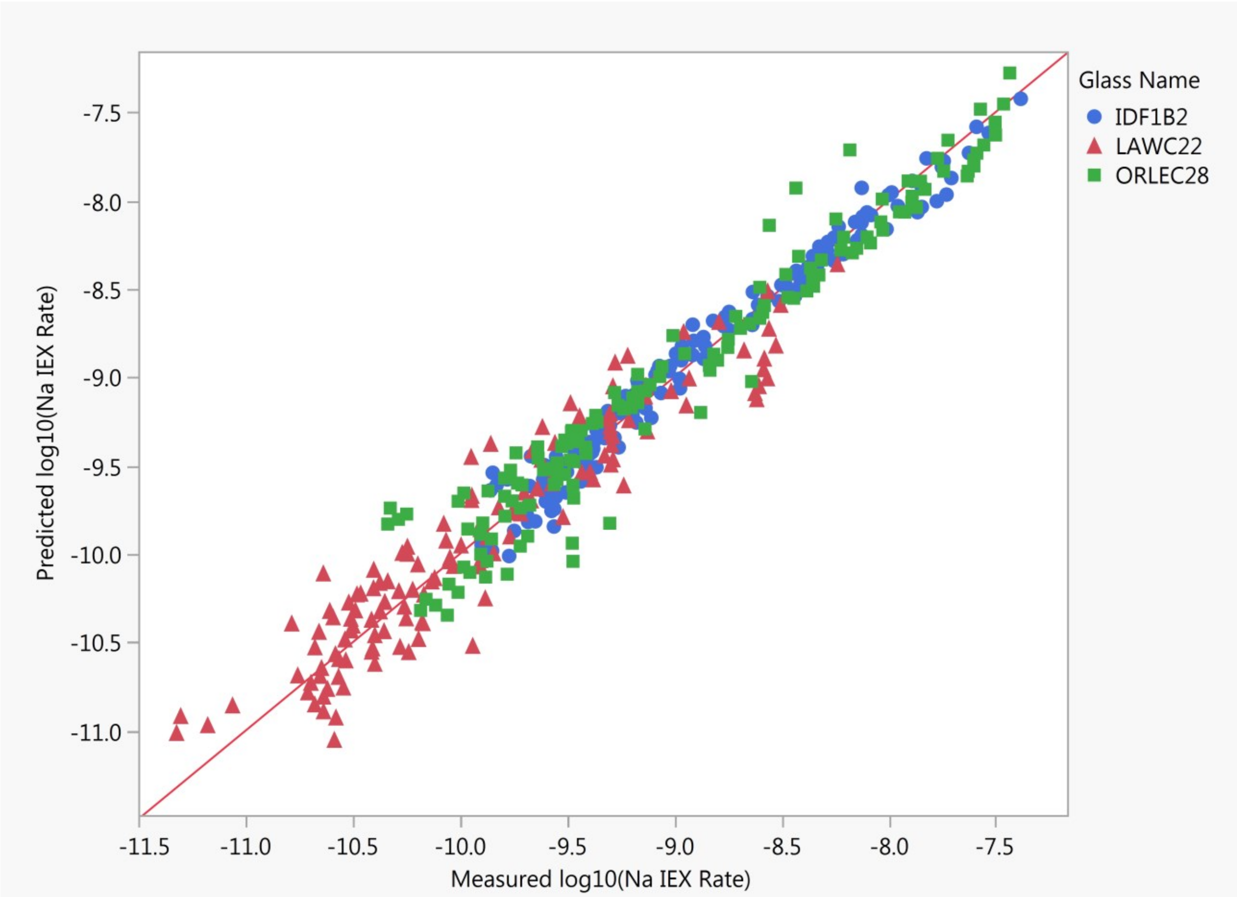

Figure 6.18. Predicted vs. measured plot for sodium ion exchange rate for all three glasses using model given by Equation 1.8.

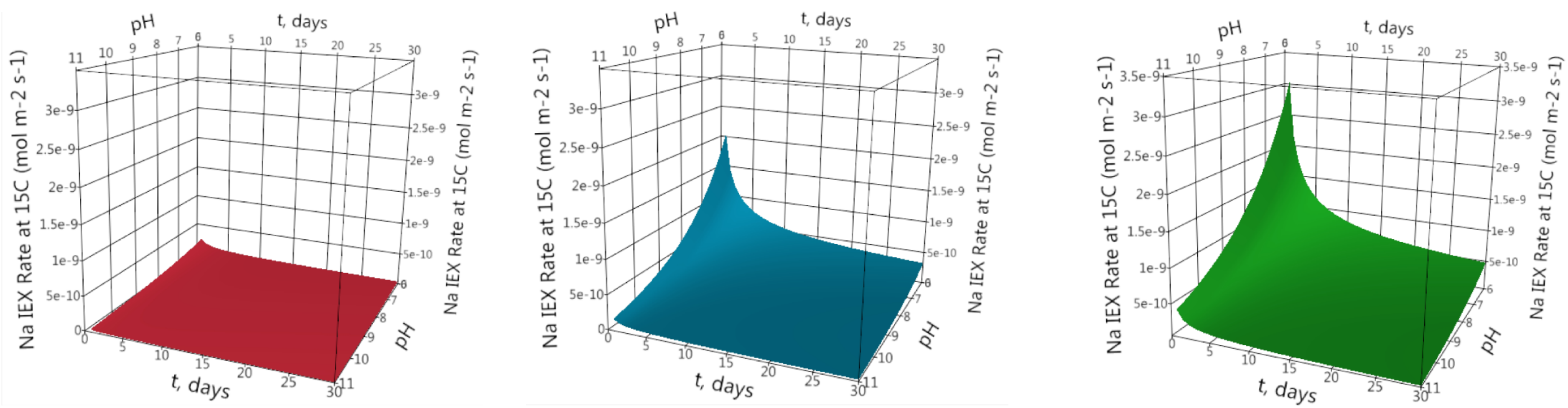

LAWC22 **ORLEC28** **IDF1B2**

Figure 6.19. Predicted sodium ion exchange rate at 15°C as a function of pH and time for the three glasses (using Equation 1.6).

APPENDIX A

SPFT TEST DATA FOR LAWC22 GLASS

Table A1. SPFT Test Results from Dissolution of Glass LAWC22 at 70 °C, dilute conditions.

Sample ID	Inf [Si] ppm	T °C	Flow Rate m^3/d	Time, days	pH 23°C	Glass Mass g	SA m^2	[B] ppm	B Rate $g\ m^{-2}\ d^{-1}$	[Li] ppm	Li Rate $g\ m^{-2}\ d^{-1}$	[Na] ppm	Na Rate $g\ m^{-2}\ d^{-1}$	[Al] ppm	Al Rate $g\ m^{-2}\ d^{-1}$	[Si] ppm	Si Rate $g\ m^{-2}\ d^{-1}$
Exp.1																	
SP-51-A1-BLK1	0	70	-	-	7	-	-	<DL	-	<DL	-	<DL	-	<DL	-	0.0760	-
SP-51-A1-BLK2	0	70	-	-	7	-	-	<DL	-	0.0020	-	0.0100	-	0.0100	-	0.0750	-
SP-51-A1-BLK3	0	70	-	-	7	-	-	<DL	-	0.0020	-	<DL	-	0.0050	-	0.0550	-
SP-51-A1-01	0	70	4.63E-05	0.88	7	1.0005	0.022	0.7760	0.0526	0.3830	0.0701	3.3880	0.0680	0.0160	0.0007	0.8090	0.0073
SP-51-A1-02	0	70	4.92E-05	1.88	7	0.9991	0.022	1.1140	0.0804	0.4810	0.0938	4.3160	0.0923	0.0320	0.0019	1.0390	0.0102
SP-51-A1-03	0	70	4.78E-05	2.88	7	0.9975	0.021	1.0440	0.0733	0.4280	0.0812	3.8000	0.0790	0.0360	0.0021	0.8380	0.0079
SP-51-A1-04	0	70	4.68E-05	3.88	7	0.9960	0.021	0.9920	0.0682	0.4030	0.0748	3.5650	0.0726	0.0400	0.0024	0.7260	0.0066
SP-51-A1-05	0	70	4.72E-05	4.88	7	0.9945	0.021	0.9330	0.0647	0.3670	0.0687	3.2390	0.0665	0.0420	0.0025	0.6310	0.0057
SP-51-A1-06	0	70	4.70E-05	5.88	7	0.9932	0.021	0.8950	0.0619	0.3450	0.0644	3.0250	0.0620	0.0430	0.0026	0.5890	0.0052
SP-51-A1-07	0	70	5.41E-05	6.88	7	0.9918	0.021	0.8030	0.0639	0.3140	0.0674	2.7290	0.0643	0.0450	0.0031	0.5380	0.0054
SP-51-A1-08	0	70	4.76E-05	7.88	7	0.9906	0.021	0.7620	0.0535	0.2950	0.0559	2.5610	0.0533	0.0440	0.0027	0.5070	0.0045
SP-51-A1-09	0	70	4.80E-05	8.88	7	0.9894	0.021	0.7630	0.0541	0.2950	0.0564	2.5620	0.0538	0.0430	0.0026	0.5030	0.0045
SP-51-A1-10	0	70	4.85E-05	9.88	7	0.9883	0.021	0.7580	0.0542	0.2920	0.0563	2.5230	0.0535	0.0440	0.0027	0.5010	0.0045
SP-51-A1-11	0	70	4.81E-05	10.88	7	0.9871	0.021	0.7430	0.0527	0.2870	0.0549	2.4770	0.0521	0.0450	0.0028	0.5010	0.0045
SP-51-A1-12	0	70	4.69E-05	11.88	8	0.9860	0.021	0.7260	0.0503	0.2860	0.0535	2.4620	0.0506	0.0490	0.0030	0.5050	0.0044
Exp.2																	
SP-51-B1-BLK1	0	70	-	-	8	-	-	<DL	-	<DL	-	<DL	-	<DL	-	0.01	-
SP-51-B1-BLK2	0	70	-	-	8	-	-	<DL	-	<DL	-	<DL	-	0.001	-	0.02	-
SP-51-B1-BLK3	0	70	-	-	8	-	-	<DL	-	<DL	-	<DL	-	<DL	-	0.02	-
SP-51-B1-02	0	70	4.76E-05	1.88	8	0.9982	0.021	0.3700	0.0257	0.2350	0.0441	2.0880	0.0433	0.1450	0.0100	1.3980	0.0141
SP-51-B1-03	0	70	4.60E-05	2.88	8	0.9974	0.021	0.3060	0.0205	0.1810	0.0326	1.6490	0.0330	0.1630	0.0108	1.3480	0.0131
SP-51-B1-04	0	70	4.52E-05	3.88	8	0.9970	0.021	0.2600	0.0171	0.1460	0.0258	1.3360	0.0263	0.1690	0.0110	1.2640	0.0121
SP-51-B1-05	0	70	4.48E-05	4.88	8	0.9967	0.021	0.2360	0.0154	0.1250	0.0218	1.1490	0.0224	0.1740	0.0113	1.2260	0.0116
SP-51-B1-06	0	70	4.65E-05	5.88	8	0.9964	0.021	0.2180	0.0147	0.1110	0.0200	1.0280	0.0208	0.1680	0.0113	1.1780	0.0116
SP-51-B1-07	0	70	5.41E-05	6.88	8	0.9960	0.021	0.1960	0.0154	0.0980	0.0205	0.9010	0.0212	0.1560	0.0122	1.0970	0.0125
SP-51-B1-08	0	70	4.78E-05	7.88	8	0.9957	0.021	0.1820	0.0126	0.0920	0.0170	0.8290	0.0173	0.1540	0.0106	1.0530	0.0106
SP-51-B1-09	0	70	4.75E-05	8.88	8	0.9955	0.021	0.1960	0.0135	0.0940	0.0173	0.8590	0.0178	0.1580	0.0109	1.1140	0.0112
SP-51-B1-10	0	70	4.70E-05	9.88	8	0.9952	0.021	0.1860	0.0127	0.0940	0.0171	0.8310	0.0170	0.1570	0.0107	1.0740	0.0107
SP-51-B1-11	0	70	4.65E-05	10.88	8	0.9949	0.021	0.1810	0.0122	0.0930	0.0167	0.8150	0.0165	0.1530	0.0103	1.0660	0.0105
SP-51-B1-12	0	70	4.93E-05	11.88	8	0.9947	0.021	0.1720	0.0123	0.0900	0.0171	0.7740	0.0166	0.1420	0.0101	1.0180	0.0106
Exp.3																	

Sample ID	Inf [Si] ppm	T °C	Flow Rate m³/d	Time, days	pH 23°C	Glass Mass g	SA m²	[B] ppm	B Rate g m⁻² d⁻¹	[Li] ppm	Li Rate g m⁻² d⁻¹	[Na] ppm	Na Rate g m⁻² d⁻¹	[Al] ppm	Al Rate g m⁻² d⁻¹	[Si] ppm	Si Rate g m⁻² d⁻¹
SP-51-C1-BLK1	0	70						<DL		<DL		0.0010		<DL		0.054	
SP-51-C1-BLK2	0	70			9			<DL		<DL		<DL		<DL		0.059	
SP-51-C1-BLK3	0	70			9			<DL		<DL		<DL		<DL		0.053	
SP-51-C1-02	0	70	5.44E-05	1.88	9	1.0009	0.022	0.5850	0.0465	0.2690	0.0575	2.3740	0.0561	0.6090	0.0480	3.9530	0.0452
SP-51-C1-03	0	70	5.47E-05	2.88	9	0.9994	0.022	0.5860	0.0469	0.2410	0.0518	2.1690	0.0516	0.6430	0.0510	4.0680	0.0468
SP-51-C1-04	0	70	5.21E-05	3.88	9	0.9984	0.022	0.5990	0.0456	0.2350	0.0481	2.0700	0.0469	0.5710	0.0431	4.1290	0.0453
SP-51-C1-05	0	70	5.40E-05	4.88	9	0.9974	0.022	0.5880	0.0465	0.2250	0.0478	1.9420	0.0456	0.5640	0.0442	4.0400	0.0460
SP-51-C1-06	0	70	5.42E-05	5.88	9	0.9964	0.021	0.5890	0.0468	0.2230	0.0475	1.9280	0.0455	0.5770	0.0454	4.0540	0.0463
SP-51-C1-07	0	70	5.07E-05	6.88	9	0.9954	0.021	0.5980	0.0445	0.2320	0.0463	2.0010	0.0442	0.6160	0.0454	4.1460	0.0444
SP-51-C1-08	0	70	5.36E-05	7.88	9	0.9945	0.021	0.5950	0.0468	0.2290	0.0483	1.9500	0.0455	0.5900	0.0459	4.0990	0.0464
SP-51-C1-09	0	70	5.38E-05	8.88	9	0.9935	0.021	0.5910	0.0467	0.2240	0.0475	1.8910	0.0444	**0.5980**	**0.0468**	4.0910	0.0466
SP-51-C1-10	0	70	5.43E-05	9.88	9	0.9925	0.021	0.5910	0.0472	0.2260	0.0484	1.9420	0.0460	**0.6060**	**0.0479**	4.0960	0.0471
SP-51-C1-11	0	70	5.31E-05	10.88	9	0.9915	0.021	0.5800	0.0453	0.2270	0.0476	1.9090	0.0443	0.2300	0.0178	3.9880	0.0448
SP-51-C1-12	0	70	5.39E-05	11.88	9	0.9905	0.021	0.5980	0.0475	0.2280	0.0486	1.9330	0.0456	**0.5920**	**0.0466**	4.0770	0.0466
Exp.4																	
SP-51-D1-BLK1	0	70						<DL		<DL		<DL		<DL		0.039	
SP-51-D1-BLK2	0	70						<DL		<DL		0.0020		<DL		0.042	
SP-51-D1-BLK3	0	70	-	-	10	-	-	<DL		<DL		<DL		<DL		0.042	
SP-51-D1-02	0	70	5.01E-05	1.88	10	0.4989	0.011	0.8710	0.1280	0.3340	0.1321	2.8710	0.1251	0.8500	0.1236	5.7050	0.1212
SP-51-D1-03	0	70	5.04E-05	2.88	10	0.4969	0.011	0.9200	0.1364	0.3350	0.1337	2.8580	0.1257	0.8300	0.1218	5.9930	0.1286
SP-51-D1-04	0	70	4.95E-05	3.88	10	0.4954	0.011	0.9610	0.1403	0.3360	0.1321	2.8630	0.1240	0.7760	0.1121	6.2280	0.1316
SP-51-D1-05	0	70	4.74E-05	4.88	10	0.4940	0.011	0.9340	0.1309	0.3410	0.1287	2.9560	0.1229	0.8350	0.1158	6.1360	0.1244
SP-51-D1-06	0	70	4.98E-05	5.88	10	0.4925	0.011	0.9500	0.1402	0.3400	0.1351	2.9180	0.1277	0.8590	0.1254	6.1940	0.1322
SP-51-D1-07	0	70	4.77E-05	6.88	10	0.4911	0.011	0.9390	0.1329	0.3500	0.1334	3.0250	0.1269	0.9280	0.1299	6.2500	0.1280
SP-51-D1-08	0	70	4.79E-05	7.88	10	0.4896	0.011	0.9500	0.1352	0.3350	0.1283	2.8870	0.1219	0.8940	0.1259	6.3110	0.1300
SP-51-D1-09	0	70	4.87E-05	8.88	10	0.4881	0.011	1.0120	0.1468	0.3650	0.1426	3.2010	0.1377	0.3320	0.0476	6.0620	0.1271
SP-51-D1-10	0	70	4.70E-05	9.88	10	0.4867	0.011	0.9370	0.1315	0.3320	0.1255	2.8370	0.1181	0.9100	0.1264	6.1970	0.1259
SP-51-D1-11	0	70	4.83E-05	10.88	10	0.4853	0.011	0.9190	0.1327	0.3380	0.1314	2.9060	0.1245	0.8930	0.1276	6.0940	0.1273
SP-51-D1-12	0	70	4.92E-05	11.88	10	0.4839	0.011	0.9210	0.1359	0.3370	0.1338	2.9000	0.1269	0.8690	0.1268	6.1390	0.1310

Exp.5																	
SP-51-E1-BLK1	0	70			11			<DL		<DL		<DL		<DL		0.40	
SP-51-E1-BLK2	0	70			11			<DL		0.009		<DL		0.1620		0.51	
SP-51-E1-BLK3	0	70	-	-	11	-	-	<DL		0.009		<DL		0.1610		0.50	
SP-51-E1-02	0	70	5.19E-05	1.88	11	0.4998	0.011	1.3740	0.2090	0.5230	0.2130	4.1860	0.1886	1.0600	0.1432	8.4560	0.1767
SP-51-E1-03	0	70	5.30E-05	2.88	11	0.4964	0.011	1.5430	0.2410	0.5890	0.2467	4.8610	0.2249	1.2370	0.1743	9.4670	0.2044
SP-51-E1-04	0	70	5.20E-05	3.88	11	0.4937	0.011	1.7370	0.2670	0.6500	0.2681	5.1170	0.2330	1.3190	0.1840	10.5760	0.2259
SP-51-E1-05	0	70	5.07E-05	4.88	11	0.4908	0.011	1.7670	0.2662	0.6720	0.2717	5.4550	0.2433	1.3590	0.1862	10.7390	0.2249
SP-51-E1-06	0	70	4.99E-05	5.88	11	0.4880	0.011	1.7980	0.2673	0.6990	0.2790	5.6170	0.2473	1.3420	0.1812	10.8110	0.2235
SP-51-E1-07	0	70	4.80E-05	6.88	11	0.4852	0.011	1.7860	0.2565	0.6760	0.2606	5.3780	0.2287	1.1960	0.1544	10.6140	0.2118
SP-51-E1-08	0	70	4.82E-05	7.88	11	0.4825	0.011	1.7640	0.2555	0.6650	0.2585	5.4330	0.2330	1.2000	0.1563	10.5450	0.2122
SP-51-E1-09	0	70	4.85E-05	8.88	11	0.4798	0.010	1.7380	0.2540	0.6670	0.2616	5.3780	0.2327	1.1110	0.1448	10.2800	0.2084
SP-51-E1-10	0	70	4.83E-05	9.88	11	0.4772	0.010	1.6990	0.2480	0.6700	0.2625	5.4410	0.2352	1.1370	0.1484	10.0670	0.2037
SP-51-E1-11	0	70	4.68E-05	10.88	11	0.4747	0.010	1.6470	0.2341	0.6530	0.2491	5.2210	0.2198	1.1120	0.1410	9.8130	0.1931
SP-51-E1-12	0	70	5.40E-05	11.88	11	0.4721	0.010	1.5720	0.2586	0.6400	0.2825	5.0710	0.2471	1.0550	0.1540	9.3990	0.2136

Table A2. SPFT Test Results from Dissolution of Glass LAWC22 at 70 °C, saturated conditions.

Sample ID	Inf [Si] ppm	T °C	Flow Rate m^3/d	Time, days	pH 23°C	Glass Mass g	SA m^2	[B] ppm	B Rate $g\ m^{-2}\ d^{-1}$	[Li] ppm	Li Rate $g\ m^{-2}\ d^{-1}$	[Na] ppm	Na Rate $g\ m^{-2}\ d^{-1}$	[K] ppm	K Rate $g\ m^{-2}\ d^{-1}$	[Al] ppm	Al Rate $g\ m^{-2}\ d^{-1}$
Exp.6																	
SP-51-A2-BLK1	55	70	-	-	7	-	-	<DL	-	0.030		0.102		0.029		0.017	-
SP-51-A2-BLK2	55	70	-	-	7	-	-	<DL	-	0.026		0.091		0.004		0.019	-
SP-51-A2-BLK3	55	70	-	-	7	-	-	<DL	-	0.026		0.091		0.003		0.018	-
SP-51-A2-02	55	70	4.91E-05	1.88	7	1.5480	0.033	1.7860	0.0831	0.4440	0.0526	6.8840	0.0936	0.0590	0.1043	0.0520	0.0016
SP-51-A2-03	55	70	5.03E-05	2.88	7	1.5441	0.033	1.6800	0.0803	0.3900	0.0470	6.0140	0.0838	0.0440	0.0729	0.0450	0.0013
SP-51-A2-04	55	70	4.75E-05	3.88	7	1.5415	0.033	1.6000	0.0722	0.3570	0.0404	5.4670	0.0718	0.0410	0.0624	0.0460	0.0012
SP-51-A2-05	55	70	4.94E-05	4.88	7	1.5392	0.033	1.4670	0.0689	0.3240	0.0378	5.0200	0.0685	0.0430	0.0694	0.0460	0.0013
SP-51-A2-06	55	70	4.81E-05	5.88	7	1.5370	0.033	1.3870	0.0636	0.3020	0.0342	4.7050	0.0626	0.0400	0.0612	0.0480	0.0014
SP-51-A2-07	55	70	5.02E-05	6.88	7	1.5349	0.033	1.3380	0.0640	0.2910	0.0342	4.4850	0.0623	0.0350	0.0525	0.0550	0.0018
SP-51-A2-08	55	70	4.92E-05	7.88	7	1.5328	0.033	1.2870	0.0603	0.2760	0.0316	4.2770	0.0581	0.0350	0.0514	0.0470	0.0013
SP-51-A2-09	55	70	4.86E-05	8.88	7	1.5309	0.033	1.2210	0.0567	0.2620	0.0296	4.0440	0.0543	0.0330	0.0465	0.0450	0.0012
SP-51-A2-10	55	70	5.01E-05	9.88	7	1.5290	0.033	1.1930	0.0570	0.2560	0.0297	3.9720	0.0549	0.0330	0.0479	0.0460	0.0013
SP-51-A2-11	55	70	4.79E-05	10.88	7	1.5272	0.033	1.1550	0.0528	0.2510	0.0278	3.8950	0.0515	0.0340	0.0480	0.0480	0.0014
SP-51-A2-12	55	70	5.05E-05	11.88	7	1.5254	0.033	1.1170	0.0539	0.2390	0.0277	3.7250	0.0519	0.0310	0.0437	0.0490	0.0015
Exp.7																	
SP-51-B2-BLK1	60	70	-	-	8	-	-	<DL	-	<DL		0.116		0.033		0.017	-
SP-51-B2-BLK2	60	70	-	-	8	-	-	<DL	-	<DL		0.108		0.002		0.020	-
SP-51-B2-BLK3	60	70	-	-	8	-	-	<DL	-	<DL		0.108		0.003		0.021	-
SP-51-B2-02	60	70	4.75E-05	1.88	8	1.5492	0.0334	0.6340	0.0284	0.3410	0.0413	3.3030	0.0426	0.0290	0.0350	0.0730	0.0024
SP-51-B2-03	60	70	5.05E-05	2.88	8	1.5479	0.0333	0.5270	0.0251	0.2470	0.0317	2.5380	0.0344	0.0280	0.0350	0.0720	0.0025
SP-51-B2-04	60	70	4.73E-05	3.88	8	1.5471	0.0333	0.4650	0.0208	0.1980	0.0237	2.0960	0.0264	0.0220	0.0200	0.0750	0.0025
SP-51-B2-05	60	70	4.77E-05	4.88	8	1.5465	0.0333	0.4190	0.0189	0.1650	0.0199	1.7820	0.0224	0.0220	0.0202	0.0690	0.0022
SP-51-B2-06	60	70	5.01E-05	5.88	8	1.5458	0.0333	0.4030	0.0191	0.1480	0.0187	1.6220	0.0213	0.0200	0.0166	0.0710	0.0024
SP-51-B2-07	60	70	4.79E-05	6.88	8	1.5452	0.0333	0.3820	0.0173	0.1370	0.0165	1.5050	0.0188	0.0220	0.0202	0.0760	0.0025
SP-51-B2-08	60	70	4.94E-05	7.88	8	1.5447	0.0333	0.3690	0.0172	0.1290	0.0160	1.4030	0.0179	0.0190	0.0142	0.0690	0.0023
SP-51-B2-09	60	70	4.77E-05	8.88	8	1.5441	0.0333	0.3540	0.0159	0.1240	0.0149	1.3430	0.0165	0.0180	0.0115	0.0710	0.0023
SP-51-B2-10	60	70	4.96E-05	9.88	8	1.5436	0.0333	0.3480	0.0163	0.1230	0.0153	1.3260	0.0170	0.0180	0.0120	0.0710	0.0024
SP-51-B2-11	60	70	4.77E-05	10.88	8	1.5431	0.0333	0.3370	0.0152	0.1180	0.0141	1.2730	0.0156	0.0180	0.0115	0.0700	0.0023
SP-51-B2-12	60	70	4.65E-05	11.88	8	1.5426	0.0333	0.3350	0.0147	0.1180	0.0138	1.2620	0.0151	0.0190	0.0133	0.0730	0.0023

Exp.8																	
SP-51-C2-BLK1	80	70	-	-	9	-	-	<DL	-	<DL		0.158		0.045		0.024	-
SP-51-C2-BLK2	80	70	-	-	9	-	-	<DL	-	<DL		0.144		0.006		0.026	-
SP-51-C2-BLK3	80	70	-	-	9	-	-	<DL	-	<DL		0.145		0.007		0.030	-
SP-51-C2-02	80	70	5.01E-05	1.88	9	1.5491	0.0333	0.3670	0.0173	0.2400	0.0305	2.3820	0.0314	0.0230	0.0374	0.0950	0.0032
SP-51-C2-03	80	70	5.17E-05	2.88	9	1.5483	0.0333	0.2700	0.0131	0.1770	0.0231	1.7980	0.0240	0.0220	0.0362	0.0850	0.0028
SP-51-C2-04	80	70	4.90E-05	3.88	9	1.5479	0.0333	0.2160	0.0099	0.1310	0.0161	1.4140	0.0174	0.0240	0.0387	0.0830	0.0026
SP-51-C2-05	80	70	5.16E-05	4.88	9	1.5476	0.0333	0.1790	0.0086	0.1040	0.0134	1.1700	0.0148	0.0180	0.0268	0.0780	0.0025
SP-51-C2-06	80	70	5.12E-05	5.88	9	1.5473	0.0333	0.1620	0.0077	0.0890	0.0113	1.0150	0.0125	0.0170	0.0243	0.0730	0.0022
SP-51-C2-07	80	70	5.17E-05	6.88	9	1.5471	0.0333	0.1620	0.0078	0.0830	0.0106	0.9810	0.0121	0.0150	0.0199	0.0770	0.0024
SP-51-C2-08	80	70	4.95E-05	7.88	9	1.5468	0.0333	0.1460	0.0067	0.0750	0.0092	0.8900	0.0103	0.0150	0.0190	0.0800	0.0025
SP-51-C2-09	80	70	5.18E-05	8.88	9	1.5466	0.0333	0.1450	0.0070	0.0720	0.0092	0.8600	0.0104	**0.0180**	**0.0270**	0.0820	0.0027
SP-51-C2-10	80	70	5.10E-05	9.88	9	1.5464	0.0333	0.1450	0.0069	0.0700	0.0088	0.8380	0.0099	**0.0160**	**0.0219**	0.0860	0.0028
SP-51-C2-11	80	70	5.00E-05	10.88	9	1.5462	0.0333	0.1440	0.0067	0.0680	0.0084	0.8190	0.0094	0.0200	0.0305	0.0930	0.0031
SP-51-C2-12	80	70	5.28E-05	11.88	9	1.5459	0.0333	0.1420	0.0070	0.0660	0.0085	0.7970	0.0096	**0.0150**	**0.0203**	0.0770	0.0025
Exp.9																	
SP-51-D2-BLK1	140	70	-	-	10	-	-	<DL	-	<DL		0.239		0.043		0.040	-
SP-51-D2-BLK2	140	70	-	-	10	-	-	<DL	-	<DL		0.232		0.011		0.035	-
SP-51-D2-BLK3	140	70	-	-	10	-	-	<DL	-	<DL		0.231		0.008		0.034	-
SP-51-D2-02	140	70	4.96E-05	1.88	10	0.9995	0.0215	0.1790	0.0128	0.1310	0.0252	1.4380	0.0260	0.0330	0.0428	0.1050	0.0049
SP-51-D2-03	140	70	4.97E-05	2.88	10	0.9992	0.0215	0.1320	0.0094	0.0960	0.0184	1.1150	0.0191	0.0160	-0.0162	0.0990	0.0045
SP-51-D2-04	140	70	4.84E-05	3.88	10	0.9990	0.0215	0.1010	0.0070	0.0750	0.0139	0.9460	0.0150	0.0170	-0.0124	0.0710	0.0024
SP-51-D2-05	140	70	5.01E-05	4.88	10	0.9989	0.0215	0.0800	0.0057	0.0610	0.0115	0.8170	0.0127	0.0160	-0.0164	0.0960	0.0043
SP-51-D2-06	140	70	5.03E-05	5.88	10	0.9988	0.0215	0.0680	0.0048	0.0530	0.0100	0.7420	0.0111	0.0170	-0.0129	0.0760	0.0029
SP-51-D2-07	140	70	4.84E-05	6.88	10	0.9987	0.0215	0.0580	0.0039	0.0470	0.0085	0.6840	0.0095	0.0160	-0.0158	0.0760	0.0028
SP-51-D2-08	140	70	5.11E-05	7.88	10	0.9986	0.0215	0.0530	0.0037	0.0410	0.0077	0.6290	0.0088	0.0160	-0.0167	0.0620	0.0019
SP-51-D2-09	140	70	5.02E-05	8.88	10	0.9985	0.0215	0.0480	0.0033	0.0380	0.0070	0.5950	0.0079	0.0140	-0.0235	0.0690	0.0024
SP-51-D2-10	140	70	5.12E-05	9.88	10	0.9984	0.0215	0.0490	0.0034	0.0380	0.0071	0.6080	0.0083	0.0160	-0.0167	0.0740	0.0028
SP-51-D2-11	140	70	5.03E-05	10.88	10	0.9984	0.0215	0.0440	0.0030	0.0330	0.0060	0.5650	0.0072	0.0170	-0.0129	0.0810	0.0033
SP-51-D2-12	140	70	4.90E-05	11.88	10	0.9983	0.0215	0.0390	0.0026	0.0320	0.0056	0.5390	0.0065	0.0160	-0.0160	0.0860	0.0035

Exp.10																	
SP-51-E2-BLK1	360	70	-	-	11	-	-	<DL	-	<DL		1.248		0.018		0.015	-
SP-51-E2-BLK2	360	70	-	-	11	-	-	<DL	-	<DL		1.317		0.021		0.018	-
SP-51-E2-BLK3	360	70	-	-	11	-	-	<DL	-	<DL		4.370		0.154		0.047	-
SP-51-E2-02	360	70	4.76E-05	1.88	11	1.0014	0.0216	0.0850	0.0057	0.0870	0.0159	2.1370	0.0177	0.0280	-0.1209	0.0600	0.0023
SP-51-E2-03	360	70	4.84E-05	2.88	11	1.0012	0.0216	0.0480	0.0032	0.0610	0.0111	1.9220	0.0134	0.0280	-0.1228	0.0470	0.0014
SP-51-E2-04	360	70	4.86E-05	3.88	11	1.0012	0.0216	0.0280	0.0018	0.0430	0.0077	1.7990	0.0109	0.0280	-0.1233	0.0410	0.0010
SP-51-E2-05	360	70	4.81E-05	4.88	11	1.0012	0.0216	0.0130	0.0007	0.0310	0.0053	1.6820	0.0083	0.0280	-0.1222	0.0320	0.0004
SP-51-E2-06	360	70	4.80E-05	5.88	11	1.0011	0.0216	0.0020	-0.0001	0.0240	0.0040	1.6030	0.0067	0.0330	-0.1052	0.0340	0.0005
SP-51-E2-07	360	70	4.75E-05	6.88	11	1.0011	0.0216	0.0150	0.0008	0.0200	0.0032	1.5070	0.0046	0.0260	-0.1272	0.0000	-0.0018
SP-51-E2-08	360	70	4.85E-05	7.88	11	1.0011	0.0216	0.0033	0.0000	0.0160	0.0025	1.5460	0.0055	0.0270	-0.1265	0.0280	0.0001
SP-51-E2-09	360	70	4.70E-05	8.88	11	1.0012	0.0216	0.0033	0.0000	0.0140	0.0020	1.5310	0.0051	0.0290	-0.1162	0.0330	0.0004
SP-51-E2-10	360	70	4.79E-05	9.88	11	1.0012	0.0216	0.0033	0.0000	0.0120	0.0017	1.5100	0.0047	0.0300	-0.1150	0.0270	0.0000
SP-51-E2-11	360	70	4.75E-05	10.88	11	1.0012	0.0216	0.0033	0.0000	0.0110	0.0015	1.5220	0.0049	0.0280	-0.1205	0.0340	0.0005
SP-51-E2-12	360	70	4.71E-05	11.88	11	1.0012	0.0216	0.0033	0.0000	0.0100	0.0013	1.5070	0.0046	0.0290	-0.1163	0.0310	0.0003

Table A3. SPFT Test Results from Dissolution of Glass LAWC22 at 40 °C, dilute conditions.

Sample ID	Inf [Si] ppm	T °C	Flow Rate m^3/d	Time, days	pH 23°C	Glass Mass g	SA m^2	[B] ppm	B Rate $g\ m^{-2}\ d^{-1}$	[Li] ppm	Li Rate $g\ m^{-2}\ d^{-1}$	[Na] ppm	Na Rate $g\ m^{-2}\ d^{-1}$	[Al] ppm	Al Rate $g\ m^{-2}\ d^{-1}$	[Si] ppm	Si Rate $g\ m^{-2}\ d^{-1}$
Exp.11																	
SP-52-A1-BLK1	0	40			7			<DL		<DL		<DL		0.0010		0.0640	
SP-52-A1-BLK2	0	40			7			<DL		<DL		<DL		0.0040		0.0730	
SP-52-A1-BLK3	0	40			7			<DL		<DL		<DL		0.0410		0.0680	
SP-52-A1-02	0	40	3.97E-05	1.92	7	0.9963	0.021	0.1900	0.0109	0.1160	0.0179	0.9800	0.0169	0.0050	0.0001	0.2750	0.0018
SP-52-A1-04	0	40	3.82E-05	3.92	7	0.9959	0.021	0.1190	0.0065	0.0670	0.0098	0.5620	0.0094	0.0060	0.0002	0.2230	0.0013
SP-52-A1-06	0	40	3.69E-05	5.92	7	0.9957	0.021	0.0840	0.0044	0.0460	0.0063	0.3830	0.0062	0.0080	0.0003	0.1940	0.0010
SP-52-A1-08	0	40	3.71E-05	7.92	7	0.9955	0.021	0.0660	0.0034	0.0350	0.0047	0.3020	0.0049	0.0090	0.0003	0.1740	0.0008
SP-52-A1-10	0	40	3.63E-05	9.92	7	0.9954	0.021	0.0570	0.0029	0.0290	0.0038	0.2500	0.0040	0.0100	0.0004	0.1650	0.0008
SP-52-A1-12	0	40	3.77E-05	11.92	7	0.9953	0.021	0.0490	0.0025	0.0260	0.0035	0.2270	0.0037	0.0110	0.0005	0.1550	0.0007
SP-52-A1-14	0	40	3.74E-05	13.92	7	0.9952	0.021	0.0430	0.0022	0.0220	0.0028	0.1940	0.0032	0.0090	0.0004	0.1530	0.0007
SP-52-A1-16	0	40	3.78E-05	15.92	7	0.9951	0.021	0.0390	0.0020	0.0200	0.0026	0.1810	0.0030	0.0100	0.0004	0.1510	0.0007
SP-52-A1-18	0	40	3.84E-05	17.92	7	0.9950	0.021	0.0370	0.0019	0.0190	0.0024	0.1670	0.0028	0.0100	0.0004	0.1540	0.0007
SP-52-A1-20	0	40	3.86E-05	19.92	7	0.9949	0.021	0.0300	0.0015	0.0170	0.0021	0.1490	0.0025	0.0060	0.0002	0.1130	0.0004
SP-52-A1-22	0	40	0.00E+00	21.92	7	0.9949	0.021	0.0370	0.0000	0.0200	0.0000	0.1780	0.0000	0.0090	0.0000	0.1000	0.0000
SP-52-A1-24	0	40	3.58E-05	23.92	8	0.9948	0.021	0.0860	0.0044	0.0390	0.0051	0.3370	0.0053	0.0150	0.0006	0.1540	0.0007
Exp.12																	
SP-52-B1-BLK1	0	40			8			<DL		<DL		<DL		0.004		0.02	
SP-52-B1-BLK2	0	40			8			<DL		<DL		<DL		0.002		0.03	
SP-52-B1-BLK3	0	40			8			<DL		<DL		0.003		0.004		0.04	
SP-52-B1-04	0	40	3.84E-05	3.92	8	1.0005	0.022	0.0620	0.0033	0.0470	0.0067	0.3930	0.0065	0.0290	0.0014	0.2440	0.0017
SP-52-B1-06	0	40	3.71E-05	5.92	8	1.0003	0.022	0.0410	0.0021	0.0300	0.0040	0.2600	0.0042	0.0290	0.0014	0.2130	0.0014
SP-52-B1-08	0	40	3.75E-05	7.92	8	1.0002	0.022	0.0290	0.0014	0.0220	0.0028	0.1930	0.0031	0.0270	0.0013	0.1900	0.0013
SP-52-B1-10	0	40	3.70E-05	9.92	8	1.0001	0.022	0.0220	0.0010	0.0180	0.0022	0.1600	0.0025	0.0250	0.0012	0.1750	0.0011
SP-52-B1-12	0	40	3.74E-05	11.92	8	1.0001	0.022	0.0190	0.0009	0.0160	0.0019	0.1450	0.0023	0.0260	0.0012	0.1620	0.0010
SP-52-B1-14	0	40	3.72E-05	13.92	8	1.0001	0.022	0.0170	0.0008	0.0140	0.0016	0.1310	0.0021	0.0230	0.0011	0.1620	0.0010
SP-52-B1-16	0	40	3.76E-05	15.92	8	1.0000	0.022	0.0140	0.0006	0.0130	0.0015	0.1230	0.0020	0.0230	0.0011	0.1510	0.0010
SP-52-B1-18	0	40	3.75E-05	17.92	8	1.0000	0.022	**0.0130**	**0.0005**	0.0120	0.0013	0.1160	0.0019	0.0220	0.0010	0.1500	0.0010
SP-52-B1-20	0	40	3.73E-05	19.92	8	1.0000	0.022	**0.0140**	**0.0006**	0.0120	0.0013	0.1150	0.0018	0.0210	0.0010	0.1460	0.0009
SP-52-B1-22	0	40	3.85E-05	21.92	8	1.0000	0.022	**0.0120**	**0.0005**	0.0110	0.0012	0.1060	0.0017	0.0210	0.0010	0.1310	0.0008
SP-52-B1-24	0	40	3.53E-05	23.92	8	0.9999	0.022	0.0190	0.0008	0.0140	0.0015	0.1320	0.0020	0.0270	0.0012	0.1680	0.0010
Exp.13																	

Sample ID	Inf [Si] ppm	T °C	Flow Rate m^3/d	Time, days	pH 23°C	Glass Mass g	SA m^2	[B] ppm	B Rate $g\ m^{-2}\ d^{-1}$	[Li] ppm	Li Rate $g\ m^{-2}\ d^{-1}$	[Na] ppm	Na Rate $g\ m^{-2}\ d^{-1}$	[Al] ppm	Al Rate $g\ m^{-2}\ d^{-1}$	[Si] ppm	Si Rate $g\ m^{-2}\ d^{-1}$
SP-52-C1-BLK1	0	40						<DL		<DL		<DL		0.002		0.030	
SP-52-C1-BLK2	0	40			9			<DL		<DL		<DL		0.002		0.029	
SP-51-C1-BLK3	0	40			9			<DL		<DL		<DL		0.003		0.030	
SP-52-C1-04	0	40	4.46E-05	3.92	9	0.9993	0.022	0.1180	0.0075	0.0550	0.0092	0.4560	0.0088	0.1150	0.0073	0.8320	0.0076
SP-52-C1-06	0	40	4.33E-05	5.92	9	0.9988	0.022	0.1120	0.0069	0.0500	0.0081	0.4260	0.0080	0.1280	0.0079	0.8530	0.0076
SP-52-C1-08	0	40	4.32E-05	7.92	9	0.9985	0.021	0.1450	0.0090	0.0600	0.0098	0.4900	0.0092	0.0530	0.0032	1.1050	0.0099
SP-52-C1-10	0	40	4.26E-05	9.92	9	0.9981	0.021	0.1110	0.0068	0.0440	0.0069	0.3690	0.0068	0.1360	0.0083	0.8810	0.0077
SP-52-C1-12	0	40	4.32E-05	11.92	9	0.9979	0.021	0.1030	0.0064	0.0440	0.0071	0.3730	0.0070	0.1300	0.0080	0.8290	0.0074
SP-52-C1-14	0	40	4.25E-05	13.92	9	0.9976	0.021	0.1060	0.0064	0.0430	0.0068	0.3460	0.0064	0.1180	0.0071	0.8520	0.0075
SP-52-C1-16	0	40	4.26E-05	15.92	9	0.9973	0.021	0.0980	0.0059	0.0380	0.0059	0.3250	0.0060	0.1010	0.0061	0.7830	0.0069
SP-52-C1-18	0	40	4.24E-05	17.92	9	0.9971	0.021	0.1000	0.0060	0.0420	0.0066	0.3470	0.0064	0.1200	0.0072	0.8090	0.0071
SP-52-C1-20	0	40	4.21E-05	19.92	9	0.9968	0.021	0.0990	0.0059	0.0430	0.0067	0.3510	0.0064	0.1200	0.0072	0.8330	0.0072
SP-52-C1-22	0	40	4.20E-05	21.92	9	0.9965	0.021	0.0970	0.0058	0.0410	0.0064	0.3390	0.0062	0.1170	0.0070	0.8450	0.0073
Exp.14																	
SP-52-D1-BLK1	0	40						<DL		<DL		0.003		<DL		0.023	
SP-52-D1-BLK2	0	40						<DL		<DL		<DL		0.001		0.031	
SP-52-D1-BLK3	0	40	-	-	10	-	-	<DL		<DL		0.022		0.008		0.053	
SP-52-D1-04	0	40	3.94E-05	3.92	10	0.5000	0.011	0.2270	0.0259	0.0870	0.0263	0.6940	0.0235	0.2180	0.0246	1.5760	0.0259
SP-52-D1-06	0	40	3.84E-05	5.92	10	0.4991	0.011	0.2350	0.0262	0.0860	0.0253	0.6910	0.0228	0.2100	0.0230	1.6250	0.0260
SP-52-D1-08	0	40	3.87E-05	7.92	10	0.4985	0.011	0.2440	0.0275	0.0880	0.0262	0.7060	0.0235	0.0790	0.0085	1.6140	0.0261
SP-52-D1-10	0	40	3.82E-05	9.92	10	0.4980	0.011	0.2280	0.0253	0.0870	0.0256	0.6960	0.0229	0.2200	0.0241	1.5760	0.0252
SP-52-D1-12	0	40	3.84E-05	11.92	10	0.4974	0.011	0.2230	0.0249	0.0850	0.0251	0.6900	0.0228	0.2210	0.0243	1.5720	0.0252
SP-52-D1-14	0	40	3.82E-05	13.92	10	0.4969	0.011	0.2250	0.0250	0.0860	0.0253	0.6890	0.0227	0.2080	0.0228	1.5730	0.0252
SP-52-D1-16	0	40	3.84E-05	15.92	10	0.4964	0.011	0.2160	0.0241	0.0830	0.0246	0.6700	0.0222	0.2100	0.0232	1.5240	0.0245
SP-52-D1-18	0	40	3.83E-05	17.92	10	0.4959	0.011	0.2200	0.0246	0.0840	0.0248	0.6770	0.0224	0.2040	0.0225	1.5450	0.0248
SP-52-D1-20	0	40	3.82E-05	19.92	10	0.4953	0.011	0.2190	0.0244	0.0860	0.0254	0.6850	0.0226	0.2110	0.0232	1.5450	0.0248
SP-52-D1-22	0	40	4.09E-05	21.92	10	0.4948	0.011	0.2140	0.0255	0.0820	0.0259	0.6630	0.0234	0.2040	0.0240	1.5200	0.0261
SP-52-D1-24	0	40	3.64E-05	23.92	10	0.4942	0.011	0.2940	0.0314	0.1170	0.0333	0.9500	0.0301	0.2880	0.0303	2.0150	0.0310

Exp.15																	
SP-52-E1-BLK1	0	40			11			<DL		0.012		<DL		<DL		0.48	
SP-52-E1-BLK2	0	40			11			<DL		0.013		<DL		0.0540		0.56	
SP-52-E1-BLK3	0	40	-	-	11	-	-	<DL		0.013		<DL		0.0550		0.57	
SP-52-E1-04	0	40	4.29E-05	3.92	11	0.4985	0.011	0.5740	0.0722	0.2250	0.0727	1.7810	0.0666	0.5040	0.0583	4.1890	0.0671
SP-52-E1-06	0	40	4.14E-05	5.92	11	0.4962	0.011	0.5800	0.0705	0.2210	0.0690	1.7370	0.0628	0.4910	0.0548	4.2220	0.0654
SP-52-E1-08	0	40	4.15E-05	7.92	11	0.4947	0.011	0.5470	0.0669	0.2130	0.0667	1.6790	0.0610	0.4900	0.0550	4.0090	0.0620
SP-52-E1-10	0	40	4.07E-05	9.92	11	0.4933	0.011	0.5260	0.0632	0.2080	0.0639	1.6240	0.0580	0.4840	0.0533	3.8890	0.0588
SP-52-E1-12	0	40	4.07E-05	11.92	11	0.4920	0.011	0.4920	0.0591	0.2010	0.0617	1.5830	0.0566	0.4420	0.0484	3.6680	0.0550
SP-52-E1-14	0	40	4.03E-05	13.92	11	0.4908	0.011	0.4610	0.0550	0.1850	0.0560	1.4400	0.0511	0.4130	0.0446	3.4930	0.0515
SP-52-E1-16	0	40	4.01E-05	15.92	11	0.4897	0.011	0.4450	0.0529	0.1780	0.0536	1.3570	0.0480	0.3940	0.0422	3.4020	0.0498
SP-52-E1-18	0	40	3.98E-05	17.92	11	0.4886	0.011	0.4050	0.0478	0.1670	0.0497	1.2660	0.0445	0.3440	0.0361	3.1410	0.0450
SP-52-E1-20	0	40	4.22E-05	19.92	11	0.4875	0.011	0.4430	0.0555	0.1730	0.0548	1.3460	0.0502	0.4040	0.0458	3.3000	0.0507
SP-52-E1-22	0	40	3.93E-05	21.92	11	0.4864	0.011	0.4730	0.0553	0.1770	0.0524	1.4310	0.0498	0.4270	0.0453	3.3070	0.0473
SP-52-E1-24	0	40	3.71E-05	23.92	11	0.4851	0.011	0.5980	0.0661	0.2310	0.0657	1.9500	0.0641	0.5480	0.0561	3.9700	0.0554

Table A4. SPFT Test Results from Dissolution of Glass LAWC22 at 40 °C, saturated conditions.

Sample ID	Inf [Si] ppm	T °C	Flow Rate m^3/d	Time, days	pH 23°C	Glass Mass g	SA m^2	[B] ppm	B Rate $g\ m^{-2}\ d^{-1}$	[Li] ppm	Li Rate $g\ m^{-2}\ d^{-1}$	[Na] ppm	Na Rate $g\ m^{-2}\ d^{-1}$	[K] ppm	K Rate $g\ m^{-2}\ d^{-1}$	[Al] ppm	Al Rate $g\ m^{-2}\ d^{-1}$
Exp.16																	
SP-52-A2-BLK1	40	40	-	-	7	-	-	<DL	-	0.031		0.060		0.011		0.015	-
SP-52-A2-BLK2	40	40	-	-	7	-	-	<DL	-	0.015		0.060		0.007		0.015	-
SP-52-A2-BLK3	40	40	-	-	7	-	-	<DL	-	0.015		0.069		0.008		0.017	-
SP-52-A2-04	40	40	1.01E-05	3.92	7	1.9996	0.043	0.5050	0.0037	0.2720	0.0051	2.5790	0.0055	0.0240	0.0054	0.0290	0.0001
SP-52-A2-06	40	40	9.81E-06	5.92	7	1.9991	0.043	0.5250	0.0038	0.2670	0.0048	2.5480	0.0053	0.0340	0.0087	0.0310	0.0001
SP-52-A2-08	40	40	1.01E-05	7.92	7	1.9988	0.043	0.4880	0.0036	0.2370	0.0043	2.2980	0.0049	0.0170	0.0029	0.0280	0.0001
SP-52-A2-10	40	40	9.84E-06	9.92	7	1.9985	0.043	0.4510	0.0032	0.2130	0.0038	2.0900	0.0043	0.0170	0.0029	0.0290	0.0001
SP-52-A2-12	40	40	9.79E-06	11.92	7	1.9982	0.043	0.4190	0.0030	0.1910	0.0033	1.9110	0.0039	0.0210	0.0042	0.0330	0.0001
SP-52-A2-14	40	40	9.94E-06	13.92	7	1.9980	0.043	0.3800	0.0028	0.1690	0.0029	1.7110	0.0036	0.0180	0.0032	0.0300	0.0001
SP-52-A2-16	40	40	9.68E-06	15.92	7	1.9978	0.043	0.3590	0.0025	0.1530	0.0026	1.5680	0.0032	0.0430	0.0116	0.0320	0.0001
SP-52-A2-18	40	40	9.72E-06	17.92	7	1.9975	0.043	0.3380	0.0024	0.1420	0.0024	1.4640	0.0030	**0.0160**	**0.0025**	0.0340	0.0001
SP-52-A2-20	40	40	9.68E-06	19.92	7	1.9973	0.043	0.3190	0.0022	0.1310	0.0021	1.3570	0.0027	0.0180	0.0032	0.0330	0.0001
SP-52-A2-22	40	40	9.71E-06	21.92	7	1.9972	0.043	0.3080	0.0022	0.1230	0.0020	1.2900	0.0026	**0.0150**	**0.0022**	0.0350	0.0001
SP-52-A2-24	40	40	9.60E-06	23.92	7	1.9970	0.043	0.3000	0.0021	0.1170	0.0019	1.2310	0.0024	**0.0140**	**0.0018**	0.0350	0.0001
Exp.17																	
SP-52-B2-BLK1	45	40	-	-	8	-	-	<DL	-	<DL		0.077		0.008		0.018	-
SP-52-B2-BLK2	45	40	-	-	8	-	-	<DL	-	0.003		0.077		0.015		0.023	-
SP-52-B2-BLK3	45	40	-	-	8	-	-	<DL	-	0.005		0.079		0.017		0.017	-
SP-52-B2-04	45	40	9.84E-06	3.92	8	1.9998	0.0430	0.3020	0.0022	0.1900	0.0036	1.9040	0.0039	0.0250	0.0040	0.0610	0.0003
SP-52-B2-06	45	40	9.58E-06	5.92	8	1.9995	0.0430	0.3030	0.0021	0.1870	0.0035	1.8560	0.0037	0.0180	0.0016	0.0550	0.0002
SP-52-B2-08	45	40	9.76E-06	7.92	8	1.9994	0.0430	0.2760	0.0020	0.1660	0.0032	1.6530	0.0033	0.0150	0.0006	0.0560	0.0003
SP-52-B2-10	45	40	9.63E-06	9.92	8	1.9992	0.0430	0.2510	0.0018	0.1490	0.0028	1.5060	0.0030	0.0150	0.0006	0.0530	0.0002
SP-52-B2-12	45	40	9.46E-06	11.92	8	1.9991	0.0430	0.2270	0.0016	0.1330	0.0024	1.3650	0.0026	0.0140	0.0002	0.0530	0.0002
SP-52-B2-14	45	40	9.58E-06	13.92	8	1.9989	0.0430	0.2030	0.0014	0.1170	0.0022	1.2090	0.0024	0.0150	0.0006	0.0520	0.0002
SP-52-B2-16	45	40	9.42E-06	15.92	8	1.9988	0.0430	0.1820	0.0012	0.1040	0.0019	1.1050	0.0021	0.0200	0.0022	0.0510	0.0002
SP-52-B2-18	45	40	9.32E-06	17.92	8	1.9987	0.0430	0.1690	0.0011	0.0950	0.0017	1.0320	0.0019	0.0550	0.0136	0.0510	0.0002
SP-52-B2-20	45	40	9.40E-06	19.92	8	1.9986	0.0430	0.1510	0.0010	0.0860	0.0015	0.9220	0.0017	0.0150	0.0005	0.0500	0.0002
SP-52-B2-22	45	40	9.32E-06	21.92	8	1.9985	0.0430	0.1420	0.0010	0.0790	0.0014	0.8630	0.0016	0.0120	-0.0004	0.0490	0.0002
SP-52-B2-24	45	40	9.13E-06	23.92	8	1.9985	0.0430	0.1350	0.0009	0.0740	0.0013	0.8080	0.0015	0.0100	-0.0011	0.0500	0.0002
Exp.18																	

Sample ID	**Inf [Si] ppm**	**T °C**	**Flow Rate m^3/d**	**Time, days**	**pH 23°C**	**Glass Mass g**	**SA m^2**	**[B] ppm**	**B Rate $g\ m^{-2}\ d^{-1}$**	**[Li] ppm**	**Li Rate $g\ m^{-2}\ d^{-1}$**	**[Na] ppm**	**Na Rate $g\ m^{-2}\ d^{-1}$**	**[K] ppm**	**K Rate $g\ m^{-2}\ d^{-1}$**	**[Al] ppm**	**Al Rate $g\ m^{-2}\ d^{-1}$**
SP-52-C2-BLK1	60	40	-	-	9	-	-	<DL	-	<DL		0.097		0.007		0.022	-
SP-52-C2-BLK2	60	40	-	-	9	-	-	<DL	-	<DL		0.097		0.006		0.023	-
SP-52-C2-BLK3	60	40	-	-	9	-	-	<DL	-	<DL		0.100		0.009		0.024	-
SP-52-C2-04	60	40	1.06E-05	3.92	9	2.0013	0.0431	0.2440	0.0019	0.1580	0.0033	1.6110	0.0035	0.0160	0.0032	0.0740	0.0004
SP-52-C2-06	60	40	1.02E-05	5.92	9	2.0011	0.0431	0.2560	0.0019	0.1580	0.0031	1.5930	0.0033	0.0140	0.0024	0.0760	0.0004
SP-52-C2-08	60	40	1.04E-05	7.92	9	2.0009	0.0431	0.2320	0.0017	0.1390	0.0028	1.4300	0.0030	0.0140	0.0024	0.0700	0.0004
SP-52-C2-10	60	40	1.02E-05	9.92	9	2.0008	0.0431	0.2120	0.0016	0.1260	0.0025	1.3060	0.0027	0.0140	0.0024	0.0680	0.0003
SP-52-C2-12	60	40	9.99E-06	11.92	9	2.0007	0.0431	0.1850	0.0013	0.1100	0.0021	1.1810	0.0024	0.0120	0.0016	0.0640	0.0003
SP-52-C2-14	60	40	1.01E-05	13.92	9	2.0006	0.0431	0.1670	0.0012	0.0970	0.0019	1.0530	0.0021	0.0260	0.0066	0.0610	0.0003
SP-52-C2-16	60	40	9.96E-06	15.92	9	2.0005	0.0431	0.1490	0.0011	0.0870	0.0017	0.9510	0.0018	0.0120	0.0016	0.0570	0.0002
SP-52-C2-18	60	40	9.81E-06	17.92	9	2.0004	0.0431	0.1340	0.0009	0.0790	0.0015	0.8780	0.0017	**0.0140**	**0.0023**	0.0580	0.0002
SP-52-C2-20	60	40	9.66E-06	19.92	9	2.0003	0.0431	0.1200	0.0008	0.0710	0.0013	0.8010	0.0015	**0.0150**	**0.0026**	0.0560	0.0002
SP-52-C2-22	60	40	1.01E-05	21.92	9	2.0002	0.0431	0.1110	0.0008	0.0650	0.0012	0.7500	0.0014	**0.0120**	**0.0016**	0.0550	0.0002
SP-52-C2-24	60	40	9.59E-06	23.92	9	2.0002	0.0431	0.1030	0.0007	0.0610	0.0011	0.7090	0.0013	0.0090	0.0006	0.0540	0.0002
Exp.19																	
SP-52-D2-BLK1	105	40	-	-	10	-	-	<DL	-	<DL		0.169		0.017		0.044	-
SP-52-D2-BLK2	105	40	-	-	10	-	-	<DL	-	<DL		0.171		0.017		0.041	-
SP-52-D2-BLK3	105	40	-	-	10	-	-	<DL	-	<DL		0.173		0.018		0.042	-
SP-52-D2-04	105	40	1.02E-05	3.92	10	1.0008	0.0215	0.1310	0.0019	0.0790	0.0031	0.9260	0.0033	0.0170	-0.0002	0.0830	0.0006
SP-52-D2-06	105	40	1.00E-05	5.92	10	1.0007	0.0215	0.1500	0.0022	0.0850	0.0033	0.9800	0.0035	0.0160	-0.0009	0.0930	0.0007
SP-52-D2-08	105	40	1.02E-05	7.92	10	1.0006	0.0215	0.1390	0.0020	0.0780	0.0030	0.9000	0.0032	0.0160	-0.0009	0.0890	0.0007
SP-52-D2-10	105	40	1.01E-05	9.92	10	1.0005	0.0215	0.1250	0.0018	0.0710	0.0027	0.8340	0.0029	0.0160	-0.0009	0.0770	0.0005
SP-52-D2-12	105	40	9.92E-06	11.92	10	1.0004	0.0215	0.1150	0.0016	0.0650	0.0024	0.7820	0.0026	0.0160	-0.0009	0.0820	0.0006
SP-52-D2-14	105	40	1.01E-05	13.92	10	1.0004	0.0215	0.0970	0.0014	0.0570	0.0022	0.7010	0.0023	0.0180	0.0005	0.0690	0.0004
SP-52-D2-16	105	40	9.98E-06	15.92	10	1.0003	0.0215	0.0860	0.0012	0.0500	0.0019	0.6550	0.0021	0.0160	-0.0009	0.0710	0.0004
SP-52-D2-18	105	40	9.91E-06	17.92	10	1.0003	0.0215	0.0750	0.0010	0.0460	0.0017	0.6090	0.0019	**0.0210**	**0.0025**	0.0630	0.0003
SP-52-D2-20	105	40	1.01E-05	19.92	10	1.0002	0.0215	0.0650	0.0009	0.0420	0.0016	0.5860	0.0018	0.0710	0.0379	0.0680	0.0004
SP-52-D2-22	105	40	9.94E-06	21.92	10	1.0002	0.0215	0.0570	0.0008	0.0380	0.0014	0.5280	0.0015	**0.0180**	**0.0005**	0.0610	0.0003
SP-52-D2-24	105	40	9.76E-06	23.92	10	1.0002	0.0215	0.0510	0.0007	0.0350	0.0012	0.5060	0.0014	**0.0220**	**0.0032**	0.0600	0.0003

Exp.20																	
SP-52-E2-BLK1	270	40	-	-	11	-	-	<DL	-	<DL		0.882		0.017		0.021	-
SP-52-E2-BLK2	270	40	-	-	11	-	-	<DL	-	<DL		0.867		0.018		0.020	-
SP-52-E2-BLK3	270	40	-	-	11	-	-	<DL	-	<DL		0.862		0.019		0.021	-
SP-52-E2-04	270	40	9.43E-06	3.92	11	1.0002	0.0215	0.1540	0.0021	0.0770	0.0028	1.7100	0.0034	0.0230	0.0033	0.1170	0.0013
SP-52-E2-06	270	40	9.09E-06	5.92	11	1.0001	0.0215	0.2090	0.0027	0.0990	0.0035	1.9060	0.0041	0.0220	0.0025	0.1580	0.0018
SP-52-E2-08	270	40	9.24E-06	7.92	11	0.9999	0.0215	0.2350	0.0032	0.1040	0.0037	1.9410	0.0043	0.0220	0.0026	0.1610	0.0019
SP-52-E2-10	270	40	9.04E-06	9.92	11	0.9998	0.0215	0.2450	0.0032	0.1050	0.0037	1.9490	0.0042	0.0220	0.0025	0.1740	0.0020
SP-52-E2-12	270	40	9.12E-06	11.92	11	0.9997	0.0215	0.2420	0.0032	0.1020	0.0036	1.9330	0.0042	0.0250	0.0045	0.1670	0.0019
SP-52-E2-14	270	40	9.49E-06	13.92	11	0.9995	0.0215	0.2250	0.0031	0.0950	0.0035	1.8600	0.0041	0.0260	0.0053	0.1580	0.0019
SP-52-E2-16	270	40	9.26E-06	15.92	11	0.9994	0.0215	0.2150	0.0029	0.0900	0.0032	1.8350	0.0039	0.0430	0.0162	0.1460	0.0017
SP-52-E2-18	270	40	9.14E-06	17.92	11	0.9993	0.0215	0.2000	0.0026	0.0840	0.0029	1.7680	0.0036	**0.0280**	**0.0064**	0.1410	0.0016
SP-52-E2-20	270	40	9.19E-06	19.92	11	0.9992	0.0215	0.1780	0.0024	0.0760	0.0027	1.6930	0.0033	**0.0210**	**0.0019**	0.1210	0.0013
SP-52-E2-22	270	40	8.76E-06	21.92	11	0.9991	0.0215	0.1580	0.0020	0.0690	0.0023	1.6140	0.0028	0.0310	0.0080	0.1140	0.0012
SP-52-E2-24	270	40	8.83E-06	23.92	11	0.9990	0.0215	0.1490	0.0019	0.0660	0.0022	1.6060	0.0028	**0.0220**	**0.0025**	0.1120	0.0012

Table A5. SPFT Test Results from Dissolution of Glass LAWC22 at 23 °C, dilute conditions.

Sample ID	Inf [Si] ppm	T °C	Flow Rate m^3/d	Time, days	pH 23°C	Glass Mass g	SA m^2	[B] ppm	B Rate $g\ m^{-2}\ d^{-1}$	[Li] ppm	Li Rate $g\ m^{-2}\ d^{-1}$	[Na] ppm	Na Rate $g\ m^{-2}\ d^{-1}$	[Al] ppm	Al Rate $g\ m^{-2}\ d^{-1}$	[Si] ppm	Si Rate $g\ m^{-2}\ d^{-1}$
Exp.21																	
SP-53-A1-BLK1	0	23			7			<DL		0.010		<DL		0.0010		-0.0040	
SP-53-A1-BLK2	0	23			7			<DL		0.010		<DL		0.0010		-0.0060	
SP-53-A1-BLK3	0	23			7			<DL		<DL		<DL		-0.0010		0.0110	
SP-53-A1-01	0	23	1.07E-05	3.00	7	1.0004	0.022	0.1720	0.0026	0.0830	0.0032	0.9720	0.0045	0.0020	0.0000	0.1650	0.0004
SP-53-A1-02	0	23	9.77E-06	6.00	7	1.0003	0.022	0.1550	0.0022	0.0700	0.0024	0.8400	0.0036	0.0040	0.0000	0.1620	0.0003
SP-53-A1-03	0	23	9.37E-06	9.00	7	1.0001	0.022	0.1260	0.0017	0.0520	0.0017	0.6640	0.0027	0.0040	0.0000	0.1410	0.0003
SP-53-A1-04	0	23	9.47E-06	12.00	7	1.0000	0.022	0.1000	0.0013	0.0360	0.0011	0.5180	0.0021	0.0040	0.0000	0.1170	0.0002
SP-53-A1-05	0	23	9.39E-06	15.00	7	1.0000	0.022	0.0780	0.0010	0.0240	0.0006	0.4010	0.0016	0.0060	0.0001	0.1040	0.0002
SP-53-A1-06	0	23	9.42E-06	18.00	7	0.9999	0.022	0.0650	0.0009	0.0140	0.0002	0.3240	0.0013	0.0060	0.0001	0.0930	0.0002
SP-53-A1-07	0	23	9.31E-06	21.00	7	0.9998	0.022	0.0540	0.0007	0.0070	0.0000	0.2650	0.0011	0.0070	0.0001	0.0810	0.0002
SP-53-A1-08	0	23	9.25E-06	24.00	7	0.9998	0.022	0.0450	0.0006	0.0030	-0.0002	0.2250	0.0009	0.0120	0.0001	0.0740	0.0001
SP-53-A1-09	0	23	9.37E-06	27.00	7	0.9998	0.022	0.0400	0.0005	-0.0010	-0.0003	0.1930	0.0008	0.0070	0.0001	0.0690	0.0001
SP-53-A1-10	0	23	9.37E-06	30.00	7	0.9997	0.022	0.0350	0.0004	-0.0030	-0.0004	0.1710	0.0007	0.0080	0.0001	0.0620	0.0001
SP-53-A1-11	0	23	9.46E-06	33.00	7	0.9997	0.022	0.0310	0.0004	-0.0060	-0.0005	0.1500	0.0006	0.0080	0.0001	0.0560	0.0001
SP-53-A1-12	0	23	9.43E-06	36.00	8	0.9997	0.022	0.0270	0.0003	-0.0080	-0.0006	0.1360	0.0006	0.0090	0.0001	0.0570	0.0001
Exp.22																	
SP-53-B1-BLK1	0	23			8			<DL		0.011		<DL		0.001		<DL	
SP-53-B1-BLK2	0	23			8			<DL		<DL		<DL		0.002		0.00	
SP-53-B1-BLK3	0	23			8			<DL		<DL		<DL		0.001		0.01	
SP-53-B1-02	0	23	9.33E-06	6.00	8	1.0010	0.022	0.1030	0.0014	0.0450	0.0015	0.6270	0.0025	0.0190	0.0002	0.1960	0.0004
SP-53-B1-03	0	23	8.96E-06	9.00	8	1.0009	0.022	0.0840	0.0011	0.0310	0.0009	0.4940	0.0019	0.0220	0.0003	0.1940	0.0004
SP-53-B1-04	0	23	9.02E-06	12.00	8	1.0008	0.022	0.0700	0.0009	0.0190	0.0005	0.3920	0.0015	0.0220	0.0003	0.1810	0.0003
SP-53-B1-05	0	23	8.96E-06	15.00	8	1.0008	0.022	0.0580	0.0007	0.0120	0.0002	0.3170	0.0012	0.0240	0.0003	0.1710	0.0003
SP-53-B1-06	0	23	8.99E-06	18.00	8	1.0007	0.022	0.0480	0.0006	0.0060	0.0000	0.2650	0.0010	0.0250	0.0003	0.1620	0.0003
SP-53-B1-07	0	23	9.19E-06	21.00	8	1.0007	0.022	0.0470	0.0006	0.0040	-0.0001	0.2390	0.0010	0.0310	0.0004	0.1860	0.0004
SP-53-B1-08	0	23	9.25E-06	24.00	8	1.0007	0.022	0.0360	0.0004	-0.0020	-0.0003	0.1940	0.0008	0.0250	0.0003	0.1460	0.0003
SP-53-B1-09	0	23	9.35E-06	27.00	8	1.0006	0.022	0.0330	0.0004	-0.0050	-0.0004	0.1670	0.0007	0.0260	0.0003	0.1390	0.0003
SP-53-B1-10	0	23	9.45E-06	30.00	8	1.0006	0.022	0.0290	0.0004	-0.0070	-0.0005	0.1470	0.0006	0.0280	0.0004	0.1330	0.0003
SP-53-B1-11	0	23	9.44E-06	33.00	8	1.0006	0.022	0.0270	0.0003	-0.0090	-0.0006	0.1330	0.0005	0.0250	0.0003	0.1230	0.0002
SP-53-B1-12	0	23	9.39E-06	36.00	8	1.0006	0.022	0.0250	0.0003	-0.0100	-0.0006	0.1210	0.0005	0.0250	0.0003	0.1230	0.0002
Exp.23																	

Sample ID	Inf [Si] ppm	T °C	Flow Rate m^3/d	Time, days	pH 23°C	Glass Mass g	SA m^2	[B] ppm	B Rate $g\ m^{-2}\ d^{-1}$	[Li] ppm	Li Rate $g\ m^{-2}\ d^{-1}$	[Na] ppm	Na Rate $g\ m^{-2}\ d^{-1}$	[Al] ppm	Al Rate $g\ m^{-2}\ d^{-1}$	[Si] ppm	Si Rate $g\ m^{-2}\ d^{-1}$
SP-53-C1-BLK1	0	23						<DL		<DL		<DL		0.002		0.116	
SP-53-C1-BLK2	0	23			9			<DL		<DL		<DL		0.001		0.111	
SP-53-C1-BLK3	0	23			9			<DL		<DL		<DL		0.001		0.110	
SP-53-C1-02	0	23	1.06E-05	6.00	9	1.0003	0.022	0.1190	0.0018	0.0490	0.0019	0.6190	0.0029	0.0520	0.0008	0.5390	0.0010
SP-53-C1-03	0	23	1.03E-05	9.00	9	1.0001	0.022	0.1100	0.0016	0.0340	0.0013	0.5090	0.0023	0.0660	0.0010	0.6100	0.0011
SP-53-C1-04	0	23	1.03E-05	12.00	9	1.0000	0.022	0.1040	0.0015	0.0270	0.0010	0.4370	0.0020	0.0730	0.0011	0.6520	0.0012
SP-53-C1-05	0	23	1.02E-05	15.00	9	0.9999	0.022	0.1000	0.0014	0.0220	0.0008	0.3920	0.0017	0.0780	0.0011	0.6800	0.0012
SP-53-C1-06	0	23	1.03E-05	18.00	9	0.9998	0.022	0.0970	0.0014	0.0190	0.0006	0.3600	0.0016	0.0820	0.0012	0.7020	0.0013
SP-53-C1-07	0	23	1.02E-05	21.00	9	0.9997	0.022	0.0960	0.0014	0.0170	0.0006	0.3430	0.0015	0.1190	0.0017	0.7230	0.0013
SP-53-C1-08	0	23	1.01E-05	24.00	9	0.9996	0.022	0.0930	0.0013	0.0160	0.0005	0.3260	0.0014	0.0870	0.0013	0.7300	0.0013
SP-53-C1-09	0	23	1.03E-05	27.00	9	0.9996	0.022	0.0920	0.0013	0.0140	0.0004	0.3100	0.0014	0.0910	0.0013	0.7420	0.0014
SP-53-C1-10	0	23	1.04E-05	30.00	9	0.9995	0.022	0.0900	0.0013	0.0130	0.0004	0.2990	0.0013	0.0900	0.0013	0.7360	0.0014
SP-53-C1-11	0	23	1.04E-05	33.00	9	0.9994	0.022	0.0880	0.0013	0.0120	0.0004	0.2870	0.0013	0.0870	0.0013	0.7270	0.0014
SP-53-C1-12	0	23	1.04E-05	36.00	10	0.9993	0.022	0.0870	0.0013	0.0120	0.0004	0.2820	0.0013	0.0860	0.0013	0.7340	0.0014
Exp.24																	
SP-53-D1-BLK1	0	23						<DL		0.010		<DL		0.002		<DL	
SP-53-D1-BLK2	0	23						<DL		<DL		<DL		0.001		<DL	
SP-53-D1-BLK3	0	23	-	-	10	-	-	<DL		<DL		<DL		0.001		<DL	
SP-53-D1-02	0	23	9.58E-06	6.00	10	0.5008	0.011	0.1520	0.0042	0.0480	0.0032	0.5790	0.0048	0.1210	0.0033	0.8290	0.0034
SP-53-D1-03	0	23	9.14E-06	9.00	10	0.5006	0.011	0.1770	0.0047	0.0540	0.0035	0.6150	0.0049	0.1600	0.0042	1.0960	0.0043
SP-53-D1-04	0	23	9.19E-06	12.00	10	0.5004	0.011	0.1900	0.0050	0.0560	0.0037	0.6280	0.0050	0.1830	0.0048	1.2350	0.0048
SP-53-D1-05	0	23	9.11E-06	15.00	10	0.5002	0.011	0.1960	0.0052	0.0580	0.0038	0.6330	0.0050	0.2050	0.0054	1.3160	0.0051
SP-53-D1-06	0	23	9.13E-06	18.00	10	0.5001	0.011	0.1980	0.0052	0.0580	0.0038	0.6310	0.0050	0.2040	0.0054	1.3480	0.0052
SP-53-D1-07	0	23	9.06E-06	21.00	10	0.4999	0.011	0.2000	0.0052	0.0580	0.0038	0.6310	0.0050	0.2470	0.0065	1.3710	0.0053
SP-53-D1-08	0	23	9.01E-06	24.00	10	0.4997	0.011	0.2010	0.0052	0.0580	0.0038	0.6340	0.0050	0.2120	0.0055	1.3950	0.0054
SP-53-D1-09	0	23	9.17E-06	27.00	10	0.4996	0.011	0.2000	0.0053	0.0580	0.0038	0.6300	0.0050	**0.2150**	**0.0057**	1.4080	0.0055
SP-53-D1-10	0	23	9.22E-06	30.00	10	0.4994	0.011	0.1990	0.0053	0.0570	0.0038	0.6240	0.0050	**0.2250**	**0.0060**	1.4100	0.0055
SP-53-D1-11	0	23	9.25E-06	33.00	10	0.4992	0.011	0.1980	0.0053	0.0560	0.0037	0.6220	0.0050	**0.2260**	**0.0060**	1.4170	0.0056
SP-53-D1-12	0	23	9.17E-06	36.00	10	0.4990	0.011	0.2020	0.0054	0.0580	0.0038	0.6280	0.0050	0.0060	0.0001	1.4310	0.0056

Exp.25																	
SP-53-E1-BLK1	0	23			11			<DL		<DL		<DL		0.0010		0.05	
SP-53-E1-BLK2	0	23			11			<DL		<DL		<DL		0.0020		0.04	
SP-53-E1-BLK3	0	23	-	-	11	-	-	<DL		<DL		<DL		0.0200		0.10	
SP-53-E1-02	0	23	1.08E-05	6.00	11	0.5001	0.011	0.3230	0.0101	0.1080	0.0090	1.0270	0.0096	0.3820	0.0117	2.4110	0.0108
SP-53-E1-03	0	23	1.02E-05	9.00	11	0.4995	0.011	0.4080	0.0122	0.1390	0.0111	1.2960	0.0115	0.4630	0.0135	2.8570	0.0122
SP-53-E1-04	0	23	1.02E-05	12.00	11	0.4991	0.011	0.4200	0.0125	0.1450	0.0116	1.3510	0.0120	0.4710	0.0137	2.9660	0.0127
SP-53-E1-05	0	23	1.01E-05	15.00	11	0.4987	0.011	0.4160	0.0122	0.1420	0.0112	1.3330	0.0117	0.4760	0.0137	2.9320	0.0123
SP-53-E1-06	0	23	1.00E-05	18.00	11	0.4984	0.011	0.4020	0.0118	0.1370	0.0107	1.2960	0.0113	0.4480	0.0128	2.7910	0.0117
SP-53-E1-07	0	23	9.90E-06	21.00	11	0.4980	0.011	0.3820	0.0111	0.1300	0.0100	1.2430	0.0107	0.4350	0.0123	2.6960	0.0112
SP-53-E1-08	0	23	9.84E-06	24.00	11	0.4976	0.011	0.3600	0.0104	0.1210	0.0093	1.1730	0.0101	0.4190	0.0118	2.5260	0.0104
SP-53-E1-09	0	23	9.97E-06	27.00	11	0.4973	0.011	0.3420	0.0100	0.1130	0.0088	1.1110	0.0097	0.3990	0.0114	2.3690	0.0098
SP-53-E1-10	0	23	1.00E-05	30.00	11	0.4970	0.011	0.3130	0.0092	0.1040	0.0081	1.0170	0.0089	0.3420	0.0098	2.2210	0.0093
SP-53-E1-11	0	23	1.01E-05	33.00	11	0.4967	0.011	0.2730	0.0080	0.0900	0.0070	0.8930	0.0078	0.2920	0.0083	1.9630	0.0082

Table A6. SPFT Test Results from Dissolution of Glass LAWC22 at 23 °C, saturated conditions.

Sample ID	Inf [Si] ppm	T °C	Flow Rate m^3/d	Time, days	pH 23°C	Glass Mass g	SA m^2	[B] ppm	B Rate $g\ m^{-2}\ d^{-1}$	[Li] ppm	Li Rate $g\ m^{-2}\ d^{-1}$	[Na] ppm	Na Rate $g\ m^{-2}\ d^{-1}$	[K] ppm	K Rate $g\ m^{-2}\ d^{-1}$	[Al] ppm	Al Rate $g\ m^{-2}\ d^{-1}$
Exp.26																	
SP-53-A2-BLK1	35	23	-	-	7	-	-	<DL	-	<DL		0.062		0.006		0.024	-
SP-53-A2-BLK2	35	23	-	-	7	-	-	<DL	-	<DL		0.063		0.006		0.017	-
SP-53-A2-BLK3	35	23	-	-	7	-	-	<DL	-	<DL		0.076		0.006		0.018	-
SP-53-A2-02	35	23	9.37E-06	6.00	7	3.9987	0.086	0.5470	0.0019	0.3100	0.0029	3.1770	0.0032	0.0210	0.0025	0.0290	0.0000
SP-53-A2-03	35	23	9.97E-06	9.00	7	3.9980	0.086	0.4450	0.0016	0.2520	0.0025	2.5000	0.0026	0.0190	0.0023	0.0310	0.0000
SP-53-A2-04	35	23	1.00E-05	12.00	7	3.9976	0.086	0.3530	0.0013	0.1990	0.0020	1.9400	0.0020	0.0150	0.0016	0.0310	0.0000
SP-53-A2-05	35	23	9.98E-06	15.00	7	3.9973	0.086	0.2870	0.0010	0.1620	0.0016	1.5510	0.0016	0.0150	0.0016	0.0320	0.0000
SP-53-A2-06	35	23	1.00E-05	18.00	7	3.9971	0.086	0.2360	0.0009	0.1350	0.0013	1.2750	0.0013	0.0130	0.0012	0.0310	0.0000
SP-53-A2-07	35	23	9.91E-06	21.00	7	3.9969	0.086	0.2030	0.0007	0.1160	0.0011	1.0830	0.0011	0.0140	0.0014	0.0330	0.0000
SP-53-A2-08	35	23	9.87E-06	24.00	7	3.9967	0.086	0.1760	0.0006	0.1010	0.0010	0.9390	0.0009	0.0130	0.0012	0.0310	0.0000
SP-53-A2-09	35	23	1.01E-05	27.00	7	3.9966	0.086	0.1570	0.0006	0.0880	0.0009	0.8300	0.0008	0.0130	0.0012	0.0310	0.0000
SP-53-A2-10	35	23	1.01E-05	30.00	7	3.9964	0.086	0.1380	0.0005	0.0780	0.0008	0.7400	0.0007	0.0130	0.0012	0.0310	0.0000
SP-53-A2-11	35	23	1.01E-05	33.00	7	3.9963	0.086	0.1250	0.0005	0.0710	0.0007	0.6760	0.0007	0.0160	0.0018	0.0300	0.0000
SP-53-A2-12	35	23	1.00E-05	36.00	7	3.9962	0.086	0.1170	0.0004	0.0660	0.0006	0.6310	0.0006	0.0160	0.0018	0.0300	0.0000
Exp.27																	
SP-53-B2-BLK1	40	23	-	-	8	-	-	<DL	-	<DL		0.071		0.006		0.013	-
SP-53-B2-BLK2	40	23	-	-	8	-	-	<DL	-	<DL		0.071		0.008		0.012	-
SP-53-B2-BLK3	40	23	-	-	8	-	-	<DL	-	<DL		0.072		0.016		0.013	-
SP-53-B2-02	40	23	8.93E-06	6.00	8	4.0005	0.0861	0.3780	0.0012	0.2520	0.0022	2.5760	0.0024	0.0160	0.0009	0.0320	0.0001
SP-53-B2-03	40	23	9.48E-06	9.00	8	4.0000	0.0861	0.3090	0.0011	0.2000	0.0019	2.0640	0.0021	0.0350	0.0041	0.0380	0.0001
SP-53-B2-04	40	23	9.50E-06	12.00	8	3.9998	0.0861	0.2480	0.0009	0.1570	0.0015	1.6090	0.0016	0.0130	0.0005	0.0340	0.0001
SP-53-B2-05	40	23	9.41E-06	15.00	8	3.9996	0.0861	0.2000	0.0007	0.1270	0.0012	1.3120	0.0013	0.0130	0.0005	0.0340	0.0001
SP-53-B2-06	40	23	9.49E-06	18.00	8	3.9994	0.0861	0.1660	0.0006	0.1060	0.0010	1.0840	0.0010	0.0130	0.0005	0.0350	0.0001
SP-53-B2-07	40	23	9.43E-06	21.00	8	3.9993	0.0861	0.1410	0.0005	0.0900	0.0008	0.9190	0.0009	0.0120	0.0003	0.0340	0.0001
SP-53-B2-08	40	23	9.40E-06	24.00	8	3.9992	0.0861	0.1240	0.0004	0.0780	0.0007	0.8050	0.0007	0.0120	0.0003	0.0330	0.0001
SP-53-B2-09	40	23	9.60E-06	27.00	8	3.9991	0.0861	0.1070	0.0004	0.0680	0.0006	0.7100	0.0007	0.0110	0.0002	0.0330	0.0001
SP-53-B2-10	40	23	9.66E-06	30.00	8	3.9990	0.0861	0.0950	0.0003	0.0610	0.0006	0.6470	0.0006	0.0130	0.0005	0.0330	0.0001
SP-53-B2-11	40	23	9.65E-06	33.00	8	3.9989	0.0861	0.0860	0.0003	0.0550	0.0005	0.5830	0.0005	0.0100	0.0000	0.0330	0.0001
SP-53-B2-12	40	23	9.56E-06	36.00	8	3.9988	0.0861	0.0790	0.0003	0.0510	0.0005	0.5430	0.0005	0.0130	0.0005	0.0320	0.0001

Exp.28																	
SP-53-C2-BLK1	52.2	23	-	-	9	-	-	<DL	-	<DL		0.096		0.006		0.016	-
SP-53-C2-BLK2	52.2	23	-	-	9	-	-	<DL	-	<DL		0.095		0.005		0.015	-
SP-53-C2-BLK3	52.2	23	-	-	9	-	-	<DL	-	<DL		0.095		0.006		0.016	-
SP-53-C2-02	52.2	23	9.79E-06	6.00	9	4.0007	0.0861	0.2690	0.0010	0.1960	0.0019	1.9540	0.0020	0.0130	0.0013	0.0420	0.0001
SP-53-C2-03	52.2	23	1.04E-05	9.00	9	4.0003	0.0861	0.2080	0.0008	0.1490	0.0015	1.5220	0.0016	0.0120	0.0012	0.0470	0.0001
SP-53-C2-04	52.2	23	1.05E-05	12.00	9	4.0001	0.0861	0.1600	0.0006	0.1130	0.0012	1.2080	0.0013	0.0160	0.0019	0.0420	0.0001
SP-53-C2-05	52.2	23	1.05E-05	15.00	9	4.0000	0.0861	0.1300	0.0005	0.0910	0.0009	0.9730	0.0010	0.0110	0.0010	0.0390	0.0001
SP-53-C2-06	52.2	23	1.06E-05	18.00	9	3.9999	0.0861	0.1070	0.0004	0.0750	0.0008	0.8180	0.0008	0.0110	0.0010	0.0390	0.0001
SP-53-C2-07	52.2	23	1.06E-05	21.00	9	3.9998	0.0861	0.0920	0.0003	0.0640	0.0006	0.7140	0.0007	0.0100	0.0008	0.0370	0.0001
SP-53-C2-08	52.2	23	1.05E-05	24.00	9	3.9997	0.0861	0.0830	0.0003	0.0560	0.0006	0.6380	0.0006	0.0120	0.0012	0.0350	0.0001
SP-53-C2-09	52.2	23	1.07E-05	27.00	9	3.9996	0.0861	0.0740	0.0003	0.0500	0.0005	0.5770	0.0006	0.0100	0.0008	0.0360	0.0001
SP-53-C2-10	52.2	23	1.09E-05	30.00	9	3.9995	0.0861	0.0670	0.0003	0.0440	0.0004	0.5270	0.0005	0.0120	0.0012	0.0350	0.0001
SP-53-C2-11	52.2	23	1.09E-05	33.00	9	3.9995	0.0861	0.0600	0.0002	0.0400	0.0004	0.4870	0.0005	0.0090	0.0006	0.0330	0.0001
SP-53-C2-12	52.2	23	1.08E-05	36.00	9	3.9994	0.0861	0.0560	0.0002	0.0370	0.0004	0.4580	0.0004	0.0130	0.0014	0.0290	0.0001
Exp.29																	
SP-53-D2-BLK1	90	23	-	-	10	-	-	<DL	-	<DL		0.163		0.008		0.029	-
SP-53-D2-BLK2	90	23	-	-	10	-	-	<DL	-	<DL		0.164		0.011		0.026	-
SP-53-D2-BLK3	90	23	-	-	10	-	-	<DL	-	<DL		0.160		0.010		0.024	-
SP-53-D2-02	90	23	9.85E-06	6.00	10	2.0000	0.04305	0.1240	0.0009	0.0900	0.0017	1.0180	0.0018	0.0100	0.0001	0.0510	0.0002
SP-53-D2-03	90	23	1.04E-05	9.00	10	1.9998	0.04305	0.1000	0.0007	0.0690	0.0014	0.8390	0.0015	0.0100	0.0001	0.0590	0.0002
SP-53-D2-04	90	23	1.05E-05	12.00	10	1.9997	0.04305	0.0830	0.0006	0.0560	0.0011	0.7020	0.0012	0.0100	0.0001	0.0510	0.0002
SP-53-D2-05	90	23	1.04E-05	15.00	10	1.9997	0.04305	0.0720	0.0005	0.0460	0.0009	0.6150	0.0010	0.0090	-0.0002	0.0490	0.0002
SP-53-D2-06	90	23	1.06E-05	18.00	10	1.9996	0.04304	0.0640	0.0005	0.0390	0.0008	0.5510	0.0009	0.0090	-0.0002	0.0460	0.0002
SP-53-D2-07	90	23	1.06E-05	21.00	10	1.9995	0.04304	0.0570	0.0004	0.0350	0.0007	0.5050	0.0008	0.0100	0.0001	0.0470	0.0002
SP-53-D2-08	90	23	1.05E-05	24.00	10	1.9995	0.04304	0.0520	0.0004	0.0310	0.0006	0.4750	0.0007	0.0100	0.0001	0.0430	0.0001
SP-53-D2-09	90	23	1.07E-05	27.00	10	1.9994	0.04304	0.0480	0.0004	0.0280	0.0005	0.4460	0.0007	0.0100	0.0001	0.0430	0.0001
SP-53-D2-10	90	23	1.07E-05	30.00	10	1.9994	0.04304	0.0440	0.0003	0.0260	0.0005	0.4250	0.0006	0.0110	0.0005	0.0420	0.0001
SP-53-D2-11	90	23	1.07E-05	33.00	10	1.9994	0.04304	0.0400	0.0003	0.0240	0.0004	0.4010	0.0006	0.0100	0.0001	0.0420	0.0001
SP-53-D2-12	90	23	1.06E-05	36.00	10	1.9993	0.04304	0.0380	0.0003	0.0230	0.0004	0.3900	0.0005	0.0110	0.0005	0.0390	0.0001

Exp.30																	
SP-53-E2-BLK1	230	23	-	-	11	-	-	<DL	-	<DL		0.607		0.017		0.017	-
SP-53-E2-BLK2	230	23	-	-	11	-	-	<DL	-	<DL		0.607		0.016		0.016	-
SP-53-E2-BLK3	230	23	-	-	11	-	-	<DL	-	<DL		0.583		0.014		0.017	-
SP-53-E2-02	230	23	8.17E-06	6.00	11	1.9998	0.04305	0.1280	0.0007	0.0880	0.0014	1.4430	0.0015	0.0140	-0.0005	0.0640	0.0003
SP-53-E2-03	230	23	9.48E-06	9.00	11	1.9997	0.04304	0.1230	0.0008	0.0740	0.0013	1.3270	0.0015	0.0150	-0.0002	0.0700	0.0004
SP-53-E2-04	230	23	9.44E-06	12.00	11	1.9995	0.04304	0.1270	0.0009	0.0650	0.0012	1.2770	0.0014	0.0170	0.0004	0.0650	0.0003
SP-53-E2-05	230	23	9.33E-06	15.00	11	1.9994	0.04304	0.1360	0.0009	0.0640	0.0011	1.2680	0.0014	0.0180	0.0008	0.0840	0.0005
SP-53-E2-06	230	23	9.33E-06	18.00	11	1.9993	0.04304	0.1450	0.0010	0.0640	0.0011	1.2620	0.0013	0.0170	0.0004	0.0910	0.0005
SP-53-E2-07	230	23	9.14E-06	21.00	11	1.9992	0.04304	0.1510	0.0010	0.0640	0.0011	1.2870	0.0014	0.0190	0.0011	0.0930	0.0005
SP-53-E2-08	**230**	**23**	**9.01E-06**	**24.00**	**11**	**1.9991**	**0.0430**	**0.1570**	**0.0010**	**0.0650**	**0.0011**	**1.2950**	**0.0014**	**0.0180**	**0.0007**	**0.0980**	**0.0005**
SP-53-E2-09	230	23	1.15E-05	27.00	11	1.9989	0.0430	0.1510	0.0012	0.0620	0.0013	1.2450	0.0016	0.0180	0.0009	0.0950	0.0007
SP-53-E2-10	**230**	**23**	**9.94E-06**	**30.00**	**11**	**1.9988**	**0.0430**	**0.1370**	**0.0010**	**0.0570**	**0.0011**	**1.1850**	**0.0013**	**0.0230**	**0.0026**	**0.0900**	**0.0005**
SP-53-E2-11	230	23	8.48E-06	33.00	11	1.9986	0.0430	0.1410	0.0009	0.0580	0.0009	1.1990	0.0011	0.0180	0.0007	0.0890	0.0004
SP-53-E2-12	**230**	**23**	**9.84E-06**	**36.00**	**11**	**1.9985**	**0.0430**	**0.1420**	**0.0010**	**0.0580**	**0.0011**	**1.1980**	**0.0013**	**0.0300**	**0.0049**	**0.0830**	**0.0005**

*In bold: Samples used to calculate steady state dissolution rates.

** Highlighted samples ignored; flow rate deviated more than 5% from average.

Table A7. Additional SPFT Test Results from Dissolution of Glass LAWC22 at 70 °C related to IEX, saturated conditions.

Sample ID	Infl [Si] ppm	T in C	[Mo] ppm	Mo Rate	[Cs] ppm	Cs Rate	[Re] ppm	Re Rate	IEX (mol m-2 s-1), Na-B	IEX (mol m-2 s-1), Na-Re	IEX (mol m-2 s-1), Na-Mo	IEX (mol m-2 s-1), Li-B	IEX (mol m-2 s-1), Li-Re	IEX (mol m-2 s-1), Li-Mo	IEX (mol m-2 s-1), Cs-B	IEX (mol m-2 s-1), Cs-Re	IEX (mol m-2 s-1), Cs-Mo
Exp.6																	
SP-51-A2-BLK1	55	70	1.01E-05		8.22E-06		5.40E-06										
SP-51-A2-BLK2	55	70	9.50E-06		8.33E-06		2.66E-06										
SP-51-A2-BLK3	55	70	1.56E-05		9.74E-06		2.01E-05										
SP-51-A2-02	55	70	0.0070	0.0192	0.0525	0.0547	0.0283	0.0451	5.63E-10	2.61E-09	4.00E-09	-5.89E-10	1.44E-10	6.44E-10	-3.50E-12	1.18E-12	4.37E-12
SP-51-A2-03	55	70	0.0035	0.0098	0.0465	0.0497	0.0187	0.0306	1.89E-10	2.86E-09	3.98E-09	-6.42E-10	3.17E-10	7.17E-10	-3.76E-12	2.36E-12	4.92E-12
SP-51-A2-04	55	70	0.0026	0.0069	0.0460	0.0464	0.0148	0.0228	-2.05E-11	2.63E-09	3.49E-09	-6.14E-10	3.38E-10	6.45E-10	-3.18E-12	2.90E-12	4.87E-12
SP-51-A2-05	55	70	0.1112	0.3097	0.0588	0.0618	0.0172	0.0277	-1.92E-11	2.19E-09	-1.30E-08	-6.00E-10	1.94E-10	-5.25E-09	-8.71E-13	4.20E-12	-3.05E-11
SP-51-A2-06	55	70	0.0853	0.2319	0.0511	0.0524	0.0130	0.0203	-5.11E-11	2.27E-09	-9.10E-09	-5.67E-10	2.66E-10	-3.81E-09	-1.37E-12	3.95E-12	-2.21E-11
SP-51-A2-07	55	70	0.0615	0.1745	0.0495	0.0529	0.0112	0.0183	-9.48E-11	2.36E-09	-6.04E-09	-5.75E-10	3.07E-10	-2.71E-09	-1.36E-12	4.27E-12	-1.50E-11
SP-51-A2-08	55	70	0.0533	0.1482	0.0508	0.0533	0.0107	0.0172	-1.19E-10	2.20E-09	-4.84E-09	-5.54E-10	2.79E-10	-2.25E-09	-8.63E-13	4.46E-12	-1.17E-11
SP-51-A2-09	55	70	**0.0392**	**0.1080**	0.0479	0.0497	0.0093	0.0148	-1.25E-10	2.12E-09	-2.89E-09	-5.23E-10	2.84E-10	-1.51E-09	-8.56E-13	4.30E-12	-7.18E-12
SP-51-A2-10	55	70	**0.0348**	**0.0989**	0.0523	0.0560	0.0085	0.0139	-1.12E-10	2.21E-09	-2.36E-09	-5.28E-10	3.05E-10	-1.33E-09	-1.30E-13	5.19E-12	-5.29E-12
SP-51-A2-11	55	70	**0.0255**	**0.0692**	0.0446	0.0456	0.0076	0.0120	-6.95E-11	2.13E-09	-9.49E-10	-4.83E-10	3.05E-10	-7.99E-10	-8.88E-13	4.14E-12	-2.90E-12
SP-51-A2-12	55	70	0.0008	0.0021	0.0352	0.0380	0.0052	0.0086	-1.05E-10	2.33E-09	2.68E-09	-5.05E-10	3.69E-10	4.93E-10	-1.96E-12	3.62E-12	4.42E-12
Exp.7																	
SP-51-B2-BLK1	60	70	8.94E-06		7.57E-06		3.22E-06										
SP-51-B2-BLK2	60	70	1.06E-05		7.34E-06		5.56E-06										
SP-51-B2-BLK3	60	70	1.26E-05		7.76E-06		3.22E-06										
SP-51-B2-02	60	70	0.02394	0.0639	0.02715	0.0273	0.01799	0.0278	7.59E-10	7.95E-10	-1.15E-09	2.47E-10	2.60E-10	-4.37E-10	-1.38E-13	-5.46E-14	-4.51E-12
SP-51-B2-03	60	70	0.01843	0.0523	0.02213	0.0237	0.01264	0.0208	5.00E-10	7.35E-10	-9.62E-10	1.26E-10	2.11E-10	-3.98E-10	-1.76E-13	3.62E-13	-3.53E-12
SP-51-B2-04	60	70	0.01401	0.0373	0.01810	0.0182	0.00890	0.0137	3.03E-10	6.83E-10	-5.85E-10	5.72E-11	1.94E-10	-2.61E-10	-3.20E-13	5.50E-13	-2.36E-12
SP-51-B2-05	60	70	0.00380	0.0102	0.01686	0.0171	0.00705	0.0109	1.91E-10	6.17E-10	6.58E-10	1.98E-11	1.73E-10	1.87E-10	-2.21E-13	7.55E-13	8.49E-13

Sample ID	Infl [Si] ppm	T in C	[Mo] ppm	Mo Rate	[Cs] ppm	Cs Rate	[Re] ppm	Re Rate	IEX (mol m-2 s-1), Na-B	IEX (mol m-2 s-1), Na-Re	IEX (mol m-2 s-1), Na-Mo	IEX (mol m-2 s-1), Li-B	IEX (mol m-2 s-1), Li-Re	IEX (mol m-2 s-1), Li-Mo	IEX (mol m-2 s-1), Cs-B	IEX (mol m-2 s-1), Cs-Re	IEX (mol m-2 s-1), Cs-Mo
SP-51-B2-06	60	70	0.00330	0.0093	0.01605	0.0171	0.00594	0.0097	1.21E-10	6.24E-10	6.46E-10	-6.81E-12	1.74E-10	1.82E-10	-2.44E-13	9.10E-13	9.59E-13
SP-51-B2-07	60	70	0.00306	0.0082	0.01462	0.0149	0.00499	0.0078	8.21E-11	5.92E-10	5.67E-10	-1.42E-11	1.69E-10	1.60E-10	-2.95E-13	8.73E-13	8.18E-13
SP-51-B2-08	60	70	0.00298	0.0083	0.01530	0.0160	0.00423	0.0068	4.13E-11	5.99E-10	5.21E-10	-2.25E-11	1.78E-10	1.49E-10	-1.41E-13	1.14E-12	9.58E-13
SP-51-B2-09	60	70	0.01018	0.0273	0.01374	0.0139	0.00405	0.0063	3.33E-11	5.51E-10	-5.81E-10	-2.05E-11	1.65E-10	-2.41E-10	-2.47E-13	9.40E-13	-1.65E-12
SP-51-B2-10	60	70	0.00925	0.0258	0.01471	0.0155	0.00420	0.0068	3.70E-11	5.47E-10	-4.77E-10	-1.83E-11	1.65E-10	-2.03E-10	-9.58E-14	1.07E-12	-1.27E-12
SP-51-B2-11	60	70	0.00804	0.0216	0.01417	0.0144	0.00385	0.0060	2.42E-11	5.18E-10	-3.22E-10	-1.98E-11	1.57E-10	-1.44E-10	-9.81E-14	1.03E-12	-8.92E-13
SP-51-B2-12	60	70	0.00895	0.0234	0.01402	0.0138	0.00376	0.0057	2.06E-11	5.04E-10	-4.50E-10	-1.76E-11	1.56E-10	-1.86E-10	-1.03E-13	1.00E-12	-1.18E-12
Exp.8																	
SP-51-C2-BLK1	80	70	8.38E-06		8.14E-06		6.60E-06										
SP-51-C2-BLK2	80	70	1.03E-05		8.07E-06		8.45E-06										
SP-51-C2-BLK3	80	70	1.09E-05		7.31E-06		6.68E-06										
SP-51-C2-02	80	70	0.01286	0.0362	0.01670	0.0177	0.01219	0.0199	7.59E-10	6.22E-10	-2.58E-10	2.55E-10	2.06E-10	-1.10E-10	5.25E-14	-2.61E-13	-2.28E-12
SP-51-C2-03	80	70	0.01015	0.0295	0.01354	0.0148	0.00920	0.0155	5.83E-10	4.57E-10	-2.99E-10	1.93E-10	1.48E-10	-1.23E-10	2.14E-13	-7.65E-14	-1.81E-12
SP-51-C2-04	80	70	0.00832	0.0229	0.01027	0.0107	0.00646	0.0103	4.03E-10	3.83E-10	-2.95E-10	1.20E-10	1.12E-10	-1.31E-10	9.40E-14	4.69E-14	-1.51E-12
SP-51-C2-05	80	70	0.00678	0.0196	0.00896	0.0098	0.00558	0.0093	3.32E-10	2.92E-10	-2.61E-10	9.21E-11	7.78E-11	-1.21E-10	1.46E-13	5.47E-14	-1.21E-12
SP-51-C2-06	80	70	0.00576	0.0166	0.00777	0.0084	0.00478	0.0080	2.55E-10	2.42E-10	-2.21E-10	6.94E-11	6.49E-11	-1.01E-10	8.75E-14	5.93E-14	-1.00E-12
SP-51-C2-07	80	70	0.00541	0.0157	0.00760	0.0083	0.00477	0.0080	2.30E-10	2.19E-10	-1.95E-10	5.46E-11	5.05E-11	-9.81E-11	6.53E-14	3.89E-14	-9.10E-13
SP-51-C2-08	80	70	0.00604	0.0168	0.00726	0.0076	0.00448	0.0072	1.93E-10	1.67E-10	-3.49E-10	4.72E-11	3.77E-11	-1.47E-10	1.11E-13	5.09E-14	-1.13E-12
SP-51-C2-09	80	70	0.00484	0.0141	0.00683	0.0075	0.00425	0.0072	1.81E-10	1.72E-10	-2.01E-10	4.26E-11	3.92E-11	-9.46E-11	6.43E-14	4.28E-14	-8.12E-13
SP-51-C2-10	80	70	0.00457	0.0131	0.00704	0.0076	0.00452	0.0075	1.62E-10	1.28E-10	-1.73E-10	3.68E-11	2.49E-11	-8.31E-11	9.13E-14	1.49E-14	-6.75E-13
SP-51-C2-11	80	70	0.00459	0.0129	0.00679	0.0072	0.00439	0.0071	1.47E-10	1.23E-10	-1.87E-10	3.21E-11	2.35E-11	-8.76E-11	6.27E-14	7.97E-15	-7.02E-13
SP-51-C2-12	80	70	0.00437	0.0130	0.00639	0.0071	0.00417	0.0071	1.43E-10	1.32E-10	-1.80E-10	3.06E-11	2.69E-11	-8.51E-11	2.34E-14	-2.34E-16	-7.15E-13
Exp.9																	
SP-51-D2-BLK1	140	70	9.78E-06		6.62E-06		4.51E-06										
SP-51-D2-BLK2	140	70	2.04E-05		8.30E-06		4.43E-06										
SP-51-D2-BLK3	140	70	1.51E-		7.65E-		3.62E-										

Sample ID	Infl [Si] ppm	T in C	[Mo] ppm	Mo Rate	[Cs] ppm	Cs Rate	[Re] ppm	Re Rate	IEX (mol m-2 s-1), Na-B	IEX (mol m-2 s-1), Na-Re	IEX (mol m-2 s-1), Na-Mo	IEX (mol m-2 s-1), Li-B	IEX (mol m-2 s-1), Li-Re	IEX (mol m-2 s-1), Li-Mo	IEX (mol m-2 s-1), Cs-B	IEX (mol m-2 s-1), Cs-Re	IEX (mol m-2 s-1), Cs-Mo
			05		06		06										
SP-51-D2-02	140	70	0.00309	0.0133	0.00663	0.0108	0.00422	0.0105	7.07E-10	8.30E-10	6.82E-10	2.40E-10	2.84E-10	2.31E-10	-2.50E-13	3.15E-14	-3.08E-13
SP-51-D2-03	140	70	0.00230	0.0099	0.00474	0.0077	0.00316	0.0079	5.18E-10	5.99E-10	4.92E-10	1.73E-10	2.02E-10	1.64E-10	-2.08E-13	-2.16E-14	-2.67E-13
SP-51-D2-04	140	70	0.00180	0.0075	0.00387	0.0061	0.00249	0.0061	4.32E-10	4.80E-10	4.01E-10	1.33E-10	1.51E-10	1.22E-10	-1.01E-13	9.86E-15	-1.71E-13
SP-51-D2-05	140	70	0.00158	0.0068	0.00337	0.0055	0.00211	0.0053	3.79E-10	3.97E-10	3.16E-10	1.14E-10	1.20E-10	9.11E-11	-1.48E-14	2.70E-14	-1.60E-13
SP-51-D2-06	140	70	0.00116	0.0050	0.00245	0.0040	0.00149	0.0038	3.40E-10	3.95E-10	3.28E-10	1.00E-10	1.20E-10	9.60E-11	-9.27E-14	3.34E-14	-1.21E-13
SP-51-D2-07	140	70	0.00116	0.0048	0.00240	0.0038	0.00147	0.0036	3.00E-10	3.17E-10	2.50E-10	8.82E-11	9.44E-11	7.02E-11	-1.13E-14	2.83E-14	-1.26E-13
SP-51-D2-08	140	70	0.00114	0.0050	0.00236	0.0040	0.00144	0.0037	2.71E-10	2.73E-10	2.03E-10	7.68E-11	7.76E-11	5.22E-11	2.61E-14	3.12E-14	-1.31E-13
SP-51-D2-09	140	70	0.00104	0.0045	0.00214	0.0035	0.00131	0.0033	2.47E-10	2.47E-10	1.83E-10	7.10E-11	7.10E-11	4.82E-11	2.65E-14	2.64E-14	-1.19E-13
SP-51-D2-10	140	70	0.00104	0.0046	0.00190	0.0032	0.00120	0.0031	2.63E-10	2.82E-10	2.02E-10	7.10E-11	7.79E-11	4.92E-11	-3.21E-14	1.22E-14	-1.71E-13
SP-51-D2-11	140	70	0.00097	0.0042	0.00184	0.0030	0.00114	0.0029	2.27E-10	2.34E-10	1.64E-10	5.75E-11	5.99E-11	3.47E-11	1.10E-15	1.64E-14	-1.45E-13
SP-51-D2-12	140	70	0.00087	0.0037	0.00174	0.0028	0.00109	0.0027	2.11E-10	2.06E-10	1.53E-10	5.92E-11	5.74E-11	3.83E-11	2.63E-14	1.47E-14	-1.08E-13

Exp.10																	
SP-51-E2-BLK1	360	70	1.12E-05		8.45E-06		4.67E-06										
SP-51-E2-BLK2	360	70	1.62E-05		7.95E-06		6.84E-06										
SP-51-E2-BLK3	360	70	1.48E-05		7.76E-06		4.19E-06										
SP-51-E2-02	360	70	0.00181	0.0074	0.00414	0.0065	0.00252	0.0060	6.43E-10	6.26E-10	5.50E-10	1.96E-10	1.90E-10	1.63E-10	9.16E-14	5.34E-14	-1.21E-13
SP-51-E2-03	360	70	0.00116	0.0048	0.00288	0.0046	0.00160	0.0039	5.51E-10	5.14E-10	4.64E-10	1.54E-10	1.40E-10	1.22E-10	1.70E-13	8.40E-14	-3.04E-14
SP-51-E2-04	360	70	0.00081	0.0034	0.00205	0.0032	0.00110	0.0027	4.91E-10	4.42E-10	4.05E-10	1.15E-10	9.70E-11	8.38E-11	1.83E-13	7.01E-14	-1.42E-14
SP-51-E2-05	360	70	0.00055	0.0023	0.00151	0.0024	0.00070	0.0017	4.12E-10	3.59E-10	3.27E-10	8.98E-11	7.08E-11	5.94E-11	2.07E-13	8.56E-14	1.28E-14
SP-51-E2-06	360	70	0.00047	0.0019	0.00129	0.0020	0.00054	0.0013	3.64E-10	2.90E-10	2.57E-10	7.88E-11	5.21E-11	4.01E-11	2.60E-13	9.00E-14	1.34E-14
SP-51-E2-07	360	70	0.00032	0.0013	0.00098	0.0015	0.00041	0.0010	2.05E-10	1.97E-10	1.80E-10	4.58E-11	4.29E-11	3.69E-11	8.50E-14	6.61E-14	2.78E-14
SP-51-E2-08	360	70	0.00029	0.0012	0.00089	0.0014	0.00034	0.0008	2.98E-10	2.55E-10	2.35E-10	4.80E-11	3.24E-11	2.53E-11	1.73E-13	7.31E-14	2.78E-14
SP-51-E2-09	360	70	**0.00027**	**0.0011**	0.00076	0.0012	0.00030	0.0007	2.73E-10	2.35E-10	2.16E-10	3.93E-11	2.58E-11	1.88E-11	1.44E-13	5.72E-14	1.26E-14
SP-51-E2-10	360	70	**0.00025**	**0.0010**	0.00070	0.0011	0.00026	0.0006	2.54E-10	2.21E-10	2.02E-10	3.27E-11	2.08E-11	1.37E-11	1.34E-13	5.75E-14	1.26E-14
SP-51-E2-11	360	70	0.00040	0.0016	0.00063	0.0010	0.00021	0.0005	2.65E-10	2.39E-10	1.81E-10	2.88E-11	1.92E-11	-1.66E-12	1.20E-13	5.86E-14	-7.43E-14
SP-51-E2-12	360	70	**0.00025**	**0.0010**	0.00059	0.0009	0.00021	0.0005	2.47E-10	2.20E-10	1.95E-10	2.49E-11	1.54E-11	6.36E-12	1.11E-13	5.03E-14	-7.67E-15

Table A8. Additional SPFT Test Results from Dissolution of Glass LAWC22 at 40 °C related to IEX, saturated conditions.

Sample ID	Infl [Si] ppm	T in C	[Mo] ppm	Mo Rate	[Cs] ppm	Cs Rate	[Re] ppm	Re Rate	IEX (mol m-2 s-1), Na-B	IEX (mol m-2 s-1), Na-Re	IEX (mol m-2 s-1), Na-Mo	IEX (mol m-2 s-1), Li-B	IEX (mol m-2 s-1), Li-Re	IEX (mol m-2 s-1), Li-Mo	IEX (mol m-2 s-1), Cs-B	IEX (mol m-2 s-1), Cs-Re	IEX (mol m-2 s-1), Cs-Mo
Exp.16																	
SP-52-A2-BLK1	40	40	4.50E-06		9.20E-07		9.80E-07										
SP-52-A2-BLK2	40	40	4.47E-06		8.70E-07		8.20E-07										
SP-52-A2-BLK3	40	40	4.25E-06		1.30E-06		1.32E-06										
SP-52-A2-04	40	40	0.00300	0.0013	0.00975	0.0016	0.00877	0.0022	9.67E-11	1.77E-10	2.26E-10	2.57E-11	5.46E-11	7.22E-11	-2.60E-13	-7.55E-14	3.68E-14
SP-52-A2-06	40	40	0.00353	0.0015	0.01244	0.0020	0.01132	0.0028	8.26E-11	1.35E-10	2.04E-10	2.03E-11	3.90E-11	6.39E-11	-2.17E-13	-9.76E-14	6.12E-14
SP-52-A2-08	40	40	0.00294	0.0013	0.01146	0.0019	0.01008	0.0026	7.00E-11	1.26E-10	1.94E-10	1.45E-11	3.45E-11	5.89E-11	-2.09E-13	-8.13E-14	7.47E-14
SP-52-A2-10	40	40	0.00246	0.0011	0.01091	0.0018	0.00867	0.0021	5.90E-11	1.18E-10	1.77E-10	1.03E-11	3.14E-11	5.25E-11	-1.82E-13	-4.75E-14	8.75E-14
SP-52-A2-12	40	40	0.00206	0.0009	0.01074	0.0017	0.00774	0.0019	5.06E-11	1.09E-10	1.64E-10	6.44E-12	2.74E-11	4.73E-11	-1.56E-13	-2.24E-14	1.05E-13
SP-52-A2-14	40	40	0.00178	0.0008	0.01056	0.0017	0.00704	0.0018	4.34E-11	9.68E-11	1.50E-10	3.64E-12	2.28E-11	4.19E-11	-1.27E-13	-4.74E-15	1.18E-13
SP-52-A2-16	40	40	0.00147	0.0006	0.00980	0.0016	0.00596	0.0015	3.42E-11	9.23E-11	1.37E-10	4.77E-13	2.13E-11	3.74E-11	-1.20E-13	1.29E-14	1.16E-13
SP-52-A2-18	40	40	0.00135	0.0006	0.01011	0.0016	0.00567	0.0014	3.06E-11	8.47E-11	1.29E-10	-7.32E-13	1.87E-11	3.45E-11	-9.61E-14	2.79E-14	1.29E-13
SP-52-A2-20	40	40	0.00120	0.0005	0.00958	0.0015	0.00500	0.0012	2.56E-11	8.10E-11	1.19E-10	-2.21E-12	1.77E-11	3.14E-11	-8.94E-14	3.75E-14	1.26E-13
SP-52-A2-22	40	40	0.00078	0.0003	0.00708	0.0011	0.00352	0.0009	2.23E-11	9.31E-11	1.22E-10	-3.69E-12	2.17E-11	3.20E-11	-1.29E-13	3.31E-14	9.87E-14
SP-52-A2-24	40	40	0.00091	0.0004	0.00896	0.0014	0.00419	0.0010	1.85E-11	7.68E-11	1.11E-10	-4.77E-12	1.61E-11	2.84E-11	-8.42E-14	4.93E-14	1.28E-13
Exp.17																	
SP-52-B2-BLK1	45	40	6.62E-06		9.30E-07		1.56E-06										
SP-52-B2-BLK2	45	40	5.61E-06		9.00E-07		6.50E-07										
SP-52-B2-BLK3	45	40	6.56E-06		9.60E-07		6.90E-07										
SP-52-B2-04	45	40	0.00390	0.0017	0.00925	0.0015	0.00779	0.0019	9.38E-11	1.06E-10	1.20E-10	2.87E-11	3.32E-11	3.82E-11	-8.22E-14	-5.36E-14	-2.15E-14
SP-52-B2-06	45	40	0.00373	0.0016	0.00881	0.0014	0.00753	0.0018	8.56E-11	1.01E-10	1.16E-10	2.67E-11	3.24E-11	3.75E-11	-8.94E-14	-5.30E-14	-2.07E-14
SP-52-B2-08	45	40	0.00337	0.0014	0.00810	0.0013	0.00689	0.0017	7.45E-11	8.88E-11	1.03E-10	2.31E-11	2.82E-11	3.33E-11	-8.13E-14	-4.87E-14	-1.63E-14
SP-52-B2-10	45	40	0.00305	0.0013	0.00757	0.0012	0.00628	0.0015	6.65E-11	7.90E-11	9.22E-11	1.99E-11	2.44E-11	2.91E-11	-6.87E-14	-4.02E-14	-9.85E-15

Sample ID	Infl [Si] ppm	T in C	[Mo] ppm	Mo Rate	[Cs] ppm	Cs Rate	[Re] ppm	Re Rate	IEX (mol m-2 s-1), Na-B	IEX (mol m-2 s-1), Na-Re	IEX (mol m-2 s-1), Na-Mo	IEX (mol m-2 s-1), Li-B	IEX (mol m-2 s-1), Li-Re	IEX (mol m-2 s-1), Li-Mo	IEX (mol m-2 s-1), Cs-B	IEX (mol m-2 s-1), Cs-Re	IEX (mol m-2 s-1), Cs-Mo
SP-52-B2-12	45	40	0.00266	0.0011	0.00675	0.0010	0.00534	0.0013	5.87E-11	7.40E-11	8.36E-11	1.70E-11	2.24E-11	2.59E-11	-6.26E-14	-2.75E-14	-5.57E-15
SP-52-B2-14	45	40	0.00236	0.0010	0.00621	0.0010	0.00476	0.0011	5.10E-11	6.50E-11	7.39E-11	1.45E-11	1.95E-11	2.27E-11	-5.30E-14	-2.11E-14	-6.77E-16
SP-52-B2-16	45	40	0.00210	0.0009	0.00544	0.0008	0.00405	0.0010	4.66E-11	6.15E-11	6.69E-11	1.24E-11	1.78E-11	1.97E-11	-4.89E-14	-1.47E-14	-2.20E-15
SP-52-B2-18	45	40	0.00188	0.0008	0.00526	0.0008	0.00368	0.0009	4.29E-11	5.76E-11	6.31E-11	1.08E-11	1.60E-11	1.80E-11	-4.08E-14	-7.22E-15	5.44E-15
SP-52-B2-20	45	40	0.00169	0.0007	0.00507	0.0008	0.00348	0.0008	3.79E-11	4.85E-11	5.58E-11	1.00E-11	1.38E-11	1.64E-11	-2.94E-14	-5.07E-15	1.15E-14
SP-52-B2-22	45	40	0.00157	0.0006	0.00482	0.0007	0.00320	0.0008	3.45E-11	4.52E-11	5.14E-11	8.61E-12	1.25E-11	1.47E-11	-2.63E-14	-1.64E-15	1.26E-14
SP-52-B2-24	45	40	0.00145	0.0006	0.00455	0.0007	0.00293	0.0007	3.04E-11	4.18E-11	4.71E-11	7.59E-12	1.17E-11	1.36E-11	-2.50E-14	1.06E-15	1.33E-14
Exp.18																	
SP-52-C2-BLK1	60	40	3.80E-06		7.80E-07		4.10E-07										
SP-52-C2-BLK2	60	40	4.75E-06		8.20E-07		2.80E-07										
SP-52-C2-BLK3	60	40	4.92E-06		7.30E-07		4.00E-07										
SP-52-C2-04	60	40	0.00352	0.0016	0.00648	0.0011	0.00569	0.0015	8.63E-11	1.05E-10	9.99E-11	2.68E-11	3.37E-11	3.16E-11	-9.19E-14	-4.80E-14	-6.08E-14
SP-52-C2-06	60	40	0.00300	0.0013	0.00537	0.0009	0.00496	0.0013	7.64E-11	1.10E-10	1.07E-10	2.41E-11	3.61E-11	3.50E-11	-1.23E-13	-4.62E-14	-5.32E-14
SP-52-C2-08	60	40	0.00277	0.0012	0.00499	0.0008	0.00452	0.0012	6.76E-11	9.79E-11	9.42E-11	2.05E-11	3.13E-11	3.00E-11	-1.10E-13	-4.07E-14	-4.92E-14
SP-52-C2-10	60	40	0.00251	0.0011	0.00467	0.0008	0.00414	0.0011	5.98E-11	8.68E-11	8.41E-11	1.79E-11	2.76E-11	2.66E-11	-9.65E-14	-3.46E-14	-4.08E-14
SP-52-C2-12	60	40	0.00227	0.0010	0.00433	0.0007	0.00379	0.0010	5.47E-11	7.52E-11	7.35E-11	1.53E-11	2.26E-11	2.20E-11	-7.70E-14	-3.00E-14	-3.40E-14
SP-52-C2-14	60	40	0.00198	0.0009	0.00399	0.0007	0.00332	0.0008	4.75E-11	6.76E-11	6.62E-11	1.30E-11	2.02E-11	1.97E-11	-6.85E-14	-2.26E-14	-2.57E-14
SP-52-C2-16	60	40	0.00173	0.0007	0.00356	0.0006	0.00283	0.0007	4.19E-11	6.12E-11	5.91E-11	1.15E-11	1.84E-11	1.77E-11	-5.98E-14	-1.57E-14	-2.05E-14
SP-52-C2-18	60	40	0.00161	0.0007	0.00347	0.0006	0.00271	0.0007	3.87E-11	5.34E-11	5.25E-11	1.04E-11	1.57E-11	1.54E-11	-4.73E-14	-1.36E-14	-1.57E-14
SP-52-C2-20	60	40	0.00137	0.0006	0.00301	0.0005	0.00227	0.0006	3.48E-11	4.97E-11	4.85E-11	9.20E-12	1.45E-11	1.41E-11	-4.33E-14	-9.21E-15	-1.20E-14
SP-52-C2-22	60	40	0.00127	0.0006	0.00293	0.0005	0.00209	0.0005	3.38E-11	4.82E-11	4.68E-11	8.54E-12	1.37E-11	1.32E-11	-3.85E-14	-5.60E-15	-8.70E-15
SP-52-C2-24	60	40	0.00117	0.0005	0.00271	0.0004	0.00194	0.0005	3.07E-11	4.33E-11	4.23E-11	7.76E-12	1.23E-11	1.19E-11	-3.41E-14	-5.15E-15	-7.42E-15

Exp.19																	
SP-52-D2-BLK1	105	40	4.02E-06		9.30E-07		6.60E-07										
SP-52-D2-BLK2	105	40	4.36E-06		8.10E-07		3.50E-07										
SP-52-D2-BLK3	105	40	6.03E-06		9.00E-07		3.04E-06										
SP-52-D2-04	105	40	0.00183	0.0016	0.00319	0.0011	0.00275	0.0014	7.66E-11	1.04E-10	9.23E-11	2.24E-11	3.21E-11	2.80E-11	-1.04E-13	-4.21E-14	-6.78E-14
SP-52-D2-06	105	40	0.00231	0.0020	0.00383	0.0013	0.00331	0.0017	7.32E-11	9.97E-11	8.13E-11	2.13E-11	3.08E-11	2.42E-11	-1.11E-13	-5.04E-14	-9.26E-14
SP-52-D2-08	105	40	0.00203	0.0018	0.00337	0.0011	0.00289	0.0015	6.42E-11	9.38E-11	7.69E-11	1.94E-11	3.00E-11	2.39E-11	-1.12E-13	-4.37E-14	-8.25E-14
SP-52-D2-10	105	40	0.00175	0.0015	0.00299	0.0010	0.00254	0.0013	5.91E-11	8.68E-11	7.37E-11	1.77E-11	2.77E-11	2.30E-11	-1.00E-13	-3.68E-14	-6.68E-14
SP-52-D2-12	105	40	0.00175	0.0015	0.00307	0.0010	0.00249	0.0012	5.41E-11	7.48E-11	6.06E-11	1.57E-11	2.32E-11	1.81E-11	-7.76E-14	-3.00E-14	-6.26E-14
SP-52-D2-14	105	40	0.00141	0.0012	0.00253	0.0008	0.00198	0.0010	5.03E-11	7.11E-11	5.87E-11	1.50E-11	2.24E-11	1.80E-11	-6.82E-14	-2.07E-14	-4.90E-14
SP-52-D2-16	105	40	0.00122	0.0011	0.00226	0.0007	0.00175	0.0009	4.76E-11	6.56E-11	5.61E-11	1.25E-11	1.90E-11	1.56E-11	-5.83E-14	-1.71E-14	-3.89E-14
SP-52-D2-18	105	40	0.00117	0.0010	0.00225	0.0007	0.00172	0.0009	4.53E-11	5.53E-11	4.74E-11	1.25E-11	1.61E-11	1.32E-11	-3.86E-14	-1.55E-14	-3.37E-14
SP-52-D2-20	105	40	0.00104	0.0009	0.00207	0.0007	0.00146	0.0007	4.87E-11	5.80E-11	4.90E-11	1.25E-11	1.59E-11	1.26E-11	-2.84E-14	-6.85E-15	-2.76E-14
SP-52-D2-22	105	40	0.00117	0.0010	0.00240	0.0008	0.00175	0.0009	4.07E-11	3.59E-11	2.87E-11	1.15E-11	9.76E-12	7.18E-12	-2.53E-16	-1.14E-14	-2.78E-14
SP-52-D2-24	105	40	0.00100	0.0008	0.00218	0.0007	0.00152	0.0007	3.96E-11	3.63E-11	3.09E-11	1.07E-11	9.52E-12	7.59E-12	1.68E-15	-5.92E-15	-1.82E-14

Exp.20																	
SP-52-E2-BLK1	270	40	5.84E-06		8.50E-07		5.40E-07										
SP-52-E2-BLK2	270	40	5.28E-06		8.50E-07		3.60E-07										
SP-52-E2-BLK3	270	40	5.50E-06		8.40E-07		9.10E-07										
SP-52-E2-04	270	40	0.00259	0.0021	0.00447	0.0014	0.00353	0.0017	7.27E-11	9.50E-11	7.10E-11	1.32E-11	2.12E-11	1.26E-11	-8.70E-14	-3.60E-14	-9.11E-14
SP-52-E2-06	270	40	0.00370	0.0029	0.00591	0.0018	0.00510	0.0023	7.22E-11	9.45E-11	6.28E-11	1.39E-11	2.19E-11	1.05E-11	-1.21E-13	-7.02E-14	-1.43E-13
SP-52-E2-08	270	40	0.00449	0.0036	0.00703	0.0021	0.00612	0.0028	6.20E-11	7.82E-11	3.72E-11	1.09E-11	1.67E-11	1.99E-12	-1.25E-13	-8.81E-14	-1.82E-13
SP-52-E2-10	270	40	0.00442	0.0035	0.00698	0.0021	0.00594	0.0027	5.52E-11	8.26E-11	4.11E-11	8.77E-12	1.86E-11	3.71E-12	-1.41E-13	-7.79E-14	-1.73E-13
SP-52-E2-12	270	40	0.00451	0.0036	0.00695	0.0021	0.00614	0.0028	5.44E-11	7.50E-11	3.42E-11	7.52E-12	1.49E-11	2.56E-13	-1.38E-13	-9.10E-14	-1.84E-13
SP-52-E2-14	270	40	0.00412	0.0034	0.00664	0.0021	0.00572	0.0027	5.32E-11	7.26E-11	3.67E-11	7.30E-12	1.43E-11	1.38E-12	-1.26E-13	-8.19E-14	-1.64E-13
SP-52-E2-16	270	40	0.00377	0.0030	0.00606	0.0018	0.00516	0.0024	5.38E-11	7.95E-11	4.56E-11	6.19E-12	1.54E-11	3.24E-12	-1.28E-13	-6.94E-14	-1.47E-13
SP-52-E2-18	270	40	0.00306	0.0024	0.00562	0.0017	0.00473	0.0022	4.97E-11	7.48E-11	6.11E-11	5.79E-12	1.48E-11	9.90E-12	-1.18E-13	-6.05E-14	-9.19E-14
SP-52-E2-20	270	40	0.00326	0.0026	0.00538	0.0016	0.00448	0.0021	4.98E-11	6.53E-11	3.67E-11	5.91E-12	1.15E-11	1.21E-12	-9.10E-14	-5.54E-14	-1.21E-13
SP-52-E2-22	270	40	0.00284	0.0022	0.00476	0.0014	0.00379	0.0017	4.51E-11	6.24E-11	3.60E-11	5.89E-12	1.21E-11	2.62E-12	-7.69E-14	-3.73E-14	-9.78E-14
SP-52-E2-24	270	40	0.00265	0.0020	0.00469	0.0014	0.00359	0.0016	5.01E-11	6.61E-11	4.25E-11	6.16E-12	1.19E-11	3.43E-12	-6.57E-14	-2.91E-14	-8.31E-14

Table A9. Additional SPFT Test Results from Dissolution of Glass LAWC22 at 23 °C related to IEX, saturated conditions.

Sample ID	Infl [Si] ppm	T in C	[Mo] ppm	Mo Rate	[Cs] ppm	Cs Rate	[Re] ppm	Re Rate	IEX (mol m-2 s-1), Na-B	IEX (mol m-2 s-1), Na-Re	IEX (mol m-2 s-1), Na-Mo	IEX (mol m-2 s-1), Li-B	IEX (mol m-2 s-1), Li-Re	IEX (mol m-2 s-1), Li-Mo	IEX (mol m-2 s-1), Cs-B	IEX (mol m-2 s-1), Cs-Re	IEX (mol m-2 s-1), Cs-Mo
Exp.26																	
SP-53-A2-BLK1	35	23	3.90E-04		1.80E-04		1.00E-05										
SP-53-A2-BLK2	35	23	3.60E-04		1.80E-04		1.00E-05										
SP-53-A2-BLK3	35	23	4.40E-04		2.80E-04		9.00E-05										
SP-53-A2-02	35	23	0.00621	0.0012	0.00793	0.0006	0.01134	0.0013	6.96E-11	9.86E-11	1.07E-10	1.91E-11	2.95E-11	3.23E-11	-1.58E-13	-9.12E-14	-7.30E-14
SP-53-A2-03	35	23	0.00460	0.0009	0.00679	0.0005	0.00910	0.0011	5.47E-11	8.07E-11	9.28E-11	1.64E-11	2.57E-11	3.01E-11	-1.33E-13	-7.39E-14	-4.62E-14
SP-53-A2-04	35	23	0.00352	0.0007	0.00599	0.0005	0.00721	0.0009	4.05E-11	6.11E-11	7.32E-11	1.29E-11	2.03E-11	2.46E-11	-1.00E-13	-5.30E-14	-2.55E-14
SP-53-A2-05	35	23	0.00262	0.0005	0.00518	0.0004	0.00553	0.0007	3.06E-11	4.95E-11	6.06E-11	1.04E-11	1.71E-11	2.11E-11	-7.82E-14	-3.49E-14	-9.40E-15
SP-53-A2-06	35	23	0.00205	0.0004	0.00474	0.0004	0.00442	0.0006	2.47E-11	4.10E-11	5.14E-11	8.85E-12	1.47E-11	1.84E-11	-5.98E-14	-2.23E-14	1.43E-15
SP-53-A2-07	35	23	0.00170	0.0003	0.00450	0.0003	0.00377	0.0005	1.97E-11	3.38E-11	4.37E-11	7.45E-12	1.25E-11	1.61E-11	-4.67E-14	-1.44E-14	8.31E-15
SP-53-A2-08	35	23	0.00150	0.0002	0.00450	0.0003	0.00332	0.0004	1.66E-11	2.84E-11	3.76E-11	6.47E-12	1.07E-11	1.40E-11	-3.44E-14	-7.48E-15	1.36E-14
SP-53-A2-09	35	23	0.00122	0.0002	0.00389	0.0003	0.00266	0.0003	1.43E-11	2.70E-11	3.52E-11	5.43E-12	9.99E-12	1.29E-11	-3.26E-14	-3.52E-15	1.52E-14
SP-53-A2-10	35	23	0.00109	0.0002	0.00381	0.0003	0.00235	0.0003	1.29E-11	2.40E-11	3.17E-11	4.90E-12	8.90E-12	1.16E-11	-2.50E-14	5.03E-16	1.80E-14
SP-53-A2-11	35	23	0.00103	0.0001	0.00372	0.0003	0.00211	0.0003	1.17E-11	2.19E-11	2.86E-11	4.47E-12	8.12E-12	1.05E-11	-2.00E-14	3.36E-15	1.87E-14
SP-53-A2-12	35	23	0.00101	0.0001	0.00365	0.0003	0.00198	0.0002	1.05E-11	1.99E-11	2.59E-11	4.03E-12	7.40E-12	9.55E-12	-1.68E-14	4.64E-15	1.84E-14
Exp.27																	
SP-53-B2-BLK1	40	23	3.90E-04		1.80E-04		1.00E-05										
SP-53-B2-BLK2	40	23	3.90E-04		1.80E-04		1.00E-05										
SP-53-B2-BLK3	40	23	3.80E-04		1.70E-04		1.00E-05										
SP-53-B2-02	40	23	0.00535	0.0010	0.00600	0.0004	0.00828	0.0009	6.46E-11	8.07E-11	7.88E-11	1.89E-11	2.47E-11	2.41E-11	-9.90E-14	-6.19E-14	-6.63E-14
SP-53-B2-03	40	23	0.00418	0.0008	0.00544	0.0004	0.00666	0.0008	5.31E-11	6.77E-11	6.83E-11	1.53E-11	2.05E-11	2.07E-11	-8.08E-14	-4.73E-14	-4.60E-14
SP-53-B2-04	40	23	0.00324	0.0006	0.00479	0.0004	0.00522	0.0006	3.94E-11	5.19E-11	5.36E-11	1.16E-11	1.61E-11	1.67E-11	-6.10E-14	-3.24E-14	-2.84E-14
SP-53-B2-05	40	23	0.00257	0.0004	0.00428	0.0003	0.00423	0.0005	3.16E-11	4.14E-11	4.42E-11	9.26E-12	1.27E-11	1.38E-11	-4.48E-14	-2.25E-14	-1.61E-14

Sample ID	Infl [Si] ppm	T in C	[Mo] ppm	Mo Rate	[Cs] ppm	Cs Rate	[Re] ppm	Re Rate	IEX (mol m-2 s-1), Na-B	IEX (mol m-2 s-1), Na-Re	IEX (mol m-2 s-1), Na-Mo	IEX (mol m-2 s-1), Li-B	IEX (mol m-2 s-1), Li-Re	IEX (mol m-2 s-1), Li-Mo	IEX (mol m-2 s-1), Cs-B	IEX (mol m-2 s-1), Cs-Re	IEX (mol m-2 s-1), Cs-Mo
SP-53-B2-06	40	23	0.00205	0.0003	0.00376	0.0003	0.00338	0.0004	2.57E-11	3.45E-11	3.77E-11	7.80E-12	1.10E-11	1.21E-11	-3.56E-14	-1.52E-14	-7.96E-15
SP-53-B2-07	40	23	0.00181	0.0003	0.00358	0.0003	0.00294	0.0003	2.11E-11	2.80E-11	3.10E-11	6.53E-12	9.03E-12	1.01E-11	-2.64E-14	-1.04E-14	-3.55E-15
SP-53-B2-08	40	23	0.00153	0.0002	0.00324	0.0002	0.00244	0.0003	1.79E-11	2.49E-11	2.77E-11	5.47E-12	7.97E-12	9.01E-12	-2.23E-14	-6.31E-15	2.88E-16
SP-53-B2-09	40	23	0.00139	0.0002	0.00313	0.0002	0.00224	0.0003	1.61E-11	2.13E-11	2.45E-11	4.90E-12	6.76E-12	7.92E-12	-1.64E-14	-4.53E-15	2.83E-15
SP-53-B2-10	40	23	0.00128	0.0002	0.00297	0.0002	0.00200	0.0002	1.50E-11	1.95E-11	2.24E-11	4.46E-12	6.07E-12	7.12E-12	-1.28E-14	-2.53E-15	4.14E-15
SP-53-B2-11	40	23	0.00116	0.0002	0.00275	0.0002	0.00175	0.0002	1.31E-11	1.75E-11	2.01E-11	3.96E-12	5.54E-12	6.48E-12	-1.10E-14	-9.28E-16	5.09E-15
SP-53-B2-12	40	23	0.00110	0.0001	0.00265	0.0002	0.00162	0.0002	1.21E-11	1.59E-11	1.84E-11	3.66E-12	5.06E-12	5.93E-12	-8.87E-15	4.15E-17	5.62E-15
Exp.28																	
SP-53-C2-BLK1	52.2	23	3.50E-04		1.70E-04		1.00E-05										
SP-53-C2-BLK2	52.2	23	3.60E-04		1.70E-04		1.00E-05										
SP-53-C2-BLK3	52.2	23	3.60E-04		1.70E-04		4.00E-05										
SP-53-C2-02	52.2	23	0.00463	0.0009	0.00426	0.0003	0.00650	0.0008	5.49E-11	6.34E-11	5.74E-11	1.78E-11	2.09E-11	1.87E-11	-7.73E-14	-5.79E-14	-7.17E-14
SP-53-C2-03	52.2	23	0.00345	0.0007	0.00377	0.0003	0.00478	0.0006	4.48E-11	5.34E-11	4.92E-11	1.41E-11	1.72E-11	1.57E-11	-5.88E-14	-3.91E-14	-4.86E-14
SP-53-C2-04	52.2	23	0.00262	0.0005	0.00325	0.0003	0.00352	0.0005	3.59E-11	4.35E-11	4.06E-11	1.05E-11	1.33E-11	1.22E-11	-4.20E-14	-2.44E-14	-3.12E-14
SP-53-C2-05	52.2	23	0.00213	0.0004	0.00294	0.0002	0.00286	0.0004	2.76E-11	3.38E-11	3.21E-11	8.31E-12	1.05E-11	9.92E-12	-3.09E-14	-1.69E-14	-2.06E-14
SP-53-C2-06	52.2	23	0.00174	0.0003	0.00258	0.0002	0.00227	0.0003	2.31E-11	2.87E-11	2.77E-11	6.85E-12	8.86E-12	8.49E-12	-2.40E-14	-1.12E-14	-1.35E-14
SP-53-C2-07	52.2	23	0.00162	0.0003	0.00256	0.0002	0.00212	0.0003	1.97E-11	2.32E-11	2.26E-11	5.72E-12	6.98E-12	6.76E-12	-1.69E-14	-8.89E-15	-1.03E-14
SP-53-C2-08	52.2	23	0.00145	0.0003	0.00241	0.0002	0.00189	0.0002	1.68E-11	2.01E-11	1.99E-11	4.75E-12	5.92E-12	5.87E-12	-1.42E-14	-6.70E-15	-7.04E-15
SP-53-C2-09	52.2	23	0.00126	0.0002	0.00215	0.0002	0.00157	0.0002	1.52E-11	1.89E-11	1.88E-11	4.28E-12	5.62E-12	5.59E-12	-1.29E-14	-4.30E-15	-4.51E-15
SP-53-C2-10	52.2	23	0.00123	0.0002	0.00214	0.0002	0.00154	0.0002	1.37E-11	1.62E-11	1.63E-11	3.62E-12	4.52E-12	4.54E-12	-9.70E-15	-3.96E-15	-3.81E-15
SP-53-C2-11	52.2	23	0.00113	0.0002	0.00192	0.0002	0.00132	0.0002	1.28E-11	1.54E-11	1.51E-11	3.35E-12	4.29E-12	4.19E-12	-8.73E-15	-2.69E-15	-3.33E-15
SP-53-C2-12	52.2	23	0.00113	0.0002	0.00200	0.0002	0.00135	0.0002	1.16E-11	1.31E-11	1.31E-11	2.99E-12	3.54E-12	3.52E-12	-5.79E-15	-2.29E-15	-2.42E-15

Exp.29																	
SP-53-D2-BLK1	90	23	3.30E-04		1.70E-04		1.00E-05										
SP-53-D2-BLK2	90	23	3.30E-04		1.70E-04		1.00E-05										
SP-53-D2-BLK3	90	23	3.60E-04		1.70E-04		1.00E-05										
SP-53-D2-02	90	23	0.00251	0.0009	0.00238	0.0004	0.00319	0.0008	5.15E-11	5.61E-11	4.84E-11	1.60E-11	1.77E-11	1.49E-11	-6.37E-14	-5.31E-14	-7.06E-14
SP-53-D2-03	90	23	0.00203	0.0008	0.00226	0.0004	0.00246	0.0006	4.26E-11	4.78E-11	4.12E-11	1.21E-11	1.40E-11	1.16E-11	-4.72E-14	-3.51E-14	-5.04E-14
SP-53-D2-04	90	23	0.00169	0.0006	0.00210	0.0003	0.00205	0.0005	3.31E-11	3.72E-11	3.30E-11	9.46E-12	1.09E-11	9.42E-12	-3.48E-14	-2.54E-14	-3.51E-14
SP-53-D2-05	90	23	0.00143	0.0005	0.00188	0.0003	0.00163	0.0004	2.69E-11	3.23E-11	2.86E-11	7.02E-12	8.98E-12	7.64E-12	-2.89E-14	-1.63E-14	-2.49E-14
SP-53-D2-06	90	23	0.00141	0.0005	0.00192	0.0003	0.00157	0.0004	2.27E-11	2.58E-11	2.16E-11	5.49E-12	6.59E-12	5.09E-12	-2.08E-14	-1.38E-14	-2.33E-14
SP-53-D2-07	90	23	0.00127	0.0004	0.00178	0.0003	0.00138	0.0004	1.99E-11	2.27E-11	1.93E-11	4.89E-12	5.91E-12	4.69E-12	-1.70E-14	-1.05E-14	-1.83E-14
SP-53-D2-08	90	23	0.00116	0.0004	0.00163	0.0003	0.00123	0.0003	1.81E-11	2.10E-11	1.82E-11	4.00E-12	5.03E-12	4.02E-12	-1.53E-14	-8.72E-15	-1.52E-14
SP-53-D2-09	90	23	0.00109	0.0003	0.00154	0.0002	0.00112	0.0003	1.66E-11	1.94E-11	1.67E-11	3.45E-12	4.47E-12	3.49E-12	-1.37E-14	-7.20E-15	-1.34E-14
SP-53-D2-10	90	23	0.00104	0.0003	0.00147	0.0002	0.00103	0.0003	1.57E-11	1.82E-11	1.54E-11	3.25E-12	4.13E-12	3.13E-12	-1.14E-14	-5.74E-15	-1.21E-14
SP-53-D2-11	90	23	0.00102	0.0003	0.00146	0.0002	0.00100	0.0003	1.43E-11	1.55E-11	1.28E-11	3.02E-12	3.44E-12	2.48E-12	-7.66E-15	-4.94E-15	-1.11E-14
SP-53-D2-12	90	23	0.00096	0.0003	0.00139	0.0002	0.00093	0.0002	1.37E-11	1.50E-11	1.28E-11	2.89E-12	3.37E-12	2.58E-12	-7.18E-15	-4.10E-15	-9.12E-15

Exp.30																		
SP-53-E2-BLK1	230	23	2.80E-04		1.70E-04		1.00E-05											
SP-53-E2-BLK2	230	23	2.80E-04		1.70E-04		1.00E-05											
SP-53-E2-BLK3	230	23	3.60E-04		1.80E-04		1.00E-05											
SP-53-E2-02	230	23	0.0026	0.0008	0.0026	0.0003	0.0034	0.0007	4.03E-11	4.29E-11	3.60E-11	1.22E-11	1.31E-11	1.06E-11	-5.31E-14	-4.72E-14	-6.31E-14
SP-53-E2-03	230	23	0.0027	0.0010	0.0031	0.0005	0.0034	0.0008	3.58E-11	3.70E-11	2.67E-11	9.72E-12	1.02E-11	6.43E-12	-4.71E-14	-4.43E-14	-6.81E-14
SP-53-E2-04	230	23	0.0027	0.0010	0.0033	0.0005	0.0034	0.0008	2.87E-11	3.18E-11	2.10E-11	5.88E-12	6.99E-12	3.14E-12	-4.55E-14	-3.84E-14	-6.30E-14
SP-53-E2-05	230	23	0.0029	0.0011	0.0037	0.0005	0.0036	0.0008	2.40E-11	2.77E-11	1.61E-11	4.26E-12	5.60E-12	1.42E-12	-4.54E-14	-3.69E-14	-6.36E-14
SP-53-E2-06	230	23	0.0031	0.0011	0.0041	0.0006	0.0038	0.0009	2.00E-11	2.42E-11	1.17E-11	3.07E-12	4.56E-12	8.36E-14	-4.64E-14	-3.69E-14	-6.55E-14
SP-53-E2-07	230	23	0.0033	0.0012	0.0044	0.0006	0.0041	0.0009	2.01E-11	2.35E-11	1.05E-11	2.23E-12	3.45E-12	-1.22E-12	-4.51E-14	-3.74E-14	-6.72E-14
SP-53-E2-08	**230**	**23**	**0.0032**	**0.0011**	**0.0044**	**0.0006**	**0.0041**	**0.0009**	**1.86E-11**	**2.39E-11**	**1.33E-11**	1.78E-12	3.70E-12	-1.03E-13	-4.77E-14	-3.55E-14	-5.98E-14
SP-53-E2-09	230	23	0.0031	0.0014	0.0044	0.0008	0.0038	0.0011	1.97E-11	2.74E-11	1.19E-11	1.92E-12	4.68E-12	-8.77E-13	-5.65E-14	-3.89E-14	-7.44E-14
SP-53-E2-10	**230**	**23**	**0.0029**	**0.0011**	**0.0043**	**0.0007**	**0.0037**	**0.0009**	**1.56E-11**	**1.89E-11**	**7.03E-12**	1.72E-12	2.91E-12	-1.33E-12	-3.71E-14	-2.95E-14	-5.66E-14
SP-53-E2-11	230	23	0.0032	0.0011	0.0045	0.0006	0.0038	0.0008	1.33E-11	1.58E-11	2.62E-12	1.32E-12	2.19E-12	-2.52E-12	-3.20E-14	-2.64E-14	-5.65E-14
SP-53-E2-12	**230**	**23**	**0.0030**	**0.0012**	**0.0044**	**0.0007**	**0.0037**	**0.0009**	**1.49E-11**	**2.00E-11**	**6.15E-12**	1.39E-12	3.21E-12	-1.77E-12	-4.00E-14	-2.83E-14	-6.01E-14

APPENDIX B

PLOTS OF SPFT TEST DATA: EFFECTS OF pH & TEMPERATURE ON NORMALIZED DISSOLUTION RATE (NDR) FOR GLASS LAWC22

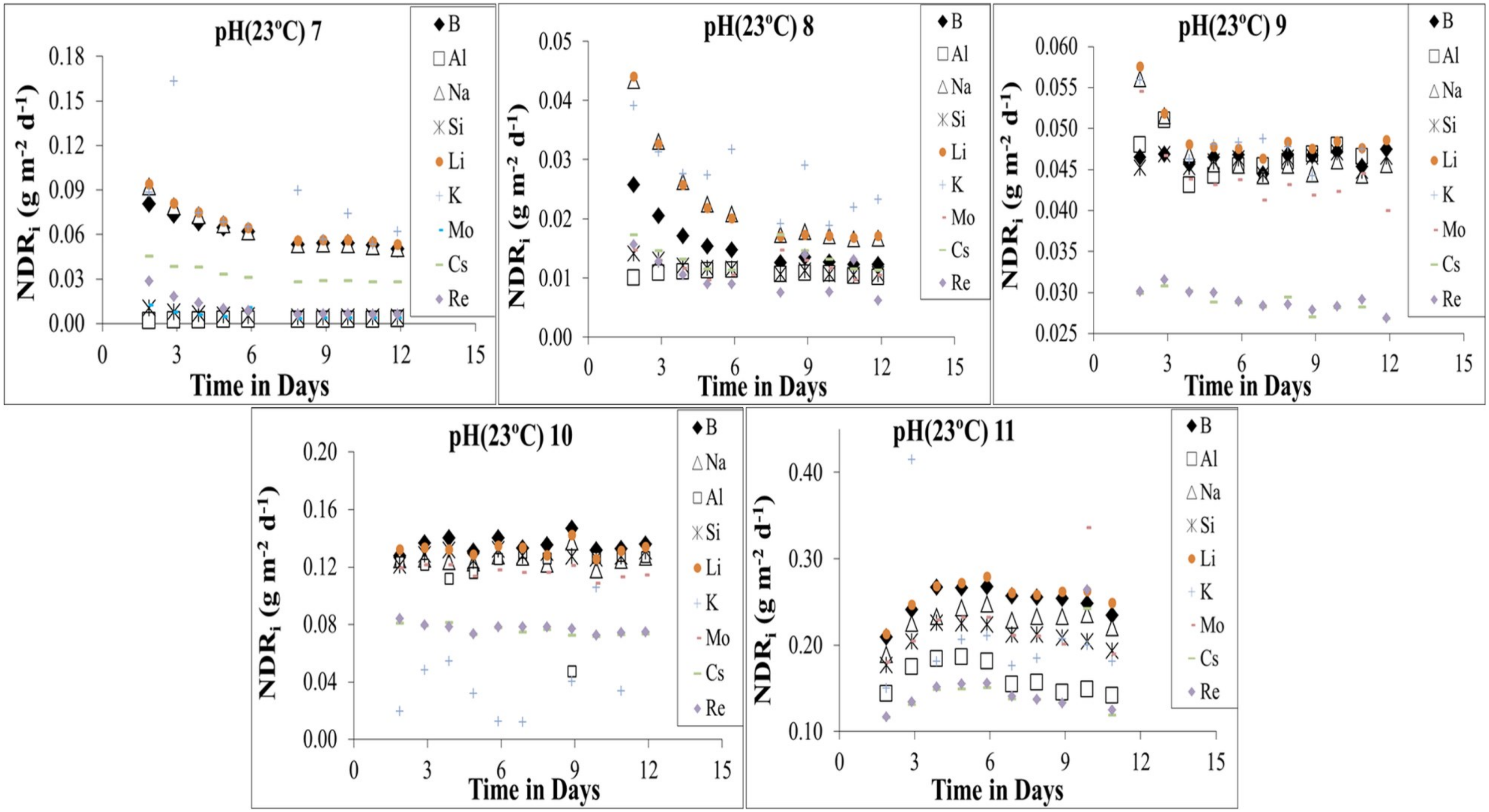

Figure B1. Dissolution under dilute conditions at 70 °C.

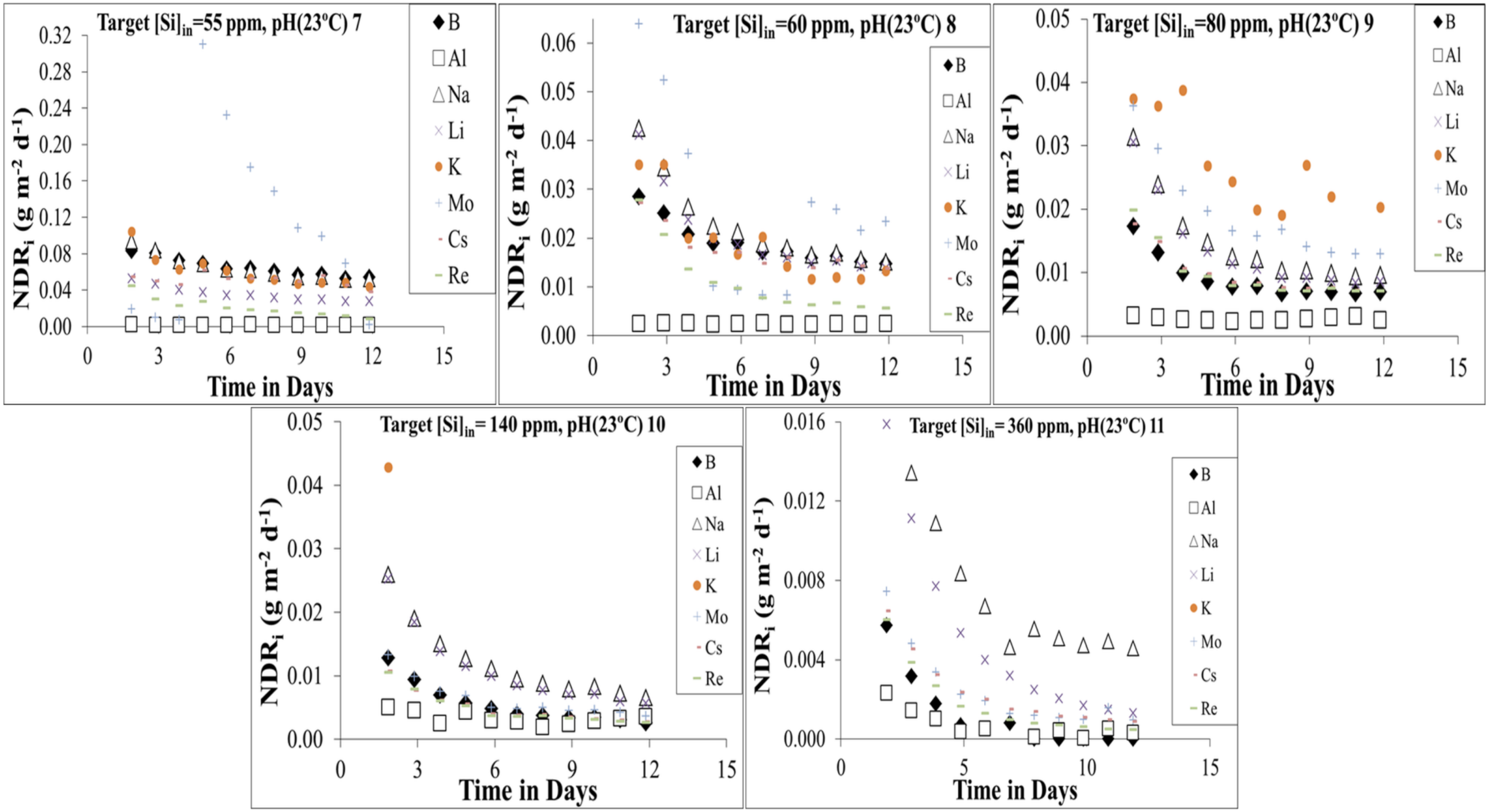

Figure B2. Dissolution under saturated conditions at 70 °C.

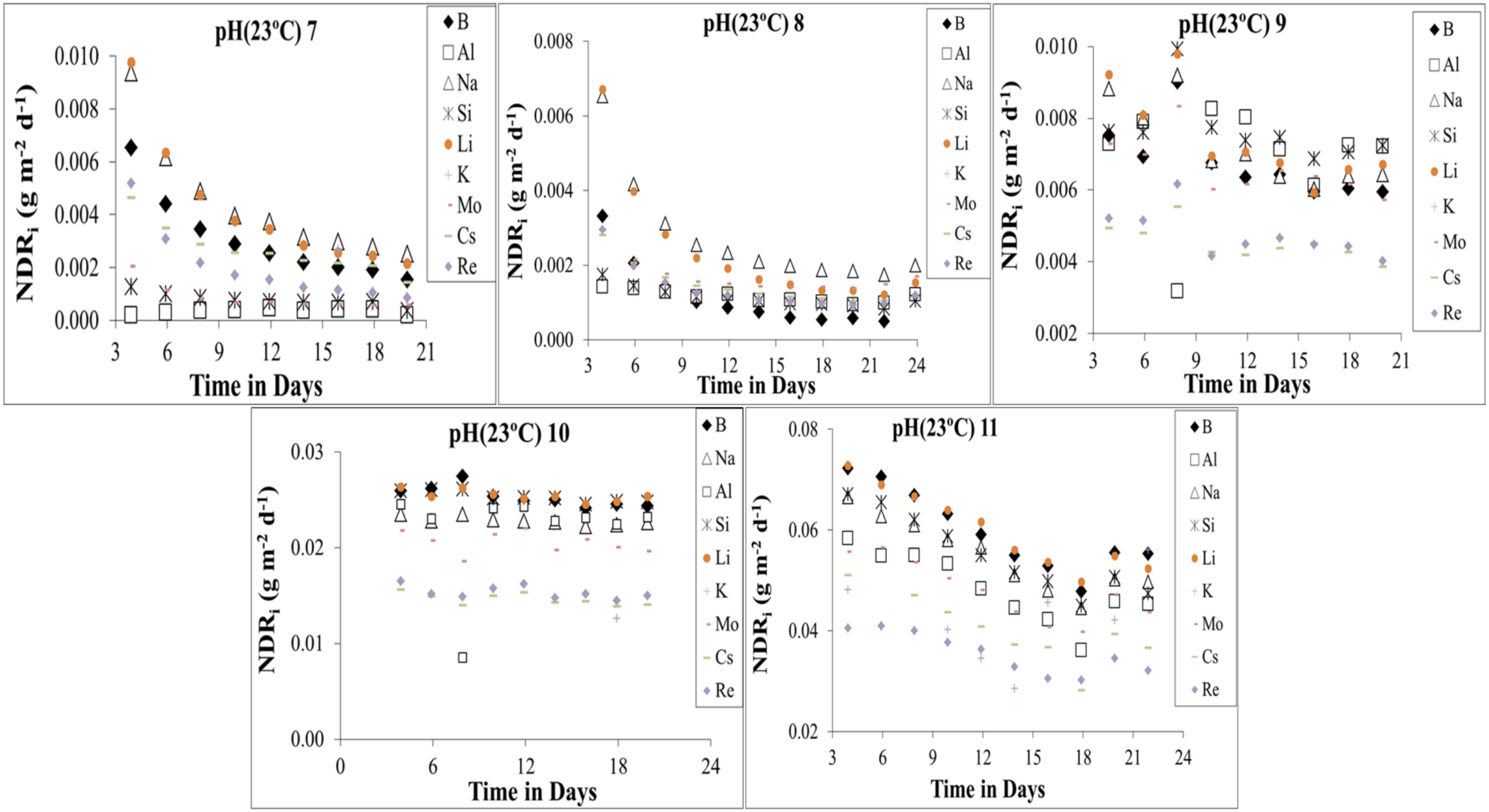

Figure B3. Dissolution under dilute conditions at 40 °C.

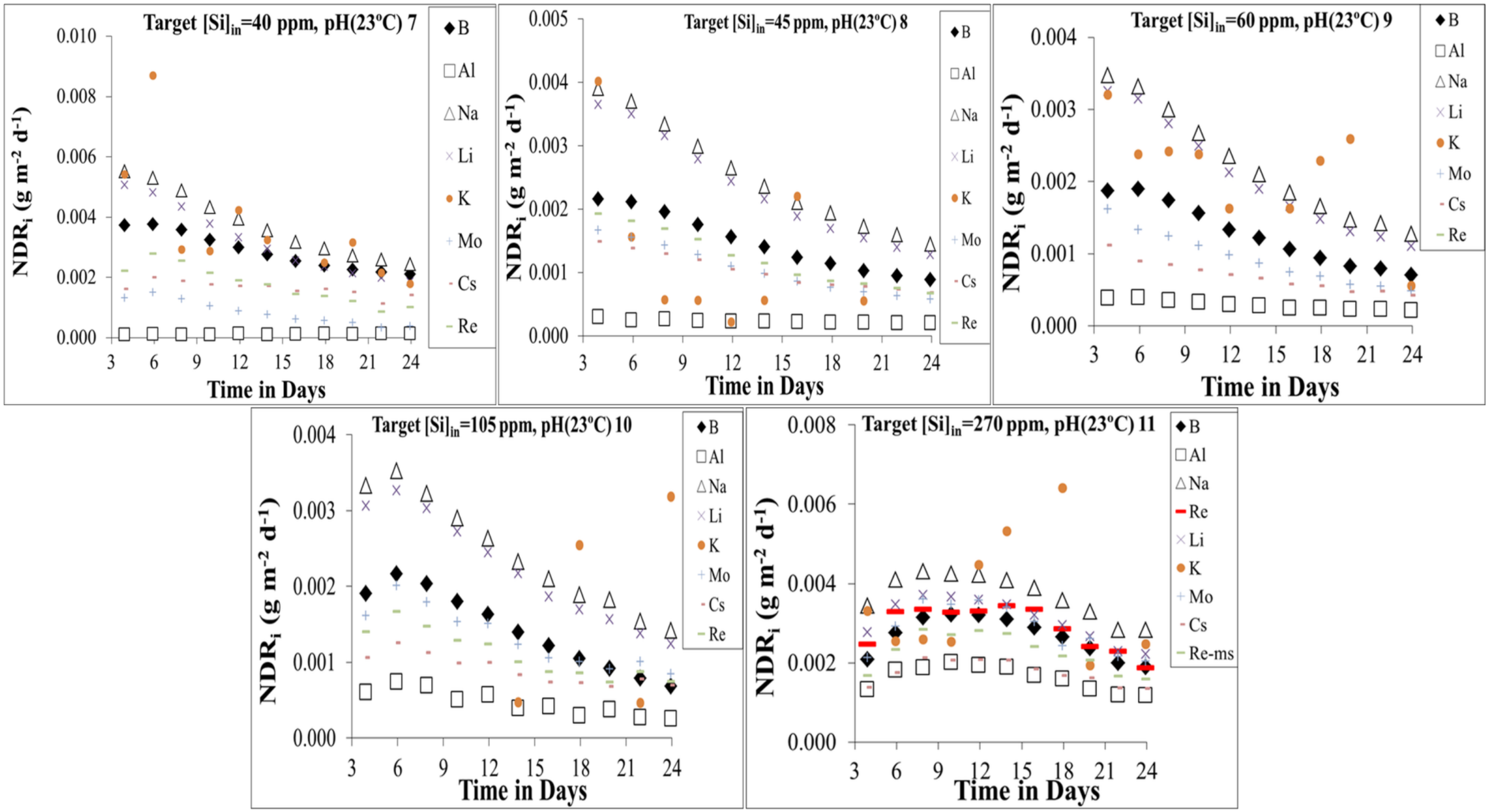

Figure B4. Dissolution under saturated conditions at 40 °C.

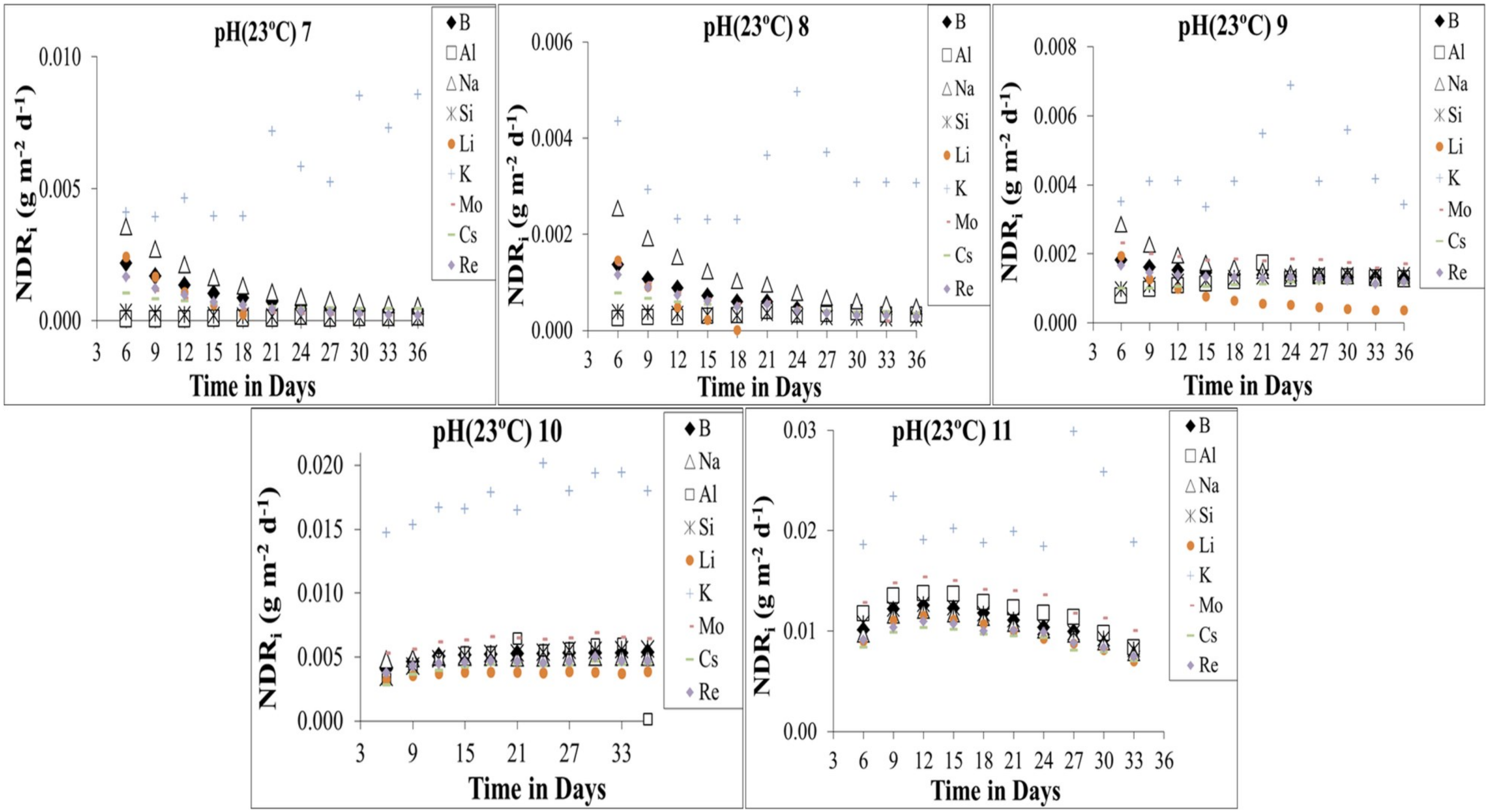

Figure B5. Dissolution under dilute conditions at 23 °C.

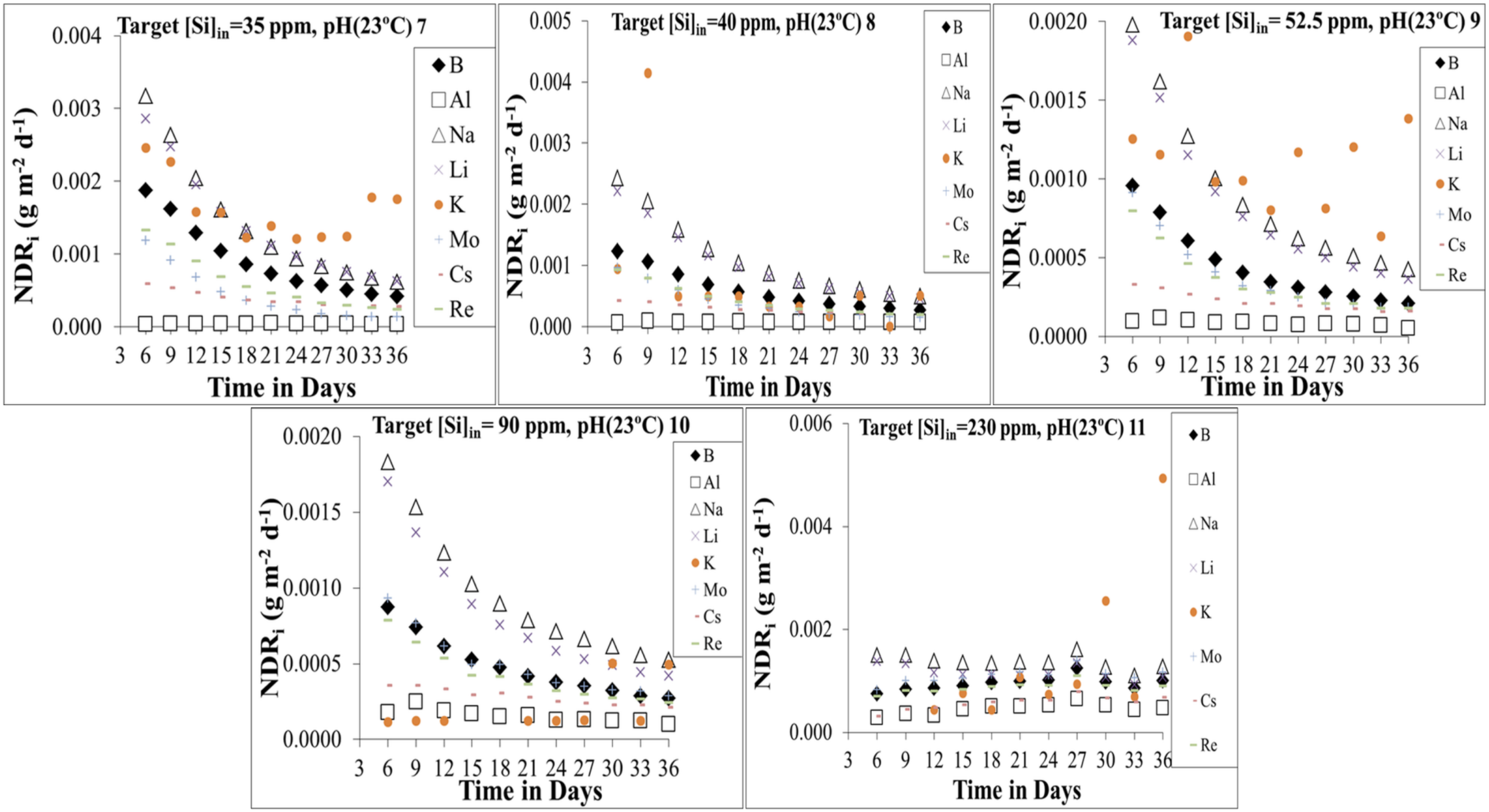

Figure B6. Dissolution under saturated conditions at 23 °C.

APPENDIX C

PLOTS OF SPFT TEST DATA: EFFECTS OF pH & TEMPERATURE ON SODIUM ION EXCHANGE FOR GLASS LAWC22

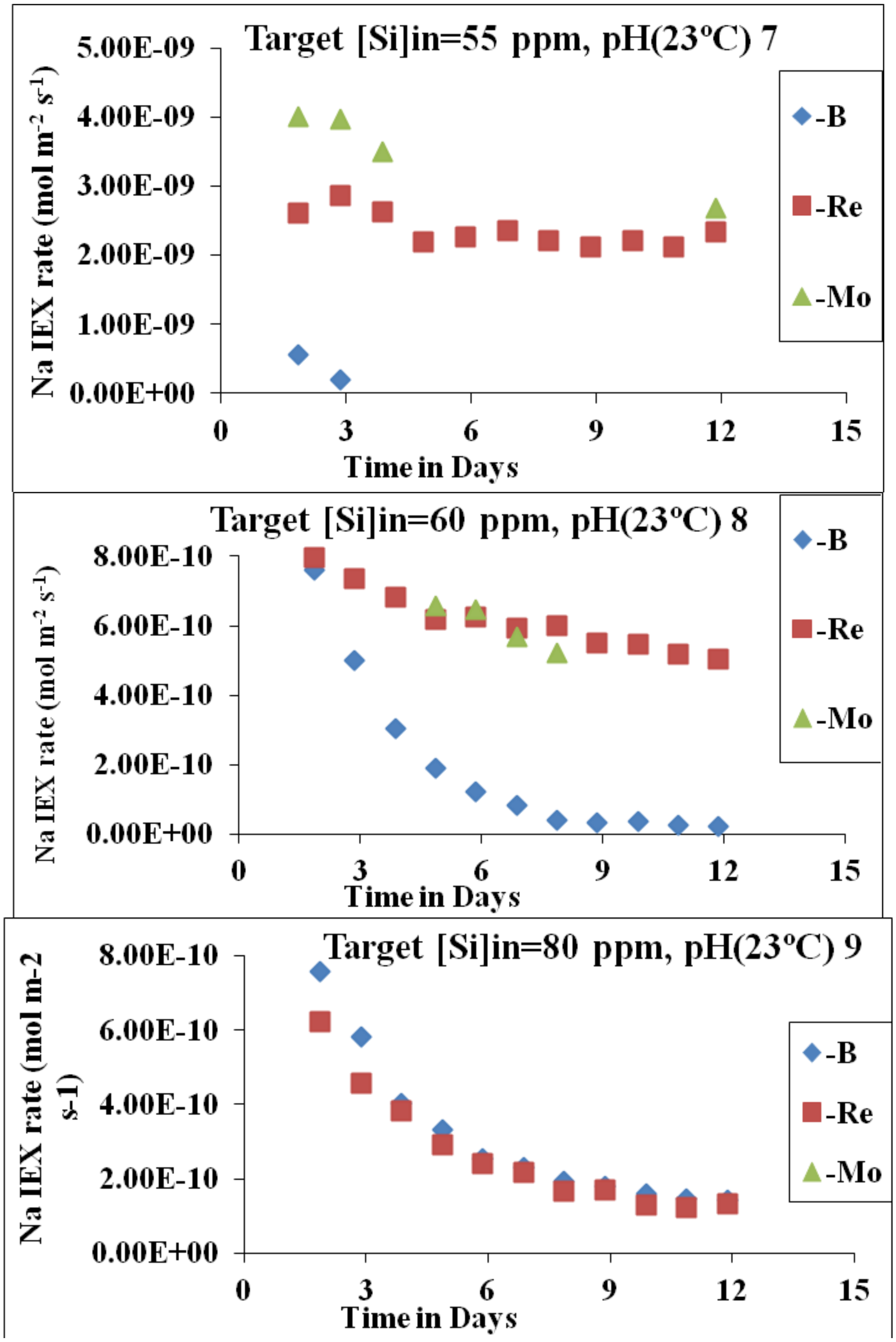

Figure C1. Na ion-exchange rates at 70 °C based on B, Mo, and Re.

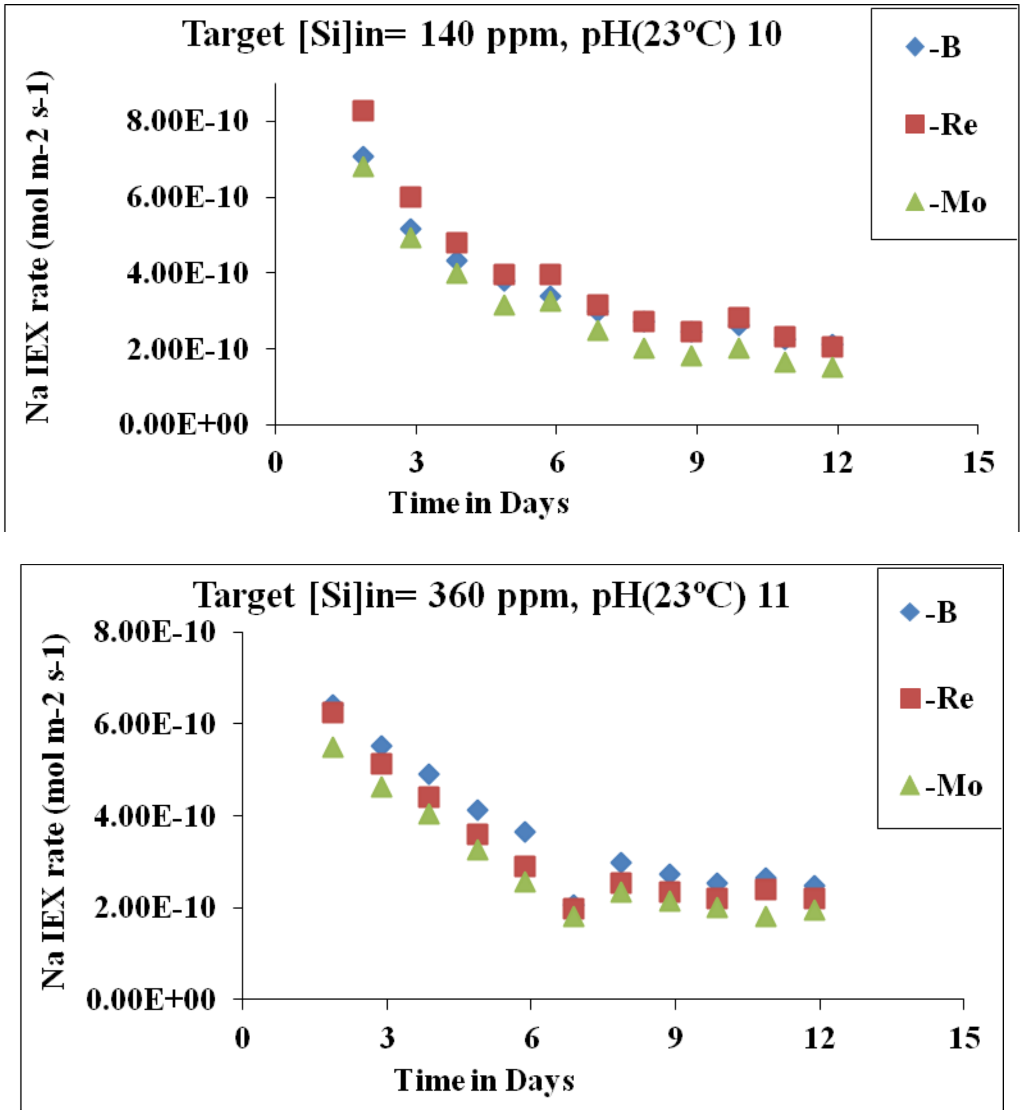

Figure C1. Na ion-exchange rates at 70 °C based on B, Mo and Re (cont'd).

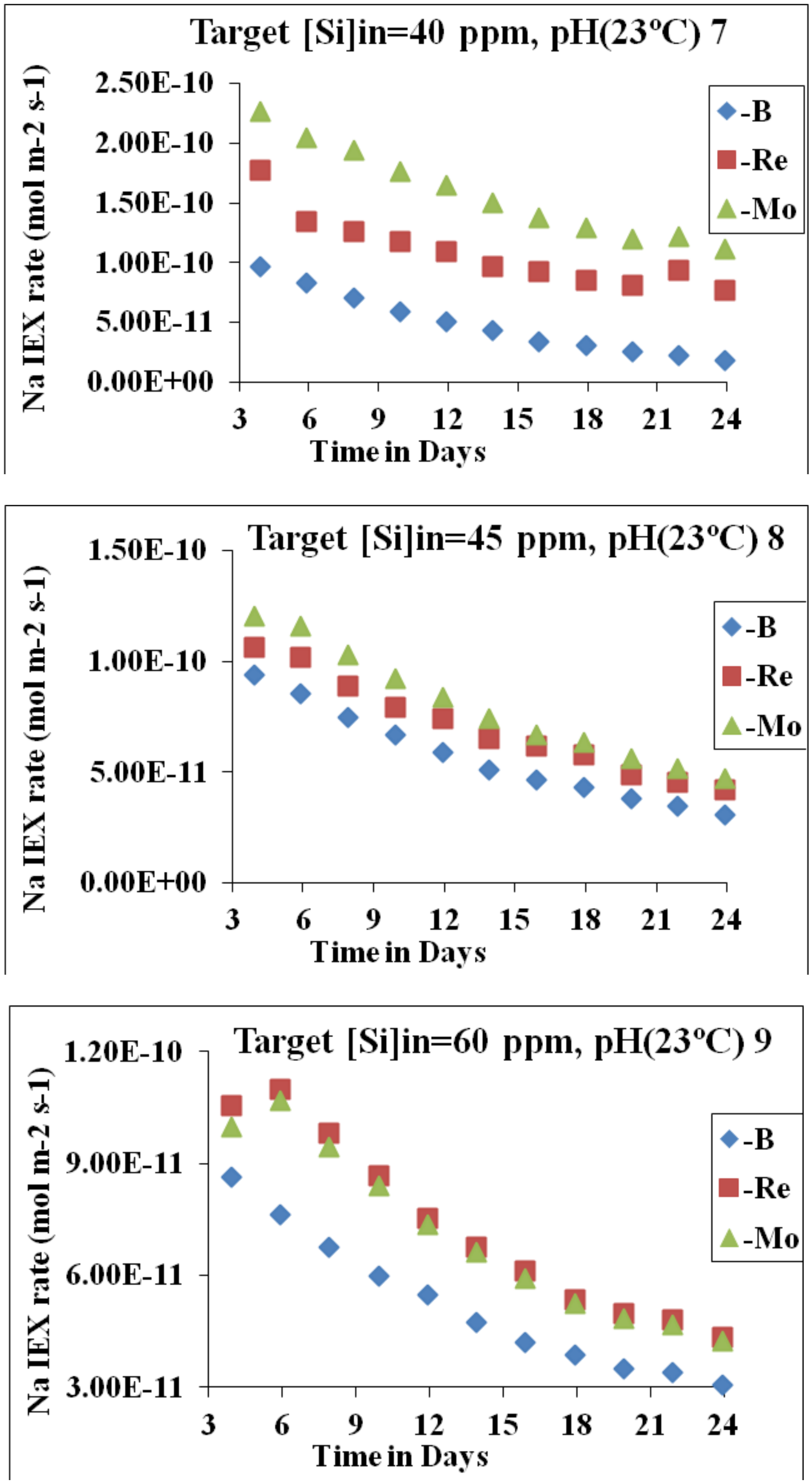

Figure C2. Na IEX Rates at 40 °C based on B, Mo and Re.

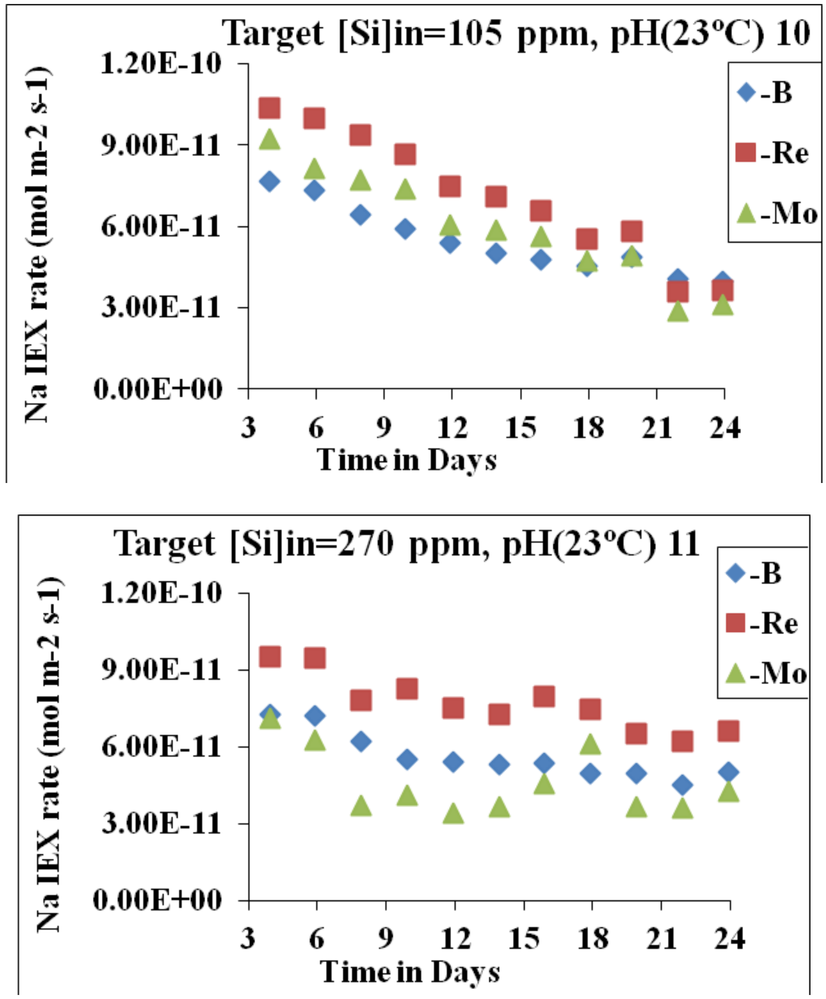

Figure C2. Na IEX Rates at 40 °C based on B, Mo, and Re (cont'd).

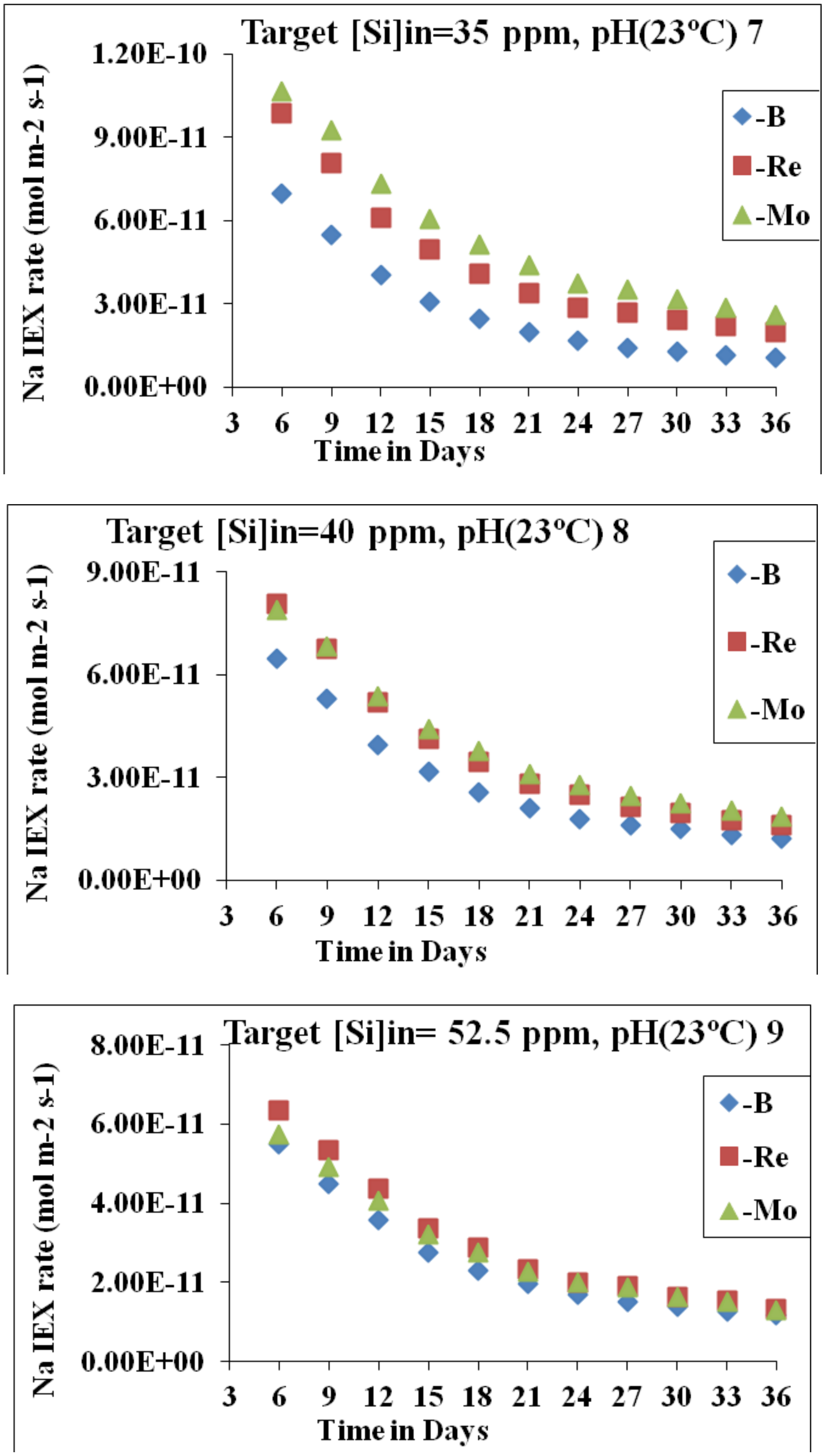

Figure C3. Na IEX Rates at 23 °C based on B, Mo, and Re.

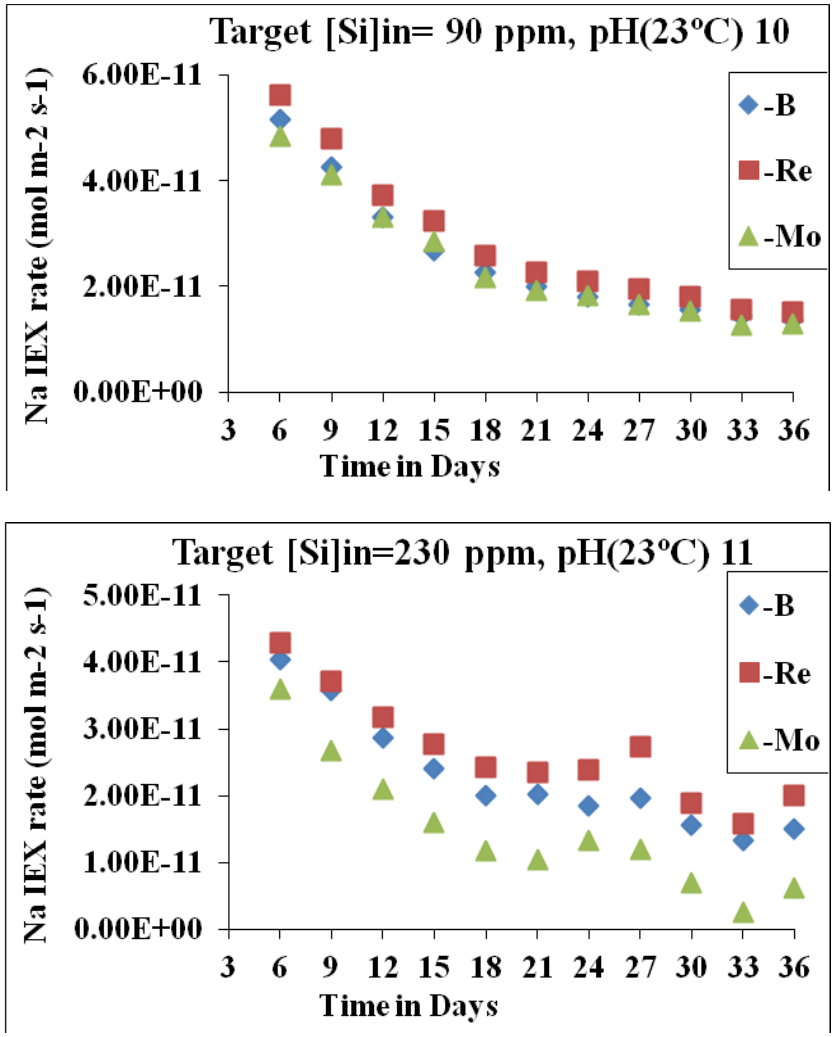

Figure C3. Na IEX Rates at 23 °C based on B, Mo and Re (cont'd).

APPENDIX D

PULSED-FLOW TEST DATA FOR LAW GLASSES LAWC22, ORLEC28 and IDF1B2

Table D1. ICP-AES Analysis Results from Dissolution of Glass LAWC22 at 70 °C: leachate concentration (ppm) and NDR_i (g m^{-2} d^{-1}).

Exp.	Sample ID	Inf [Si] ppm	T °C	Flow Rate, m^3/d	Time, days	pH 23°C	Glass Mass g	SA m^2	[B] ppm	B Rate g_{glass} m^{-2} d^{-1}	[Li] ppm	Li Rate g_{glass} m^{-2} d^{-1}	[Na] ppm	Na Rate g_{glass} m^{-2} d^{-1}	[K] ppm	K Rate g_{glass} m^{-2} d^{-1}	[Al] ppm	Al Rate g_{glass} m^{-2} d^{-1}	[Re] ppm	Re Rate g_{glass} m^{-2} d^{-1}
1	C22IX70-1D1	55	70	2.50E-05	1	7	0.77	0.0166	1.441	0.1390	0.3790	0.0972	5.7950	0.1608	0.0380	0.0327	0.0410	0.0023	0.0240	0.0759
	C22IX70-1D2	55	70	2.50E-05	2	7	0.77	0.0166	1.455	0.0709	0.3480	0.0406	5.4290	0.0701	0.0400	0.0237	0.0430	0.0013	0.0190	0.0216
	C22IX70-1D3	55	70	2.50E-05	3	7	0.77	0.0166	1.362	0.0614	0.3120	0.0354	4.8740	0.0597	0.0360	0.0055	0.0450	0.0014	0.0150	0.0167
	C22IX70-1D4	55	70	2.50E-05	4	7	0.77	0.0166	1.363	0.0662	0.3020	0.0376	4.7060	0.0630	0.0360	0.0128	0.0470	0.0015	0.0120	0.0135
	C22IX70-1D5	55	70	2.50E-05	5	7	0.77	0.0166	1.288	0.0591	0.2810	0.0336	4.3990	0.0569	0.0360	0.0129	0.0560	0.0023	0.0100	0.0119
	C22IX70-1D6	55	70	2.50E-05	6	7	0.77	0.0166	1.231	0.0574	0.2630	0.0317	4.1440	0.0543	0.0340	0.0055	0.0480	0.0011	0.0080	0.0086
	C22IX70-1D7	55	70	2.50E-05	7	7	0.77	0.0166	1.194	0.0569	0.2560	0.0324	4.0560	0.0557	0.0360	0.0167	0.0530	0.0020	0.0080	0.0120
	C22IX70-1D8	55	70	2.50E-05	8	7	0.77	0.0166	1.143	0.0540	0.2460	0.0309	3.8860	0.0524	0.0340	0.0056	0.0490	0.0014	0.0070	0.0087
	C22IX70-1D9	55	70	2.50E-05	9	7	0.77	0.0166	1.090	0.0516	0.2340	0.0292	3.6750	0.0490	0.0320	0.0019	0.0460	0.0013	0.0060	0.0071
	C22IX70-1D10	55	70	2.50E-05	10	7	0.77	0.0166	1.014	0.0470	0.2150	0.0259	3.3800	0.0438	0.0320	0.0057	0.0460	0.0014	0.0050	0.0054
2	C22IX70-2D1	60	70	2.50E-05	1	8	0.77	0.0166	0.617	0.0593	0.3510	0.0900	3.4380	0.0938	0.0260	-0.0255	0.0780	0.0057	0.0150	0.0464
	C22IX70-2D2	60	70	2.50E-05	2	8	0.77	0.0166	0.545	0.0227	0.2690	0.0238	2.7560	0.0277	0.0230	-0.0236	0.0770	0.0028	0.0120	0.0134
	C22IX70-2D3	60	70	2.50E-05	3	8	0.77	0.0166	0.470	0.0189	0.2060	0.0181	2.2030	0.0217	0.0190	-0.0328	0.0800	0.0031	0.0090	0.0085
	C22IX70-2D4	60	70	2.50E-05	4	8	0.77	0.0166	0.440	0.0197	0.1740	0.0180	1.9000	0.0209	0.0180	-0.0291	0.0810	0.0031	0.0070	0.0069
	C22IX70-2D5	60	70	2.50E-05	5	8	0.77	0.0166	0.398	0.0171	0.1480	0.0154	1.6600	0.0184	0.0170	-0.0310	0.0790	0.0028	0.0060	0.0069
	C22IX70-2D6	60	70	2.50E-05	6	8	0.77	0.0166	0.374	0.0168	0.1340	0.0151	1.5050	0.0175	0.0180	-0.0255	0.0790	0.0029	0.0060	0.0085
	C22IX70-2D7	60	70	2.50E-05	7	8	0.77	0.0166	0.352	0.0158	0.1230	0.0141	1.4050	0.0168	0.0210	-0.0164	0.0740	0.0025	0.0050	0.0052
	C22IX70-2D8	60	70	2.50E-05	8	8	0.77	0.0166	0.333	0.0151	0.1150	0.0135	1.2930	0.0151	0.0160	-0.0401	0.0720	0.0025	0.0040	0.0036
	C22IX70-2D9	60	70	2.50E-05	9	8	0.77	0.0166	0.331	0.0158	0.1120	0.0137	1.2750	0.0162	0.0160	-0.0310	0.0760	0.0030	0.0040	0.0052
	C22IX70-2D10	60	70	2.50E-05	10	8	0.77	0.0166	0.314	0.0142	0.1060	0.0126	1.1980	0.0142	0.0150	-0.0346	0.0710	0.0023	0.0030	0.0020
3	C22IX70-3D1	80	70	2.50E-05	1	9	0.77	0.0166	0.422	0.0405	0.2620	0.0670	2.6820	0.0713	0.0410	-0.0145	0.0940	0.0066	0.0120	0.0366
	C22IX70-3D2	80	70	2.50E-05	2	9	0.77	0.0166	0.338	0.0121	0.2000	0.0174	2.1220	0.0198	0.0230	-0.0727	0.1070	0.0045	0.0100	0.0118
	C22IX70-3D3	80	70	2.50E-05	3	9	0.77	0.0166	0.265	0.0091	0.1480	0.0120	1.6510	0.0144	0.0190	-0.0546	0.0970	0.0030	0.0080	0.0085
	C22IX70-3D4	80	70	2.50E-05	4	9	0.77	0.0166	0.241	0.0103	0.1260	0.0131	1.4370	0.0150	0.0160	-0.0582	0.1230	0.0059	0.0070	0.0085
	C22IX70-3D5	80	70	2.50E-05	5	9	0.77	0.0166	0.201	0.0076	0.1010	0.0094	1.2030	0.0115	0.0170	-0.0491	0.1010	0.0026	0.0060	0.0069
	C22IX70-3D6	80	70	2.50E-05	6	9	0.77	0.0166	0.168	0.0064	0.0850	0.0085	1.0180	0.0095	0.0150	-0.0582	0.0860	0.0022	0.0050	0.0052
	C22IX70-3D7	80	70	2.50E-05	7	9	0.77	0.0166	0.160	0.0072	0.0790	0.0090	0.9620	0.0106	0.0200	-0.0364	0.0910	0.0034	0.0050	0.0069
	C22IX70-3D8	80	70	2.50E-05	8	9	0.77	0.0166	0.152	0.0068	0.0720	0.0080	0.8920	0.0094	0.0140	-0.0673	0.0870	0.0028	0.0050	0.0069
	C22IX70-3D9	80	70	2.50E-05	9	9	0.77	0.0166	0.152	0.0072	0.0700	0.0084	0.8600	0.0095	0.0140	-0.0564	0.0850	0.0028	0.0050	0.0069
	C22IX70-3D10	80	70	2.50E-05	10	9	0.77	0.0166	0.146	0.0066	0.0670	0.0079	0.8170	0.0087	0.0130	-0.0601	0.0730	0.0017	0.0050	0.0069
4	C22IX70-4D1	140	70	2.50E-05	1	10	0.50	0.0107	0.220	0.0304	0.1420	0.0447	1.5960	0.0691	0.0160	-0.1527	0.1550	0.0169	0.0070	0.0315
	C22IX70-4D2	140	70	2.50E-05	2	10	0.50	0.0107	0.174	0.0094	0.1110	0.0155	1.3070	0.0218	0.0160	-0.0764	0.1180	0.0030	0.0050	0.0056
	C22IX70-4D3	140	70	2.50E-05	3	10	0.50	0.0107	0.128	0.0059	0.0840	0.0108	1.0330	0.0162	0.0130	-0.0934	0.0970	0.0026	0.0040	0.0056
	C22IX70-4D4	140	70	2.50E-05	4	10	0.50	0.0107	0.111	0.0068	0.0700	0.0106	0.9270	0.0175	0.0140	-0.0792	0.1110	0.0062	0.0040	0.0081
	C22IX70-4D5	140	70	2.50E-05	5	10	0.50	0.0107	0.077	0.0030	0.0520	0.0062	0.7610	0.0126	0.0120	-0.0934	0.0970	0.0032	0.0020	0.0000
	C22IX70-4D6	140	70	2.50E-05	6	10	0.50	0.0107	0.059	0.0028	0.0450	0.0070	0.6690	0.0122	0.0110	-0.0934	0.0840	0.0023	0.0020	0.0031
	C22IX70-4D7	140	70	2.50E-05	7	10	0.50	0.0107	0.047	0.0024	0.0380	0.0056	0.6070	0.0115	0.0120	-0.0849	0.0760	0.0021	0.0020	0.0031
	C22IX70-4D8	140	70	2.50E-05	8	10	0.50	0.0107	0.036	0.0016	0.0340	0.0054	0.5500	0.0103	0.0110	-0.0934	0.0740	0.0023	0.0010	0.0000
	C22IX70-4D9	140	70	2.50E-05	9	10	0.50	0.0107	0.030	0.0016	0.0300	0.0046	0.5120	0.0099	0.0120	-0.0849	0.0690	0.0018	0.0010	0.0005
	C22IX70-4D10	140	70	2.50E-05	10	10	0.50	0.0107	0.025	0.0013	0.0250	0.0034	0.5580	0.0128	0.0370	0.0538	0.0710	0.0024	0.0010	0.0005
5	C22IX70-5D1	360	70	2.50E-05	1	11	0.50	0.0107	0.104	0.0151	0.0890	0.0346	2.2590	0.0429	0.0380	0.0961	0.0600	0.0066	0.0040	0.0163
	C22IX70-5D2	360	70	2.50E-05	2	11	0.50	0.0107	0.066	0.0019	0.0650	0.0076	2.0250	0.0112	0.0350	0.0311	0.0500	0.0018	0.0030	0.0031
	C22IX70-5D3	360	70	2.50E-05	3	11	0.50	0.0107	0.037	0.0004	0.0460	0.0048	1.8290	0.0077	0.0330	0.0283	0.0420	0.0014	0.0020	0.0005
	C22IX70-5D4	360	70	2.50E-05	4	11	0.50	0.0107	0.018	-0.0003	0.0340	0.0038	1.7150	0.0070	0.0310	0.0226	0.0400	0.0017	0.0010	-0.0020
	C22IX70-5D5	360	70	2.50E-05	5	11	0.50	0.0107	0.006	-0.0007	0.0250	0.0026	1.6310	0.0058	0.0300	0.0226	0.0370	0.0014	0.0010	0.0005
	C22IX70-5D6	360	70	2.50E-05	6	11	0.50	0.0107	0.003	-0.0002	0.0190	0.0020	1.6000	0.0063	0.0330	0.0424	0.0570	0.0045	0.0010	0.0005
	C22IX70-5D7	360	70	2.50E-05	7	11	0.50	0.0107	<DL	-	0.0150	0.0016	1.5460	0.0046	0.0300	0.0170	0.0320	-0.0006	0.0010	0.0005
	C22IX70-5D8	360	70	2.50E-05	8	11	0.50	0.0107	<DL	-	0.0120	0.0012	1.5220	0.0047	0.0420	0.0933	0.0320	0.0012	0.0010	0.0005
	C22IX70-5D9	360	70	2.50E-05	9	11	0.50	0.0107	<DL	-	0.0100	0.0010	1.4840	0.0036	0.0390	0.0424	0.0320	0.0012	0.0010	0.0005
	C22IX70-5D10	360	70	2.50E-05	10	11	0.50	0.0107	<DL	-	0.0080	0.0006	1.4860	0.0045	0.0360	0.0339	0.0310	0.0011	0.0010	0.0005

Table D2. ICP-AES Analysis Results from Dissolution of Glass LAWC22 at 40 °C.

Exp.	Sample ID	Inf [Si] ppm	T °C	Flow Rate, m^3/d	Time, days	pH 23°C	Glass Mass g	SA m^2	[B] ppm	B Rate $g_{glass}\ m^{-2}\ d^{-1}$	[Li] ppm	Li Rate $g_{glass}\ m^{-2}\ d^{-1}$	[Na] ppm	Na Rate $g_{glass}\ m^{-2}\ d^{-1}$	[K] ppm	K Rate $g_{glass}\ m^{-2}\ d^{-1}$	[Al] ppm	Al Rate $g_{glass}\ m^{-2}\ d^{-1}$	[Re] ppm	Re Rate $g_{glass}\ m^{-2}\ d^{-1}$
1	C22IX40-1D1	40	40	8.33E-06	3	7	1.65	0.0355	1.057	0.0158	0.5950	0.0231	5.4650	**0.0237**	0.0460	0.0211	0.0340	0.0003	0.0240	0.0118
	C22IX40-1D2	40	40	8.33E-06	6	7	1.65	0.0355	0.870	0.0051	0.4180	0.0044	4.1610	0.0061	0.0400	0.0072	0.0390	0.0002	0.0180	0.0028
	C22IX40-1D3	40	40	8.33E-06	9	7	1.65	0.0355	0.723	0.0043	0.3110	0.0037	3.2580	0.0050	0.0500	0.0145	0.0380	0.0002	0.0130	0.0018
	C22IX40-1D4	40	40	8.33E-06	12	7	1.65	0.0355	0.637	0.0041	0.2480	0.0033	2.6410	0.0043	0.0300	0.0004	0.0430	0.0002	0.0100	0.0016
	C22IX40-1D5	40	40	8.33E-06	15	7	1.65	0.0355	0.551	0.0035	0.2030	0.0028	2.2000	0.0037	0.0260	0.0038	0.0390	0.0001	0.0070	0.0008
	C22IX40-1D6	40	40	8.33E-06	18	7	1.65	0.0355	0.503	0.0034	0.1770	0.0026	1.9610	0.0037	0.0400	0.0129	0.0450	0.0003	0.0060	0.0010
	C22IX40-1D7	40	40	8.33E-06	21	7	1.65	0.0355	0.462	0.0032	0.1580	0.0024	1.7520	0.0033	0.0270	0.0015	0.0400	0.0001	0.0050	0.0008
	C22IX40-1D8	40	40	8.33E-06	24	7	1.65	0.0355	0.441	0.0031	0.1480	0.0024	1.6600	0.0033	0.0240	0.0035	0.0410	0.0002	0.0040	0.0005
	C22IX40-1D9	40	40	8.33E-06	27	7	1.65	0.0355	0.423	0.0030	0.1400	0.0023	1.5550	0.0031	0.0240	0.0044	0.0390	0.0002	0.0040	0.0008
	C22IX40-1D10	40	40	8.33E-06	30	7	1.65	0.0355	0.409	0.0030	0.1360	0.0023	1.4930	0.0030	0.0250	0.0049	0.0360	0.0001	0.0040	0.0008
2	C22IX40-2D1	45	40	8.33E-06	3	8	1.65	0.0355	0.635	0.0095	0.3830	0.0153	3.8530	0.0166	0.0300	0.0094	0.0660	0.0007	0.0160	0.0081
	C22IX40-2D2	45	40	8.33E-06	6	8	1.65	0.0355	0.477	0.0024	0.2700	0.0028	2.8100	0.0037	0.0200	-0.0009	0.0630	0.0003	0.0110	0.0015
	C22IX40-2D3	45	40	8.33E-06	9	8	1.65	0.0355	0.359	0.0018	0.1960	0.0020	2.0930	0.0029	0.0180	0.0008	0.0630	0.0003	0.0090	0.0018
	C22IX40-2D4	45	40	8.33E-06	12	8	1.65	0.0355	0.291	0.0017	0.1510	0.0017	1.6470	0.0025	0.0150	-0.0004	0.0610	0.0003	0.0060	0.0008
	C22IX40-2D5	45	40	8.33E-06	15	8	1.65	0.0355	0.231	0.0013	0.1170	0.0013	1.3090	0.0020	0.0160	0.0010	0.0570	0.0003	0.0050	0.0010
	C22IX40-2D6	45	40	8.33E-06	18	8	1.65	0.0355	0.199	0.0012	0.0970	0.0011	1.1120	0.0018	0.0200	0.0030	0.0590	0.0003	0.0040	0.0008
	C22IX40-2D7	45	40	8.33E-06	21	8	1.65	0.0355	0.172	0.0011	0.0840	0.0010	0.9610	0.0016	0.0160	-0.0004	0.0550	0.0002	0.0030	0.0005
	C22IX40-2D8	45	40	8.33E-06	24	8	1.65	0.0355	0.157	0.0010	0.0750	0.0009	0.8680	0.0015	0.0130	-0.0009	0.0570	0.0003	0.0030	0.0008
	C22IX40-2D9	45	40	8.33E-06	27	8	1.65	0.0355	0.141	0.0009	0.0670	0.0008	0.7770	0.0013	0.0140	0.0005	0.0520	0.0002	0.0030	0.0008
	C22IX40-2D10	45	40	8.33E-06	30	8	1.65	0.0355	0.133	0.0009	0.0620	0.0007	0.7310	0.0013	0.0170	0.0019	0.0530	0.0003	0.0020	0.0003
3	C22IX40-3D1	60	40	8.33E-06	3	9	1.65	0.0355	1.333	0.0200	0.6000	0.0240	5.8340	0.0252	0.0560	0.0277	1.0400	0.0149	0.0380	0.0193
	C22IX40-3D2	60	40	8.33E-06	6	9	1.65	0.0355	0.378	-0.0044	0.2280	-0.0033	2.2450	-0.0032	0.0270	-0.0025	0.0850	-0.0065	0.0100	-0.0046
	C22IX40-3D3	60	40	8.33E-06	9	9	1.65	0.0355	0.292	0.0015	0.1730	0.0020	1.6940	0.0023	0.0200	0.0017	0.0770	0.0003	0.0080	0.0015
	C22IX40-3D4	60	40	8.33E-06	12	9	1.65	0.0355	0.242	0.0014	0.1390	0.0017	1.3640	0.0021	0.0170	0.0020	0.0730	0.0003	0.0060	0.0010
	C22IX40-3D5	60	40	8.33E-06	15	9	1.65	0.0355	0.191	0.0010	0.1100	0.0012	1.0960	0.0016	0.0170	0.0028	0.0640	0.0002	0.0050	0.0010
	C22IX40-3D6	60	40	8.33E-06	18	9	1.65	0.0355	0.162	0.0010	0.0920	0.0011	0.9300	0.0015	0.0150	0.0017	0.0610	0.0003	0.0040	0.0008
	C22IX40-3D7	60	40	8.33E-06	21	9	1.65	0.0355	0.137	0.0008	0.0780	0.0009	0.8280	0.0014	0.0170	0.0034	0.0580	0.0002	0.0040	0.0010
	C22IX40-3D8	60	40	8.33E-06	24	9	1.65	0.0355	0.122	0.0008	0.0690	0.0008	0.7530	0.0013	0.0150	0.0017	0.0570	0.0002	0.0030	0.0005
	C22IX40-3D9	60	40	8.33E-06	27	9	1.65	0.0355	0.111	0.0007	0.0630	0.0007	0.6830	0.0011	0.0130	0.0011	0.0580	0.0003	0.0030	0.0008
	C22IX40-3D10	60	40	8.33E-06	30	9	1.65	0.0355	0.105	0.0007	0.0570	0.0006	0.6240	0.0010	0.0140	0.0023	0.0540	0.0002	0.0030	0.0008
4	C22IX40-4D1	105	40	8.33E-06	3	10	0.83	0.0178	0.257	0.0076	0.1490	0.0118	1.5930	0.0138	0.0240	0.0079	0.1300	0.0025	0.0070	0.0071
	C22IX40-4D2	105	40	8.33E-06	6	10	0.83	0.0178	0.243	0.0034	0.1290	0.0036	1.3530	0.0048	0.0180	-0.0028	0.1220	0.0010	0.0070	0.0036
	C22IX40-4D3	105	40	8.33E-06	9	10	0.83	0.0178	0.199	0.0023	0.1050	0.0024	1.1400	0.0040	0.0220	0.0051	0.1040	0.0006	0.0060	0.0025
	C22IX40-4D4	105	40	8.33E-06	12	10	0.83	0.0178	0.169	0.0020	0.0890	0.0021	0.9580	0.0033	0.0160	-0.0040	0.0970	0.0007	0.0050	0.0020
	C22IX40-4D5	105	40	8.33E-06	15	10	0.83	0.0178	0.133	0.0014	0.0700	0.0012	0.7950	0.0027	0.0150	-0.0017	0.0840	0.0004	0.0040	0.0015
	C22IX40-4D6	105	40	8.33E-06	18	10	0.83	0.0178	0.103	0.0010	0.0580	0.0010	0.6850	0.0025	0.0150	-0.0011	0.0700	0.0002	0.0030	0.0010
	C22IX40-4D7	105	40	8.33E-06	21	10	0.83	0.0178	0.078	0.0007	0.0470	0.0006	0.5950	0.0021	0.0160	0.0000	0.0620	0.0001	0.0020	0.0005
	C22IX40-4D8	105	40	8.33E-06	24	10	0.83	0.0178	0.062	0.0006	0.0390	0.0004	0.5320	0.0020	0.0130	-0.0040	0.0580	0.0001	0.0020	0.0010
	C22IX40-4D9	105	40	8.33E-06	27	10	0.83	0.0178	0.050	0.0005	0.0330	0.0003	0.4820	0.0018	0.0140	-0.0011	0.0570	0.0002	0.0010	0.0000
	C22IX40-4D10	105	40	8.33E-06	30	10	0.83	0.0178	0.041	0.0004	0.0280	0.0001	0.4310	0.0016	0.0200	0.0051	0.0520	0.0000	0.0010	0.0005
5	C22IX40-5D1	270	40	8.33E-06	3	11	0.83	0.0178	0.229	0.0068	0.1250	0.0098	1.8100	0.0081	0.0210	0.0218	0.1270	0.0031	0.0070	0.0063
	C22IX40-5D2	270	40	8.33E-06	6	11	0.83	0.0178	0.271	0.0047	0.1290	0.0045	1.7850	0.0039	0.0220	0.0120	0.1470	0.0021	0.0080	0.0042
	C22IX40-5D3	270	40	8.33E-06	9	11	0.83	0.0178	0.266	0.0039	0.1200	0.0036	1.6570	0.0028	0.0230	0.0126	0.1380	0.0016	0.0080	0.0037
	C22IX40-5D4	270	40	8.33E-06	12	11	0.83	0.0178	0.245	0.0033	0.1080	0.0030	1.5150	0.0022	0.0210	0.0098	0.1280	0.0014	0.0070	0.0026
	C22IX40-5D5	270	40	8.33E-06	15	11	0.83	0.0178	0.209	0.0026	0.0900	0.0021	1.3560	0.0014	0.0190	0.0086	0.1140	0.0012	0.0060	0.0021
	C22IX40-5D6	270	40	8.33E-06	18	11	0.83	0.0178	0.177	0.0021	0.0770	0.0018	1.2530	0.0012	0.0240	0.0154	0.0940	0.0008	0.0050	0.0016
	C22IX40-5D7	270	40	8.33E-06	21	11	0.83	0.0178	0.153	0.0019	0.0660	0.0014	1.1620	0.0008	0.0580	0.0511	0.0840	0.0008	0.0040	0.0011
	C22IX40-5D8	270	40	8.33E-06	24	11	0.83	0.0178	0.134	0.0017	0.0570	0.0011	1.0970	0.0007	0.0390	0.0103	0.0740	0.0006	0.0040	0.0016
	C22IX40-5D9	270	40	8.33E-06	27	11	0.83	0.0178	0.121	0.0016	0.0530	0.0012	1.0410	0.0005	0.0420	0.0245	0.0720	0.0007	0.0030	0.0006
	C22IX40-5D10	270	40	8.33E-06	30	11	0.83	0.0178	0.113	0.0015	0.0480	0.0009	0.9620	0.0000	0.0300	0.0092	0.0630	0.0005	0.0030	0.0011

Table D3. ICP-AES Analysis Results from Dissolution of Glass LAWC22 at 23 °C.

Exp.	Sample ID	Inf [Si] ppm	T °C	Flow Rate, m^3/d	Time, days	pH 23°C	Glass Mass g	SA m^2	[B] ppm	B Rate $g_{glass}\ m^{-2}\ d^{-1}$	[Li] ppm	Li Rate $g_{glass}\ m^{-2}\ d^{-1}$	[Na] ppm	Na Rate $g_{glass}\ m^{-2}\ d^{-1}$	[K] ppm	K Rate $g_{glass}\ m^{-2}\ d^{-1}$	[Al] ppm	Al Rate $g_{glass}\ m^{-2}\ d^{-1}$	[Re] ppm	Re Rate $g_{glass}\ m^{-2}\ d^{-1}$
	C22IX23-1D1	35	23	8.33E-06	3	7	1.65	0.0355	0.721	0.0108	0.4350	0.0174	4.4240	0.0191	0.0280	0.0124	0.0370	0.0003	0.0200	0.0097
	C22IX23-1D2	35	23	8.33E-06	6	7	1.65	0.0355	0.537	0.0026	0.3140	0.0038	3.1110	0.0038	0.0240	0.0040	0.0350	0.0001	0.0140	0.0018
	C22IX23-1D3	35	23	8.33E-06	9	7	1.65	0.0355	0.387	0.0018	0.2250	0.0027	2.1510	0.0025	0.0210	0.0034	0.0350	0.0001	0.0090	0.0008
	C22IX23-1D4	35	23	8.33E-06	12	7	1.65	0.0355	0.291	0.0014	0.1690	0.0022	1.5820	0.0021	0.0190	0.0031	0.0320	0.0001	0.0070	0.0010
1	C22IX23-1D5	35	23	8.33E-06	15	7	1.65	0.0355	0.216	0.0010	0.1290	0.0017	1.1780	0.0016	0.0160	0.0020	0.0310	0.0001	0.0050	0.0005
	C22IX23-1D6	35	23	8.33E-06	18	7	1.65	0.0355	0.158	0.0007	0.0970	0.0012	0.8880	0.0012	0.0140	0.0017	0.0300	0.0001	0.0040	0.0005
	C22IX23-1D7	35	23	8.33E-06	21	7	1.65	0.0355	0.064	-0.0003	0.0440	-0.0002	0.5630	0.0004	0.1690	0.0901	0.0280	0.0000	0.0020	-0.0003
	C22IX23-1D8	35	23	8.33E-06	24	7	1.65	0.0355	0.063	0.0004	0.0450	0.0009	0.4960	0.0008	0.0910	0.0020	0.0270	0.0000	0.0010	-0.0003
	C22IX23-1D9	35	23	8.33E-06	27	7	1.65	0.0355	0.073	0.0006	0.0480	0.0010	0.4980	0.0010	0.0690	0.0116	0.0250	0.0000	0.0020	0.0005
	C22IX23-1D10	35	23	8.33E-06	30	7	1.65	0.0355	0.235	0.0030	0.1080	0.0033	0.9750	0.0030	0.0530	0.0088	0.2070	0.0027	0.0070	0.0028
	C22IX23-2D1	40	23	8.33E-06	3	8	1.65	0.0355	0.497	0.0074	0.3450	0.0138	3.5460	0.0153	0.0220	0.0068	0.0300	0.0003	0.0130	0.0062
	C22IX23-2D2	40	23	8.33E-06	6	8	1.65	0.0355	0.341	0.0014	0.2350	0.0025	2.3600	0.0024	0.0180	0.0011	0.0330	0.0002	0.0090	0.0010
	C22IX23-2D3	40	23	8.33E-06	9	8	1.65	0.0355	0.236	0.0010	0.1630	0.0018	1.6300	0.0018	0.0180	0.0023	0.0320	0.0001	0.0060	0.0005
	C22IX23-2D4	40	23	8.33E-06	12	8	1.65	0.0355	0.176	0.0008	0.1220	0.0016	1.2060	0.0016	0.0140	0.0000	0.0340	0.0002	0.0040	0.0003
2	C22IX23-2D5	40	23	8.33E-06	15	8	1.65	0.0355	0.128	0.0006	0.0920	0.0012	0.9050	0.0012	0.0100	-0.0011	0.0340	0.0002	0.0030	0.0003
	C22IX23-2D6	40	23	8.33E-06	18	8	1.65	0.0355	0.088	0.0003	0.0680	0.0008	0.6790	0.0008	0.0150	0.0028	0.0300	0.0001	0.0030	0.0005
	C22IX23-2D7	40	23	8.33E-06	21	8	1.65	0.0355	0.065	0.0003	0.0540	0.0007	0.5460	0.0008	0.0100	-0.0014	0.0320	0.0002	0.0020	0.0000
	C22IX23-2D8	40	23	8.33E-06	24	8	1.65	0.0355	0.047	0.0002	0.0430	0.0006	0.4420	0.0006	0.0090	-0.0006	0.0260	0.0001	0.0010	-0.0002
	C22IX23-2D9	40	23	8.33E-06	27	8	1.65	0.0355	0.046	0.0003	0.0410	0.0007	0.4320	0.0008	0.0090	-0.0003	0.0260	0.0001	0.0010	0.0000
	C22IX23-2D10	40	23	8.33E-06	30	8	1.65	0.0355	0.052	0.0004	0.0440	0.0009	0.4440	0.0008	0.0100	0.0003	0.0240	0.0001	0.0010	0.0000
	C22IX23-3D1	52	23	8.33E-06	3	9	1.65	0.0355	0.371	0.0055	0.2860	0.0114	2.7910	0.0118	0.0200	0.0081	0.0390	0.0003	0.0110	0.0051
	C22IX23-3D2	52	23	8.33E-06	6	9	1.65	0.0355	0.242	0.0008	0.1910	0.0019	1.8850	0.0019	0.0160	0.0018	0.0420	0.0002	0.0070	0.0005
	C22IX23-3D3	52	23	8.33E-06	9	9	1.65	0.0355	0.164	0.0006	0.1340	0.0015	1.3510	0.0016	0.0130	0.0012	0.0420	0.0002	0.0050	0.0005
	C22IX23-3D4	52	23	8.33E-06	12	9	1.65	0.0355	0.118	0.0005	0.1000	0.0013	1.0120	0.0013	0.0150	0.0032	0.0420	0.0002	0.0030	0.0000
3	C22IX23-3D5	52	23	8.33E-06	15	9	1.65	0.0355	0.280	0.0004	0.0790	0.0011	0.8190	0.0012	0.0150	0.0026	0.0390	0.0001	0.0025	0.0003
	C22IX23-3D6	52	23	8.33E-06	18	9	1.65	0.0355	0.062	0.0002	0.0580	0.0007	0.6260	0.0007	0.0150	0.0026	0.0360	0.0001	0.0020	0.0001
	C22IX23-3D7	52	23	8.33E-06	21	9	1.65	0.0355	0.045	0.0002	0.0450	0.0006	0.5060	0.0006	0.0110	0.0004	0.0330	0.0001	0.0010	-0.0003
	C22IX23-3D8	52	23	8.33E-06	24	9	1.65	0.0355	0.033	0.0001	0.0380	0.0006	0.4350	0.0006	0.0090	0.0004	0.0320	0.0001	0.0010	0.0000
	C22IX23-3D9	52	23	8.33E-06	27	9	1.65	0.0355	0.031	0.0002	0.0350	0.0006	0.4120	0.0006	0.0090	0.0009	0.0310	0.0001	0.0010	0.0000
	C22IX23-3D10	52	23	8.33E-06	30	9	1.65	0.0355	0.037	0.0003	0.0380	0.0008	0.4280	0.0008	0.0100	0.0015	0.0310	0.0001	0.0010	0.0000
	C22IX23-4D1	90	23	8.33E-06	3	10	0.83	0.0178	0.194	0.0057	0.1450	0.0114	1.4390	0.0112	0.0160	0.0071	0.0660	0.0012	0.0060	0.0000
	C22IX23-4D2	90	23	8.33E-06	6	10	0.83	0.0178	0.121	0.0007	0.0950	0.0017	1.0210	0.0019	0.0330	0.0228	0.0580	0.0003	0.0030	-0.0030
	C22IX23-4D3	90	23	8.33E-06	9	10	0.83	0.0178	0.083	0.0006	0.0650	0.0013	0.7670	0.0015	0.0190	-0.0027	0.0480	0.0002	0.0020	-0.0025
	C22IX23-4D4	90	23	8.33E-06	12	10	0.83	0.0178	0.061	0.0005	0.0490	0.0012	0.6150	0.0013	0.0170	0.0030	0.0460	0.0003	0.0020	-0.0020
4	C22IX23-4D5	90	23	8.33E-06	15	10	0.83	0.0178	0.045	0.0004	0.0390	0.0010	0.5100	0.0011	0.0130	-0.0004	0.0430	0.0002	0.0010	-0.0030
	C22IX23-4D6	90	23	8.33E-06	18	10	0.83	0.0178	0.033	0.0003	0.0300	0.0007	0.4350	0.0009	0.0150	0.0041	0.0390	0.0001	0.0000	-0.0036
	C22IX23-4D7	90	23	8.33E-06	21	10	0.83	0.0178	0.024	0.0002	0.0240	0.0006	0.3810	0.0007	0.0120	-0.0004	0.0380	0.0002	0.0010	-0.0020
	C22IX23-4D8	90	23	8.33E-06	24	10	0.83	0.0178	0.018	0.0001	0.0200	0.0005	0.3420	0.0006	0.0110	0.0002	0.0360	0.0001	0.0000	-0.0036
	C22IX23-4D9	90	23	8.33E-06	27	10	0.83	0.0178	0.018	0.0002	0.0190	0.0006	0.3400	0.0008	0.0120	0.0019	0.0320	0.0000	0.0000	-0.0030
	C22IX23-4D10	90	23	8.33E-06	30	10	0.83	0.0178	0.021	0.0003	0.0210	0.0008	0.3440	0.0008	0.0120	0.0013	0.0330	0.0001	0.0000	-0.0030
	C22IX23-5D1	230	23	8.33E-06	3	11	0.83	0.0178	0.144	0.0042	0.1210	0.0095	1.6370	0.0090	0.0170	0.0173	0.0550	0.0011	0.0050	0.0043
	C22IX23-5D2	230	23	8.33E-06	6	11	0.83	0.0178	0.093	0.0006	0.0800	0.0014	1.3060	0.0016	0.0160	0.0075	0.0670	0.0009	0.0030	0.0001
	C22IX23-5D3	230	23	8.33E-06	9	11	0.83	0.0178	0.073	0.0007	0.0600	0.0015	1.1200	0.0014	0.0160	0.0081	0.0690	0.0008	0.0020	0.0001
	C22IX23-5D4	230	23	8.33E-06	12	11	0.83	0.0178	0.245	0.0010	0.0535	0.0018	1.0600	0.0017	0.0165	0.0086	0.0730	0.0009	0.0020	0.0006
5	C22IX23-5D5	230	23	8.33E-06	15	11	0.83	0.0178	0.068	0.0009	0.0470	0.0015	1.0000	0.0015	0.0170	0.0089	0.0770	0.0009	0.0020	0.0006
	C22IX23-5D6	230	23	8.33E-06	18	11	0.83	0.0178	0.068	0.0010	0.0440	0.0015	0.9710	0.0015	0.0190	0.0109	0.0740	0.0008	0.0020	0.0006
	C22IX23-5D7	230	23	8.33E-06	21	11	0.83	0.0178	0.068	0.0010	0.0430	0.0016	0.9550	0.0015	0.0190	0.0098	0.0800	0.0010	0.0020	0.0006
	C22IX23-5D8	230	23	8.33E-06	24	11	0.83	0.0178	0.066	0.0009	0.0400	0.0014	0.9330	0.0013	0.0180	0.0086	0.0750	0.0008	0.0020	0.0006
	C22IX23-5D9	230	23	8.33E-06	27	11	0.83	0.0178	0.140	0.0032	0.0670	0.0037	1.2050	0.0038	0.0690	0.0669	0.1490	0.0030	0.0040	0.0026
	C22IX23-5D10	230	23	8.33E-06	30	11	0.83	0.0178	0.096	0.0007	0.0530	0.0014	1.0320	0.0011	0.0210	-0.0162	0.0940	0.0003	0.0030	0.0006

Table D4. ICP-AES Analysis Results from Dissolution of Glass ORLEC28 at 70 °C.

Exp.	Sample ID	Inf [Si] ppm	T °C	Flow Rate, m^3/d	Time, days	pH 23°C	Glass Mass g	SA m^2	[B] ppm	B Rate $g_{glass}\ m^{-2}\ d^{-1}$	[Na] ppm	Na Rate $g_{glass}\ m^{-2}\ d^{-1}$	[K] ppm	K Rate $g_{glass}\ m^{-2}\ d^{-1}$	[Al] ppm	Al Rate $g_{glass}\ m^{-2}\ d^{-1}$	[Re] ppm	Re Rate $g_{glass}\ m^{-2}\ d^{-1}$
1	C28IX70-1D1	55	70	2.50E-05	1	7	0.77	0.0166	7.419	0.7223	42.3250	0.7785	5.4780	0.5911	0.0830	0.0038	0.1650	0.5295
	C28IX70-1D2	55	70	2.50E-05	2	7	0.77	0.0166	8.018	0.4218	43.1570	0.4068	5.8800	0.3410	0.0820	0.0018	0.0940	0.0360
	C28IX70-1D3	55	70	2.50E-05	3	7	0.77	0.0166	8.051	0.3979	43.4150	0.4062	6.0990	0.3449	0.0800	0.0018	0.0560	0.0280
	C28IX70-1D4	55	70	2.50E-05	4	7	0.77	0.0166	8.025	0.3960	42.9110	0.3966	6.2490	0.3514	0.0880	0.0023	0.0350	0.0216
	C28IX70-1D5	55	70	2.50E-05	5	7	0.77	0.0166	7.535	0.3507	40.0450	0.3496	5.9610	0.3131	0.0850	0.0019	0.0240	0.0201
	C28IX70-1D6	55	70	2.50E-05	6	7	0.77	0.0166	7.088	0.3324	37.0320	0.3215	5.5750	0.2878	0.0790	0.0016	0.0170	0.0153
	C28IX70-1D7	55	70	2.50E-05	7	7	0.77	0.0166	6.535	0.3009	34.3530	0.3008	5.2310	0.2723	0.0750	0.0016	0.0130	0.0137
	C28IX70-1D8	55	70	2.50E-05	8	7	0.77	0.0166	6.327	0.3092	33.7310	0.3159	5.3650	0.3080	0.0730	0.0016	0.0110	0.0137
	C28IX70-1D9	55	70	2.50E-05	9	7	0.77	0.0166	6.088	0.2969	32.1830	0.2936	5.1630	0.2790	0.0840	0.0023	0.0090	0.0104
	C28IX70-1D10	55	70	2.50E-05	10	7	0.77	0.0166	5.916	0.2929	31.0890	0.2887	4.8320	0.2541	0.0740	0.0014	0.0080	0.0105
2	C28IX70-2D1	60	70	2.50E-05	1	8	0.77	0.0166	4.576	0.4449	27.0240	0.4956	3.0980	0.3322	0.1920	0.0100	0.1640	0.5257
	C28IX70-2D2	60	70	2.50E-05	2	8	0.77	0.0166	4.685	0.2338	26.5020	0.2390	3.1120	0.1681	0.1550	0.0029	0.0880	0.0181
	C28IX70-2D3	60	70	2.50E-05	3	8	0.77	0.0166	4.479	0.2091	24.7000	0.2112	3.0100	0.1568	0.1420	0.0032	0.0490	0.0149
	C28IX70-2D4	60	70	2.50E-05	4	8	0.77	0.0166	4.439	0.2159	24.5640	0.2261	3.1140	0.1743	0.1430	0.0037	0.0280	0.0101
	C28IX70-2D5	60	70	2.50E-05	5	8	0.77	0.0166	3.997	0.1750	21.7050	0.1747	2.7450	0.1286	0.1330	0.0031	0.0170	0.0085
	C28IX70-2D6	60	70	2.50E-05	6	8	0.77	0.0166	3.800	0.1778	20.7870	0.1847	2.6770	0.1418	0.1230	0.0028	0.0120	0.0101
	C28IX70-2D7	60	70	2.50E-05	7	8	0.77	0.0166	3.491	0.1575	19.0710	0.1617	2.4760	0.1237	0.1170	0.0027	0.0080	0.0052
	C28IX70-2D8	60	70	2.50E-05	8	8	0.77	0.0166	3.296	0.1538	18.1280	0.1605	2.4090	0.1277	0.1140	0.0027	0.0060	0.0053
	C28IX70-2D9	60	70	2.50E-05	9	8	0.77	0.0166	3.193	0.1536	18.0110	0.1675	2.4060	0.1314	0.1220	0.0033	0.0050	0.0053
	C28IX70-2D10	60	70	2.50E-05	10	8	0.77	0.0166	3.016	0.1415	16.4350	0.1392	2.1680	0.1054	0.1110	0.0024	0.0040	0.0036
3	C28IX70-3D1	80	70	2.50E-05	1	9	0.77	0.0166	2.639	0.2563	17.4930	0.3191	1.6600	0.1749	0.2680	0.0139	0.1180	0.3773
	C28IX70-3D2	80	70	2.50E-05	2	9	0.77	0.0166	2.799	0.1440	17.0460	0.1516	1.6530	0.0869	0.2320	0.0049	0.0630	0.0116
	C28IX70-3D3	80	70	2.50E-05	3	9	0.77	0.0166	2.592	0.1162	15.2300	0.1225	1.4870	0.0694	0.1970	0.0040	0.0340	0.0068
	C28IX70-3D4	80	70	2.50E-05	4	9	0.77	0.0166	2.598	0.1272	15.3000	0.1408	1.5510	0.0855	0.1170	0.0004	0.0200	0.0084
	C28IX70-3D5	80	70	2.50E-05	5	9	0.77	0.0166	2.458	0.1134	14.0280	0.1168	1.4570	0.0719	0.1540	0.0048	0.0110	0.0019
	C28IX70-3D6	80	70	2.50E-05	6	9	0.77	0.0166	2.349	0.1097	13.4910	0.1188	1.4130	0.0724	0.1700	0.0047	0.0080	0.0068
	C28IX70-3D7	80	70	2.50E-05	7	9	0.77	0.0166	2.176	0.0983	12.2110	0.1002	1.3110	0.0637	0.1100	0.0007	0.0030	-0.0046
	C28IX70-3D8	80	70	2.50E-05	8	9	0.77	0.0166	2.064	0.0959	11.7890	0.1044	1.2900	0.0671	0.1610	0.0054	0.0050	0.0101
	C28IX70-3D9	80	70	2.50E-05	9	9	0.77	0.0166	1.905	0.0859	10.7670	0.0894	1.1840	0.0567	0.1520	0.0034	0.0040	0.0036
	C28IX70-3D10	80	70	2.50E-05	10	9	0.77	0.0166	1.743	0.0779	10.0910	0.0865	1.0760	0.0507	0.1460	0.0034	0.0040	0.0052
4	C28IX70-4D1	140	70	2.50E-05	1	10	0.50	0.0107	0.960	0.1446	6.9030	0.1969	0.5460	0.0847	0.1620	0.0108	0.0610	0.3013
	C28IX70-4D2	140	70	2.50E-05	2	10	0.50	0.0107	0.967	0.0735	6.1080	0.0758	0.4830	0.0318	0.1280	0.0024	0.0330	0.0105
	C28IX70-4D3	140	70	2.50E-05	3	10	0.50	0.0107	0.946	0.0698	5.5730	0.0719	0.4540	0.0322	0.1020	0.0016	0.0180	0.0055
	C28IX70-4D4	140	70	2.50E-05	4	10	0.50	0.0107	0.959	0.0735	5.4190	0.0752	0.4650	0.0366	0.0970	0.0023	0.0090	-0.0020
	C28IX70-4D5	140	70	2.50E-05	5	10	0.50	0.0107	0.889	0.0619	4.9110	0.0629	0.4180	0.0277	0.1050	0.0033	0.0050	0.0005
	C28IX70-4D6	140	70	2.50E-05	6	10	0.50	0.0107	0.828	0.0580	4.4740	0.0577	0.3800	0.0253	0.0940	0.0019	0.0030	0.0005
	C28IX70-4D7	140	70	2.50E-05	7	10	0.50	0.0107	0.766	0.0533	4.2380	0.0573	0.3610	0.0253	0.0860	0.0017	0.0020	0.0005
	C28IX70-4D8	140	70	2.50E-05	8	10	0.50	0.0107	0.741	0.0542	4.0650	0.0557	0.3680	0.0281	0.0790	0.0014	0.0010	-0.0020
	C28IX70-4D9	140	70	2.50E-05	9	10	0.50	0.0107	0.723	0.0534	3.9710	0.0556	0.3500	0.0245	0.0770	0.0016	0.0010	0.0005
	C28IX70-4D10	140	70	2.50E-05	10	10	0.50	0.0107	0.681	0.0485	3.7820	0.0515	0.3240	0.0217	0.0720	0.0012	0.0010	0.0005
5	C28IX70-5D1	360	70	2.50E-05	1	11	0.50	0.0107	0.535	0.0804	6.1340	0.1388	0.3910	0.0623	0.0850	0.0062	0.0440	0.2162
	C28IX70-5D2	360	70	2.50E-05	2	11	0.50	0.0107	0.576	0.0464	5.5780	0.0535	0.3580	0.0256	0.0770	0.0024	0.0230	0.0030
	C28IX70-5D3	360	70	2.50E-05	3	11	0.50	0.0107	0.537	0.0374	4.9410	0.0433	0.3150	0.0212	0.0610	0.0013	0.0120	0.0005
	C28IX70-5D4	360	70	2.50E-05	4	11	0.50	0.0107	0.514	0.0369	4.5770	0.0420	0.2960	0.0216	0.0500	0.0011	0.0060	-0.0020
	C28IX70-5D5	360	70	2.50E-05	5	11	0.50	0.0107	0.459	0.0304	4.2130	0.0368	0.2730	0.0193	0.0440	0.0010	0.0030	-0.0020
	C28IX70-5D6	360	70	2.50E-05	6	11	0.50	0.0107	0.416	0.0280	3.8760	0.0324	0.2460	0.0167	0.0410	0.0010	0.0010	-0.0045
	C28IX70-5D7	360	70	2.50E-05	7	11	0.50	0.0107	0.377	0.0254	3.7080	0.0324	0.2380	0.0177	0.0420	0.0012	0.0010	0.0005
	C28IX70-5D8	360	70	2.50E-05	8	11	0.50	0.0107	0.353	0.0247	3.5870	0.0314	0.2330	0.0175	0.0400	0.0010	<DL	-0.0045
	C28IX70-5D9	360	70	2.50E-05	9	11	0.50	0.0107	0.330	0.0230	3.4460	0.0291	0.2180	0.0154	0.0390	0.0010	<DL	-0.0020
	C28IX70-5D10	360	70	2.50E-05	10	11	0.50	0.0107	0.305	0.0210	3.2600	0.0257	0.1970	0.0131	0.0390	0.0011	<DL	-0.0020

Table D5. ICP-AES Analysis Results from Dissolution of Glass ORLEC28 at 40 °C.

Exp.	Sample ID	Inf [Si] ppm	T °C	Flow Rate, m^3/d	Time, days	pH 23°C	Glass Mass g	SA m^2	[B] ppm	B Rate $g_{glass}\ m^{-2}\ d^{-1}$	[Na] ppm	Na Rate $g_{glass}\ m^{-2}\ d^{-1}$	[K] ppm	K Rate $g_{glass}\ m^{-2}\ d^{-1}$	[Al] ppm	Al Rate $g_{glass}\ m^{-2}\ d^{-1}$	[Re] ppm	Re Rate $g_{glass}\ m^{-2}\ d^{-1}$
1	C28IX40-1D1	40	40	8.33E-06	3	7	1.65	0.0355	0.304	0.0045	4.4010	0.0124	0.3160	0.0052	0.0990	0.0007	0.0960	0.0476
	C28IX40-1D2	40	40	8.33E-06	6	7	1.65	0.0355	3.671	0.0532	22.9580	0.0593	2.6120	0.0413	0.0670	0.0001	0.0970	0.0243
	C28IX40-1D3	40	40	8.33E-06	9	7	1.65	0.0355	3.579	0.0264	20.3170	0.0252	2.5210	0.0204	0.0670	0.0002	0.0580	0.0045
	C28IX40-1D4	40	40	8.33E-06	12	7	1.65	0.0355	3.559	0.0268	19.7710	0.0275	2.6040	0.0226	0.0750	0.0003	0.0380	0.0043
	C28IX40-1D5	40	40	8.33E-06	15	7	1.65	0.0355	3.301	0.0231	18.0780	0.0234	2.4170	0.0188	0.0740	0.0003	0.0260	0.0033
	C28IX40-1D6	40	40	8.33E-06	18	7	1.65	0.0355	3.126	0.0224	17.1090	0.0231	2.3800	0.0197	0.0750	0.0003	0.0190	0.0028
	C28IX40-1D7	40	40	8.33E-06	21	7	1.65	0.0355	2.988	0.0216	16.0830	0.0216	2.3060	0.0188	0.0770	0.0003	0.0160	0.0030
	C28IX40-1D8	40	40	8.33E-06	24	7	1.65	0.0355	2.854	0.0207	15.4150	0.0212	2.2070	0.0178	0.0720	0.0002	0.0140	0.0028
	C28IX40-1D9	40	40	8.33E-06	27	7	1.65	0.0355	2.755	0.0202	14.5470	0.0196	2.1140	0.0171	0.0710	0.0002	0.0130	0.0028
	C28IX40-1D10	40	40	8.33E-06	30	7	1.65	0.0355	2.654	0.0194	14.1190	0.0197	2.0150	0.0162	0.0660	0.0002	0.0120	0.0025
2	C28IX40-2D1	45	40	8.33E-06	3	8	1.65	0.0355	0.380	0.0057	4.5260	0.0127	0.3420	0.0055	0.1520	0.0012	0.0660	0.0330
	C28IX40-2D2	45	40	8.33E-06	6	8	1.65	0.0355	1.768	0.0238	13.4160	0.0318	1.2390	0.0179	0.1330	0.0004	0.0870	0.0270
	C28IX40-2D3	45	40	8.33E-06	9	8	1.65	0.0355	1.655	0.0116	11.3780	0.0133	1.1310	0.0085	0.1150	0.0004	0.0480	0.0023
	C28IX40-2D4	45	40	8.33E-06	12	8	1.65	0.0355	1.612	0.0118	9.8030	0.0117	1.0780	0.0085	0.1150	0.0004	0.0280	0.0020
	C28IX40-2D5	45	40	8.33E-06	15	8	1.65	0.0355	1.486	0.0103	8.8170	0.0111	1.0070	0.0078	0.1150	0.0004	0.0170	0.0015
	C28IX40-2D6	45	40	8.33E-06	18	8	1.65	0.0355	1.396	0.0099	8.0920	0.0105	0.9570	0.0075	0.1140	0.0004	0.0110	0.0013
	C28IX40-2D7	45	40	8.33E-06	21	8	1.65	0.0355	1.313	0.0093	7.4390	0.0096	0.9120	0.0072	0.1070	0.0004	0.0080	0.0013
	C28IX40-2D8	45	40	8.33E-06	24	8	1.65	0.0355	1.240	0.0088	6.8340	0.0088	0.8550	0.0066	0.0990	0.0003	0.0070	0.0015
	C28IX40-2D9	45	40	8.33E-06	27	8	1.65	0.0355	1.201	0.0088	6.6370	0.0091	0.8490	0.0070	0.1000	0.0004	0.0060	0.0013
	C28IX40-2D10	45	40	8.33E-06	30	8	1.65	0.0355	1.163	0.0085	6.3020	0.0085	0.8130	0.0065	0.0960	0.0003	0.0050	0.0010
3	C28IX40-3D1	60	40	8.33E-06	3	9	1.65	0.0355	1.082	0.0163	11.8620	0.0337	0.8470	0.0141	0.1890	0.0015	0.1950	0.0976
	C28IX40-3D2	60	40	8.33E-06	6	9	1.65	0.0355	0.949	0.0061	9.3360	0.0096	0.6630	0.0040	0.1740	0.0006	0.1020	0.0023
	C28IX40-3D3	60	40	8.33E-06	9	9	1.65	0.0355	0.828	0.0053	7.1740	0.0070	0.5430	0.0035	0.1470	0.0004	0.0540	0.0015
	C28IX40-3D4	60	40	8.33E-06	12	9	1.65	0.0355	0.770	0.0054	6.0960	0.0070	0.4840	0.0035	0.1340	0.0004	0.0290	0.0010
	C28IX40-3D5	60	40	8.33E-06	15	9	1.65	0.0355	0.690	0.0046	5.1020	0.0057	0.4210	0.0030	0.1270	0.0004	0.0160	0.0008
	C28IX40-3D6	60	40	8.33E-06	18	9	1.65	0.0355	0.642	0.0045	4.5330	0.0055	0.3850	0.0029	0.1210	0.0004	0.0100	0.0010
	C28IX40-3D7	60	40	8.33E-06	21	9	1.65	0.0355	0.603	0.0042	4.1100	0.0051	0.3640	0.0028	0.1200	0.0004	0.0070	0.0010
	C28IX40-3D8	60	40	8.33E-06	24	9	1.65	0.0355	0.584	0.0043	3.8370	0.0050	0.3510	0.0028	0.1270	0.0005	0.0050	0.0008
	C28IX40-3D9	60	40	8.33E-06	27	9	1.65	0.0355	0.552	0.0039	3.6180	0.0047	0.3380	0.0027	0.1190	0.0004	0.0040	0.0008
	C28IX40-3D10	60	40	8.33E-06	30	9	1.65	0.0355	0.536	0.0039	3.3550	0.0043	0.3240	0.0026	0.1140	0.0004	0.0030	0.0005
4	C28IX40-4D1	105	40	8.33E-06	3	10	0.83	0.0178	1.679	0.0506	16.2140	0.0926	1.3570	0.0451	0.1630	0.0021	0.1590	0.1590
	C28IX40-4D2	105	40	8.33E-06	6	10	0.83	0.0178	0.297	-0.0164	3.5390	-0.0262	0.2390	-0.0151	0.1290	0.0005	0.0340	-0.0455
	C28IX40-4D3	105	40	8.33E-06	9	10	0.83	0.0178	0.245	0.0029	2.6710	0.0051	0.1800	0.0018	0.1050	0.0003	0.0160	-0.0010
	C28IX40-4D4	105	40	8.33E-06	12	10	0.83	0.0178	0.228	0.0031	2.3890	0.0060	0.1600	0.0021	0.0940	0.0003	0.0100	0.0020
	C28IX40-4D5	105	40	8.33E-06	15	10	0.83	0.0178	0.202	0.0026	1.9940	0.0045	0.1360	0.0016	0.0800	0.0002	0.0050	0.0000
	C28IX40-4D6	105	40	8.33E-06	18	10	0.83	0.0178	0.192	0.0027	1.7970	0.0045	0.1290	0.0018	0.0770	0.0003	0.0030	0.0005
	C28IX40-4D7	105	40	8.33E-06	21	10	0.83	0.0178	0.181	0.0025	1.6330	0.0042	0.1190	0.0015	0.0700	0.0002	0.0020	0.0005
	C28IX40-4D8	105	40	8.33E-06	24	10	0.83	0.0178	0.180	0.0027	1.5450	0.0041	0.1140	0.0015	0.0690	0.0002	0.0010	0.0000
	C28IX40-4D9	105	40	8.33E-06	27	10	0.83	0.0178	0.174	0.0025	1.4590	0.0039	0.1110	0.0015	0.0620	0.0001	0.0010	0.0005
	C28IX40-4D10	105	40	8.33E-06	30	10	0.83	0.0178	0.173	0.0026	1.3920	0.0037	0.1050	0.0014	0.0590	0.0001	0.0010	0.0005
5	C28IX40-5D1	270	40	8.33E-06	3	11	0.83	0.0178	3.410	0.1029	23.9540	0.1320	2.6810	0.0902	0.0830	0.0011	0.1670	0.1663
	C28IX40-5D2	270	40	8.33E-06	6	11	0.83	0.0178	0.207	-0.0454	3.3110	-0.0522	0.2020	-0.0384	0.0850	0.0006	0.0490	-0.0350
	C28IX40-5D3	270	40	8.33E-06	9	11	0.83	0.0178	0.138	0.0010	2.5470	0.0026	0.1580	0.0019	0.0750	0.0004	0.0250	0.0001
	C28IX40-5D4	270	40	8.33E-06	12	11	0.83	0.0178	0.102	0.0009	2.1210	0.0023	0.1210	0.0014	0.0640	0.0003	0.0130	0.0001
	C28IX40-5D5	270	40	8.33E-06	15	11	0.83	0.0178	0.074	0.0006	1.7670	0.0015	0.0960	0.0012	0.0560	0.0002	0.0070	0.0001
	C28IX40-5D6	270	40	8.33E-06	18	11	0.83	0.0178	0.059	0.0006	1.5880	0.0015	0.0860	0.0013	0.0520	0.0002	0.0030	-0.0009
	C28IX40-5D7	270	40	8.33E-06	21	11	0.83	0.0178	0.055	0.0007	1.4760	0.0014	0.0860	0.0014	0.0440	0.0001	0.0020	0.0001
	C28IX40-5D8	270	40	8.33E-06	24	11	0.83	0.0178	0.047	0.0005	1.3780	0.0011	0.0750	0.0011	0.0430	0.0002	0.0010	-0.0004
	C28IX40-5D9	270	40	8.33E-06	27	11	0.83	0.0178	0.041	0.0005	1.3190	0.0011	0.0710	0.0011	0.0430	0.0002	0.0000	-0.0009
	C28IX40-5D10	270	40	8.33E-06	30	11	0.83	0.0178	0.035	0.0004	1.2550	0.0009	0.0680	0.0011	0.0400	0.0001	0.0000	-0.0004

Table D6. ICP-AES Analysis Results from Dissolution of Glass ORLEC28 at 23 °C.

Exp.	Sample ID	Inf [Si] ppm	T °C	Flow Rate, m^3/d	Time, days	pH 23°C	Glass Mass g	SA m^2	[B] ppm	B Rate $g_{glass}\ m^{-2}\ d^{-1}$	[Na] ppm	Na Rate $g_{glass}\ m^{-2}\ d^{-1}$	[K] ppm	K Rate $g_{glass}\ m^{-2}\ d^{-1}$	[Al] ppm	Al Rate $g_{glass}\ m^{-2}\ d^{-1}$	[Re] ppm	Re Rate $g_{glass}\ m^{-2}\ d^{-1}$
1	C28IX23-1D1	35	23	8.33E-06	3	7	1.65	0.0355	1.239	0.0187	14.6800	0.0418	1.2020	0.0201	0.0770	0.0005	0.2980	0.1486
	C28IX23-1D2	35	23	8.33E-06	6	7	1.65	0.0355	1.063	0.0067	10.9080	0.0101	0.9120	0.0052	0.0830	0.0003	0.1540	0.0023
	C28IX23-1D3	35	23	8.33E-06	9	7	1.65	0.0355	0.907	0.0057	8.2700	0.0080	0.7380	0.0047	0.0780	0.0002	0.0820	0.0023
	C28IX23-1D4	35	23	8.33E-06	12	7	1.65	0.0355	0.789	0.0051	6.4490	0.0065	0.6170	0.0041	0.0630	0.0001	0.0450	0.0018
	C28IX23-1D5	35	23	8.33E-06	15	7	1.65	0.0355	0.946	0.0083	6.4860	0.0092	0.7560	0.0075	0.6620	0.0055	0.0340	0.0055
	C28IX23-1D6	35	23	8.33E-06	18	7	1.65	0.0355	0.524	0.0007	3.9520	0.0019	0.4180	0.0006	0.0530	-0.0026	0.0150	-0.0013
	C28IX23-1D7	35	23	8.33E-06	21	7	1.65	0.0355	0.425	0.0024	3.1780	0.0033	0.3480	0.0023	0.0480	0.0001	0.0080	0.0000
	C28IX23-1D8	35	23	8.33E-06	24	7	1.65	0.0355	0.344	0.0020	2.5220	0.0026	0.2870	0.0019	0.0430	0.0001	0.0060	0.0008
	C28IX23-1D9	35	23	8.33E-06	27	7	1.65	0.0355	0.352	0.0027	2.4970	0.0034	0.2960	0.0025	0.0390	0.0001	0.0040	0.0003
	C28IX23-1D10	35	23	8.33E-06	30	7	1.65	0.0355	0.422	0.0037	2.7600	0.0042	0.3330	0.0031	0.0450	0.0001	0.0040	0.0008
2	C28IX23-2D1	40	23	8.33E-06	3	8	1.65	0.0355	0.963	0.0145	12.8120	0.0365	0.9270	0.0154	0.1130	0.0009	0.3410	0.1702
	C28IX23-2D2	40	23	8.33E-06	6	8	1.65	0.0355	0.677	0.0029	8.6530	0.0063	0.6110	0.0024	0.1010	0.0003	0.1720	0.0005
	C28IX23-2D3	40	23	8.33E-06	9	8	1.65	0.0355	0.504	0.0025	6.1510	0.0051	0.4360	0.0021	0.0850	0.0002	0.0880	0.0008
	C28IX23-2D4	40	23	8.33E-06	12	8	1.65	0.0355	0.399	0.0022	4.6110	0.0043	0.3310	0.0018	0.0630	0.0001	0.0460	0.0008
	C28IX23-2D5	40	23	8.33E-06	15	8	1.65	0.0355	0.311	0.0017	3.5210	0.0034	0.2590	0.0015	0.0560	0.0002	0.0240	0.0003
	C28IX23-2D6	40	23	8.33E-06	18	8	1.65	0.0355	0.690	0.0081	5.0590	0.0093	0.5880	0.0076	0.0000	-0.0003	0.0280	0.0078
	C28IX23-2D7	40	23	8.33E-06	21	8	1.65	0.0355	0.193	-0.0023	2.1980	-0.0011	0.1760	-0.0021	0.0000	-0.0001	0.0070	-0.0037
	C28IX23-2D8	40	23	8.33E-06	24	8	1.65	0.0355	0.149	0.0008	1.7420	0.0017	0.1410	0.0008	0.0430	0.0003	0.0040	0.0000
	C28IX23-2D9	40	23	8.33E-06	27	8	1.65	0.0355	0.146	0.0011	1.6780	0.0022	0.1430	0.0011	0.0360	0.0001	0.0020	-0.0002
	C28IX23-2D10	40	23	8.33E-06	30	8	1.65	0.0355	0.168	0.0014	1.7270	0.0024	0.1460	0.0012	0.0330	0.0001	0.0020	0.0003
3	C28IX23-3D1	52	23	8.33E-06	3	9	1.65	0.0355	0.924	0.0139	11.5420	0.0328	0.7600	0.0127	0.1160	0.0009	0.4150	0.2072
	C28IX23-3D2	52	23	8.33E-06	6	9	1.65	0.0355	0.563	0.0015	7.5400	0.0049	0.4730	0.0015	0.0980	0.0003	0.2100	0.0010
	C28IX23-3D3	52	23	8.33E-06	9	9	1.65	0.0355	0.361	0.0012	5.0800	0.0036	0.3170	0.0013	0.0850	0.0002	0.1060	0.0003
	C28IX23-3D4	52	23	8.33E-06	12	9	1.65	0.0355	0.247	0.0010	3.6370	0.0030	0.2260	0.0011	0.0730	0.0002	0.0530	-0.0003
	C28IX23-3D5	52	23	8.33E-06	15	9	1.65	0.0355	0.179	0.0008	2.7260	0.0025	0.1700	0.0009	0.0700	0.0002	0.0270	0.0000
	C28IX23-3D6	52	23	8.33E-06	18	9	1.65	0.0355	0.131	0.0006	2.1260	0.0020	0.1390	0.0009	0.0610	0.0002	0.0140	0.0000
	C28IX23-3D7	52	23	8.33E-06	21	9	1.65	0.0355	0.105	0.0006	1.7180	0.0017	0.1130	0.0007	0.0670	0.0003	0.0070	-0.0003
	C28IX23-3D8	52	23	8.33E-06	24	9	1.65	0.0355	0.076	0.0003	1.3900	0.0014	0.0910	0.0005	0.0530	0.0001	0.0030	-0.0005
	C28IX23-3D9	52	23	8.33E-06	27	9	1.65	0.0355	0.072	0.0005	1.3070	0.0016	0.0890	0.0007	0.0520	0.0002	0.0020	0.0000
	C28IX23-3D10	52	23	8.33E-06	30	9	1.65	0.0355	0.083	0.0007	1.3630	0.0019	0.0910	0.0007	0.0520	0.0002	0.0010	-0.0003
4	C28IX23-4D1	90	23	8.33E-06	3	10	0.83	0.0178	0.511	0.0153	6.0920	0.0339	0.3930	0.0129	0.0820	0.0010	0.2530	0.2469
	C28IX23-4D2	90	23	8.33E-06	6	10	0.83	0.0178	0.289	0.0010	3.7970	0.0038	0.2380	0.0012	0.0670	0.0002	0.1280	-0.0015
	C28IX23-4D3	90	23	8.33E-06	9	10	0.83	0.0178	0.164	0.0005	2.5080	0.0030	0.1550	0.0010	0.0600	0.0002	0.0640	-0.0030
	C28IX23-4D4	90	23	8.33E-06	12	10	0.83	0.0178	0.100	0.0005	1.7880	0.0026	0.1120	0.0010	0.0550	0.0002	0.0330	-0.0020
	C28IX23-4D5	90	23	8.33E-06	15	10	0.83	0.0178	0.222	0.0051	2.0980	0.0064	0.2160	0.0052	0.3280	0.0051	0.0200	0.0005
	C28IX23-4D6	90	23	8.33E-06	18	10	0.83	0.0178	0.042	-0.0021	1.0560	-0.0004	0.0700	-0.0014	0.0470	-0.0023	0.0080	-0.0050
	C28IX23-4D7	90	23	8.33E-06	21	10	0.83	0.0178	0.028	0.0002	0.9040	0.0017	0.0710	0.0010	0.0380	0.0000	0.0040	-0.0030
	C28IX23-4D8	90	23	8.33E-06	24	10	0.83	0.0178	0.016	0.0000	0.7480	0.0012	0.0560	0.0005	0.0360	0.0001	0.0020	-0.0030
	C28IX23-4D9	90	23	8.33E-06	27	10	0.83	0.0178	0.014	0.0001	0.7190	0.0015	0.0540	0.0007	0.0390	0.0001	0.0010	-0.0030
	C28IX23-4D10	90	23	8.33E-06	30	10	0.83	0.0178	0.015	0.0002	0.7300	0.0017	0.0490	0.0006	0.0370	0.0001	0.0000	-0.0035
5	C28IX23-5D1	230	23	8.33E-06	3	11	0.83	0.0178	0.651	0.0196	6.7400	0.0351	0.5980	0.0201	0.6510	0.0112	0.2020	0.2011
	C28IX23-5D2	230	23	8.33E-06	6	11	0.83	0.0178	0.176	-0.0046	3.2510	-0.0024	0.1880	-0.0038	0.0680	-0.0047	0.0970	-0.0044
	C28IX23-5D3	230	23	8.33E-06	9	11	0.83	0.0178	0.093	0.0001	2.3140	0.0022	0.1310	0.0012	0.0600	0.0003	0.0490	0.0001
	C28IX23-5D4	230	23	8.33E-06	12	11	0.83	0.0178	0.048	0.0000	1.7770	0.0018	0.0990	0.0011	0.0570	0.0003	0.0240	-0.0009
	C28IX23-5D5	230	23	8.33E-06	15	11	0.83	0.0178	0.022	-0.0001	1.4510	0.0015	0.0790	0.0010	0.0500	0.0002	0.0120	-0.0004
	C28IX23-5D6	230	23	8.33E-06	18	11	0.83	0.0178	0.005	-0.0002	1.2440	0.0012	0.0680	0.0009	0.0480	0.0003	0.0060	-0.0004
	C28IX23-5D7	230	23	8.33E-06	21	11	0.83	0.0178	0.000	-0.0001	1.1110	0.0011	0.0610	0.0009	0.0480	0.0003	0.0030	-0.0004
	C28IX23-5D8	230	23	8.33E-06	24	11	0.83	0.0178	0.000	-0.0004	1.0030	0.0008	0.0510	0.0007	0.0380	0.0001	0.0020	0.0001
	C28IX23-5D9	230	23	8.33E-06	27	11	0.83	0.0178	0.000	-0.0002	0.9860	0.0010	0.0520	0.0009	0.0410	0.0002	0.0000	-0.0014
	C28IX23-5D10	230	23	8.33E-06	30	11	0.83	0.0178	0.000	-0.0002	1.0000	0.0012	0.0510	0.0008	0.0390	0.0002	0.0000	-0.0004

Table D7. ICP-AES Analysis Results from Dissolution of Glass IDF1B2 at 70 °C.

Exp.	Sample ID	Inf [Si] ppm	T °C	Flow Rate, m^3/d	Time, days	pH 23°C	Glass Mass g	SA m^2	[B] ppm	B Rate $g_{glass}\ m^{-2}\ d^{-1}$	[Na] ppm	Na Rate $g_{glass}\ m^{-2}\ d^{-1}$	[K] ppm	K Rate $g_{glass}\ m^{-2}\ d^{-1}$	[Al] ppm	Al Rate $g_{glass}\ m^{-2}\ d^{-1}$	[Re] ppm	Re Rate $g_{glass}\ m^{-2}\ d^{-1}$
1	B2IX70-1D1	55	70	2.50E-05	1	7	0.77	0.01657	3.189	0.4246	38.5380	0.6261	0.1200	0.2761	0.1340	0.0067	0.0740	0.2397
	B2IX70-1D2	55	70	2.50E-05	2	7	0.77	0.0166	3.694	0.2805	40.4350	0.3451	0.1390	0.1964	0.1970	0.0070	0.0560	0.0611
	B2IX70-1D3	55	70	2.50E-05	3	7	0.77	0.0166	3.596	0.2345	37.9770	0.2904	0.1370	0.1619	0.2200	0.0065	0.0420	0.0448
	B2IX70-1D4	55	70	2.50E-05	4	7	0.77	0.0166	3.311	0.2035	32.4600	0.2208	0.1270	0.1349	0.2420	0.0071	0.0320	0.0351
	B2IX70-1D5	55	70	2.50E-05	5	7	0.77	0.0166	3.083	0.1926	30.9830	0.2427	0.1280	0.1537	0.2320	0.0059	0.0270	0.0352
	B2IX70-1D6	55	70	2.50E-05	6	7	0.77	0.0166	2.801	0.1704	25.7980	0.1698	0.1150	0.1126	0.1980	0.0043	0.0210	0.0236
	B2IX70-1D7	55	70	2.50E-05	7	7	0.77	0.0166	2.721	0.1791	26.3380	0.2222	0.1190	0.1453	0.2020	0.0055	0.0190	0.0270
	B2IX70-1D8	55	70	2.50E-05	8	7	0.77	0.0166	2.661	0.1769	25.3830	0.2024	0.1190	0.1395	0.1990	0.0052	0.0180	0.0271
	B2IX70-1D9	55	70	2.50E-05	9	7	0.77	0.0166	2.561	0.1678	23.2580	0.1755	0.1130	0.1212	0.1940	0.0050	0.0170	0.0255
	B2IX70-1D10	55	70	2.50E-05	10	7	0.77	0.0166	2.395	0.1523	21.4480	0.1634	0.1000	0.0904	0.1770	0.0042	0.0160	0.0239
2	B2IX70-2D1	60	70	2.50E-05	1	8	0.77	0.0166	1.733	0.2304	25.8390	0.4187	0.0660	0.1001	0.1910	0.0099	0.0560	0.1807
	B2IX70-2D2	60	70	2.50E-05	2	8	0.77	0.0166	2.040	0.1564	25.7490	0.2083	0.0710	0.0653	0.2410	0.0078	0.0380	0.0315
	B2IX70-2D3	60	70	2.50E-05	3	8	0.77	0.0166	1.960	0.1254	22.6090	0.1581	0.0670	0.0457	0.2530	0.0071	0.0270	0.0250
	B2IX70-2D4	60	70	2.50E-05	4	8	0.77	0.0166	1.794	0.1088	19.0410	0.1257	0.0590	0.0274	0.2320	0.0056	0.0200	0.0201
	B2IX70-2D5	60	70	2.50E-05	5	8	0.77	0.0166	1.640	0.0994	17.6940	0.1331	0.0560	0.0305	0.2260	0.0058	0.0150	0.0152
	B2IX70-2D6	60	70	2.50E-05	6	8	0.77	0.0166	1.469	0.0870	15.2500	0.1042	0.0560	0.0352	0.2580	0.0079	0.0140	0.0201
	B2IX70-2D7	60	70	2.50E-05	7	8	0.77	0.0166	1.417	0.0916	14.0990	0.1055	0.0620	0.0536	0.2450	0.0062	0.0130	0.0185
	B2IX70-2D8	60	70	2.50E-05	8	8	0.77	0.0166	1.377	0.0898	14.1580	0.1161	0.0530	0.0169	0.2800	0.0086	0.0120	0.0169
	B2IX70-2D9	60	70	2.50E-05	9	8	0.77	0.0166	1.322	0.0852	13.1450	0.0991	0.0540	0.0338	0.2700	0.0070	0.0120	0.0186
	B2IX70-2D10	60	70	2.50E-05	10	8	0.77	0.0166	1.234	0.0772	12.2560	0.0929	0.0490	0.0169	0.2580	0.0066	0.0120	0.0186
3	B2IX70-3D1	80	70	2.50E-05	1	9	0.77	0.0166	0.919	0.1219	17.0100	0.2678	0.0440	0.0000	0.2790	0.0145	0.0430	0.1158
	B2IX70-3D2	80	70	2.50E-05	2	9	0.77	0.0166	0.968	0.0675	15.6200	0.1146	0.0390	0.0000	0.2950	0.0082	0.0270	0.0140
	B2IX70-3D3	80	70	2.50E-05	3	9	0.77	0.0166	0.922	0.0582	13.6800	0.0944	0.0330	0.0000	0.2940	0.0077	0.0180	0.0113
	B2IX70-3D4	80	70	2.50E-05	4	9	0.77	0.0166	0.830	0.0490	11.2640	0.0709	0.0290	0.0000	0.2630	0.0059	0.0120	0.0072
	B2IX70-3D5	80	70	2.50E-05	5	9	0.77	0.0166	0.765	0.0465	9.8560	0.0677	0.0270	0.0000	0.2580	0.0065	0.0090	0.0072
	B2IX70-3D6	80	70	2.50E-05	6	9	0.77	0.0166	0.685	0.0402	8.4750	0.0567	0.0250	0.0000	0.2170	0.0044	0.0080	0.0085
	B2IX70-3D7	80	70	2.50E-05	7	9	0.77	0.0166	0.703	0.0480	8.7680	0.0728	0.0260	0.0000	0.2460	0.0072	0.0070	0.0072
	B2IX70-3D8	80	70	2.50E-05	8	9	0.77	0.0166	0.702	0.0467	8.6220	0.0680	0.0260	0.0000	0.2600	0.0072	0.0070	0.0086
	B2IX70-3D9	80	70	2.50E-05	9	9	0.77	0.0166	0.684	0.0444	8.0500	0.0599	0.0260	0.0000	0.2490	0.0061	0.0070	0.0086
	B2IX70-3D10	80	70	2.50E-05	10	9	0.77	0.0166	0.632	0.0386	7.2520	0.0516	0.0240	0.0000	0.2350	0.0057	0.0060	0.0058
4	B2IX70-4D1	140	70	2.50E-05	1	10	0.50	0.0107	0.415	0.0853	8.3020	0.2088	0.0000	0.0000	0.1880	0.0131	0.0310	0.1289
	B2IX70-4D2	140	70	2.50E-05	2	10	0.50	0.0107	0.416	0.0429	7.1960	0.0768	<0.023	0.0000	0.1590	0.0040	0.0180	0.0090
	B2IX70-4D3	140	70	2.50E-05	3	10	0.50	0.0107	0.382	0.0357	6.0050	0.0607	<0.023	0.0000	0.1360	0.0032	0.0100	0.0026
	B2IX70-4D4	140	70	2.50E-05	4	10	0.50	0.0107	0.349	0.0324	5.0610	0.0519	<0.023	0.0000	0.1220	0.0030	0.0060	0.0026
	B2IX70-4D5	140	70	2.50E-05	5	10	0.50	0.0107	0.327	0.0313	4.4240	0.0477	<0.023	0.0000	0.1200	0.0035	0.0040	0.0026
	B2IX70-4D6	140	70	2.50E-05	6	10	0.50	0.0107	0.295	0.0270	3.9010	0.0426	<0.023	0.0000	0.1150	0.0031	0.0030	0.0026
	B2IX70-4D7	140	70	2.50E-05	7	10	0.50	0.0107	0.287	0.0286	3.6880	0.0438	<0.023	0.0000	0.0980	0.0018	0.0020	0.0004
	B2IX70-4D8	140	70	2.50E-05	8	10	0.50	0.0107	0.284	0.0289	3.4520	0.0405	<0.023	0.0000	0.0970	0.0025	0.0010	0.0000
	B2IX70-4D9	140	70	2.50E-05	9	10	0.50	0.0107	0.278	0.0279	3.3530	0.0410	<0.023	0.0000	0.0920	0.0021	0.0010	0.0004
	B2IX70-4D10	140	70	2.50E-05	10	10	0.50	0.0107	0.257	0.0242	3.0610	0.0349	<0.023	0.0000	0.0940	0.0025	0.0010	0.0004
5	B2IX70-5D1	360	70	2.50E-05	1	11	0.50	0.0107	0.246	0.0502	7.3180	0.1527	<0.023	0.0000	0.1350	0.0106	0.0170	0.0692
	B2IX70-5D2	360	70	2.50E-05	2	11	0.50	0.0107	0.222	0.0202	6.4450	0.0543	<0.023	0.0000	0.0740	0.0000	0.0080	0.0000
	B2IX70-5D3	360	70	2.50E-05	3	11	0.50	0.0107	0.207	0.0195	5.5030	0.0415	<0.023	0.0000	0.0770	0.0029	0.0050	0.0026
	B2IX70-5D4	360	70	2.50E-05	4	11	0.50	0.0107	0.182	0.0159	4.8160	0.0360	<0.023	0.0000	0.0590	0.0012	0.0020	0.0000
	B2IX70-5D5	360	70	2.50E-05	5	11	0.50	0.0107	0.166	0.0152	4.2450	0.0303	<0.023	0.0000	0.0520	0.0013	0.0020	0.0026
	B2IX70-5D6	360	70	2.50E-05	6	11	0.50	0.0107	0.142	0.0119	3.8320	0.0271	<0.023	0.0000	0.0460	0.0011	0.0010	0.0000
	B2IX70-5D7	360	70	2.50E-05	7	11	0.50	0.0107	0.137	0.0133	3.6890	0.0287	<0.023	0.0000	0.0450	0.0013	0.0000	0.0000
	B2IX70-5D8	360	70	2.50E-05	8	11	0.50	0.0107	0.131	0.0126	3.4980	0.0257	<0.023	0.0000	0.0430	0.0012	0.0000	0.0000
	B2IX70-5D9	360	70	2.50E-05	9	11	0.50	0.0107	0.120	0.0110	3.4040	0.0257	<0.023	0.0000	0.0460	0.0015	0.0000	0.0000
	B2IX70-5D10	360	70	2.50E-05	10	11	0.50	0.0107	0.108	0.0096	3.1280	0.0199	<0.023	0.0000	0.0400	0.0008	0.0000	0.0000

Table D8. ICP-AES Analysis Results from Dissolution of Glass IDF1B2 at 40 °C.

Exp.	Sample ID	Inf [Si] ppm	T °C	Flow Rate, m^3/d	Time, days	pH 23°C	Glass Mass g	SA m^2	[B] ppm	B Rate $g_{glass}\ m^{-2}\ d^{-1}$	[Na] ppm	Na Rate $g_{glass}\ m^{-2}\ d^{-1}$	[K] ppm	K Rate $g_{glass}\ m^{-2}\ d^{-1}$	[Al] ppm	Al Rate $g_{glass}\ m^{-2}\ d^{-1}$	[Re] ppm	Re Rate $g_{glass}\ m^{-2}\ d^{-1}$
1	B2IX40-1D1	40	40	8.33E-06	3	7	1.65	0.0355	1.587	0.0328	31.4320	0.0794	0.0710	0.0294	0.0770	0.0005	0.0840	0.0355
	B2IX40-1D2	40	40	8.33E-06	6	7	1.65	0.0355	1.470	0.0140	26.9220	0.0283	0.0570	0.0003	0.0960	0.0004	0.0530	0.0045
	B2IX40-1D3	40	40	8.33E-06	9	7	1.65	0.0355	1.309	0.0119	22.0890	0.0218	0.0480	0.0003	0.0950	0.0003	0.0350	0.0034
	B2IX40-1D4	40	40	8.33E-06	12	7	1.65	0.0355	1.246	0.0122	19.7410	0.0220	0.0470	0.0003	0.1330	0.0007	0.0270	0.0039
	B2IX40-1D5	40	40	8.33E-06	15	7	1.65	0.0355	1.116	0.0102	16.6170	0.0170	0.0450	0.0003	0.1250	0.0005	0.0200	0.0026
	B2IX40-1D6	40	40	8.33E-06	18	7	1.65	0.0355	1.025	0.0097	15.4620	0.0181	0.0470	0.0003	0.1670	0.0009	0.0180	0.0032
	B2IX40-1D7	40	40	8.33E-06	21	7	1.65	0.0355	0.956	0.0092	14.0960	0.0161	0.0400	0.0002	0.1840	0.0008	0.0170	0.0032
	B2IX40-1D8	40	40	8.33E-06	24	7	1.65	0.0355	0.898	0.0087	12.9800	0.0150	0.0400	0.0003	0.1920	0.0008	0.0160	0.0030
	B2IX40-1D9	40	40	8.33E-06	27	7	1.65	0.0355	0.842	0.0081	11.1930	0.0119	0.0380	0.0002	0.1620	0.0005	0.0140	0.0024
	B2IX40-1D10	40	40	8.33E-06	30	7	1.65	0.0355	0.815	0.0082	10.7790	0.0131	0.0390	0.0003	0.1600	0.0006	0.0140	0.0028
2	B2IX40-2D1	45	40	8.33E-06	3	8	1.65	0.0355	1.071	0.0221	24.8130	0.0626	0.0420	0.0135	0.4540	0.0039	0.0690	0.0295
	B2IX40-2D2	45	40	8.33E-06	6	8	1.65	0.0355	0.819	0.0058	19.0880	0.0168	0.0320	0.0001	0.1560	-0.0007	0.0390	0.0019
	B2IX40-2D3	45	40	8.33E-06	9	8	1.65	0.0355	0.672	0.0054	15.2750	0.0144	0.0260	0.0001	0.1410	0.0005	0.0230	0.0015
	B2IX40-2D4	45	40	8.33E-06	12	8	1.65	0.0355	0.623	0.0059	13.3380	0.0143	0.0280	0.0001	0.1540	0.0007	0.0160	0.0019
	B2IX40-2D5	45	40	8.33E-06	15	8	1.65	0.0355	0.546	0.0048	11.1110	0.0112	0.0210	0.0000	0.1430	0.0005	0.0110	0.0013
	B2IX40-2D6	45	40	8.33E-06	18	8	1.65	0.0355	0.498	0.0046	9.5740	0.0101	0.0210	0.0001	0.1470	0.0006	0.0090	0.0015
	B2IX40-2D7	45	40	8.33E-06	21	8	1.65	0.0355	0.454	0.0042	8.4680	0.0092	0.0200	0.0000	0.1440	0.0005	0.0070	0.0011
	B2IX40-2D8	45	40	8.33E-06	24	8	1.65	0.0355	0.424	0.0041	8.0100	0.0095	0.0230	0.0001	0.1540	0.0006	0.0070	0.0015
	B2IX40-2D9	45	40	8.33E-06	27	8	1.65	0.0355	0.410	0.0041	7.3340	0.0083	0.0240	0.0001	0.1510	0.0006	0.0060	0.0011
	B2IX40-2D10	45	40	8.33E-06	30	8	1.65	0.0355	0.389	0.0038	6.8590	0.0080	0.0190	0.0000	0.1470	0.0006	0.0070	0.0017
3	B2IX40-3D1	60	40	8.33E-06	3	9	1.65	0.0355	0.642	0.0132	17.0580	0.0427	0.0260	0.0090	0.2270	0.0018	0.0630	0.0269
	B2IX40-3D2	60	40	8.33E-06	6	9	1.65	0.0355	0.489	0.0034	13.7560	0.0131	0.0190	0.0000	0.2170	0.0008	0.0360	0.0019
	B2IX40-3D3	60	40	8.33E-06	9	9	1.65	0.0355	0.375	0.0027	10.7210	0.0096	0.0190	0.0001	0.1790	0.0005	0.0210	0.0013
	B2IX40-3D4	60	40	8.33E-06	12	9	1.65	0.0355	0.312	0.0025	8.8950	0.0088	0.0150	0.0000	0.1690	0.0006	0.0130	0.0011
	B2IX40-3D5	60	40	8.33E-06	15	9	1.65	0.0355	0.254	0.0020	7.2410	0.0070	0.0130	0.0000	0.1430	0.0004	0.0090	0.0011
	B2IX40-3D6	60	40	8.33E-06	18	9	1.65	0.0355	0.222	0.0019	6.5030	0.0072	0.0120	0.0000	0.1440	0.0005	0.0070	0.0011
	B2IX40-3D7	60	40	8.33E-06	21	9	1.65	0.0355	0.194	0.0017	5.7840	0.0063	0.0170	0.0001	0.1390	0.0005	0.0050	0.0006
	B2IX40-3D8	60	40	8.33E-06	24	9	1.65	0.0355	0.178	0.0016	5.3390	0.0061	0.0160	0.0001	0.1460	0.0006	0.0040	0.0006
	B2IX40-3D9	60	40	8.33E-06	27	9	1.65	0.0355	0.163	0.0015	4.8810	0.0055	0.0130	0.0000	0.1470	0.0006	0.0040	0.0009
	B2IX40-3D10	60	40	8.33E-06	30	9	1.65	0.0355	0.153	0.0014	4.6120	0.0054	0.0150	0.0001	0.1370	0.0005	0.0040	0.0009
4	B2IX40-4D1	105	40	8.33E-06	3	10	0.83	0.0178	2.522	0.1043	25.2060	0.1273	0.0870	0.0660	5.7470	0.1011	0.1310	0.1118
	B2IX40-4D2	105	40	8.33E-06	6	10	0.83	0.0178	0.218	-0.0433	5.4850	-0.0361	<DL	-	0.1350	-0.0490	0.0180	-0.0406
	B2IX40-4D3	105	40	8.33E-06	9	10	0.83	0.0178	0.157	0.0019	4.2900	0.0078	<DL	-	0.1090	0.0003	0.0100	0.0009
	B2IX40-4D4	105	40	8.33E-06	12	10	0.83	0.0178	0.124	0.0018	3.6050	0.0074	<DL	-	0.0960	0.0003	0.0060	0.0009
	B2IX40-4D5	105	40	8.33E-06	15	10	0.83	0.0178	0.097	0.0014	2.9420	0.0057	<DL	-	0.0800	0.0002	0.0040	0.0009
	B2IX40-4D6	105	40	8.33E-06	18	10	0.83	0.0178	0.083	0.0014	2.6210	0.0058	<DL	-	0.0750	0.0002	0.0020	0.0000
	B2IX40-4D7	105	40	8.33E-06	21	10	0.83	0.0178	0.071	0.0012	2.3430	0.0052	<DL	-	0.0680	0.0002	0.0010	0.0000
	B2IX40-4D8	105	40	8.33E-06	24	10	0.83	0.0178	0.064	0.0011	2.1480	0.0049	<DL	-	0.0630	0.0001	0.0010	0.0004
	B2IX40-4D9	105	40	8.33E-06	27	10	0.83	0.0178	0.060	0.0011	2.0220	0.0048	<DL	-	0.0640	0.0002	0.0010	0.0004
	B2IX40-4D10	105	40	8.33E-06	30	10	0.83	0.0178	0.058	0.0011	1.9000	0.0045	<DL	-	0.0600	0.0001	0.0010	0.0004
5	B2IX40-5D1	270	40	8.33E-06	3	11	0.83	0.0178	0.185	0.0075	6.0590	0.0262	<DL	-	0.1080	0.0015	0.0300	0.0249
	B2IX40-5D2	270	40	8.33E-06	6	11	0.83	0.0178	0.115	0.0009	4.6500	0.0060	<DL	-	0.0960	0.0006	0.0160	0.0005
	B2IX40-5D3	270	40	8.33E-06	9	11	0.83	0.0178	0.040	-0.0008	3.6230	0.0043	0.0140	-	0.0860	0.0005	0.0090	0.0005
	B2IX40-5D4	270	40	8.33E-06	12	11	0.83	0.0178	0.013	-0.0004	3.0470	0.0040	0.0100	0.0001	0.0800	0.0005	0.0040	-0.0008
	B2IX40-5D5	270	40	8.33E-06	15	11	0.83	0.0178	<DL	-	2.5290	0.0029	0.0100	0.0001	0.0670	0.0003	0.0020	-0.0003
	B2IX40-5D6	270	40	8.33E-06	18	11	0.83	0.0178	<DL	-	2.2500	0.0028	0.0110	0.0002	0.0590	0.0003	0.0010	-0.0003
	B2IX40-5D7	270	40	8.33E-06	21	11	0.83	0.0178	<DL	-	2.0610	0.0025	0.0100	0.0001	0.0550	0.0003	0.0010	0.0001
	B2IX40-5D8	270	40	8.33E-06	24	11	0.83	0.0178	<DL	-	1.8960	0.0021	0.0100	0.0001	0.0540	0.0003	0.0010	0.0001
	B2IX40-5D9	270	40	8.33E-06	27	11	0.83	0.0178	<DL	-	1.7850	0.0020	0.0120	0.0002	0.0510	0.0002	0.0010	0.0001
	B2IX40-5D10	270	40	8.33E-06	30	11	0.83	0.0178	<DL	-	1.7100	0.0019	0.0110	0.0001	0.0460	0.0002	0.0000	-0.0008

Table D9. ICP-AES Analysis Results from Dissolution of Glass IDF1B2 at 23 °C.

Exp.	Sample ID	Inf [Si] ppm	T °C	Flow Rate, m^3/d	Time, days	pH 23°C	Glass Mass g	SA m^2	[B] ppm	B Rate $g_{glass}\ m^{-2}\ d^{-1}$	[Na] ppm	Na Rate $g_{glass}\ m^{-2}\ d^{-1}$	[K] ppm	K Rate $g_{glass}\ m^{-2}\ d^{-1}$	[Al] ppm	Al Rate $g_{glass}\ m^{-2}\ d^{-1}$	[Re] ppm	Re Rate $g_{glass}\ m^{-2}\ d^{-1}$
1	B2IX23-1D1	35	23	8.33E-06	3	7	1.65	0.0355	0.885	0.0183	23.1030	0.0583	0.0490	0.0203	0.1470	0.0011	0.1090	0.0461
	B2IX23-1D2	35	23	8.33E-06	6	7	1.65	0.0355	0.658	0.0044	17.7960	0.0157	0.0370	0.0002	0.1060	0.0002	0.0580	0.0013
	B2IX23-1D3	35	23	8.33E-06	9	7	1.65	0.0355	0.511	0.0037	13.7350	0.0122	0.0320	0.0002	0.0890	0.0002	0.0330	0.0015
	B2IX23-1D4	35	23	8.33E-06	12	7	1.65	0.0355	0.406	0.0031	10.8030	0.0099	0.0230	0.0001	0.0800	0.0002	0.0200	0.0013
	B2IX23-1D5	35	23	8.33E-06	15	7	1.65	0.0355	0.316	0.0023	8.5410	0.0079	0.0210	0.0001	0.0780	0.0002	0.0120	0.0006
	B2IX23-1D6	35	23	8.33E-06	18	7	1.65	0.0355	0.245	0.0018	6.9410	0.0067	0.0190	0.0001	0.0790	0.0003	0.0080	0.0006
	B2IX23-1D7	35	23	8.33E-06	21	7	1.65	0.0355	0.187	0.0013	5.5190	0.0051	0.0150	0.0000	0.0660	0.0001	0.0060	0.0006
	B2IX23-1D8	35	23	8.33E-06	24	7	1.65	0.0355	0.149	0.0011	4.6000	0.0046	0.0140	0.0001	0.0560	0.0001	0.0040	0.0002
	B2IX23-1D9	35	23	8.33E-06	27	7	1.65	0.0355	0.216	0.0029	5.0700	0.0069	0.0180	0.0001	0.2510	0.0019	0.0070	0.0019
	B2IX23-1D10	35	23	8.33E-06	30	7	1.65	0.0355	0.279	0.0035	5.7920	0.0082	0.0210	0.0002	0.2980	0.0014	0.0090	0.0021
2	B2IX23-2D1	40	23	8.33E-06	3	8	1.65	0.0355	0.683	0.0141	18.8400	0.0475	0.0370	0.0127	0.1200	0.0010	0.1100	0.0466
	B2IX23-2D2	40	23	8.33E-06	6	8	1.65	0.0355	0.465	0.0025	13.5530	0.0104	0.0220	0.0000	0.0990	0.0003	0.0570	0.0007
	B2IX23-2D3	40	23	8.33E-06	9	8	1.65	0.0355	0.325	0.0019	10.1540	0.0085	0.0180	0.0000	0.0830	0.0002	0.0310	0.0009
	B2IX23-2D4	40	23	8.33E-06	12	8	1.65	0.0355	0.246	0.0017	8.0820	0.0075	0.0170	0.0001	0.0790	0.0003	0.0170	0.0004
	B2IX23-2D5	40	23	8.33E-06	15	8	1.65	0.0355	0.181	0.0012	6.2950	0.0056	0.0140	0.0000	0.0690	0.0002	0.0090	0.0000
	B2IX23-2D6	40	23	8.33E-06	18	8	1.65	0.0355	0.134	0.0009	5.0590	0.0048	0.0140	0.0000	0.0620	0.0002	0.0060	0.0004
	B2IX23-2D7	40	23	8.33E-06	21	8	1.65	0.0355	0.099	0.0006	4.0890	0.0039	0.0120	0.0000	0.0580	0.0002	0.0030	-0.0002
	B2IX23-2D8	40	23	8.33E-06	24	8	1.65	0.0355	0.074	0.0005	3.3140	0.0031	0.0110	0.0000	0.0430	0.0001	0.0020	0.0000
	B2IX23-2D9	40	23	8.33E-06	27	8	1.65	0.0355	0.096	0.0012	3.5240	0.0046	0.0120	0.0000	0.1060	0.0007	0.0030	0.0007
	B2IX23-2D10	40	23	8.33E-06	30	8	1.65	0.0355	0.086	0.0008	3.5660	0.0045	0.0120	0.0000	0.0460	-0.0001	0.0010	-0.0004
3	B2IX23-3D1	52	23	8.33E-06	3	9	1.65	0.0355	0.669	0.0138	15.2300	0.0384	0.0910	0.0402	0.0960	0.0007	0.1240	0.0525
	B2IX23-3D2	52	23	8.33E-06	6	9	1.65	0.0355	0.406	0.0014	10.5870	0.0074	0.0200	-0.0005	0.0880	0.0003	0.0640	0.0006
	B2IX23-3D3	52	23	8.33E-06	9	9	1.65	0.0355	0.253	0.0010	7.6410	0.0058	0.0150	0.0000	0.0810	0.0003	0.0320	-0.0002
	B2IX23-3D4	52	23	8.33E-06	12	9	1.65	0.0355	0.168	0.0008	5.7210	0.0047	0.0130	0.0000	0.0720	0.0002	0.0170	0.0002
	B2IX23-3D5	52	23	8.33E-06	15	9	1.65	0.0355	0.113	0.0006	4.3680	0.0037	0.0140	0.0001	0.0660	0.0002	0.0090	0.0000
	B2IX23-3D6	52	23	8.33E-06	18	9	1.65	0.0355	0.080	0.0005	3.5680	0.0034	0.0120	0.0000	0.0610	0.0002	0.0050	0.0000
	B2IX23-3D7	52	23	8.33E-06	21	9	1.65	0.0355	0.059	0.0004	2.9360	0.0028	0.0110	0.0000	0.0620	0.0002	0.0030	0.0000
	B2IX23-3D8	52	23	8.33E-06	24	9	1.65	0.0355	0.042	0.0002	2.4520	0.0024	0.0090	0.0000	0.0550	0.0001	0.0010	-0.0004
	B2IX23-3D9	52	23	8.33E-06	27	9	1.65	0.0355	0.039	0.0003	2.3820	0.0028	0.0100	0.0000	0.0540	0.0002	0.0010	0.0000
	B2IX23-3D10	52	23	8.33E-06	30	9	1.65	0.0355	0.046	0.0005	2.5000	0.0032	0.0100	0.0000	0.0590	0.0002	0.0010	0.0000
4	B2IX23-4D1	90	23	8.33E-06	3	10	0.83	0.0178	0.293	0.0120	7.0470	0.0351	0.0310	0.0201	0.1100	0.0015	0.0560	0.0426
	B2IX23-4D2	90	23	8.33E-06	6	10	0.83	0.0178	0.172	0.0010	4.7920	0.0060	0.0150	-0.0002	0.0880	0.0004	0.0280	-0.0026
	B2IX23-4D3	90	23	8.33E-06	9	10	0.83	0.0178	0.106	0.0008	3.3980	0.0047	0.0100	-0.0001	0.0710	0.0002	0.0140	-0.0026
	B2IX23-4D4	90	23	8.33E-06	12	10	0.83	0.0178	0.069	0.0006	2.6000	0.0041	0.0100	0.0000	0.0610	0.0002	0.0070	-0.0026
	B2IX23-4D5	90	23	8.33E-06	15	10	0.83	0.0178	0.047	0.0004	2.0690	0.0035	0.0090	0.0000	0.0590	0.0003	0.0040	-0.0021
	B2IX23-4D6	90	23	8.33E-06	18	10	0.83	0.0178	0.035	0.0004	1.7100	0.0030	0.0090	0.0000	0.0550	0.0002	0.0020	-0.0026
	B2IX23-4D7	90	23	8.33E-06	21	10	0.83	0.0178	0.030	0.0004	1.5320	0.0030	0.0100	0.0000	0.0490	0.0001	0.0000	-0.0034
	B2IX23-4D8	90	23	8.33E-06	24	10	0.83	0.0178	0.020	0.0001	1.2970	0.0023	0.0120	0.0001	0.0490	0.0002	0.0000	-0.0026
	B2IX23-4D9	90	23	8.33E-06	27	10	0.83	0.0178	0.016	0.0002	1.2360	0.0026	0.0090	-0.0001	0.0460	0.0001	0.0000	-0.0026
	B2IX23-4D10	90	23	8.33E-06	30	10	0.83	0.0178	0.018	0.0003	1.3100	0.0031	0.0100	0.0000	0.0470	0.0002	0.0000	-0.0026
5	B2IX23-5D1	230	23	8.33E-06	3	11	0.83	0.0178	0.218	0.0089	6.0530	0.0275	0.0170	0.0144	0.0840	0.0012	0.0520	0.0437
	B2IX23-5D2	230	23	8.33E-06	6	11	0.83	0.0178	0.126	0.0006	4.1340	0.0041	0.0130	0.0001	0.0820	0.0006	0.0260	-0.0003
	B2IX23-5D3	230	23	8.33E-06	9	11	0.83	0.0178	0.072	0.0003	3.0290	0.0033	0.0110	0.0001	0.0710	0.0004	0.0120	-0.0012
	B2IX23-5D4	230	23	8.33E-06	12	11	0.83	0.0178	0.047	0.0004	2.4220	0.0031	0.0120	0.0002	0.0750	0.0005	0.0060	-0.0003
	B2IX23-5D5	230	23	8.33E-06	15	11	0.83	0.0178	0.028	0.0001	1.9870	0.0024	0.0110	0.0001	0.0640	0.0003	0.0030	-0.0003
	B2IX23-5D6	230	23	8.33E-06	18	11	0.83	0.0178	0.015	0.0000	1.6820	0.0019	0.0110	0.0002	0.0560	0.0003	0.0010	-0.0008
	B2IX23-5D7	230	23	8.33E-06	21	11	0.83	0.0178	0.009	0.0000	1.4590	0.0016	0.0100	0.0001	0.0520	0.0003	0.0010	0.0001
	B2IX23-5D8	230	23	8.33E-06	24	11	0.83	0.0178	0.005	0.0000	1.3150	0.0014	0.0100	0.0001	0.0490	0.0003	0.0000	-0.0008
	B2IX23-5D9	230	23	8.33E-06	27	11	0.83	0.0178	0.003	0.0000	1.2880	0.0017	0.0140	0.0003	0.0450	0.0002	-0.0010	-0.0012
	B2IX23-5D10	230	23	8.33E-06	30	11	0.83	0.0178	0.005	0.0001	1.3450	0.0020	0.0120	0.0001	0.0500	0.0003	0.0000	0.0001

Table D10. ICP-MS Analysis Results from Dissolution of Glass LAWC22 at 70 °C.

Exp.	Sample ID	Inf [Si] ppm	T °C	Flow Rate, m^3/d	Time, days	pH 23°C	Glass Mass g	SA m^2	[Mo] ppm	Mo Rate $g_{glass}\ m^{-2}\ d^{-1}$	[Cs] ppm	Cs Rate $g_{glass}\ m^{-2}\ d^{-1}$	[Re] ppm	Re Rate $g_{glass}\ m^{-2}\ d^{-1}$
1	C22IX70-1D1	55	70	2.50E-05	1	7	0.77	0.0166	0.00665	0.0376	0.03979	0.0849	0.0211	0.0691
	C22IX70-1D2	55	70	2.50E-05	2	7	0.77	0.0165	0.00410	0.0044	0.04011	0.0432	0.0164	0.0190
	C22IX70-1D3	55	70	2.50E-05	3	7	0.77	0.0165	0.00265	0.0034	0.03490	0.0318	0.0122	0.0130
	C22IX70-1D4	55	70	2.50E-05	4	7	0.77	0.0165	0.00186	0.0030	0.03396	0.0354	0.0098	0.0121
	C22IX70-1D5	55	70	2.50E-05	5	7	0.77	0.0164	0.00156	0.0036	0.03312	0.0348	0.0086	0.0123
	C22IX70-1D6	55	70	2.50E-05	6	7	0.77	0.0163	0.00122	0.0025	0.03084	0.0309	0.0069	0.0087
	C22IX70-1D7	55	70	2.50E-05	7	7	0.77	0.0162	0.00100	0.0022	0.02883	0.0292	0.0058	0.0077
	C22IX70-1D8	55	70	2.50E-05	8	7	0.77	0.0162	0.00095	0.0026	0.03015	0.0344	0.0058	0.0096
	C22IX70-1D9	55	70	2.50E-05	9	7	0.77	0.0160	0.00084	0.0021	0.02704	0.0263	0.0050	0.0072
	C22IX70-1D10	55	70	2.50E-05	10	7	0.77	0.0159	0.00041	-0.0001	0.00896	-0.0101	0.0017	-0.0027
2	C22IX70-2D1	60	70	2.50E-05	1	8	0.77	0.0166	0.00755	0.0427	0.02027	0.0432	0.0133	0.0433
	C22IX70-2D2	60	70	2.50E-05	2	8	0.77	0.0166	0.00465	0.0049	0.01669	0.0140	0.0094	0.0091
	C22IX70-2D3	60	70	2.50E-05	3	8	0.77	0.0166	0.00446	0.0121	0.01473	0.0136	0.0074	0.0087
	C22IX70-2D4	60	70	2.50E-05	4	8	0.77	0.0166	0.00301	0.0044	0.01322	0.0125	0.0055	0.0060
	C22IX70-2D5	60	70	2.50E-05	5	8	0.77	0.0165	0.00217	0.0037	0.01180	0.0111	0.0045	0.0056
	C22IX70-2D6	60	70	2.50E-05	6	8	0.77	0.0165	0.00164	0.0031	0.01056	0.0099	0.0036	0.0045
	C22IX70-2D7	60	70	2.50E-05	7	8	0.77	0.0165	0.00015	-0.0038	0.00082	-0.0095	0.0003	-0.0050
	C22IX70-2D8	60	70	2.50E-05	8	8	0.77	0.0165	0.00094	0.0049	0.00703	0.0141	0.0021	0.0065
	C22IX70-2D9	60	70	2.50E-05	9	8	0.77	0.0165	0.00117	0.0039	0.00997	0.0138	0.0027	0.0055
	C22IX70-2D10	60	70	2.50E-05	10	8	0.77	0.0165	0.00128	0.0039	0.01094	0.0127	0.0032	0.0058
3	C22IX70-3D1	80	70	2.50E-05	1	9	0.77	0.0166	0.00817	0.0462	0.01540	0.0328	0.0110	0.0361
	C22IX70-3D2	80	70	2.50E-05	2	9	0.77	0.0166	0.00592	0.0104	0.01277	0.0108	0.0084	0.0096
	C22IX70-3D3	80	70	2.50E-05	3	9	0.77	0.0166	0.00383	0.0049	0.00910	0.0058	0.0057	0.0047
	C22IX70-3D4	80	70	2.50E-05	4	9	0.77	0.0166	0.00361	0.0096	0.00891	0.0093	0.0054	0.0083
	C22IX70-3D5	80	70	2.50E-05	5	9	0.77	0.0166	0.00266	0.0048	0.00682	0.0050	0.0041	0.0046
	C22IX70-3D6	80	70	2.50E-05	6	9	0.77	0.0166	0.00223	0.0051	0.00582	0.0051	0.0036	0.0050
	C22IX70-3D7	80	70	2.50E-05	7	9	0.77	0.0166	0.00130	0.0010	0.00355	0.0014	0.0021	0.0009
	C22IX70-3D8	80	70	2.50E-05	8	9	0.77	0.0166	0.00188	0.0069	0.00505	0.0070	0.0031	0.0066
	C22IX70-3D9	80	70	2.50E-05	9	9	0.77	0.0166	0.00193	0.0056	0.00500	0.0053	0.0031	0.0053
	C22IX70-3D10	80	70	2.50E-05	10	9	0.77	0.0165	0.00243	0.0083	0.00632	0.0081	0.0042	0.0086
4	C22IX70-4D1	140	70	2.50E-05	1	10	0.50	0.0107	0.01054	0.0927	0.00773	0.0256	0.0058	0.0296
	C22IX70-4D2	140	70	2.50E-05	2	10	0.50	0.0107	0.00429	-0.0087	0.00630	0.0081	0.0044	0.0076
	C22IX70-4D3	140	70	2.50E-05	3	10	0.50	0.0106	0.00311	0.0085	0.00494	0.0059	0.0033	0.0054
	C22IX70-4D4	140	70	2.50E-05	4	10	0.50	0.0106	0.00282	0.0111	0.00427	0.0060	0.0026	0.0051
	C22IX70-4D5	140	70	2.50E-05	5	10	0.50	0.0106	0.00180	0.0034	0.00304	0.0030	0.0019	0.0027
	C22IX70-4D6	140	70	2.50E-05	6	10	0.50	0.0106	0.00135	0.0039	0.00271	0.0039	0.0015	0.0028
	C22IX70-4D7	140	70	2.50E-05	7	10	0.50	0.0106	0.00093	0.0022	0.00214	0.0026	0.0011	0.0018
	C22IX70-4D8	140	70	2.50E-05	8	10	0.50	0.0106	0.00093	0.0041	0.00214	0.0035	0.0011	0.0028
	C22IX70-4D9	140	70	2.50E-05	9	10	0.50	0.0106	0.00073	0.0023	0.00189	0.0027	0.0009	0.0019
	C22IX70-4D10	140	70	2.50E-05	10	10	0.50	0.0106	0.00062	0.0022	0.00160	0.0022	0.0008	0.0016
5	C22IX70-5D1	360	70	2.50E-05	1	11	0.50	0.0107	0.00292	0.0256	0.00522	0.0173	0.0032	0.0165
	C22IX70-5D2	360	70	2.50E-05	2	11	0.50	0.0107	0.00170	0.0021	0.00355	0.0031	0.0020	0.0020
	C22IX70-5D3	360	70	2.50E-05	3	11	0.50	0.0107	0.00116	0.0027	0.00279	0.0033	0.0015	0.0024
	C22IX70-5D4	360	70	2.50E-05	4	11	0.50	0.0107	0.00096	0.0033	0.00231	0.0030	0.0011	0.0018
	C22IX70-5D5	360	70	2.50E-05	5	11	0.50	0.0107	0.00053	0.0004	0.00160	0.0014	0.0007	0.0009
	C22IX70-5D6	360	70	2.50E-05	6	11	0.50	0.0107	0.00048	0.0018	0.00121	0.0013	0.0005	0.0008
	C22IX70-5D7	360	70	2.50E-05	7	11	0.50	0.0107	0.00034	0.0008	0.00109	0.0016	0.0005	0.0010
	C22IX70-5D8	360	70	2.50E-05	8	11	0.50	0.0107	0.00028	0.0009	0.00087	0.0011	0.0003	0.0005
	C22IX70-5D9	360	70	2.50E-05	9	11	0.50	0.0107	0.00025	0.0009	0.00078	0.0011	0.0003	0.0006
	C22IX70-5D10	360	70	2.50E-05	10	11	0.50	0.0107	0.00026	0.0011	0.00080	0.0013	0.0003	0.0007

Table D11. ICP-MS Analysis Results from Dissolution of Glass LAWC22 at 40 °C.

Exp.	Sample ID	Inf [Si] ppm	T °C	Flow Rate, m^3/d	Time, days	pH 23°C	Glass Mass g	SA m^2	[Mo] ppm	Mo Rate $g_{glass}\ m^{-2}\ d^{-1}$	[Cs] ppm	Cs Rate $g_{glass}\ m^{-2}\ d^{-1}$	[Re] ppm	Re Rate $g_{glass}\ m^{-2}\ d^{-1}$
1	C22IX40-1D1	40	40	8.33E-06	3	7	1.65	0.0355	0.00851	0.0075	0.02463	0.0082	0.0237	0.0120
	C22IX40-1D2	40	40	8.33E-06	6	7	1.65	0.0355	0.00286	-0.0012	0.00974	-0.0009	0.0088	-0.0016
	C22IX40-1D3	40	40	8.33E-06	9	7	1.65	0.0355	0.00351	0.0018	0.01592	0.0037	0.0123	0.0040
	C22IX40-1D4	40	40	8.33E-06	12	7	1.65	0.0355	0.00238	0.0005	0.01391	0.0020	0.0092	0.0016
	C22IX40-1D5	40	40	8.33E-06	15	7	1.65	0.0354	0.00289	0.0015	0.01229	0.0018	0.0073	0.0014
	C22IX40-1D6	40	40	8.33E-06	18	7	1.65	0.0354	0.00135	-0.0001	0.01066	0.0015	0.0056	0.0010
	C22IX40-1D7	40	40	8.33E-06	21	7	1.65	0.0354	0.00161	0.0008	0.01439	0.0030	0.0066	0.0019
	C22IX40-1D8	40	40	8.33E-06	24	7	1.65	0.0353	0.00119	0.0003	0.01225	0.0017	0.0051	0.0009
	C22IX40-1D9	40	40	8.33E-06	27	7	1.65	0.0353	0.00103	0.0004	0.01147	0.0018	0.0047	0.0011
	C22IX40-1D10	40	40	8.33E-06	30	7	1.65	0.0352	0.00095	0.0004	0.01075	0.0017	0.0043	0.0010
2	C22IX40-2D1	45	40	8.33E-06	3	8	1.65	0.0355	0.00736	0.0065	0.01543	0.0051	0.0145	0.0074
	C22IX40-2D2	45	40	8.33E-06	6	8	1.65	0.0355	0.00537	0.0015	0.01182	0.0014	0.0107	0.0017
	C22IX40-2D3	45	40	8.33E-06	9	8	1.65	0.0355	0.00394	0.0011	0.00977	0.0013	0.0082	0.0015
	C22IX40-2D4	45	40	8.33E-06	12	8	1.65	0.0355	0.00283	0.0008	0.00789	0.0010	0.0060	0.0010
	C22IX40-2D5	45	40	8.33E-06	15	8	1.65	0.0355	0.00235	0.0008	0.00697	0.0010	0.0050	0.0010
	C22IX40-2D6	45	40	8.33E-06	18	8	1.65	0.0355	0.00184	0.0006	0.00606	0.0009	0.0039	0.0007
	C22IX40-2D7	45	40	8.33E-06	21	8	1.65	0.0355	0.00218	0.0011	0.00746	0.0015	0.0044	0.0013
	C22IX40-2D8	45	40	8.33E-06	24	8	1.65	0.0355	0.00183	0.0006	0.00628	0.0008	0.0036	0.0007
	C22IX40-2D9	45	40	8.33E-06	27	8	1.65	0.0355	0.00150	0.0005	0.00536	0.0007	0.0031	0.0007
	C22IX40-2D10	45	40	8.33E-06	30	8	1.65	0.0355	0.00150	0.0007	0.00514	0.0008	0.0031	0.0008
3	C22IX40-3D1	60	40	8.33E-06	3	9	1.65	0.0355	0.02620	0.0231	0.04927	0.0163	0.0370	0.0188
	C22IX40-3D2	60	40	8.33E-06	6	9	1.65	0.0355	0.00578	-0.0064	0.01000	-0.0049	0.0096	-0.0045
	C22IX40-3D3	60	40	8.33E-06	9	9	1.65	0.0355	0.00433	0.0013	0.00816	0.0010	0.0074	0.0013
	C22IX40-3D4	60	40	8.33E-06	12	9	1.65	0.0355	0.00376	0.0014	0.00725	0.0011	0.0061	0.0012
	C22IX40-3D5	60	40	8.33E-06	15	9	1.65	0.0355	0.00280	0.0008	0.00579	0.0007	0.0047	0.0008
	C22IX40-3D6	60	40	8.33E-06	18	9	1.65	0.0355	0.00234	0.0008	0.00525	0.0008	0.0040	0.0008
	C22IX40-3D7	60	40	8.33E-06	21	9	1.65	0.0355	0.00268	0.0013	0.00599	0.0011	0.0043	0.0012
	C22IX40-3D8	60	40	8.33E-06	24	9	1.65	0.0355	0.00212	0.0007	0.00504	0.0007	0.0034	0.0007
	C22IX40-3D9	60	40	8.33E-06	27	9	1.65	0.0355	0.00181	0.0007	0.00452	0.0007	0.0030	0.0007
	C22IX40-3D10	60	40	8.33E-06	30	9	1.65	0.0355	0.00178	0.0008	0.00450	0.0007	0.0028	0.0007
4	C22IX40-4D1	105	40	8.33E-06	3	10	0.83	0.0178	0.00515	0.0090	0.00776	0.0051	0.0072	0.0073
	C22IX40-4D2	105	40	8.33E-06	6	10	0.83	0.0178	0.00453	0.0034	0.00679	0.0019	0.0064	0.0028
	C22IX40-4D3	105	40	8.33E-06	9	10	0.83	0.0178	0.00386	0.0028	0.00617	0.0018	0.0056	0.0024
	C22IX40-4D4	105	40	8.33E-06	12	10	0.83	0.0178	0.00246	0.0009	0.00419	0.0007	0.0036	0.0008
	C22IX40-4D5	105	40	8.33E-06	15	10	0.83	0.0178	0.00249	0.0022	0.00419	0.0014	0.0034	0.0016
	C22IX40-4D6	105	40	8.33E-06	18	10	0.83	0.0178	0.00199	0.0013	0.00361	0.0010	0.0028	0.0011
	C22IX40-4D7	105	40	8.33E-06	21	10	0.83	0.0178	0.00181	0.0014	0.00388	0.0014	0.0026	0.0012
	C22IX40-4D8	105	40	8.33E-06	24	10	0.83	0.0178	0.00136	0.0008	0.00334	0.0009	0.0021	0.0008
	C22IX40-4D9	105	40	8.33E-06	27	10	0.83	0.0178	0.00000	-0.0012	0.00270	0.0007	0.0016	0.0006
	C22IX40-4D10	105	40	8.33E-06	30	10	0.83	0.0178	0.00098	0.0017	0.00264	0.0009	0.0013	0.0005
5	C22IX40-5D1	270	40	8.33E-06	3	11	0.83	0.01778	0.00522	0.0092	0.00778	0.0052	0.0070	0.0071
	C22IX40-5D2	270	40	8.33E-06	6	11	0.83	0.01778	0.00578	0.0056	0.00880	0.0033	0.0078	0.0044
	C22IX40-5D3	270	40	8.33E-06	9	11	0.83	0.01777	0.00570	0.0049	0.00908	0.0031	0.0079	0.0040
	C22IX40-5D4	270	40	8.33E-06	12	11	0.83	0.01777	0.00485	0.0035	0.00814	0.0024	0.0068	0.0029
	C22IX40-5D5	270	40	8.33E-06	15	11	0.83	0.01777	0.00419	0.0031	0.00723	0.0021	0.0059	0.0026
	C22IX40-5D6	270	40	8.33E-06	18	11	0.83	0.01776	0.00352	0.0025	0.00630	0.0018	0.0049	0.0020
	C22IX40-5D7	270	40	8.33E-06	21	11	0.83	0.01776	0.00404	0.0040	0.00758	0.0029	0.0054	0.0030
	C22IX40-5D8	270	40	8.33E-06	24	11	0.83	0.01776	0.00328	0.0022	0.00643	0.0018	0.0046	0.0019
	C22IX40-5D9	270	40	8.33E-06	27	11	0.83	0.01776	0.00287	0.0022	0.00575	0.0017	0.0041	0.0018
	C22IX40-5D10	270	40	8.33E-06	30	11	0.83	0.01776	0.00278	0.0024	0.00592	0.0020	0.0036	0.0016

Table D12. ICP-MS Analysis Results from Dissolution of Glass LAWC22 at 23 °C.

Exp.	Sample ID	Inf [Si] ppm	T °C	Flow Rate, m^3/d	Time, days	pH 23°C	Glass Mass g	SA m^2	[Mo] ppm	Mo Rate $g_{glass}\ m^{-2}\ d^{-1}$	[Cs] ppm	Cs Rate $g_{glass}\ m^{-2}\ d^{-1}$	[Re] ppm	Re Rate $g_{glass}\ m^{-2}\ d^{-1}$
1	C22IX23-1D1	35	23	8.33E-06	3	7	1.65	0.0355	0.01066	0.0090	0.01238	0.0040	0.0198	0.0100
	C22IX23-1D2	35	23	8.33E-06	6	7	1.65	0.0355	0.00626	0.0006	0.00944	0.0010	0.0138	0.0020
	C22IX23-1D3	35	23	8.33E-06	9	7	1.65	0.0355	0.00383	0.0004	0.00737	0.0008	0.0093	0.0012
	C22IX23-1D4	35	23	8.33E-06	12	7	1.65	0.0355	0.00258	0.0004	0.00601	0.0007	0.0064	0.0009
	C22IX23-1D5	35	23	8.33E-06	15	7	1.65	0.0355	0.00184	0.0003	0.00512	0.0007	0.0049	0.0009
	C22IX23-1D6	35	23	8.33E-06	18	7	1.65	0.0355	0.00129	0.0002	0.00418	0.0005	0.0035	0.0005
	C22IX23-1D7	35	23	8.33E-06	21	7	1.65	0.0354	0.00076	-0.0001	0.00452	0.0008	0.0016	-0.0001
	C22IX23-1D8	35	23	8.33E-06	24	7	1.65	0.0354	0.00065	0.0001	0.00354	0.0004	0.0016	0.0004
	C22IX23-1D9	35	23	8.33E-06	27	7	1.65	0.0354	0.00077	0.0002	0.00386	0.0007	0.0018	0.0005
	C22IX23-1D10	35	23	8.33E-06	30	7	1.65	0.0354	0.00368	0.0027	0.00921	0.0024	0.0059	0.0025
2	C22IX23-2D1	40	23	8.33E-06	3	8	1.65	0.0355	0.00895	0.0075	0.00841	0.0027	0.0143	0.0073
	C22IX23-2D2	40	23	8.33E-06	6	8	1.65	0.0355	0.00508	0.0004	0.00670	0.0008	0.0091	0.0010
	C22IX23-2D3	40	23	8.33E-06	9	8	1.65	0.0355	0.00335	0.0005	0.00541	0.0007	0.0063	0.0009
	C22IX23-2D4	40	23	8.33E-06	12	8	1.65	0.0355	0.00231	0.0004	0.00459	0.0006	0.0045	0.0007
	C22IX23-2D5	40	23	8.33E-06	15	8	1.65	0.0355	0.00171	0.0003	0.00383	0.0005	0.0034	0.0006
	C22IX23-2D6	40	23	8.33E-06	18	8	1.65	0.0355	0.00124	0.0002	0.00301	0.0003	0.0024	0.0003
	C22IX23-2D7	40	23	8.33E-06	21	8	1.65	0.0355	0.00095	0.0001	0.00264	0.0003	0.0018	0.0003
	C22IX23-2D8	40	23	8.33E-06	24	8	1.65	0.0355	0.00078	0.0001	0.00230	0.0003	0.0015	0.0003
	C22IX23-2D9	40	23	8.33E-06	27	8	1.65	0.0355	0.00082	0.0002	0.00267	0.0005	0.0014	0.0004
	C22IX23-2D10	40	23	8.33E-06	30	8	1.65	0.0355	0.00083	0.0002	0.00247	0.0003	0.0015	0.0004
3	C22IX23-3D1	52	23	8.33E-06	3	9	1.65	0.0355	0.00708	0.0059	0.00545	0.0018	0.0110	0.0056
	C22IX23-3D2	52	23	8.33E-06	6	9	1.65	0.0355	0.00436	0.0006	0.00473	0.0006	0.0071	0.0008
	C22IX23-3D3	52	23	8.33E-06	9	9	1.65	0.0355	0.00291	0.0005	0.00403	0.0005	0.0047	0.0006
	C22IX23-3D4	52	23	8.33E-06	12	9	1.65	0.0355	0.00214	0.0004	0.00361	0.0005	0.0035	0.0006
	C22IX23-3D5	52	23	8.33E-06	15	9	1.65	0.0355	0.00548	0.0004	0.00304	0.0004	0.0028	0.0005
	C22IX23-3D6	52	23	8.33E-06	18	9	1.65	0.0355	0.00122	0.0002	0.00246	0.0003	0.0020	0.0003
	C22IX23-3D7	52	23	8.33E-06	21	9	1.65	0.0355	0.00097	0.0002	0.00212	0.0003	0.0015	0.0003
	C22IX23-3D8	52	23	8.33E-06	24	9	1.65	0.0355	0.00080	0.0001	0.00192	0.0003	0.0012	0.0002
	C22IX23-3D9	52	23	8.33E-06	27	9	1.65	0.0355	0.00084	0.0002	0.00208	0.0003	0.0012	0.0003
	C22IX23-3D10	52	23	8.33E-06	30	9	1.65	0.0355	0.00090	0.0003	0.00199	0.0003	0.0014	0.0004
4	C22IX23-4D1	90	23	8.33E-06	3	10	0.83	0.0178	0.00455	0.0074	0.00272	0.0017	0.0059	0.0060
	C22IX23-4D2	90	23	8.33E-06	6	10	0.83	0.0178	0.00282	0.0007	0.00250	0.0007	0.0036	0.0007
	C22IX23-4D3	90	23	8.33E-06	9	10	0.83	0.0178	0.00189	0.0005	0.00225	0.0006	0.0024	0.0006
	C22IX23-4D4	90	23	8.33E-06	12	10	0.83	0.0178	0.00142	0.0005	0.00197	0.0005	0.0018	0.0006
	C22IX23-4D5	90	23	8.33E-06	15	10	0.83	0.0178	0.00119	0.0005	0.00189	0.0005	0.0015	0.0006
	C22IX23-4D6	90	23	8.33E-06	18	10	0.83	0.0178	0.00092	0.0003	0.00162	0.0004	0.0011	0.0004
	C22IX23-4D7	90	23	8.33E-06	21	10	0.83	0.0178	0.00076	0.0002	0.00147	0.0004	0.0009	0.0004
	C22IX23-4D8	90	23	8.33E-06	24	10	0.83	0.0178	0.00063	0.0001	0.00132	0.0003	0.0008	0.0003
	C22IX23-4D9	90	23	8.33E-06	27	10	0.83	0.0178	0.00067	0.0003	0.00144	0.0005	0.0007	0.0004
	C22IX23-4D10	90	23	8.33E-06	30	10	0.83	0.0178	0.00065	0.0003	0.00130	0.0003	0.0008	0.0004
5	C22IX23-5D1	230	23	8.33E-06	3	11	0.83	0.0178	0.00362	0.0059	0.00242	0.0015	0.0054	0.0054
	C22IX23-5D2	230	23	8.33E-06	6	11	0.83	0.0178	0.00246	0.0009	0.00259	0.0008	0.0036	0.0009
	C22IX23-5D3	230	23	8.33E-06	9	11	0.83	0.0178	0.00201	0.0011	0.00270	0.0008	0.0029	0.0011
	C22IX23-5D4	230	23	8.33E-06	12	11	0.83	0.0178	0.00540	0.0014	0.00275	0.0008	0.0027	0.0013
	C22IX23-5D5	230	23	8.33E-06	15	11	0.83	0.0178	0.00188	0.0013	0.00280	0.0008	0.0026	0.0013
	C22IX23-5D6	230	23	8.33E-06	18	11	0.83	0.0178	0.00191	0.0015	0.00298	0.0009	0.0027	0.0014
	C22IX23-5D7	230	23	8.33E-06	21	11	0.83	0.0178	0.00188	0.0014	0.00305	0.0009	0.0026	0.0013
	C22IX23-5D8	230	23	8.33E-06	24	11	0.83	0.0178	0.00180	0.0013	0.00297	0.0008	0.0025	0.0012
	C22IX23-5D9	230	23	8.33E-06	27	11	0.83	0.0178	0.00346	0.0043	0.00600	0.0029	0.0045	0.0033
	C22IX23-5D10	230	23	8.33E-06	30	11	0.83	0.0178	0.00262	0.0013	0.00403	0.0006	0.0035	0.0012

Table D13. ICP-MS Analysis Results from Dissolution of Glass ORLEC28 at 70 °C.

Exp.	**Sample ID**	**Inf [Si]** ppm	**T** °C	**Flow Rate,** m^3/d	**Time,** days	**pH** 23°C	**Glass Mass** g	**SA** m^2	**[Mo]** ppm	**Mo Rate** $g_{glass}\ m^{-2}\ d^{-1}$	**[Cs]** ppm	**Cs Rate** $g_{glass}\ m^{-2}\ d^{-1}$	**[Re]** ppm	**Re Rate** $g_{glass}\ m^{-2}\ d^{-1}$
1	C28IX70-1D1	55	70	2.50E-05	1	7	0.77	0.0165	0.03661	0.2076	0.11873	0.2538	0.1419	0.4574
	C28IX70-1D2	55	70	2.50E-05	2	7	0.77	0.0164	0.01708	-0.0070	0.10805	0.1046	0.0668	-0.0133
	C28IX70-1D3	55	70	2.50E-05	3	7	0.77	0.0163	0.01071	0.0124	0.12574	0.1550	0.0450	0.0378
	C28IX70-1D4	55	70	2.50E-05	4	7	0.77	0.0163	0.00652	0.0067	0.13090	0.1479	0.0289	0.0211
	C28IX70-1D5	55	70	2.50E-05	5	7	0.77	0.0162	0.00438	0.0065	0.12870	0.1383	0.0198	0.0175
	C28IX70-1D6	55	70	2.50E-05	6	7	0.77	0.0161	0.00316	0.0056	0.11194	0.1046	0.0132	0.0108
	C28IX70-1D7	55	70	2.50E-05	7	7	0.77	0.0160	0.00130	-0.0017	0.06138	0.0119	0.0059	-0.0024
	C28IX70-1D8	55	70	2.50E-05	8	7	0.77	0.0159	0.00184	0.0070	0.10885	0.1735	0.0084	0.0182
	C28IX70-1D9	55	70	2.50E-05	9	7	0.77	0.0158	0.00183	0.0054	0.11491	0.1349	0.0076	0.0114
	C28IX70-1D10	55	70	2.50E-05	10	7	0.77	0.0158	0.00154	0.0037	0.09859	0.0921	0.0063	0.0084
2	C28IX70-2D1	60	70	2.50E-05	1	8	0.77	0.0165	0.02100	0.1189	0.06082	0.1299	0.0690	0.2223
	C28IX70-2D2	60	70	2.50E-05	2	8	0.77	0.0165	0.01144	0.0053	0.05749	0.0580	0.0388	0.0138
	C28IX70-2D3	60	70	2.50E-05	3	8	0.77	0.0164	0.00638	0.0037	0.05816	0.0632	0.0216	0.0071
	C28IX70-2D4	60	70	2.50E-05	4	8	0.77	0.0164	0.00405	0.0049	0.05235	0.0502	0.0138	0.0096
	C28IX70-2D5	60	70	2.50E-05	5	8	0.77	0.0163	0.00258	0.0032	0.04648	0.0439	0.0084	0.0051
	C28IX70-2D6	60	70	2.50E-05	6	8	0.77	0.0163	0.00201	0.0041	0.04361	0.0442	0.0061	0.0062
	C28IX70-2D7	60	70	2.50E-05	7	8	0.77	0.0163	0.00175	0.0043	0.04606	0.0527	0.0050	0.0065
	C28IX70-2D8	60	70	2.50E-05	8	8	0.77	0.0162	0.00170	0.0047	0.04653	0.0512	0.0042	0.0055
	C28IX70-2D9	60	70	2.50E-05	9	8	0.77	0.0162	0.00146	0.0035	0.03983	0.0362	0.0034	0.0044
	C28IX70-2D10	60	70	2.50E-05	10	8	0.77	0.0161	0.00000	-0.0043	0.00000	-0.0436	0.0000	-0.0057
3	C28IX70-3D1	80	70	2.50E-05	1	9	0.77	0.0166	0.03143	0.1779	0.03557	0.0759	0.0935	0.3009
	C28IX70-3D2	80	70	2.50E-05	2	9	0.77	0.0165	0.01578	0.0003	0.03057	0.0273	0.0479	0.0039
	C28IX70-3D3	80	70	2.50E-05	3	9	0.77	0.0165	0.00891	0.0058	0.02720	0.0255	0.0278	0.0124
	C28IX70-3D4	80	70	2.50E-05	4	9	0.77	0.0165	0.00499	0.0030	0.02665	0.0280	0.0157	0.0058
	C28IX70-3D5	80	70	2.50E-05	5	9	0.77	0.0164	0.00313	0.0036	0.02434	0.0237	0.0100	0.0070
	C28IX70-3D6	80	70	2.50E-05	6	9	0.77	0.0164	0.00254	0.0055	0.02161	0.0203	0.0063	0.0043
	C28IX70-3D7	80	70	2.50E-05	7	9	0.77	0.0164	0.00179	0.0030	0.02020	0.0203	0.0047	0.0050
	C28IX70-3D8	80	70	2.50E-05	8	9	0.77	0.0164	0.00162	0.0041	0.02068	0.0228	0.0039	0.0050
	C28IX70-3D9	80	70	2.50E-05	9	9	0.77	0.0163	0.00138	0.0032	0.01826	0.0171	0.0031	0.0036
	C28IX70-3D10	80	70	2.50E-05	10	9	0.77	0.0163	0.00152	0.0047	0.01698	0.0170	0.0027	0.0039
4	C28IX70-4D1	140	70	2.50E-05	1	10	0.50	0.0106	0.01729	0.1521	0.01445	0.0479	0.0509	0.2546
	C28IX70-4D2	140	70	2.50E-05	2	10	0.50	0.0106	0.00903	0.0033	0.01169	0.0148	0.0275	0.0105
	C28IX70-4D3	140	70	2.50E-05	3	10	0.50	0.0106	0.00423	-0.0026	0.00904	0.0106	0.0131	-0.0033
	C28IX70-4D4	140	70	2.50E-05	4	10	0.50	0.0106	0.00232	0.0018	0.00881	0.0143	0.0072	0.0034
	C28IX70-4D5	140	70	2.50E-05	5	10	0.50	0.0106	0.00174	0.0051	0.00765	0.0108	0.0042	0.0031
	C28IX70-4D6	140	70	2.50E-05	6	10	0.50	0.0106	0.00114	0.0023	0.00883	0.0167	0.0037	0.0082
	C28IX70-4D7	140	70	2.50E-05	7	10	0.50	0.0106	0.00061	0.0003	0.00655	0.0071	0.0018	-0.0005
	C28IX70-4D8	140	70	2.50E-05	8	10	0.50	0.0106	0.00044	0.0012	0.00619	0.0097	0.0015	0.0030
	C28IX70-4D9	140	70	2.50E-05	9	10	0.50	0.0106	0.00041	0.0016	0.00604	0.0098	0.0010	0.0011
	C28IX70-4D10	140	70	2.50E-05	10	10	0.50	0.0106	0.00033	0.0011	0.00512	0.0070	0.0007	0.0011
5	C28IX70-5D1	360	70	2.50E-05	1	11	0.50	0.0107	0.01196	0.1052	0.01111	0.0368	0.0355	0.1777
	C28IX70-5D2	360	70	2.50E-05	2	11	0.50	0.0106	0.00671	0.0064	0.00941	0.0128	0.0194	0.0083
	C28IX70-5D3	360	70	2.50E-05	3	11	0.50	0.0106	0.00363	0.0024	0.00796	0.0108	0.0105	0.0037
	C28IX70-5D4	360	70	2.50E-05	4	11	0.50	0.0106	0.00437	0.0225	0.00693	0.0098	0.0054	0.0007
	C28IX70-5D5	360	70	2.50E-05	5	11	0.50	0.0106	0.00107	-0.0099	0.00609	0.0087	0.0029	0.0011
	C28IX70-5D6	360	70	2.50E-05	6	11	0.50	0.0106	0.00061	0.0006	0.00497	0.0064	0.0015	0.0003
	C28IX70-5D7	360	70	2.50E-05	7	11	0.50	0.0106	0.00045	0.0012	0.00468	0.0073	0.0009	0.0008
	C28IX70-5D8	360	70	2.50E-05	8	11	0.50	0.0106	0.00034	0.0010	0.00484	0.0083	0.0006	0.0009
	C28IX70-5D9	360	70	2.50E-05	9	11	0.50	0.0106	0.00043	0.0022	0.00559	0.0105	0.0006	0.0013
	C28IX70-5D10	360	70	2.50E-05	10	11	0.50	0.0106	0.00036	0.0012	0.00471	0.0064	0.0005	0.0008

Table D14. ICP-MS Analysis Results from Dissolution of Glass ORLEC28 at 40 °C.

Exp.	**Sample ID**	**Inf [Si]** ppm	**T** °C	**Flow Rate,** m^3/d	**Time,** days	**pH** 23°C	**Glass Mass** g	**SA** m^2	**[Mo]** ppm	**Mo Rate** $g_{glass}\ m^{-2}\ d^{-1}$	**[Cs]** ppm	**Cs Rate** $g_{glass}\ m^{-2}\ d^{-1}$	**[Re]** ppm	**Re Rate** $g_{glass}\ m^{-2}\ d^{-1}$
1	C28IX40-1D1	40	40	8.33E-06	3	7	1.65	0.0355	0.02519	0.0222	0.00958	0.0032	0.0910	0.0455
	C28IX40-1D2	40	40	8.33E-06	6	7	1.65	0.0355	0.02106	0.0075	0.05487	0.0166	0.0925	0.0235
	C28IX40-1D3	40	40	8.33E-06	9	7	1.65	0.0354	0.01133	0.0007	0.05105	0.0078	0.0520	0.0029
	C28IX40-1D4	40	40	8.33E-06	12	7	1.65	0.0354	0.00699	0.0012	0.05381	0.0094	0.0339	0.0040
	C28IX40-1D5	40	40	8.33E-06	15	7	1.65	0.0354	0.00432	0.0007	0.04787	0.0070	0.0226	0.0028
	C28IX40-1D6	40	40	8.33E-06	18	7	1.65	0.0353	0.00299	0.0007	0.04481	0.0070	0.0161	0.0024
	C28IX40-1D7	40	40	8.33E-06	21	7	1.65	0.0353	0.00320	0.0015	0.05793	0.0119	0.0171	0.0046
	C28IX40-1D8	40	40	8.33E-06	24	7	1.65	0.0353	0.00262	0.0009	0.05210	0.0077	0.0140	0.0027
	C28IX40-1D9	40	40	8.33E-06	27	7	1.65	0.0352	0.00232	0.0009	0.05160	0.0085	0.0131	0.0031
	C28IX40-1D10	40	40	8.33E-06	30	7	1.65	0.0352	0.00210	0.0008	0.04849	0.0076	0.0122	0.0028
2	C28IX40-2D1	45	40	8.33E-06	3	8	1.65	0.0355	0.01795	0.0158	0.00981	0.0033	0.0616	0.0308
	C28IX40-2D2	45	40	8.33E-06	6	8	1.65	0.0355	0.02174	0.0112	0.02949	0.0082	0.0877	0.0285
	C28IX40-2D3	45	40	8.33E-06	9	8	1.65	0.0355	0.01077	-0.0001	0.02331	0.0028	0.0427	-0.0006
	C28IX40-2D4	45	40	8.33E-06	12	8	1.65	0.0355	0.00599	0.0005	0.02132	0.0032	0.0245	0.0016
	C28IX40-2D5	45	40	8.33E-06	15	8	1.65	0.0354	0.00350	0.0004	0.01784	0.0024	0.0143	0.0010
	C28IX40-2D6	45	40	8.33E-06	18	8	1.65	0.0354	0.00253	0.0007	0.01795	0.0030	0.0102	0.0015
	C28IX40-2D7	45	40	8.33E-06	21	8	1.65	0.0354	0.00237	0.0010	0.02074	0.0039	0.0088	0.0019
	C28IX40-2D8	45	40	8.33E-06	24	8	1.65	0.0354	0.00197	0.0007	0.01942	0.0030	0.0073	0.0014
	C28IX40-2D9	45	40	8.33E-06	27	8	1.65	0.0354	0.00173	0.0007	0.01847	0.0029	0.0061	0.0012
	C28IX40-2D10	45	40	8.33E-06	30	8	1.65	0.0354	0.00151	0.0006	0.01650	0.0024	0.0051	0.0010
3	C28IX40-3D1	60	40	8.33E-06	3	9	1.65	0.0355	0.04931	0.0434	0.02360	0.0078	0.1892	0.0947
	C28IX40-3D2	60	40	8.33E-06	6	9	1.65	0.0355	0.02502	0.0003	0.01710	0.0018	0.0996	0.0025
	C28IX40-3D3	60	40	8.33E-06	9	9	1.65	0.0355	0.01347	0.0008	0.01344	0.0016	0.0507	0.0004
	C28IX40-3D4	60	40	8.33E-06	12	9	1.65	0.0355	0.00707	0.0003	0.01102	0.0014	0.0264	0.0005
	C28IX40-3D5	60	40	8.33E-06	15	9	1.65	0.0355	0.00397	0.0004	0.00915	0.0012	0.0145	0.0007
	C28IX40-3D6	60	40	8.33E-06	18	9	1.65	0.0355	0.00240	0.0004	0.00773	0.0010	0.0086	0.0006
	C28IX40-3D7	60	40	8.33E-06	21	9	1.65	0.0355	0.00213	0.0008	0.00912	0.0017	0.0070	0.0014
	C28IX40-3D8	60	40	8.33E-06	24	9	1.65	0.0354	0.00166	0.0005	0.00845	0.0013	0.0051	0.0008
	C28IX40-3D9	60	40	8.33E-06	27	9	1.65	0.0354	0.00139	0.0005	0.00765	0.0011	0.0040	0.0007
	C28IX40-3D10	60	40	8.33E-06	30	9	1.65	0.0354	0.00133	0.0006	0.00730	0.0012	0.0035	0.0008
4	C28IX40-4D1	105	40	8.33E-06	3	10	0.83	0.0178	0.03685	0.0648	0.03367	0.0223	0.1465	0.1465
	C28IX40-4D2	105	40	8.33E-06	6	10	0.83	0.0178	0.00912	-0.0164	0.00688	-0.0066	0.0310	-0.0422
	C28IX40-4D3	105	40	8.33E-06	9	10	0.83	0.0178	0.00480	0.0004	0.00508	0.0011	0.0164	0.0009
	C28IX40-4D4	105	40	8.33E-06	12	10	0.83	0.0178	0.00325	0.0015	0.00444	0.0013	0.0110	0.0028
	C28IX40-4D5	105	40	8.33E-06	15	10	0.83	0.0177	0.00157	-0.0001	0.00340	0.0008	0.0053	-0.0003
	C28IX40-4D6	105	40	8.33E-06	18	10	0.83	0.0177	0.00099	0.0004	0.00295	0.0008	0.0031	0.0005
	C28IX40-4D7	105	40	8.33E-06	21	10	0.83	0.0177	0.00090	0.0007	0.00339	0.0013	0.0026	0.0011
	C28IX40-4D8	105	40	8.33E-06	24	10	0.83	0.0177	0.00062	0.0003	0.00290	0.0008	0.0018	0.0005
	C28IX40-4D9	105	40	8.33E-06	27	10	0.83	0.0177	0.00052	0.0004	0.00268	0.0008	0.0014	0.0005
	C28IX40-4D10	105	40	8.33E-06	30	10	0.83	0.0177	0.00045	0.0003	0.00250	0.0008	0.0012	0.0005
5	C28IX40-5D1	270	40	8.33E-06	3	11	0.83	0.0178	0.02953	0.0520	0.04453	0.0295	0.1226	0.1227
	C28IX40-5D2	270	40	8.33E-06	6	11	0.83	0.0177	0.01331	-0.0026	0.00670	-0.0103	0.0454	-0.0160
	C28IX40-5D3	270	40	8.33E-06	9	11	0.83	0.0177	0.00699	0.0006	0.00480	0.0010	0.0231	0.0004
	C28IX40-5D4	270	40	8.33E-06	12	11	0.83	0.0177	0.00361	0.0002	0.00367	0.0008	0.0115	0.0000
	C28IX40-5D5	270	40	8.33E-06	15	11	0.83	0.0177	0.00196	0.0003	0.00281	0.0006	0.0060	0.0002
	C28IX40-5D6	270	40	8.33E-06	18	11	0.83	0.0177	0.00119	0.0004	0.00242	0.0007	0.0033	0.0003
	C28IX40-5D7	270	40	8.33E-06	21	11	0.83	0.0177	0.00141	0.0014	0.00308	0.0012	0.0024	0.0008
	C28IX40-5D8	270	40	8.33E-06	24	11	0.83	0.0177	0.00098	0.0005	0.00259	0.0007	0.0017	0.0004
	C28IX40-5D9	270	40	8.33E-06	27	11	0.83	0.0177	0.00082	0.0006	0.00233	0.0007	0.0012	0.0003
	C28IX40-5D10	270	40	8.33E-06	30	11	0.83	0.0177	0.00063	0.0004	0.00200	0.0006	0.0009	0.0003

Table D15. ICP-MS Analysis Results from Dissolution of Glass ORLEC28 at 23 °C.

Exp.	Sample ID	**Inf [Si]** ppm	**T** °C	**Flow Rate,** m^3/d	**Time,** days	**pH** 23°C	**Glass Mass** g	**SA** m^2	**[Mo]** ppm	**Mo Rate** $g_{glass}\ m^{-2}\ d^{-1}$	**[Cs]** ppm	**Cs Rate** $g_{glass}\ m^{-2}\ d^{-1}$	**[Re]** ppm	**Re Rate** $g_{glass}\ m^{-2}\ d^{-1}$
1	C28IX23-1D1	35	23	8.33E-06	3	7	1.65	0.0355	0.07996	0.0700	0.03642	0.0120	0.3169	0.1586
	C28IX23-1D2	35	23	8.33E-06	6	7	1.65	0.0355	0.04013	0.0000	0.02548	0.0024	0.1633	0.0024
	C28IX23-1D3	35	23	8.33E-06	9	7	1.65	0.0355	0.02113	0.0008	0.02055	0.0026	0.0838	0.0011
	C28IX23-1D4	35	23	8.33E-06	12	7	1.65	0.0355	0.01156	0.0007	0.01732	0.0023	0.0455	0.0018
	C28IX23-1D5	35	23	8.33E-06	15	7	1.65	0.0355	0.01193	0.0052	0.02655	0.0059	0.0331	0.0052
	C28IX23-1D6	35	23	8.33E-06	18	7	1.65	0.0355	0.00352	-0.0023	0.01069	-0.0009	0.0140	-0.0013
	C28IX23-1D7	35	23	8.33E-06	21	7	1.65	0.0355	0.00223	0.0002	0.00929	0.0013	0.0088	0.0009
	C28IX23-1D8	35	23	8.33E-06	24	7	1.65	0.0354	0.00147	0.0001	0.00774	0.0010	0.0055	0.0006
	C28IX23-1D9	35	23	8.33E-06	27	7	1.65	0.0354	0.00132	0.0003	0.00854	0.0015	0.0046	0.0009
	C28IX23-1D10	35	23	8.33E-06	30	7	1.65	0.0354	0.00130	0.0004	0.00931	0.0016	0.0047	0.0012
2	C28IX23-2D1	40	23	8.33E-06	3	8	1.65	0.0355	0.09228	0.0809	0.02936	0.0097	0.3714	0.1858
	C28IX23-2D2	40	23	8.33E-06	6	8	1.65	0.0355	0.04446	-0.0016	0.01791	0.0010	0.1789	-0.0034
	C28IX23-2D3	40	23	8.33E-06	9	8	1.65	0.0355	0.02287	0.0004	0.01290	0.0013	0.0904	0.0005
	C28IX23-2D4	40	23	8.33E-06	12	8	1.65	0.0355	0.01213	0.0004	0.00997	0.0011	0.0456	0.0002
	C28IX23-2D5	40	23	8.33E-06	15	8	1.65	0.0355	0.00652	0.0002	0.00770	0.0009	0.0240	0.0006
	C28IX23-2D6	40	23	8.33E-06	18	8	1.65	0.0355	0.01202	0.0075	0.02380	0.0066	0.0264	0.0072
	C28IX23-2D7	40	23	8.33E-06	21	8	1.65	0.0355	0.00204	-0.0037	0.00491	-0.0024	0.0069	-0.0032
	C28IX23-2D8	40	23	8.33E-06	24	8	1.65	0.0355	0.00122	0.0000	0.00398	0.0005	0.0038	0.0002
	C28IX23-2D9	40	23	8.33E-06	27	8	1.65	0.0355	0.00096	0.0001	0.00431	0.0007	0.0026	0.0004
	C28IX23-2D10	40	23	8.33E-06	30	8	1.65	0.0355	0.00082	0.0001	0.00449	0.0007	0.0023	0.0005
3	C28IX23-3D1	52	23	8.33E-06	3	9	1.65	0.0355	0.10737	0.0942	0.02418	0.0080	0.4292	0.2148
	C28IX23-3D2	52	23	8.33E-06	6	9	1.65	0.0355	0.05557	0.0015	0.01470	0.0008	0.2273	0.0063
	C28IX23-3D3	52	23	8.33E-06	9	9	1.65	0.0355	0.02768	-0.0002	0.00988	0.0008	0.1123	-0.0007
	C28IX23-3D4	52	23	8.33E-06	12	9	1.65	0.0355	0.01391	-0.0001	0.00697	0.0006	0.0519	-0.0021
	C28IX23-3D5	52	23	8.33E-06	15	9	1.65	0.0355	0.00724	0.0001	0.00512	0.0005	0.0263	0.0002
	C28IX23-3D6	52	23	8.33E-06	18	9	1.65	0.0355	0.00385	0.0000	0.00393	0.0004	0.0134	0.0001
	C28IX23-3D7	52	23	8.33E-06	21	9	1.65	0.0355	0.00222	0.0001	0.00352	0.0005	0.0073	0.0003
	C28IX23-3D8	52	23	8.33E-06	24	9	1.65	0.0355	0.00127	0.0000	0.00281	0.0003	0.0039	0.0002
	C28IX23-3D9	52	23	8.33E-06	27	9	1.65	0.0355	0.00088	0.0001	0.00279	0.0004	0.0023	0.0002
	C28IX23-3D10	52	23	8.33E-06	30	9	1.65	0.0355	0.00071	0.0001	0.00290	0.0005	0.0018	0.0003
4	C28IX23-4D1	90	23	8.33E-06	3	10	0.83	0.0178	0.06598	0.1154	0.01326	0.0087	0.2620	0.2619
	C28IX23-4D2	90	23	8.33E-06	6	10	0.83	0.0178	0.03324	0.0001	0.00773	0.0007	0.1334	0.0024
	C28IX23-4D3	90	23	8.33E-06	9	10	0.83	0.0178	0.01658	-0.0004	0.00510	0.0008	0.0610	-0.0057
	C28IX23-4D4	90	23	8.33E-06	12	10	0.83	0.0178	0.00847	0.0000	0.00365	0.0007	0.0306	0.0001
	C28IX23-4D5	90	23	8.33E-06	15	10	0.83	0.0178	0.00695	0.0045	0.00897	0.0047	0.0191	0.0037
	C28IX23-4D6	90	23	8.33E-06	18	10	0.83	0.0178	0.00236	-0.0023	0.00208	-0.0017	0.0079	-0.0016
	C28IX23-4D7	90	23	8.33E-06	21	10	0.83	0.0178	0.00132	-0.0001	0.00261	0.0010	0.0042	0.0002
	C28IX23-4D8	90	23	8.33E-06	24	10	0.83	0.0178	0.00078	-0.0001	0.00194	0.0004	0.0021	0.0000
	C28IX23-4D9	90	23	8.33E-06	27	10	0.83	0.0178	0.00061	0.0001	0.00191	0.0006	0.0013	0.0002
	C28IX23-4D10	90	23	8.33E-06	30	10	0.83	0.0178	0.00043	-0.0001	0.00170	0.0004	0.0008	0.0002
5	C28IX23-5D1	230	23	8.33E-06	3	11	0.83	0.0178	0.05669	0.0992	0.02528	0.0166	0.2107	0.2106
	C28IX23-5D2	230	23	8.33E-06	6	11	0.83	0.0178	0.02499	-0.0061	0.00642	-0.0042	0.0986	-0.0068
	C28IX23-5D3	230	23	8.33E-06	9	11	0.83	0.0178	0.01260	-0.0001	0.00458	0.0008	0.0456	-0.0037
	C28IX23-5D4	230	23	8.33E-06	12	11	0.83	0.0178	0.00640	-0.0001	0.00333	0.0006	0.0224	-0.0004
	C28IX23-5D5	230	23	8.33E-06	15	11	0.83	0.0178	0.00346	0.0002	0.00265	0.0005	0.0118	0.0006
	C28IX23-5D6	230	23	8.33E-06	18	11	0.83	0.0178	0.00189	0.0000	0.00224	0.0005	0.0060	0.0000
	C28IX23-5D7	230	23	8.33E-06	21	11	0.83	0.0178	0.00117	0.0001	0.00216	0.0006	0.0033	0.0003
	C28IX23-5D8	230	23	8.33E-06	24	11	0.83	0.0178	0.00065	-0.0001	0.00169	0.0003	0.0016	-0.0001
	C28IX23-5D9	230	23	8.33E-06	27	11	0.83	0.0178	0.00056	0.0002	0.00187	0.0006	0.0011	0.0003
	C28IX23-5D10	230	23	8.33E-06	30	11	0.83	0.0178	0.00043	0.0000	0.00176	0.0004	0.0007	0.0002

Table D16. ICP-MS Analysis Results from Dissolution of Glass IDF1B2 at 70 °C.

Exp.	Sample ID	Inf [Si] ppm	T °C	Flow Rate, m^3/d	Time, days	pH 23°C	Glass Mass g	SA m^2	[Mo] ppm	Mo Rate $g_{\text{-glass}}\ m^{-2}\ d^{-1}$	[Cs] ppm	Cs Rate $g_{\text{-glass}}\ m^{-2}\ d^{-1}$	[Re] ppm	Re Rate $g_{\text{-glass}}\ m^{-2}\ d^{-1}$
1	B2IX70-1D1	55	70	2.50E-05	1	7	0.77	0.0165	0.02429	0.1375	0.06058	0.1294	0.0694	0.2273
	B2IX70-1D2	55	70	2.50E-05	2	7	0.77	0.0165	0.01748	0.0303	0.05870	0.0609	0.0442	0.0313
	B2IX70-1D3	55	70	2.50E-05	3	7	0.77	0.0164	0.01469	0.0339	0.05722	0.0599	0.0334	0.0373
	B2IX70-1D4	55	70	2.50E-05	4	7	0.77	0.0164	0.01237	0.0287	0.05501	0.0569	0.0266	0.0327
	B2IX70-1D5	55	70	2.50E-05	5	7	0.77	0.0163	0.01161	0.0311	0.05886	0.0678	0.0230	0.0323
	B2IX70-1D6	55	70	2.50E-05	6	7	0.77	0.0163	0.00862	0.0162	0.04727	0.0387	0.0166	0.0170
	B2IX70-1D7	55	70	2.50E-05	7	7	0.77	0.0162	0.00826	0.0228	0.05025	0.0579	0.0150	0.0223
	B2IX70-1D8	55	70	2.50E-05	8	7	0.77	0.0162	0.00809	0.0229	0.05257	0.0599	0.0143	0.0227
	B2IX70-1D9	55	70	2.50E-05	9	7	0.77	0.0162	0.00784	0.0220	0.05102	0.0541	0.0137	0.0220
	B2IX70-1D10	55	70	2.50E-05	10	7	0.77	0.0161	0.00687	0.0171	0.04397	0.0405	0.0122	0.0181
2	B2IX70-2D1	60	70	2.50E-05	1	8	0.77	0.0166	0.02156	0.1220	0.03214	0.0686	0.0501	0.1640
	B2IX70-2D2	60	70	2.50E-05	2	8	0.77	0.0165	0.01285	0.0117	0.02947	0.0286	0.0302	0.0169
	B2IX70-2D3	60	70	2.50E-05	3	8	0.77	0.0165	0.00987	0.0196	0.02560	0.0233	0.0212	0.0200
	B2IX70-2D4	60	70	2.50E-05	4	8	0.77	0.0165	0.00798	0.0173	0.02301	0.0219	0.0165	0.0195
	B2IX70-2D5	60	70	2.50E-05	5	8	0.77	0.0164	0.00665	0.0151	0.01991	0.0181	0.0127	0.0145
	B2IX70-2D6	60	70	2.50E-05	6	8	0.77	0.0164	0.00627	0.0168	0.01826	0.0179	0.0106	0.0140
	B2IX70-2D7	60	70	2.50E-05	7	8	0.77	0.0164	0.00737	0.0242	0.02238	0.0286	0.0132	0.0263
	B2IX70-2D8	60	70	2.50E-05	8	8	0.77	0.0164	0.00602	0.0133	0.01683	0.0122	0.0092	0.0087
	B2IX70-2D9	60	70	2.50E-05	9	8	0.77	0.0164	0.00659	0.0205	0.01720	0.0190	0.0097	0.0169
	B2IX70-2D10	60	70	2.50E-05	10	8	0.77	0.0163	0.00634	0.0175	0.01617	0.0164	0.0094	0.0149
3	B2IX70-3D1	80	70	2.50E-05	1	9	0.77	0.0166	0.01852	0.1048	0.02070	0.0441	0.0396	0.1086
	B2IX70-3D2	80	70	2.50E-05	2	9	0.77	0.0166	0.00961	0.0020	0.01507	0.0101	0.0216	0.0050
	B2IX70-3D3	80	70	2.50E-05	3	9	0.77	0.0165	0.00636	0.0088	0.01304	0.0118	0.0144	0.0099
	B2IX70-3D4	80	70	2.50E-05	4	9	0.77	0.0165	0.00470	0.0086	0.01045	0.0084	0.0100	0.0077
	B2IX70-3D5	80	70	2.50E-05	5	9	0.77	0.0165	0.00373	0.0078	0.00970	0.0096	0.0079	0.0081
	B2IX70-3D6	80	70	2.50E-05	6	9	0.77	0.0165	0.00292	0.0060	0.00786	0.0064	0.0059	0.0053
	B2IX70-3D7	80	70	2.50E-05	7	9	0.77	0.0165	0.00288	0.0081	0.00744	0.0075	0.0051	0.0058
	B2IX70-3D8	80	70	2.50E-05	8	9	0.77	0.0165	0.00310	0.0094	0.00765	0.0084	0.0053	0.0076
	B2IX70-3D9	80	70	2.50E-05	9	9	0.77	0.0165	0.00367	0.0120	0.00760	0.0081	0.0057	0.0084
	B2IX70-3D10	80	70	2.50E-05	10	9	0.77	0.0165	0.00119	0.0000	0.00684	0.0065	0.0054	0.0069
4	B2IX70-4D1	140	70	2.50E-05	1	10	0.50	0.0107	0.01565	0.1377	0.00889	0.0295	0.0279	0.1193
	B2IX70-4D2	140	70	2.50E-05	2	10	0.50	0.0106	0.00779	0.0000	0.00652	0.0069	0.0150	0.0042
	B2IX70-4D3	140	70	2.50E-05	3	10	0.50	0.0106	0.00434	0.0039	0.00528	0.0067	0.0088	0.0057
	B2IX70-4D4	140	70	2.50E-05	4	10	0.50	0.0106	0.00283	0.0058	0.00414	0.0050	0.0051	0.0028
	B2IX70-4D5	140	70	2.50E-05	5	10	0.50	0.0106	0.00163	0.0019	0.00357	0.0050	0.0033	0.0032
	B2IX70-4D6	140	70	2.50E-05	6	10	0.50	0.0106	0.00097	0.0013	0.00286	0.0036	0.0020	0.0017
	B2IX70-4D7	140	70	2.50E-05	7	10	0.50	0.0106	0.00074	0.0022	0.00262	0.0039	0.0015	0.0020
	B2IX70-4D8	140	70	2.50E-05	8	10	0.50	0.0106	0.00071	0.0030	0.00278	0.0049	0.0014	0.0028
	B2IX70-4D9	140	70	2.50E-05	9	10	0.50	0.0106	0.00057	0.0019	0.00241	0.0034	0.0011	0.0017
	B2IX70-4D10	140	70	2.50E-05	10	10	0.50	0.0106	0.00050	0.0019	0.00225	0.0035	0.0010	0.0017
5	B2IX70-5D1	360	70	2.50E-05	1	11	0.50	0.0107	0.00864	0.0759	0.00822	0.0272	0.0158	0.0674
	B2IX70-5D2	360	70	2.50E-05	2	11	0.50	0.0106	0.00420	0.0000	0.00549	0.0046	0.0076	0.0000
	B2IX70-5D3	360	70	2.50E-05	3	11	0.50	0.0106	0.00227	0.0014	0.00412	0.0045	0.0043	0.0020
	B2IX70-5D4	360	70	2.50E-05	4	11	0.50	0.0106	0.00137	0.0020	0.00387	0.0060	0.0027	0.0023
	B2IX70-5D5	360	70	2.50E-05	5	11	0.50	0.0106	0.00082	0.0011	0.00312	0.0039	0.0016	0.0009
	B2IX70-5D6	360	70	2.50E-05	6	11	0.50	0.0106	0.00050	0.0007	0.00256	0.0033	0.0009	0.0006
	B2IX70-5D7	360	70	2.50E-05	7	11	0.50	0.0106	0.00041	0.0014	0.00251	0.0041	0.0007	0.0010
	B2IX70-5D8	360	70	2.50E-05	8	11	0.50	0.0106	0.00032	0.0010	0.00231	0.0035	0.0005	0.0007
	B2IX70-5D9	360	70	2.50E-05	9	11	0.50	0.0106	0.00030	0.0012	0.00216	0.0033	0.0004	0.0006
	B2IX70-5D10	360	70	2.50E-05	10	11	0.50	0.0106	0.00023	0.0007	0.00190	0.0027	0.0003	0.0005

Table D17. ICP-MS Analysis Results from Dissolution of Glass IDF1B2 at 40 °C.

Exp.	Sample ID	Inf [Si] ppm	T °C	Flow Rate, m^3/d	Time, days	pH 23°C	Glass Mass g	SA m^2	[Mo] ppm	Mo Rate $g_{glass}\ m^{-2}\ d^{-1}$	[Cs] ppm	Cs Rate $g_{glass}\ m^{-2}\ d^{-1}$	[Re] ppm	Re Rate $g_{glass}\ m^{-2}\ d^{-1}$
1	B2IX40-1D1	40	40	8.33E-06	3	7	1.65	0.0355	0.03092	0.0272	0.03123	0.0104	0.0804	0.0343
	B2IX40-1D2	40	40	8.33E-06	6	7	1.65	0.0355	0.01842	0.0026	0.02423	0.0029	0.0499	0.0041
	B2IX40-1D3	40	40	8.33E-06	9	7	1.65	0.0355	0.01158	0.0021	0.01967	0.0025	0.0316	0.0028
	B2IX40-1D4	40	40	8.33E-06	12	7	1.65	0.0354	0.01015	0.0038	0.02008	0.0034	0.0243	0.0036
	B2IX40-1D5	40	40	8.33E-06	15	7	1.65	0.0354	0.00771	0.0023	0.01627	0.0021	0.0177	0.0024
	B2IX40-1D6	40	40	8.33E-06	18	7	1.65	0.0354	0.00782	0.0035	0.01600	0.0026	0.0153	0.0028
	B2IX40-1D7	40	40	8.33E-06	21	7	1.65	0.0354	0.01047	0.0058	0.01996	0.0040	0.0182	0.0045
	B2IX40-1D8	40	40	8.33E-06	24	7	1.65	0.0354	0.00952	0.0038	0.01820	0.0027	0.0164	0.0031
	B2IX40-1D9	40	40	8.33E-06	27	7	1.65	0.0354	0.00802	0.0029	0.01609	0.0023	0.0142	0.0026
	B2IX40-1D10	40	40	8.33E-06	30	7	1.65	0.0353	0.00770	0.0033	0.01563	0.0025	0.0134	0.0027
2	B2IX40-2D1	45	40	8.33E-06	3	8	1.65	0.0355	0.02903	0.0255	0.02543	0.0084	0.0653	0.0279
	B2IX40-2D2	45	40	8.33E-06	6	8	1.65	0.0355	0.01429	-0.0002	0.01506	0.0008	0.0357	0.0013
	B2IX40-2D3	45	40	8.33E-06	9	8	1.65	0.0355	0.00807	0.0008	0.01167	0.0014	0.0214	0.0015
	B2IX40-2D4	45	40	8.33E-06	12	8	1.65	0.0355	0.00534	0.0011	0.01018	0.0014	0.0140	0.0014
	B2IX40-2D5	45	40	8.33E-06	15	8	1.65	0.0355	0.00364	0.0009	0.00784	0.0009	0.0092	0.0009
	B2IX40-2D6	45	40	8.33E-06	18	8	1.65	0.0355	0.00331	0.0013	0.00755	0.0012	0.0077	0.0013
	B2IX40-2D7	45	40	8.33E-06	21	8	1.65	0.0354	0.00402	0.0021	0.00884	0.0017	0.0082	0.0019
	B2IX40-2D8	45	40	8.33E-06	24	8	1.65	0.0354	0.00380	0.0016	0.00797	0.0012	0.0072	0.0013
	B2IX40-2D9	45	40	8.33E-06	27	8	1.65	0.0354	0.00363	0.0015	0.00725	0.0011	0.0065	0.0012
	B2IX40-2D10	45	40	8.33E-06	30	8	1.65	0.0354	0.00369	0.0017	0.00698	0.0011	0.0065	0.0014
3	B2IX40-3D1	60	40	8.33E-06	3	9	1.65	0.0355	0.02692	0.0237	0.01444	0.0048	0.0577	0.0246
	B2IX40-3D2	60	40	8.33E-06	6	9	1.65	0.0355	0.01486	0.0012	0.01111	0.0013	0.0334	0.0019
	B2IX40-3D3	60	40	8.33E-06	9	9	1.65	0.0355	0.00794	0.0004	0.00801	0.0008	0.0187	0.0008
	B2IX40-3D4	60	40	8.33E-06	12	9	1.65	0.0355	0.00481	0.0007	0.00672	0.0009	0.0119	0.0011
	B2IX40-3D5	60	40	8.33E-06	15	9	1.65	0.0355	0.00297	0.0005	0.00514	0.0006	0.0075	0.0007
	B2IX40-3D6	60	40	8.33E-06	18	9	1.65	0.0355	0.00221	0.0006	0.00471	0.0007	0.0055	0.0008
	B2IX40-3D7	60	40	8.33E-06	21	9	1.65	0.0355	0.00218	0.0009	0.00517	0.0009	0.0052	0.0010
	B2IX40-3D8	60	40	8.33E-06	24	9	1.65	0.0355	0.00190	0.0007	0.00464	0.0007	0.0043	0.0007
	B2IX40-3D9	60	40	8.33E-06	27	9	1.65	0.0355	0.00181	0.0008	0.00437	0.0007	0.0038	0.0007
	B2IX40-3D10	60	40	8.33E-06	30	9	1.65	0.0355	0.00172	0.0007	0.00418	0.0007	0.0036	0.0007
4	B2IX40-4D1	105	40	8.33E-06	3	10	0.83	0.0178	0.06893	0.1213	0.12400	0.0822	0.1290	0.1101
	B2IX40-4D2	105	40	8.33E-06	6	10	0.83	0.0177	0.00837	-0.0460	0.00454	-0.0382	0.0169	-0.0407
	B2IX40-4D3	105	40	8.33E-06	9	10	0.83	0.0177	0.00477	0.0010	0.00350	0.0008	0.0099	0.0012
	B2IX40-4D4	105	40	8.33E-06	12	10	0.83	0.0177	0.00263	0.0004	0.00277	0.0007	0.0056	0.0006
	B2IX40-4D5	105	40	8.33E-06	15	10	0.83	0.0177	0.00153	0.0004	0.00199	0.0004	0.0032	0.0003
	B2IX40-4D6	105	40	8.33E-06	18	10	0.83	0.0177	0.00105	0.0005	0.00180	0.0005	0.0022	0.0005
	B2IX40-4D7	105	40	8.33E-06	21	10	0.83	0.0177	0.00107	0.0010	0.00204	0.0008	0.0020	0.0008
	B2IX40-4D8	105	40	8.33E-06	24	10	0.83	0.0177	0.00077	0.0004	0.00179	0.0005	0.0015	0.0004
	B2IX40-4D9	105	40	8.33E-06	27	10	0.83	0.0177	0.00069	0.0005	0.00163	0.0005	0.0012	0.0004
	B2IX40-4D10	105	40	8.33E-06	30	10	0.83	0.0177	0.00066	0.0006	0.00163	0.0005	0.0011	0.0004
5	B2IX40-5D1	270	40	8.33E-06	3	11	0.83	0.0178	0.01408	0.0247	0.00566	0.0037	0.0278	0.0237
	B2IX40-5D2	270	40	8.33E-06	6	11	0.83	0.0178	0.00737	0.0006	0.00405	0.0008	0.0149	0.0008
	B2IX40-5D3	270	40	8.33E-06	9	11	0.83	0.0178	0.00405	0.0006	0.00318	0.0008	0.0082	0.0006
	B2IX40-5D4	270	40	8.33E-06	12	11	0.83	0.0178	0.00213	0.0002	0.00237	0.0005	0.0042	0.0001
	B2IX40-5D5	270	40	8.33E-06	15	11	0.83	0.0178	0.00141	0.0006	0.00205	0.0006	0.0027	0.0005
	B2IX40-5D6	270	40	8.33E-06	18	11	0.83	0.0178	0.00079	0.0001	0.00141	0.0003	0.0014	0.0000
	B2IX40-5D7	270	40	8.33E-06	21	11	0.83	0.0178	0.00108	0.0012	0.00226	0.0010	0.0016	0.0008
	B2IX40-5D8	270	40	8.33E-06	24	11	0.83	0.0178	0.00078	0.0004	0.00189	0.0005	0.0011	0.0003
	B2IX40-5D9	270	40	8.33E-06	27	11	0.83	0.0178	0.00067	0.0005	0.00177	0.0005	0.0010	0.0003
	B2IX40-5D10	270	40	8.33E-06	30	11	0.83	0.0178	0.00063	0.0005	0.00168	0.0005	0.0009	0.0003

Table D18. ICP-MS Analysis Results from Dissolution of Glass IDF1B2 at 23 °C.

Exp.	Sample ID	Inf [Si] ppm	T °C	Flow Rate, m^3/d	Time, days	pH 23°C	Glass Mass g	SA m^2	[Mo] ppm	Mo Rate $g_{glass}\ m^{-2}\ d^{-1}$	[Cs] ppm	Cs Rate $g_{glass}\ m^{-2}\ d^{-1}$	[Re] ppm	Re Rate $g_{glass}\ m^{-2}\ d^{-1}$
1	B2IX23-1D1	35	23	8.33E-06	3	7	1.65	0.0355	0.04790	0.0418	0.01974	0.0065	0.1139	0.0486
	B2IX23-1D2	35	23	8.33E-06	6	7	1.65	0.0355	0.02508	0.0008	0.01336	0.0011	0.0597	0.0012
	B2IX23-1D3	35	23	8.33E-06	9	7	1.65	0.0355	0.01309	0.0003	0.01029	0.0012	0.0330	0.0013
	B2IX23-1D4	35	23	8.33E-06	12	7	1.65	0.0355	0.00712	0.0003	0.00792	0.0009	0.0184	0.0008
	B2IX23-1D5	35	23	8.33E-06	15	7	1.65	0.0355	0.00438	0.0005	0.00637	0.0008	0.0117	0.0011
	B2IX23-1D6	35	23	8.33E-06	18	7	1.65	0.0355	0.00308	0.0006	0.00544	0.0007	0.0079	0.0009
	B2IX23-1D7	35	23	8.33E-06	21	7	1.65	0.0355	0.00224	0.0004	0.00438	0.0005	0.0053	0.0006
	B2IX23-1D8	35	23	8.33E-06	24	7	1.65	0.0355	0.00197	0.0006	0.00401	0.0006	0.0042	0.0006
	B2IX23-1D9	35	23	8.33E-06	27	7	1.65	0.0355	0.00388	0.0024	0.00780	0.0019	0.0065	0.0019
	B2IX23-1D10	35	23	8.33E-06	30	7	1.65	0.0355	0.00606	0.0035	0.01143	0.0025	0.0096	0.0027
2	B2IX23-2D1	40	23	8.33E-06	3	8	1.65	0.0355	0.05065	0.0442	0.01465	0.0048	0.1192	0.0509
	B2IX23-2D2	40	23	8.33E-06	6	8	1.65	0.0355	0.02493	-0.0005	0.00950	0.0007	0.0561	-0.0015
	B2IX23-2D3	40	23	8.33E-06	9	8	1.65	0.0355	0.01299	0.0003	0.00702	0.0007	0.0301	0.0009
	B2IX23-2D4	40	23	8.33E-06	12	8	1.65	0.0355	0.00697	0.0002	0.00570	0.0007	0.0162	0.0005
	B2IX23-2D5	40	23	8.33E-06	15	8	1.65	0.0355	0.00380	0.0001	0.00439	0.0005	0.0092	0.0005
	B2IX23-2D6	40	23	8.33E-06	18	8	1.65	0.0355	0.00224	0.0001	0.00354	0.0004	0.0054	0.0003
	B2IX23-2D7	40	23	8.33E-06	21	8	1.65	0.0355	0.00143	0.0001	0.00291	0.0003	0.0034	0.0003
	B2IX23-2D8	40	23	8.33E-06	24	8	1.65	0.0355	0.00094	0.0000	0.00235	0.0003	0.0021	0.0002
	B2IX23-2D9	40	23	8.33E-06	27	8	1.65	0.0355	0.00138	0.0006	0.00386	0.0009	0.0026	0.0007
	B2IX23-2D10	40	23	8.33E-06	30	8	1.65	0.0355	0.00083	0.0000	0.00279	0.0003	0.0019	0.0002
3	B2IX23-3D1	52	23	8.33E-06	3	9	1.65	0.0355	0.05847	0.0511	0.01156	0.0038	0.1312	0.0560
	B2IX23-3D2	52	23	8.33E-06	6	9	1.65	0.0355	0.02884	-0.0005	0.00711	0.0004	0.0622	-0.0015
	B2IX23-3D3	52	23	8.33E-06	9	9	1.65	0.0355	0.01463	0.0000	0.00514	0.0005	0.0319	0.0003
	B2IX23-3D4	52	23	8.33E-06	12	9	1.65	0.0355	0.00767	0.0002	0.00443	0.0006	0.0167	0.0003
	B2IX23-3D5	52	23	8.33E-06	15	9	1.65	0.0355	0.00426	0.0002	0.00309	0.0003	0.0093	0.0004
	B2IX23-3D6	52	23	8.33E-06	18	9	1.65	0.0355	0.00221	-0.0001	0.00233	0.0002	0.0048	0.0001
	B2IX23-3D7	52	23	8.33E-06	21	9	1.65	0.0355	0.00142	0.0001	0.00214	0.0003	0.0029	0.0002
	B2IX23-3D8	52	23	8.33E-06	24	9	1.65	0.0355	0.00093	0.0000	0.00184	0.0002	0.0019	0.0002
	B2IX23-3D9	52	23	8.33E-06	27	9	1.65	0.0355	0.00079	0.0001	0.00195	0.0003	0.0014	0.0002
	B2IX23-3D10	52	23	8.33E-06	30	9	1.65	0.0355	0.00070	0.0001	0.00201	0.0003	0.0013	0.0003
4	B2IX23-4D1	90	23	8.33E-06	3	10	0.83	0.0178	0.02584	0.0448	0.00593	0.0038	0.0550	0.0469
	B2IX23-4D2	90	23	8.33E-06	6	10	0.83	0.0178	0.01298	-0.0002	0.00358	0.0004	0.0280	0.0004
	B2IX23-4D3	90	23	8.33E-06	9	10	0.83	0.0178	0.00657	-0.0002	0.00252	0.0004	0.0142	0.0002
	B2IX23-4D4	90	23	8.33E-06	12	10	0.83	0.0178	0.00352	0.0001	0.00195	0.0004	0.0074	0.0003
	B2IX23-4D5	90	23	8.33E-06	15	10	0.83	0.0178	0.00195	0.0000	0.00156	0.0003	0.0040	0.0002
	B2IX23-4D6	90	23	8.33E-06	18	10	0.83	0.0178	0.00132	0.0003	0.00139	0.0003	0.0024	0.0003
	B2IX23-4D7	90	23	8.33E-06	21	10	0.83	0.0178	0.00081	0.0000	0.00194	0.0008	0.0014	0.0001
	B2IX23-4D8	90	23	8.33E-06	24	10	0.83	0.0178	0.00057	0.0000	0.00154	0.0003	0.0009	0.0001
	B2IX23-4D9	90	23	8.33E-06	27	10	0.83	0.0178	0.00052	0.0001	0.00149	0.0004	0.0007	0.0002
	B2IX23-4D10	90	23	8.33E-06	30	10	0.83	0.0178	0.00046	0.0001	0.00139	0.0004	0.0006	0.0002
5	B2IX23-5D1	230	23	8.33E-06	3	11	0.83	0.0178	0.02332	0.0405	0.00498	0.0032	0.0496	0.0422
	B2IX23-5D2	230	23	8.33E-06	6	11	0.83	0.0178	0.01167	-0.0002	0.00328	0.0004	0.0249	0.0001
	B2IX23-5D3	230	23	8.33E-06	9	11	0.83	0.0178	0.00618	0.0004	0.00250	0.0005	0.0130	0.0005
	B2IX23-5D4	230	23	8.33E-06	12	11	0.83	0.0178	0.00331	0.0001	0.00213	0.0005	0.0068	0.0002
	B2IX23-5D5	230	23	8.33E-06	15	11	0.83	0.0178	0.00187	0.0001	0.00172	0.0003	0.0036	0.0002
	B2IX23-5D6	230	23	8.33E-06	18	11	0.83	0.0178	0.00106	0.0000	0.00135	0.0002	0.0019	0.0001
	B2IX23-5D7	230	23	8.33E-06	21	11	0.83	0.0178	0.00076	0.0002	0.00127	0.0003	0.0012	0.0002
	B2IX23-5D8	230	23	8.33E-06	24	11	0.83	0.0178	0.00052	0.0000	0.00115	0.0002	0.0008	0.0001
	B2IX23-5D9	230	23	8.33E-06	27	11	0.83	0.0178	0.00047	0.0001	0.00119	0.0003	0.0006	0.0001
	B2IX23-5D10	230	23	8.33E-06	30	11	0.83	0.0178	0.00046	0.0001	0.00124	0.0003	0.0006	0.0002

APPENDIX E

PLOTS OF PULSED-FLOW TEST DATA: EFFECTS OF pH & TEMPERATURE ON ION EXCHANGE FOR GLASSES LAWC22, ORLEC28, & IDF1B2

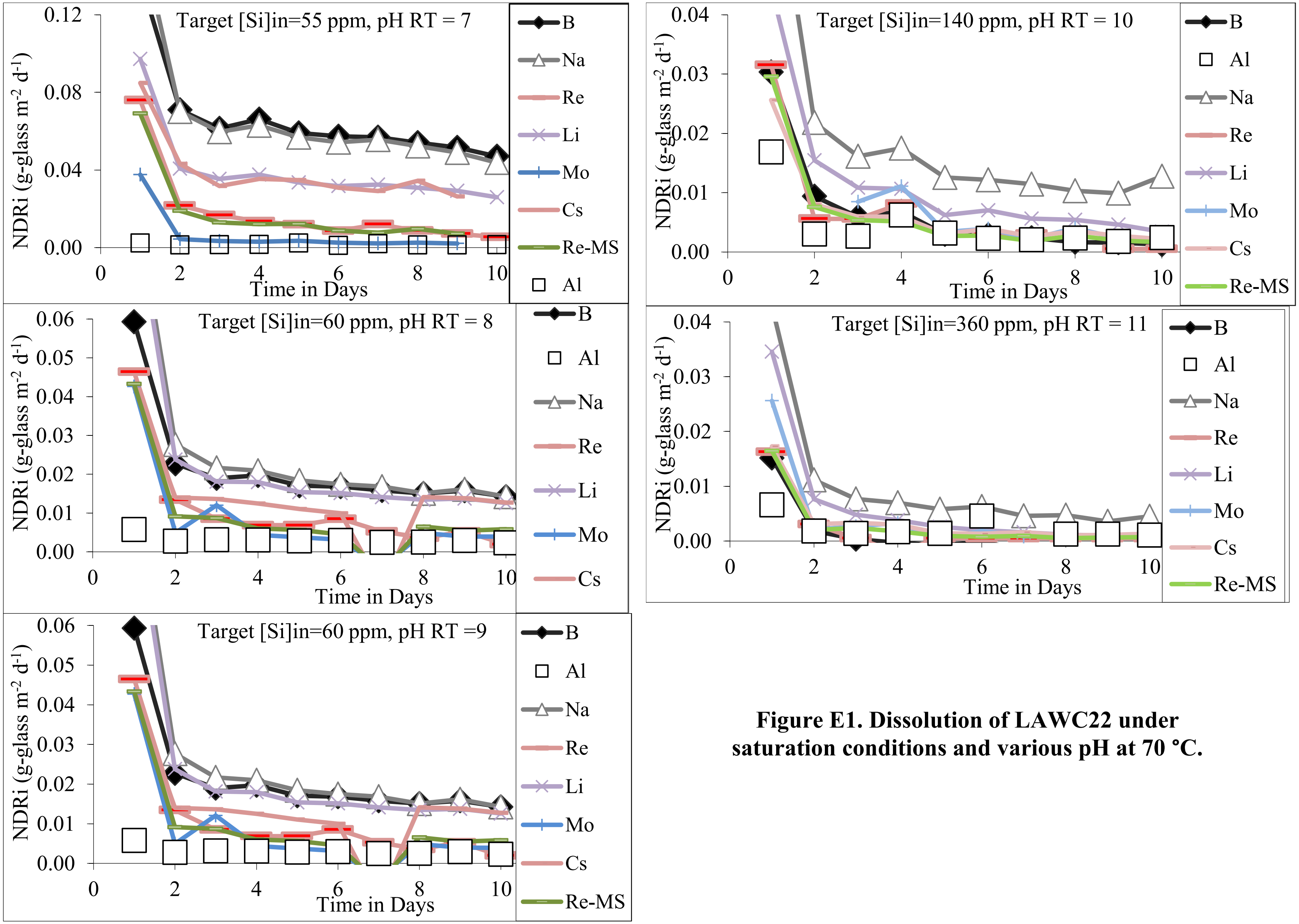

Figure E1. Dissolution of LAWC22 under saturation conditions and various pH at 70 °C.

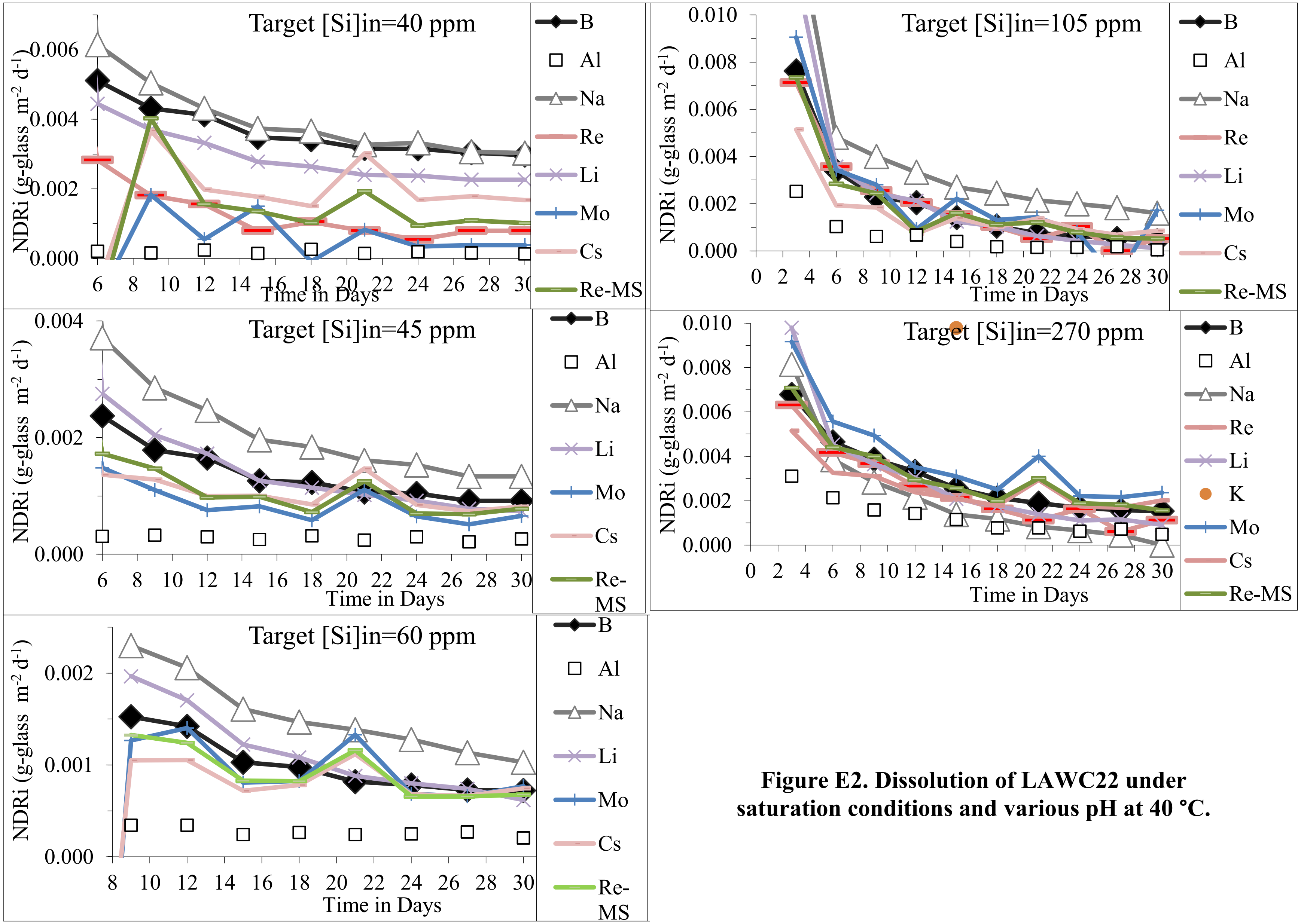

Figure E2. Dissolution of LAWC22 under saturation conditions and various pH at 40 °C.

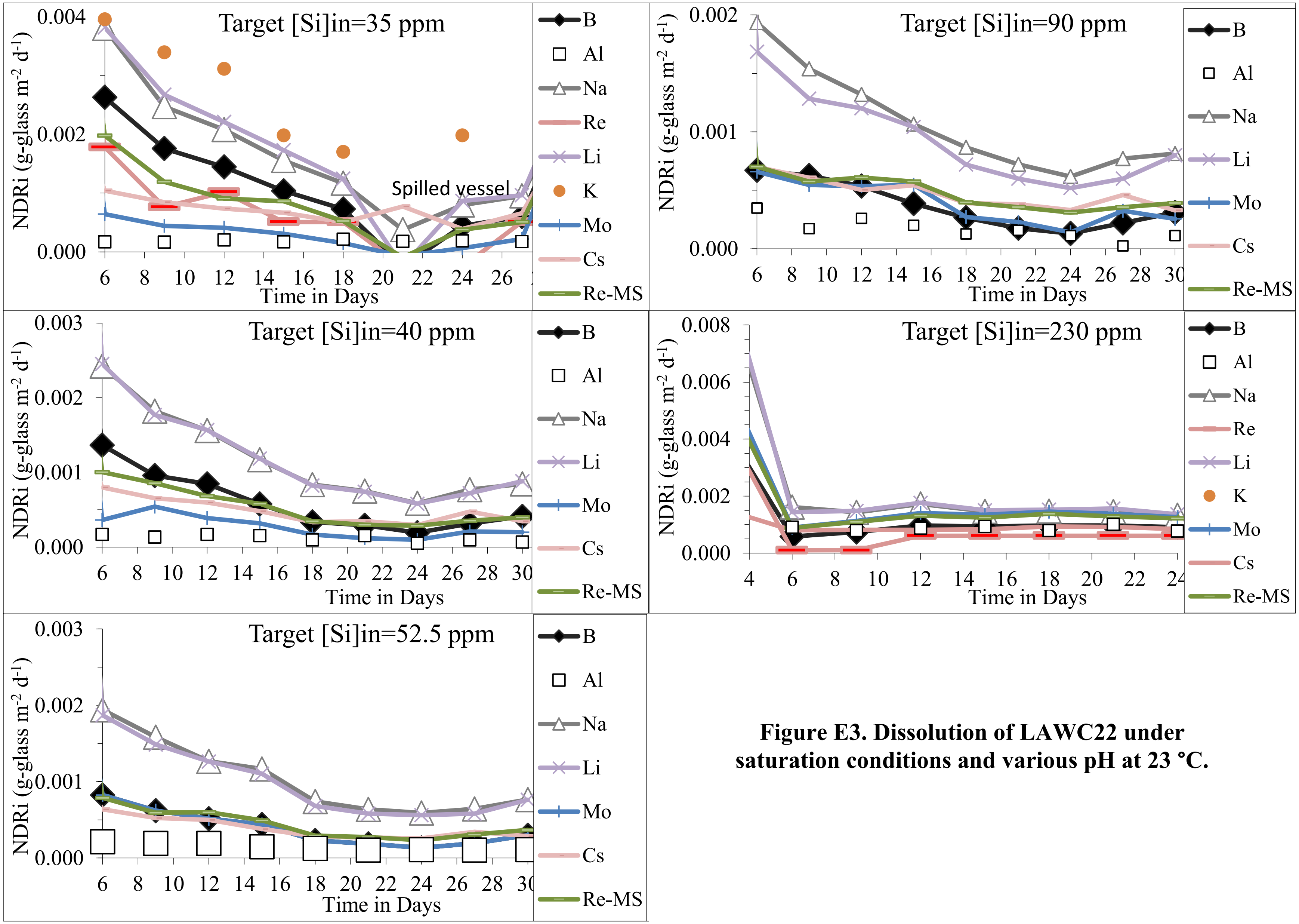

Figure E3. Dissolution of LAWC22 under saturation conditions and various pH at 23 °C.

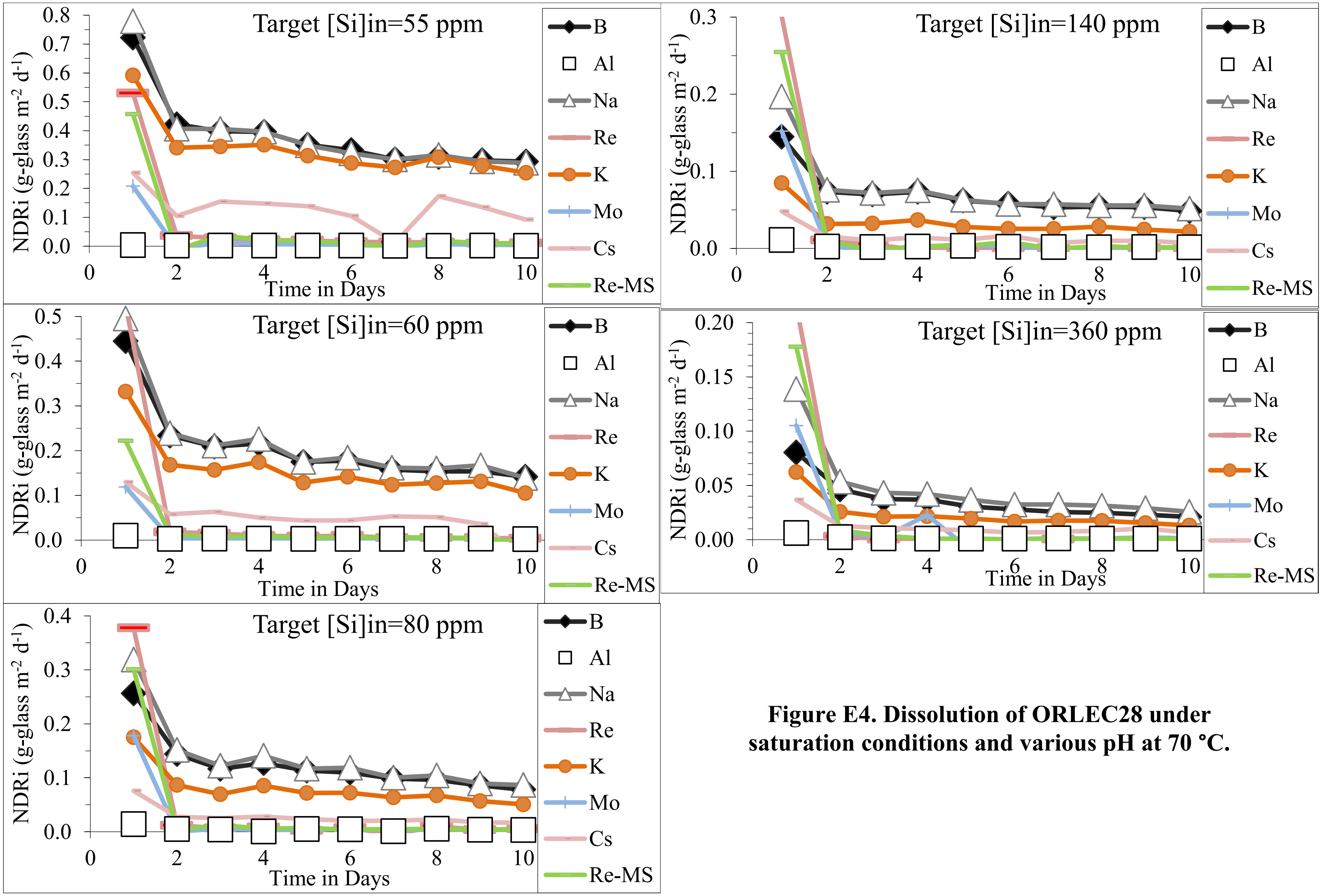

Figure E4. Dissolution of ORLEC28 under saturation conditions and various pH at 70 °C.

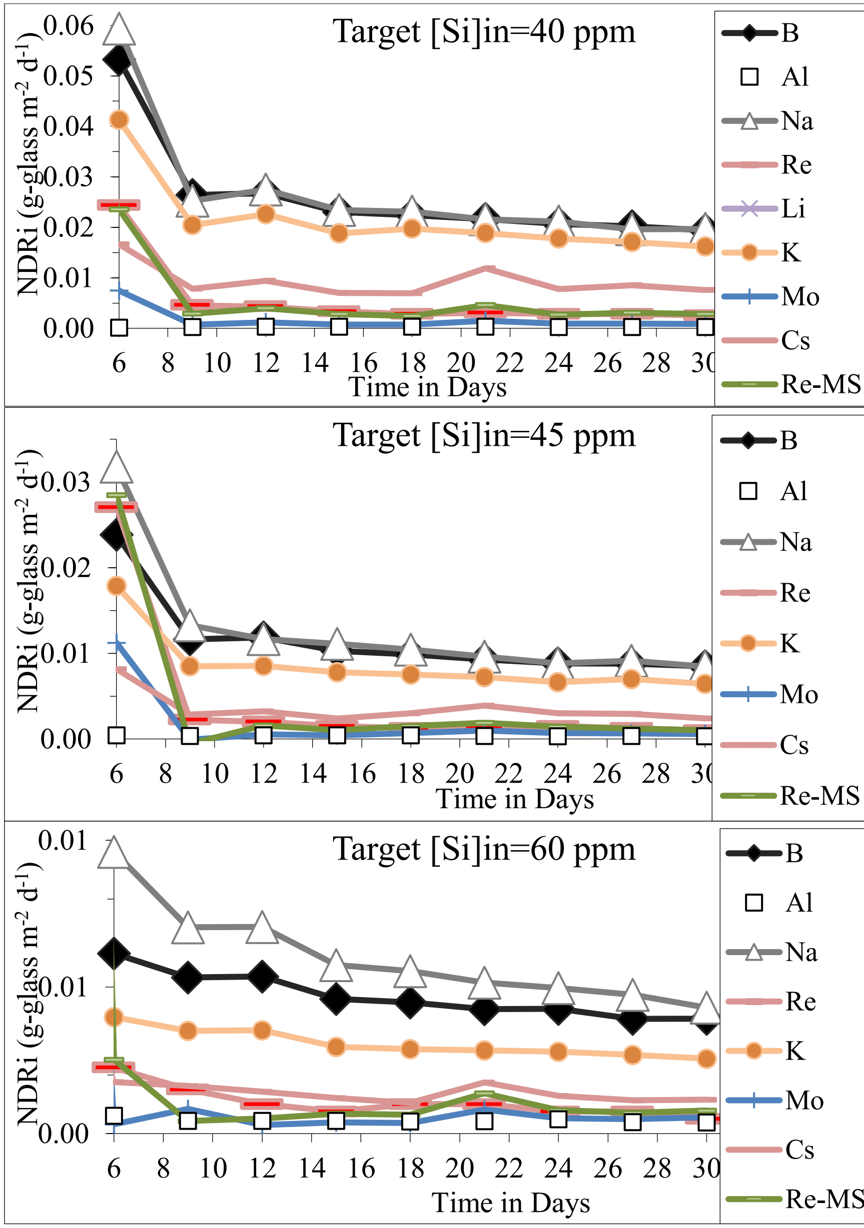

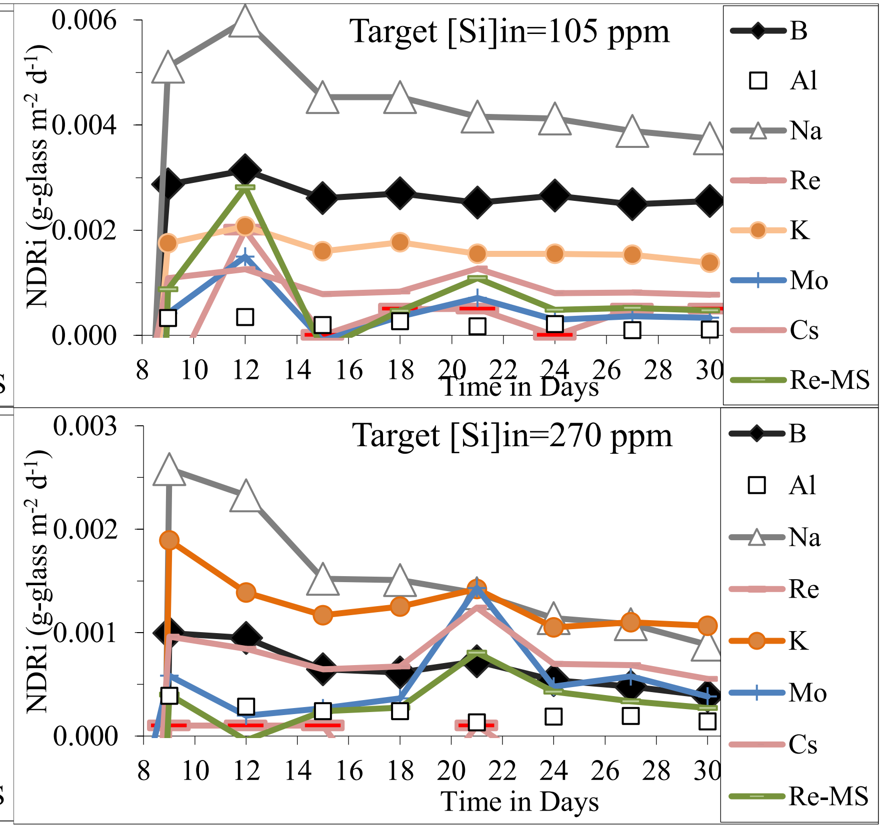

Figure E5. Dissolution of ORLEC28 under saturation conditions and various pH at 40 °C.

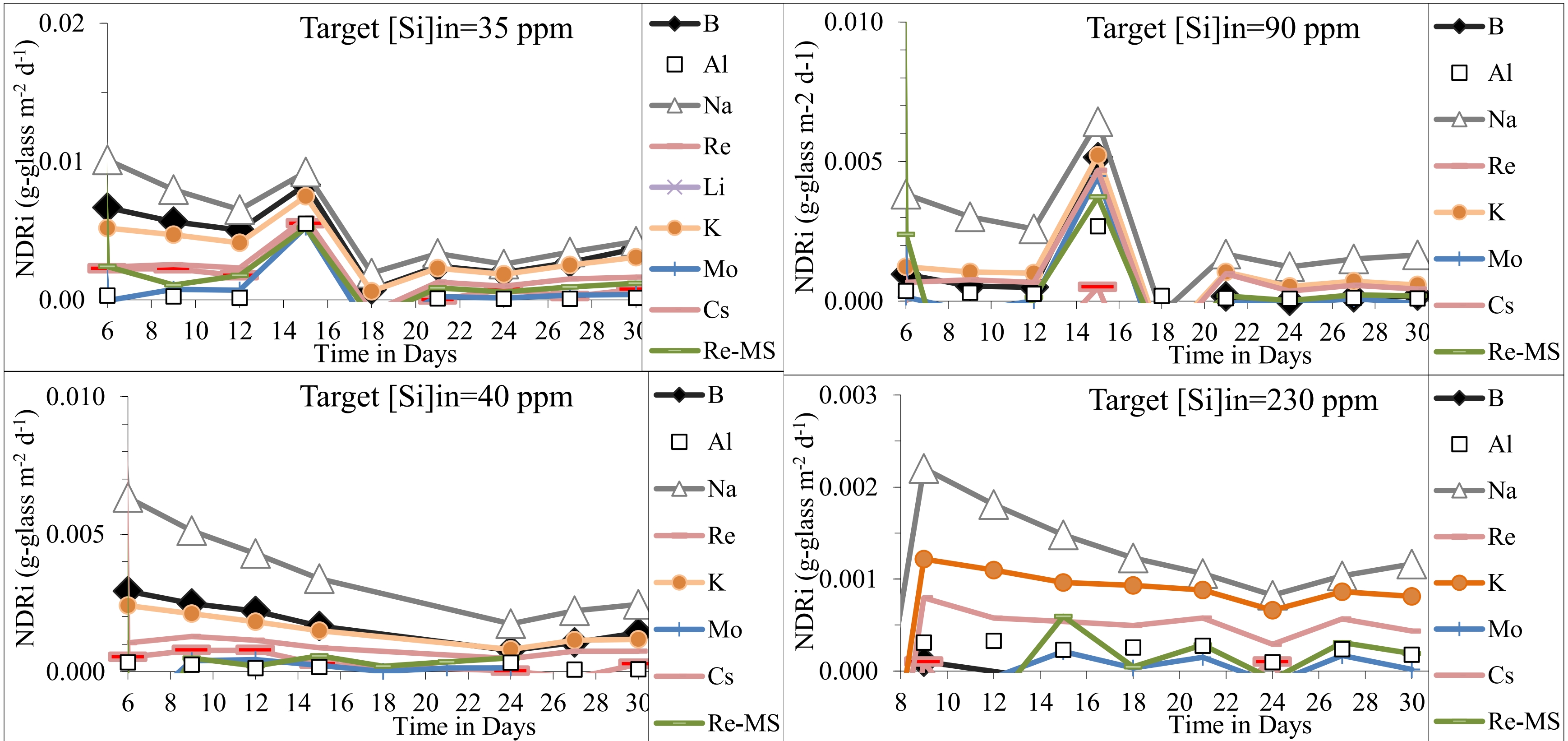

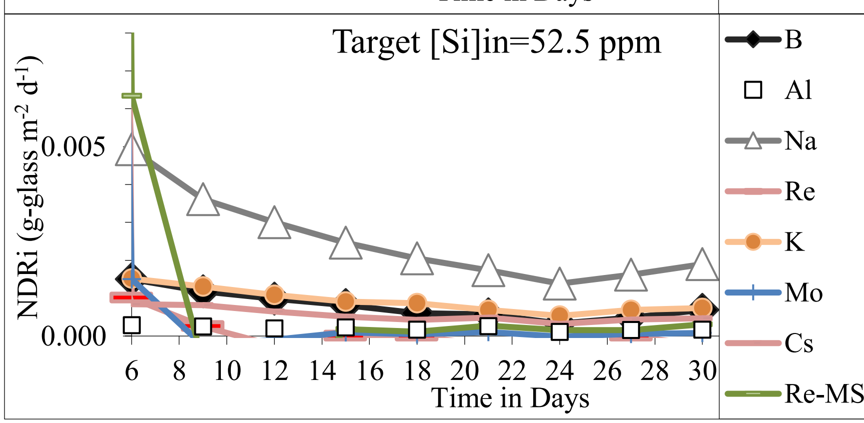

Figure E6. Dissolution of ORLEC28 under saturation conditions and various pH at 23 °C.

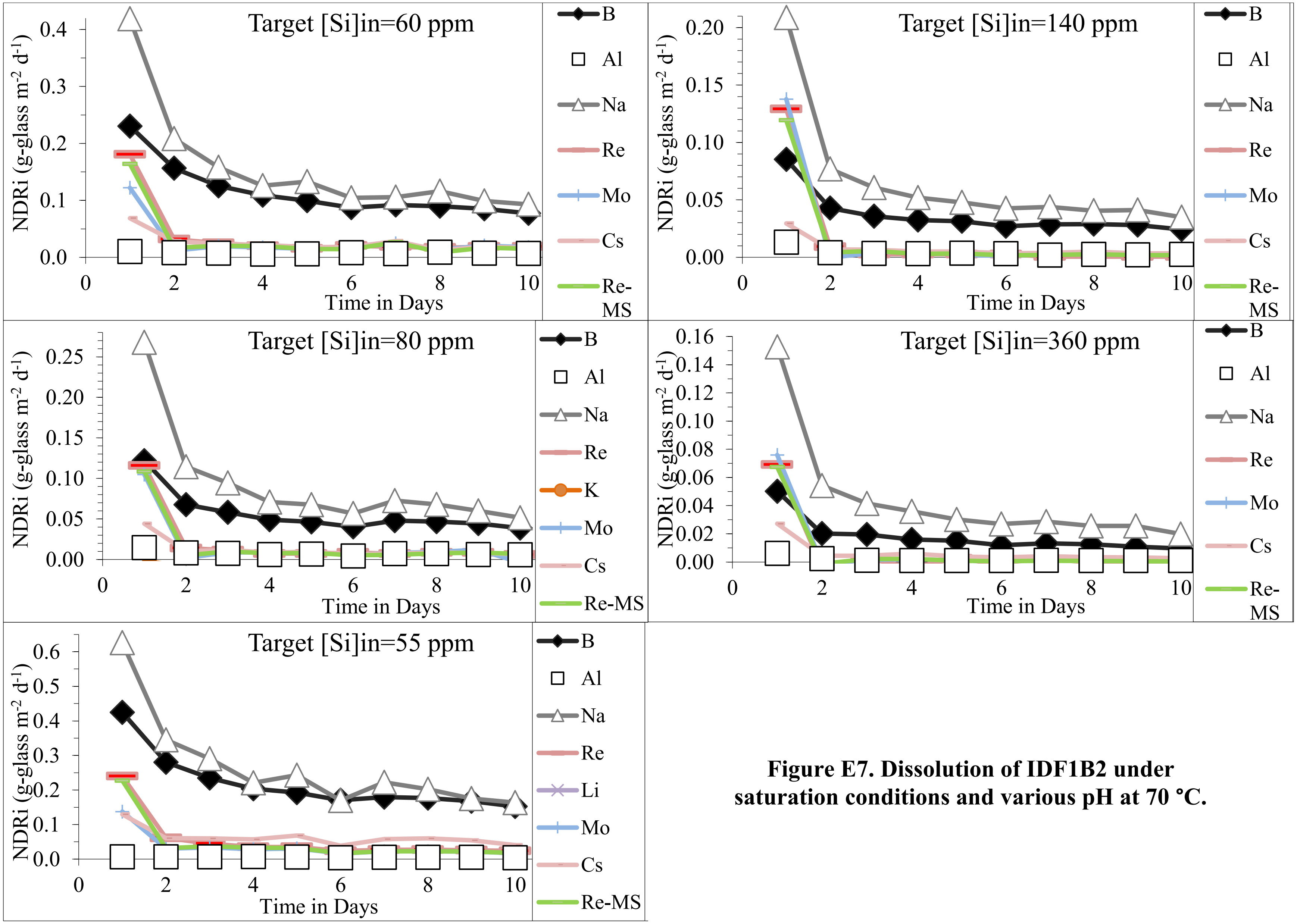

Figure E7. Dissolution of IDF1B2 under saturation conditions and various pH at 70 °C.

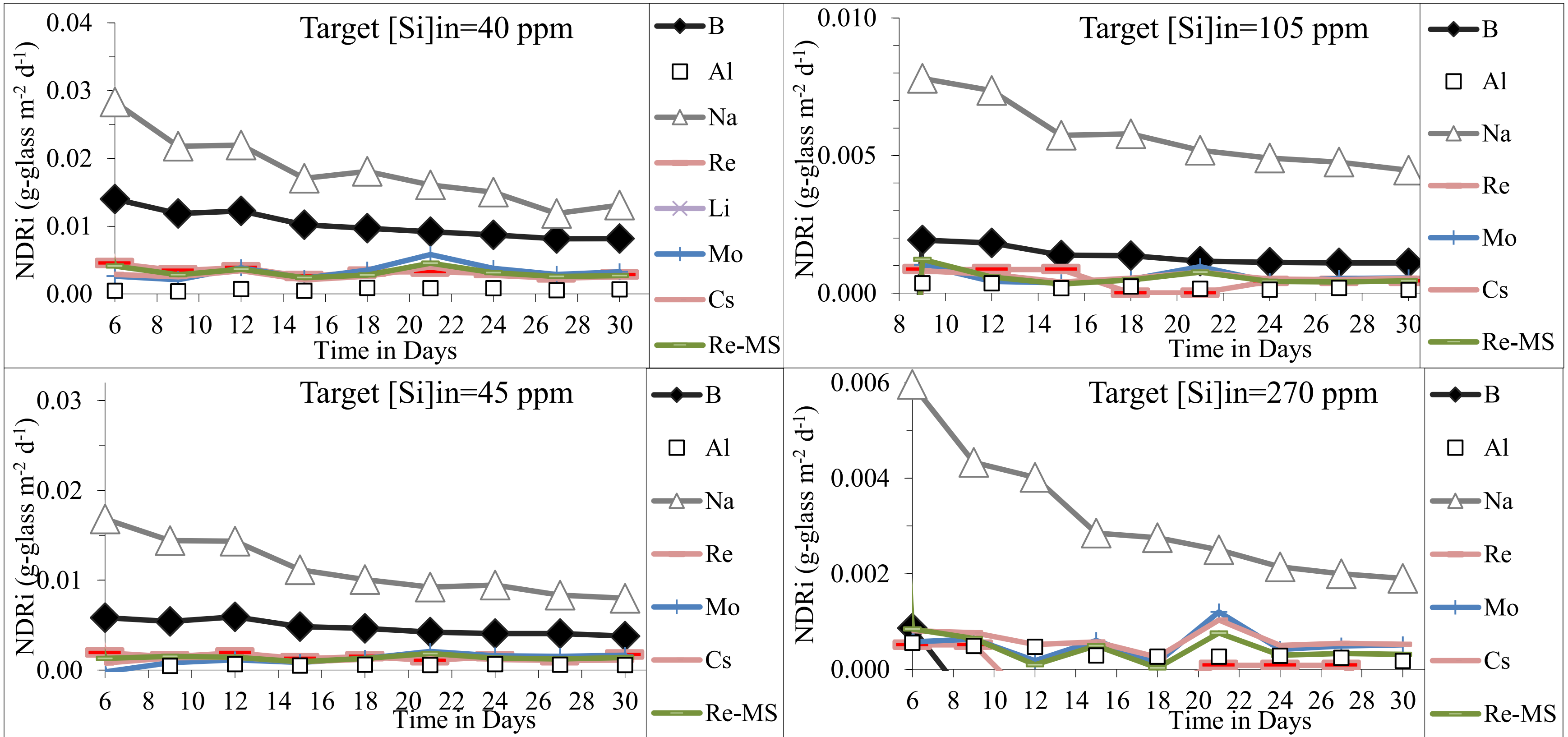

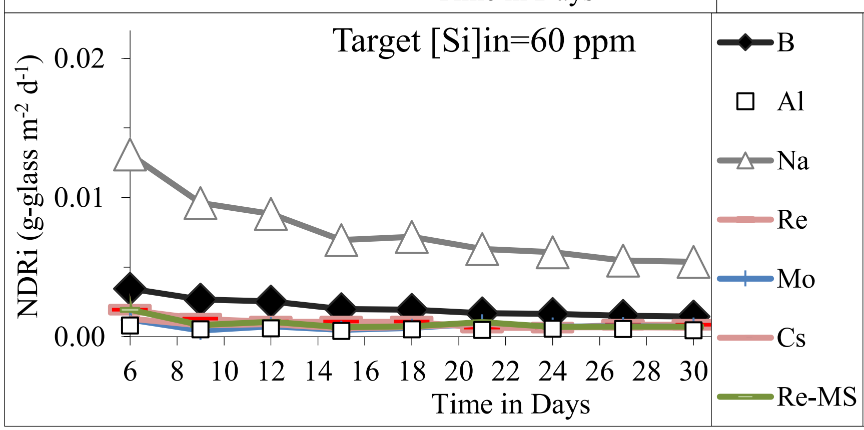

Figure E8. Dissolution of IDF1B2 under saturation conditions and various pH at 40 °C.

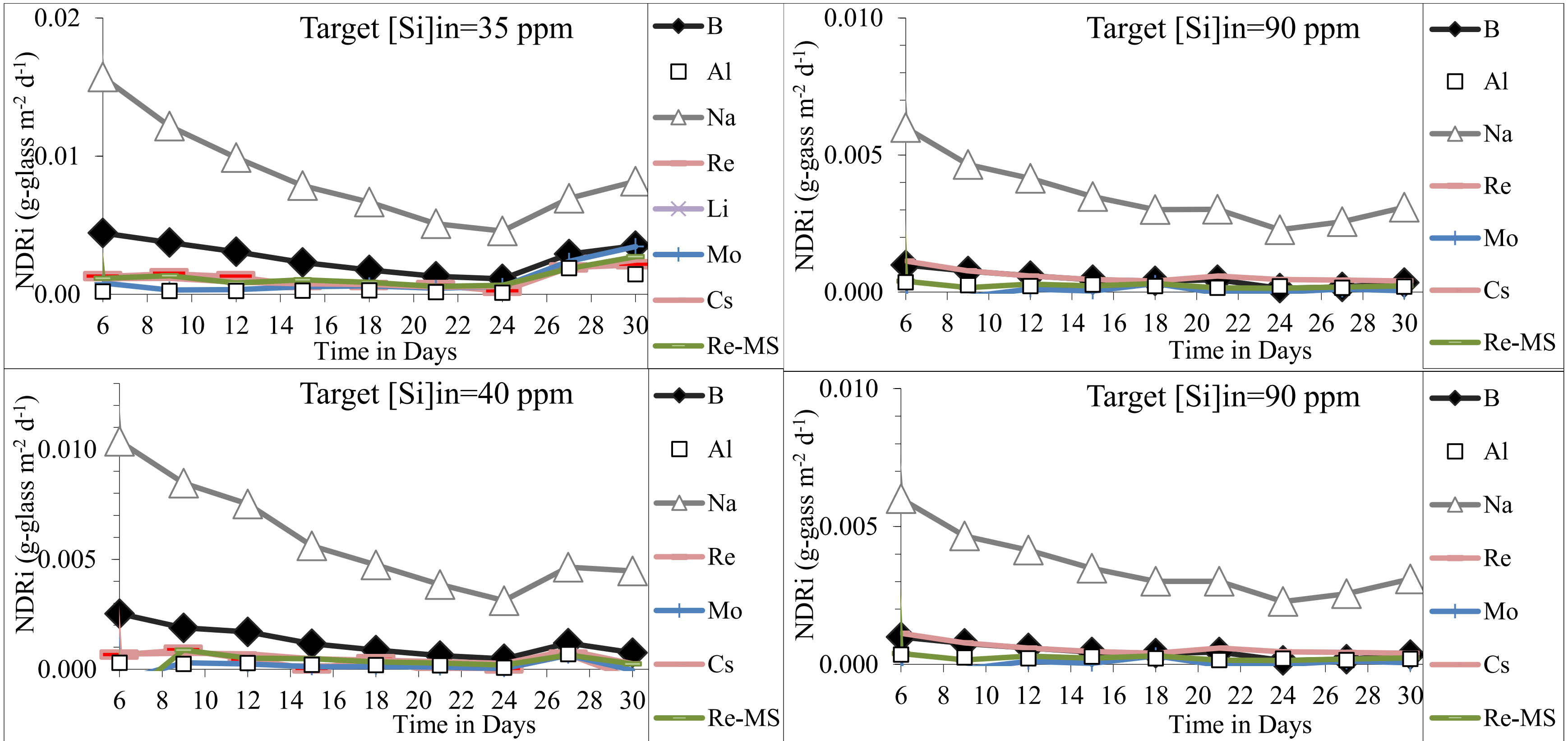

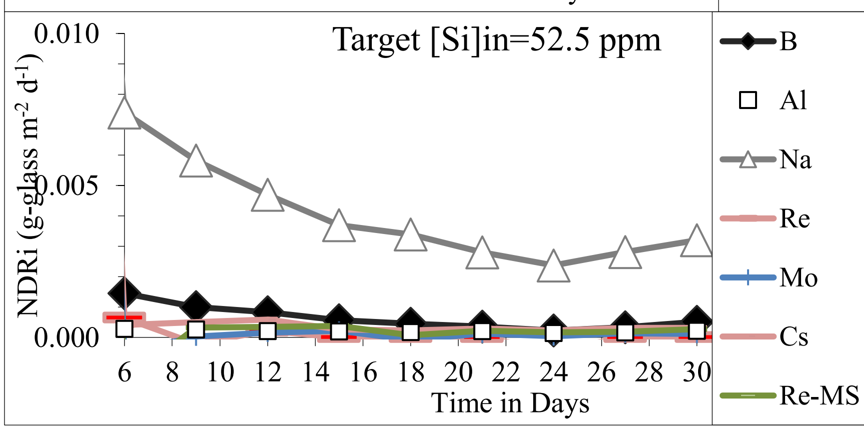

Figure E9. Dissolution of IDF1B2 under saturation conditions and various pH at 23 °C.

APPENDIX F

SODIUM ION EXCHANGE PLOTS COMPARING THE VALUES BY DIFFERENCE OF NDR_{Na} TO NDR_{B}, NDR_{Re}, AND NDR_{Mo} FOR GLASSES LAWC22, ORLEC28 and IDF1B2

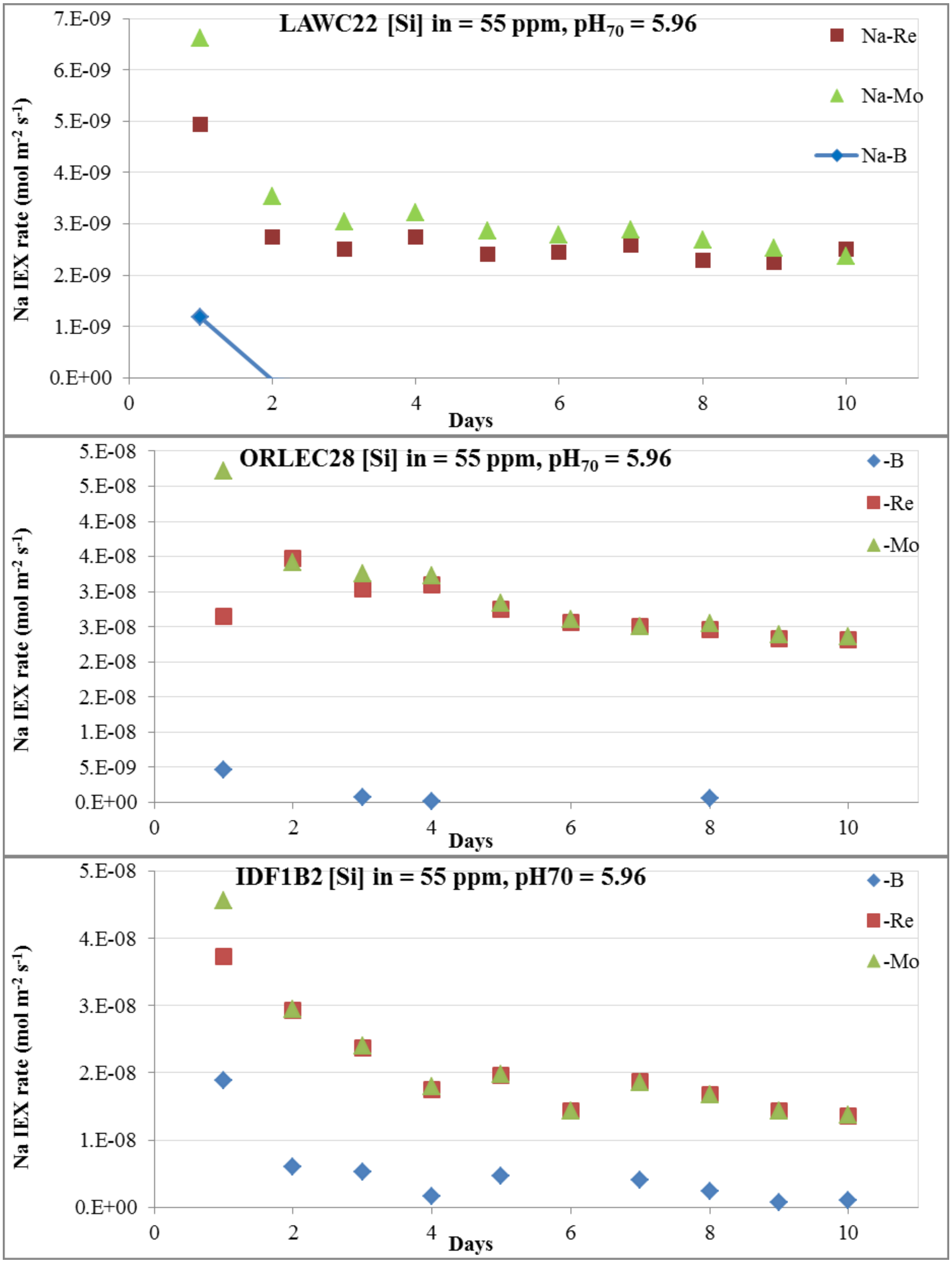

Figure F1. Plot of sodium ion exchange rate calculated from difference of sodium normalized release rate to that of boron, rhenium, or molybdenum, at 70 °C, pH_{23} =7.

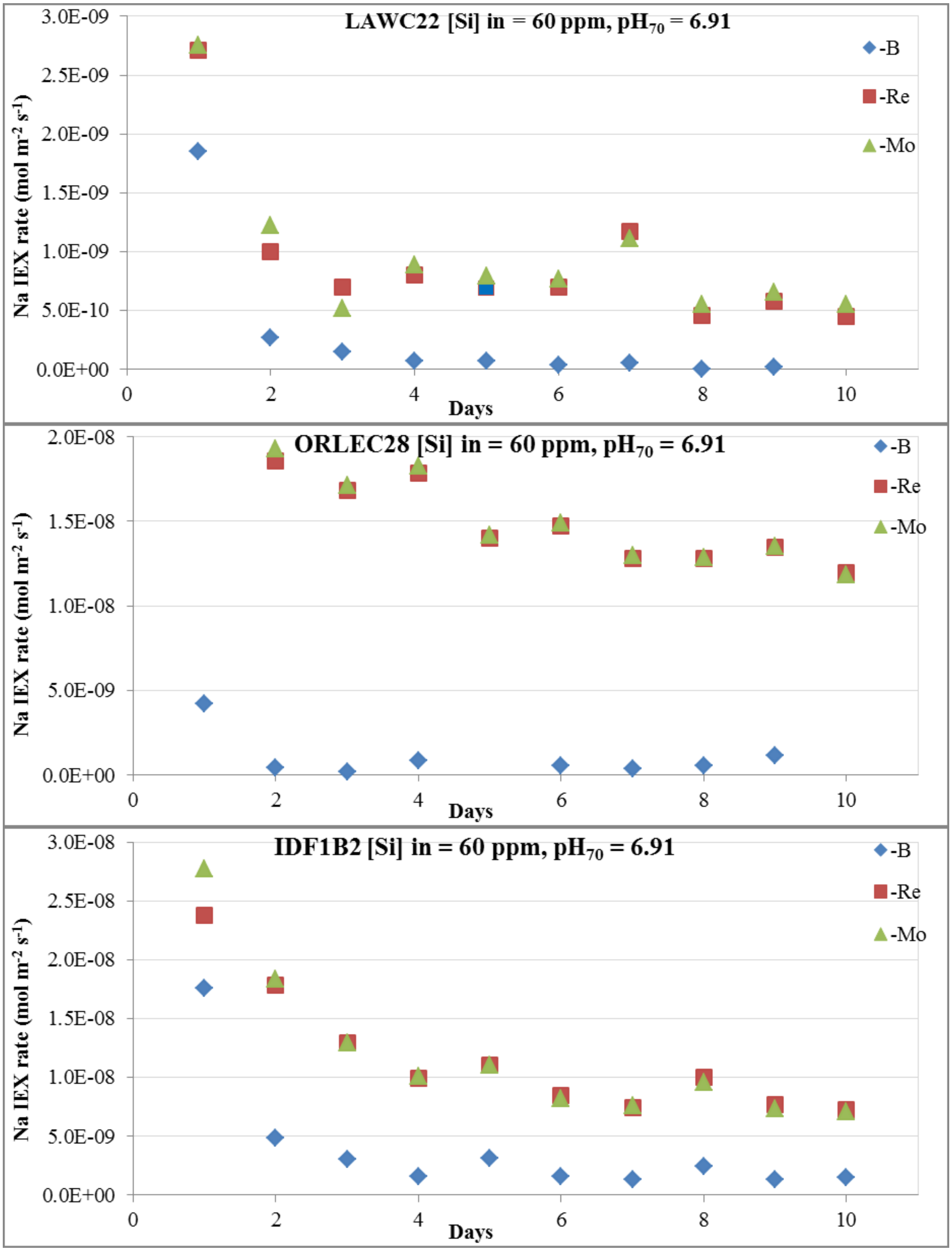

Figure F2. Plot of sodium ion exchange rate calculated from difference of sodium normalized release rate to that of boron, rhenium, or molybdenum, at 70 °C, pH_{23} =8.

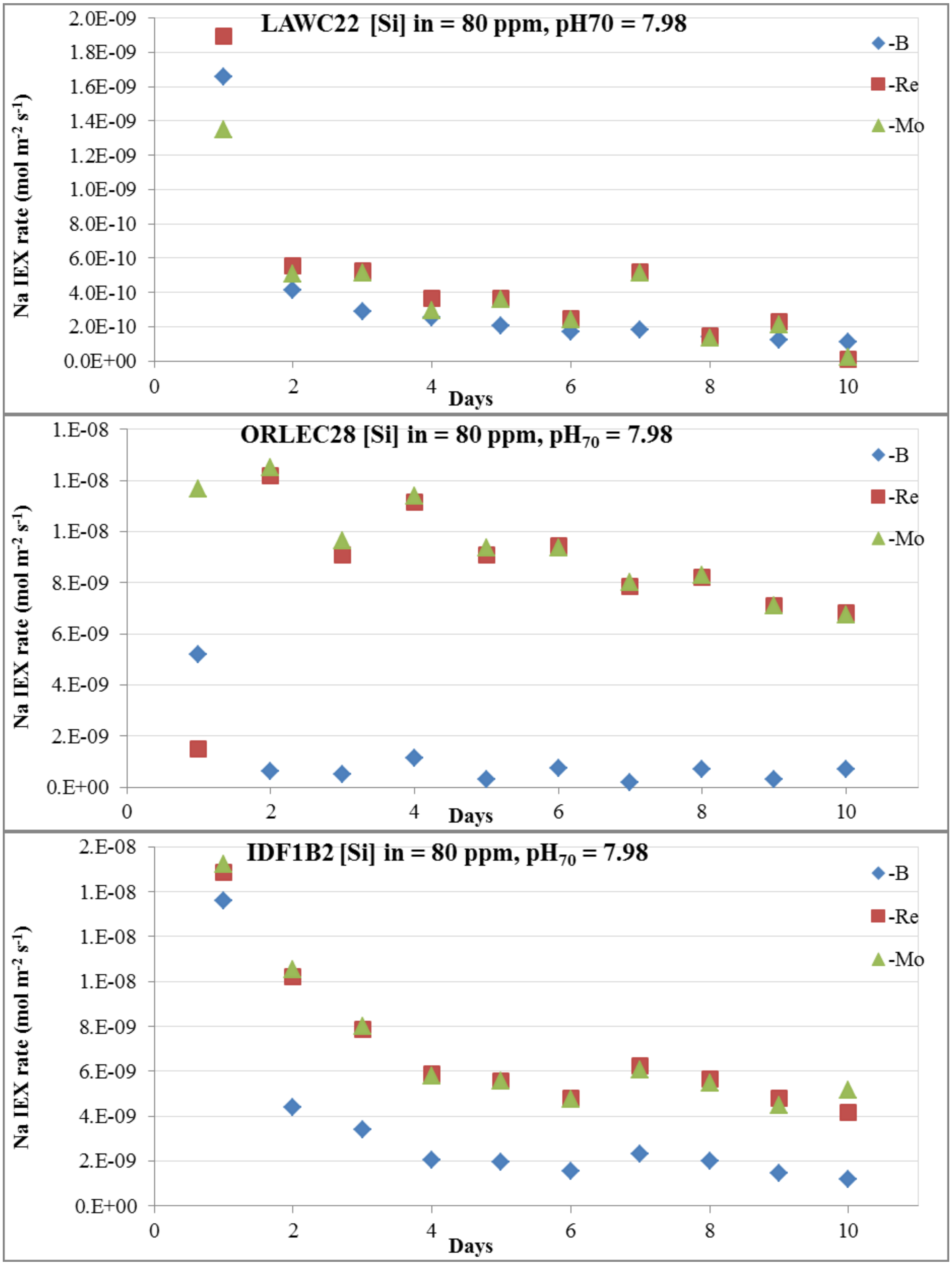

Figure F3. Plot of sodium ion exchange rate calculated from difference of sodium normalized release rate to that of boron, rhenium, or molybdenum, at 70 °C, pH_{23} =9.

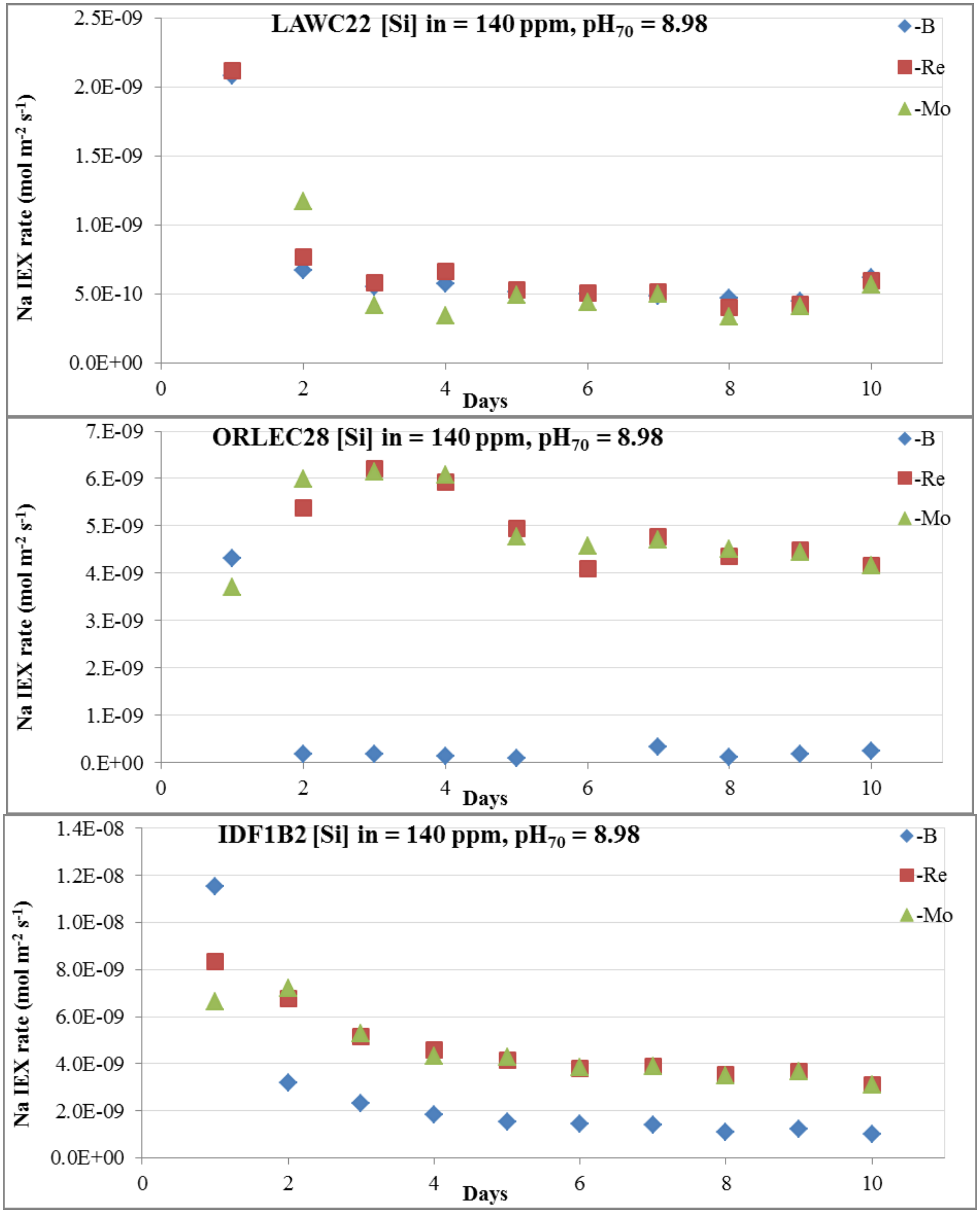

Figure F4. Plot of sodium ion exchange rate calculated from difference of sodium normalized release rate to that of boron, rhenium, or molybdenum, at 70 °C, pH_{23} =10.

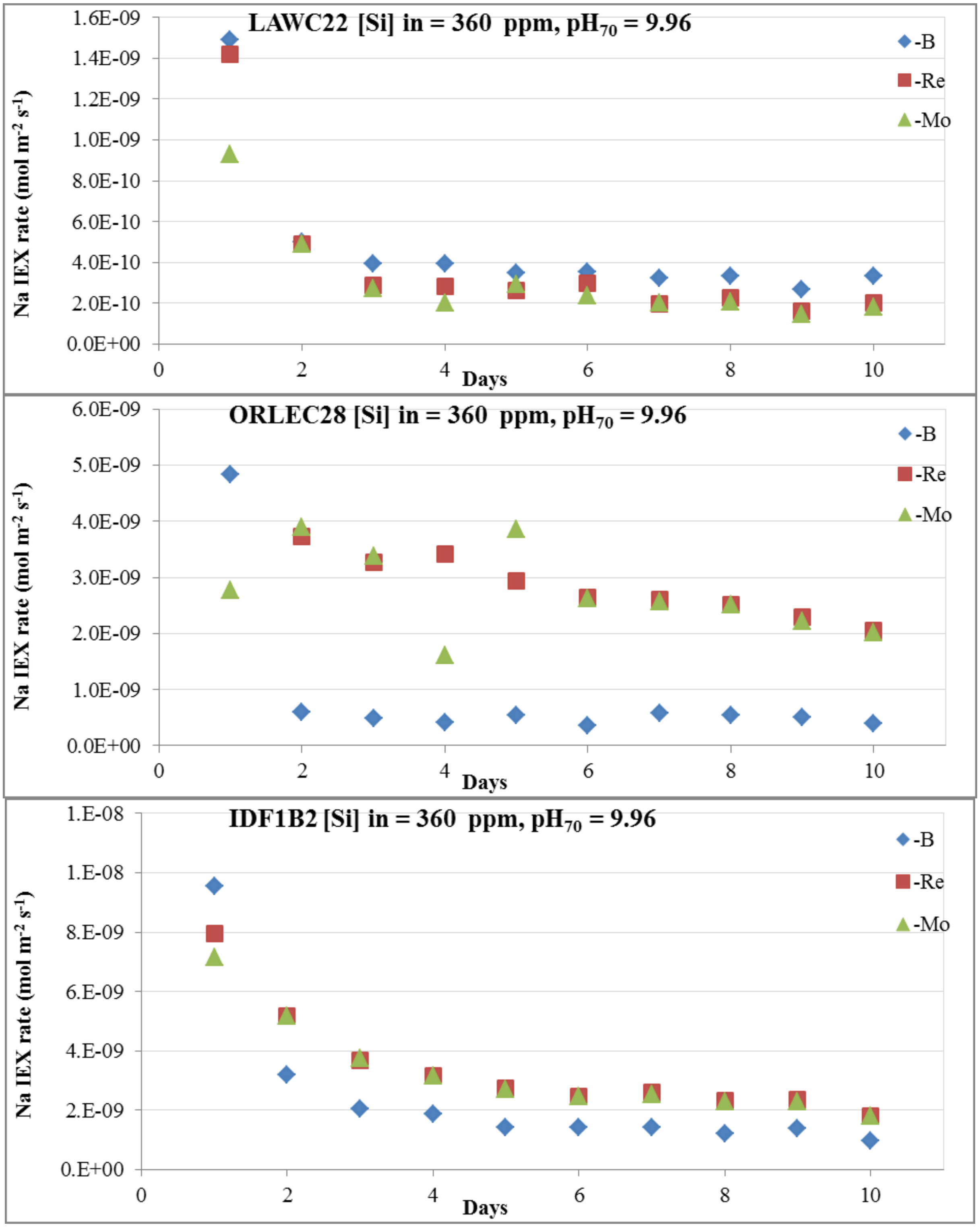

Figure F5. Plot of sodium ion exchange rate calculated from difference of sodium normalized release rate to that of boron, rhenium, or molybdenum, at 70 °C, pH_{23} =11.

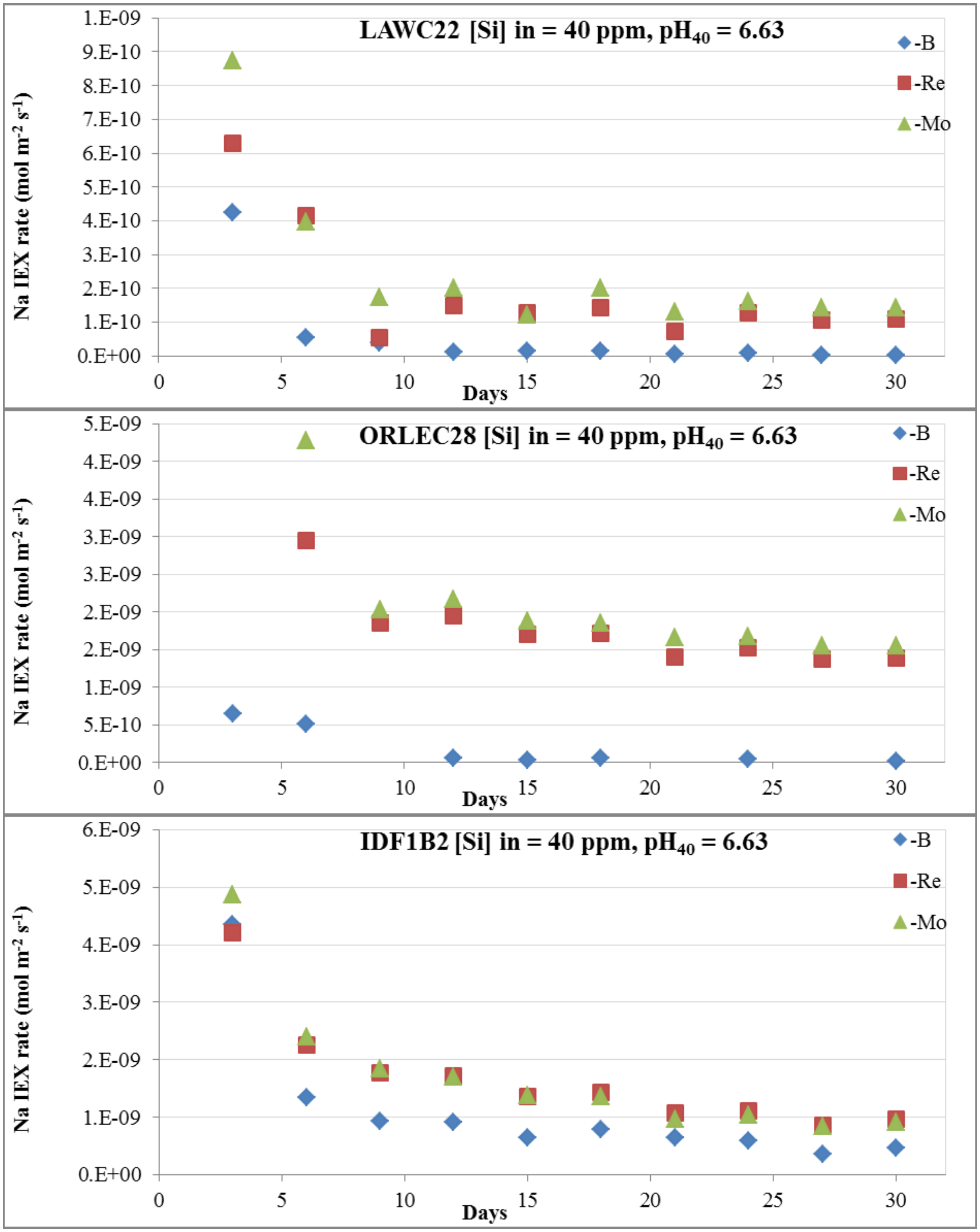

Figure F6. Plot of sodium ion exchange rate calculated from difference of sodium normalized release rate to that of boron, rhenium or molybdenum, at 40 °C, pH_{23} =7.

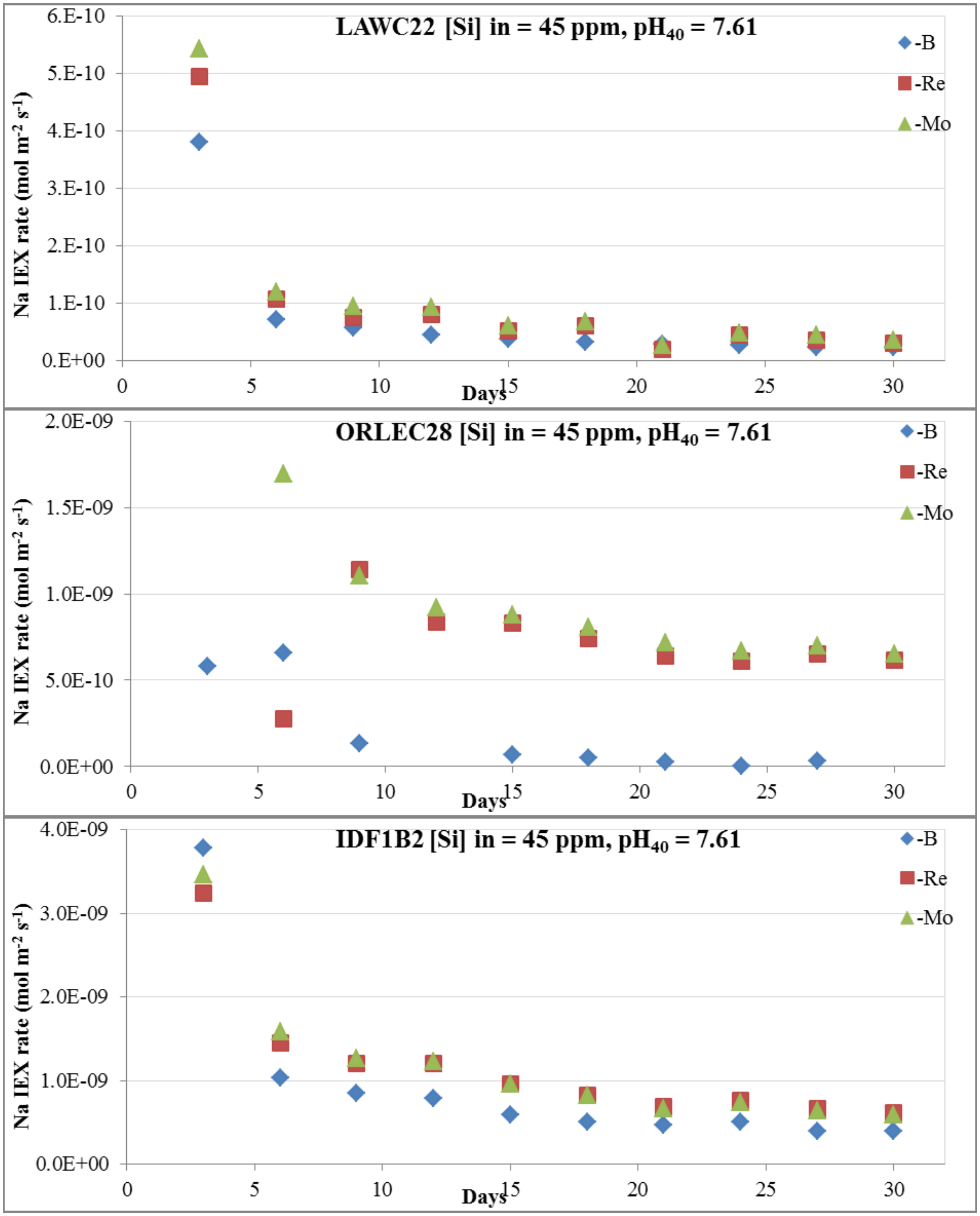

Figure F7. Plot of sodium ion exchange rate calculated from difference of sodium normalized release rate to that of boron, rhenium, or molybdenum, at 40 °C, pH_{23} =8.

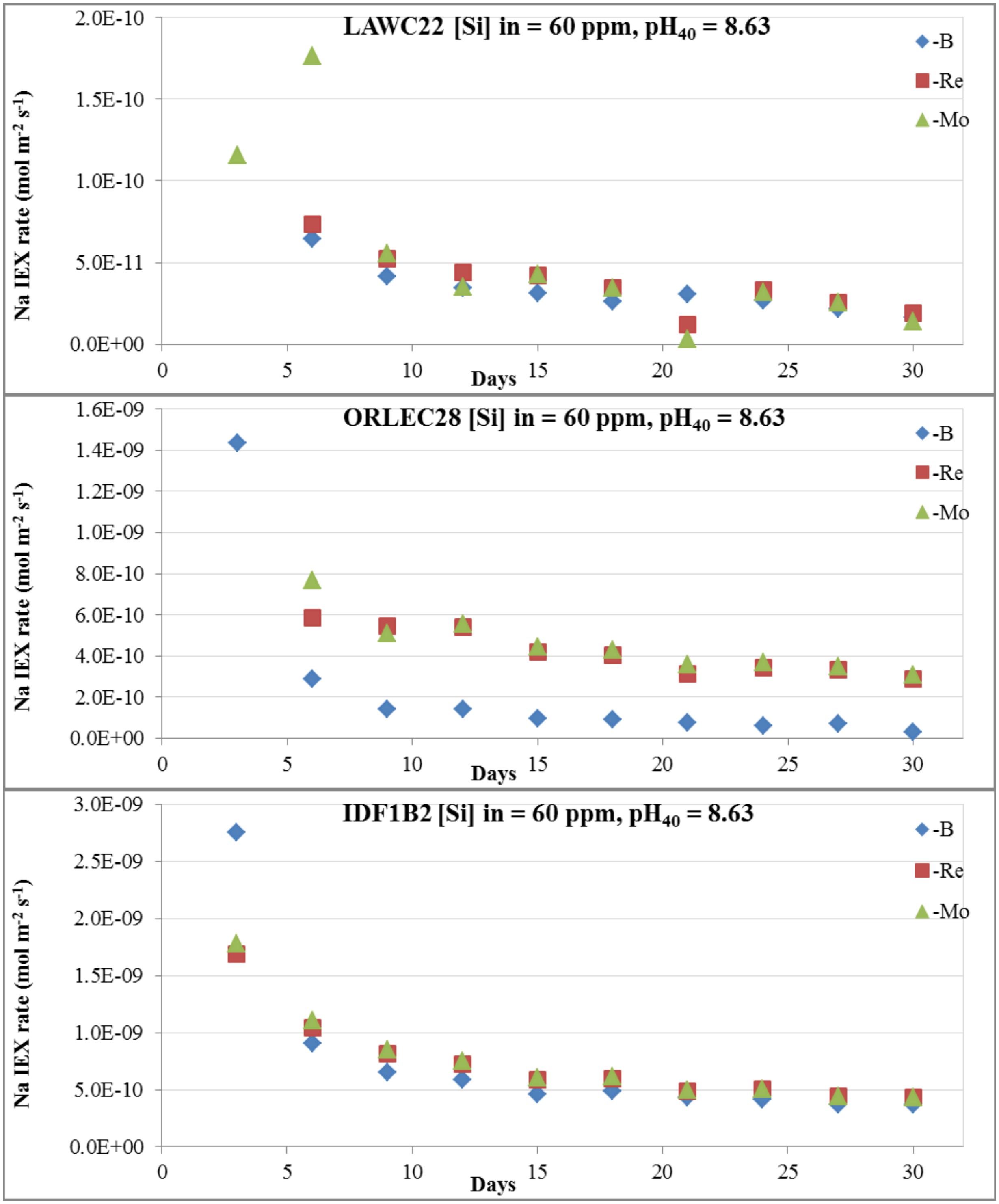

Figure F8. Plot of sodium ion exchange rate calculated from difference of sodium normalized release rate to that of boron, rhenium, or molybdenum, at 40 °C, pH_{23} =9.

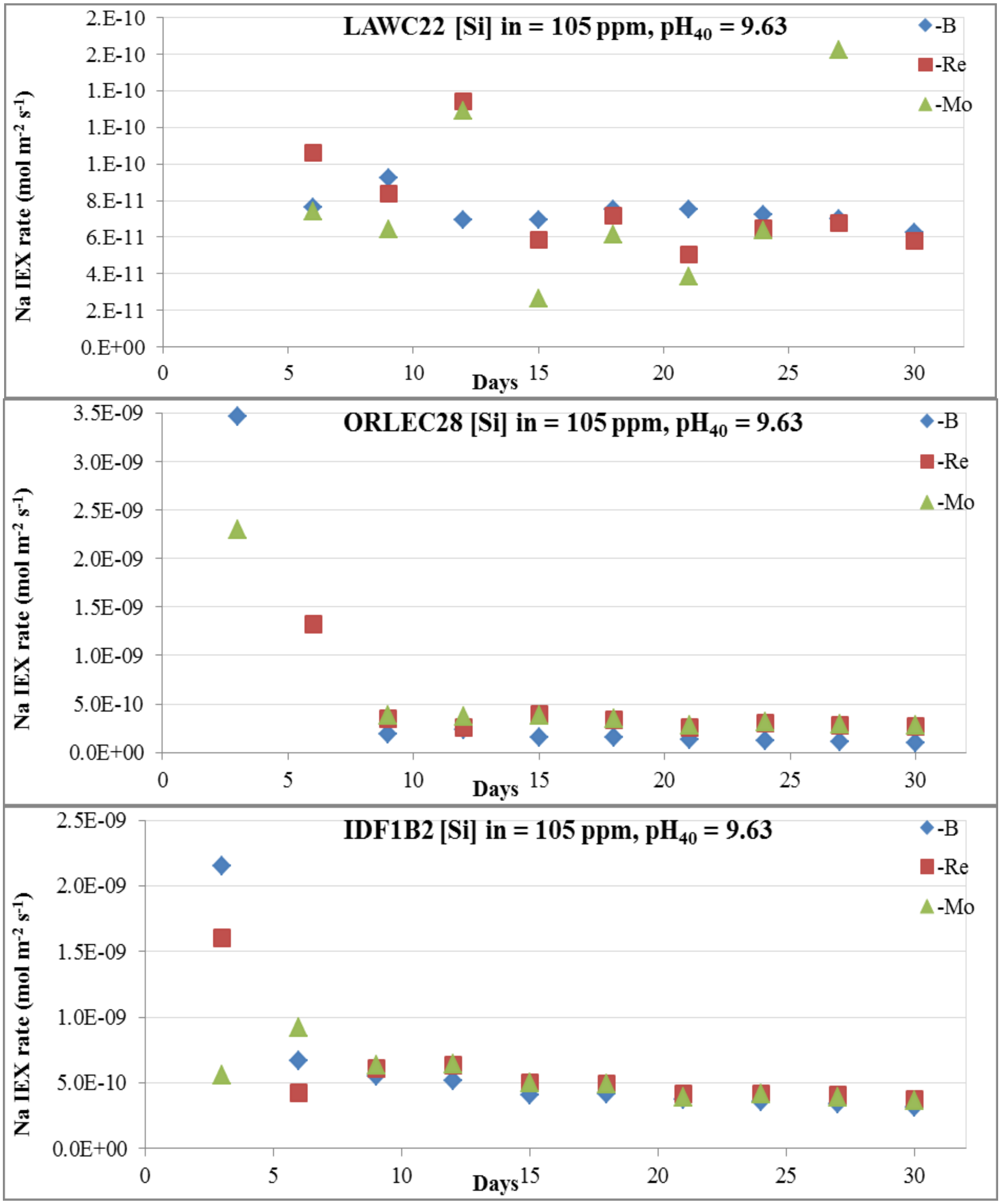

Figure F9. Plot of sodium ion exchange rate calculated from difference of sodium normalized release rate to that of boron, rhenium, or molybdenum, at 40 °C, pH_{23} =10.

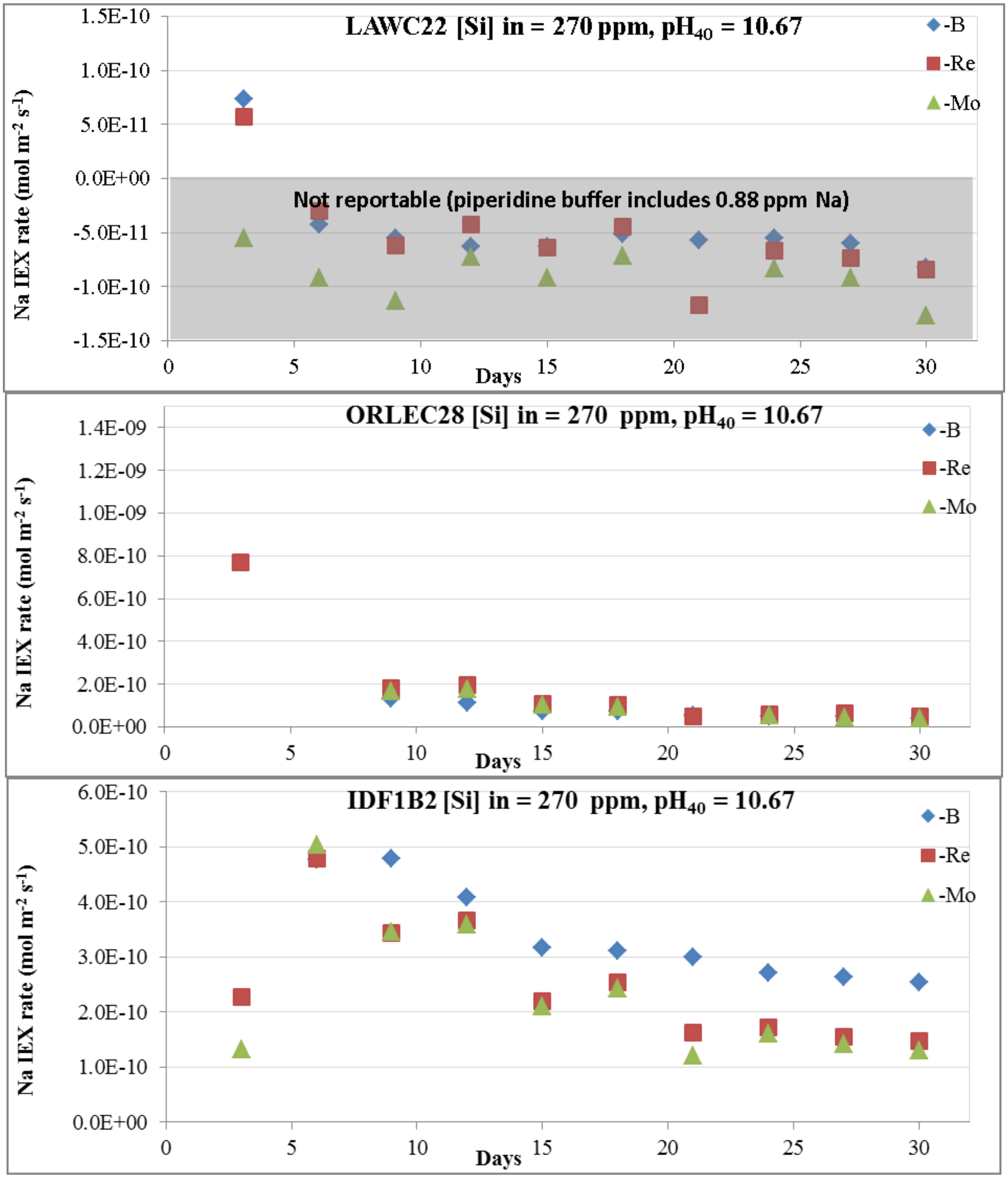

Figure F10. Plot of sodium ion exchange rate calculated from difference of sodium normalized release rate to that of boron, rhenium, or molybdenum, at 40 °C, pH_{23} =11.

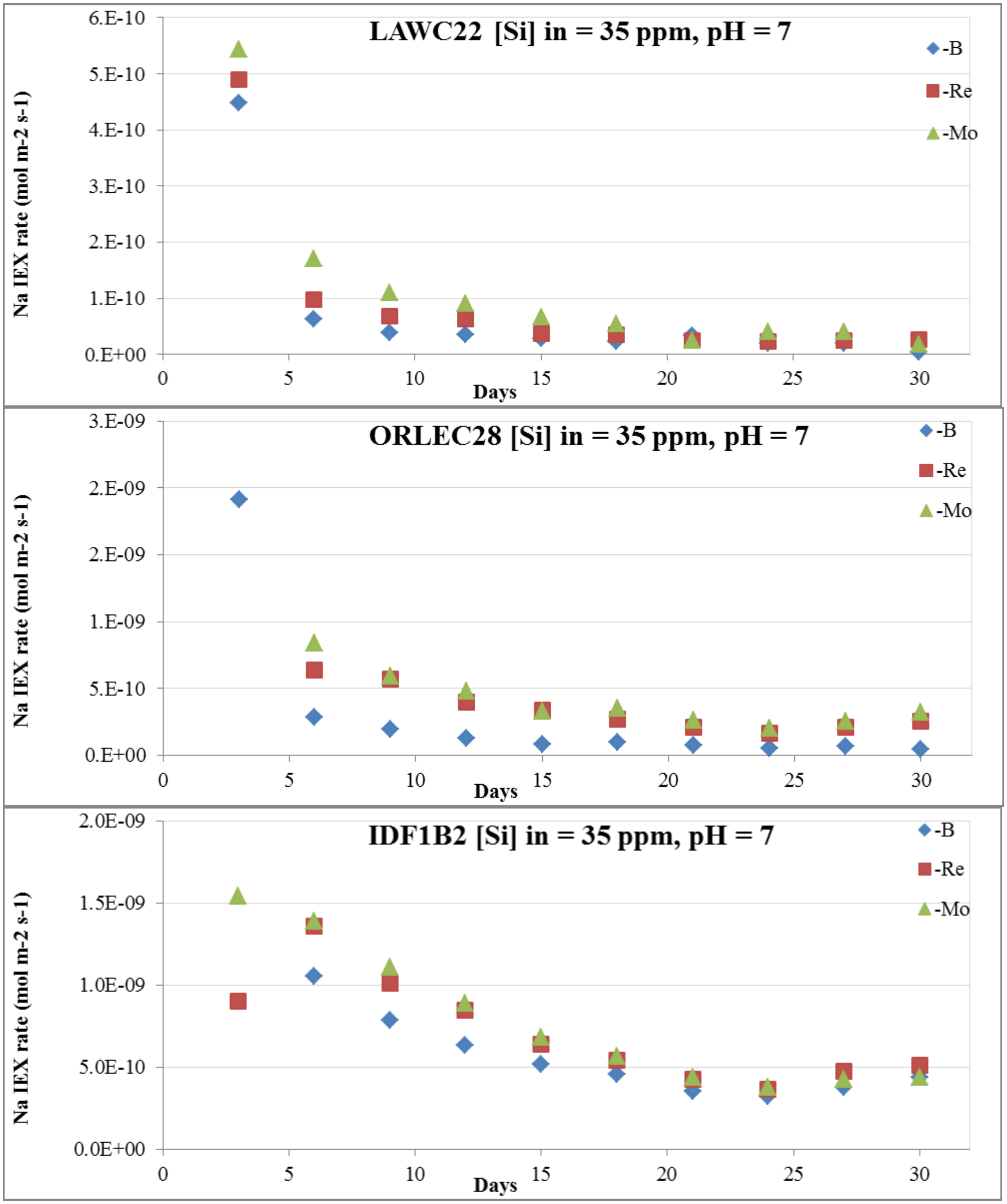

Figure F11. Plot of sodium and lithium ion exchange rate calculated from difference of respective normalized release rates to that of boron, rhenium, or molybdenum, at 23 °C, pH_{23} =7.

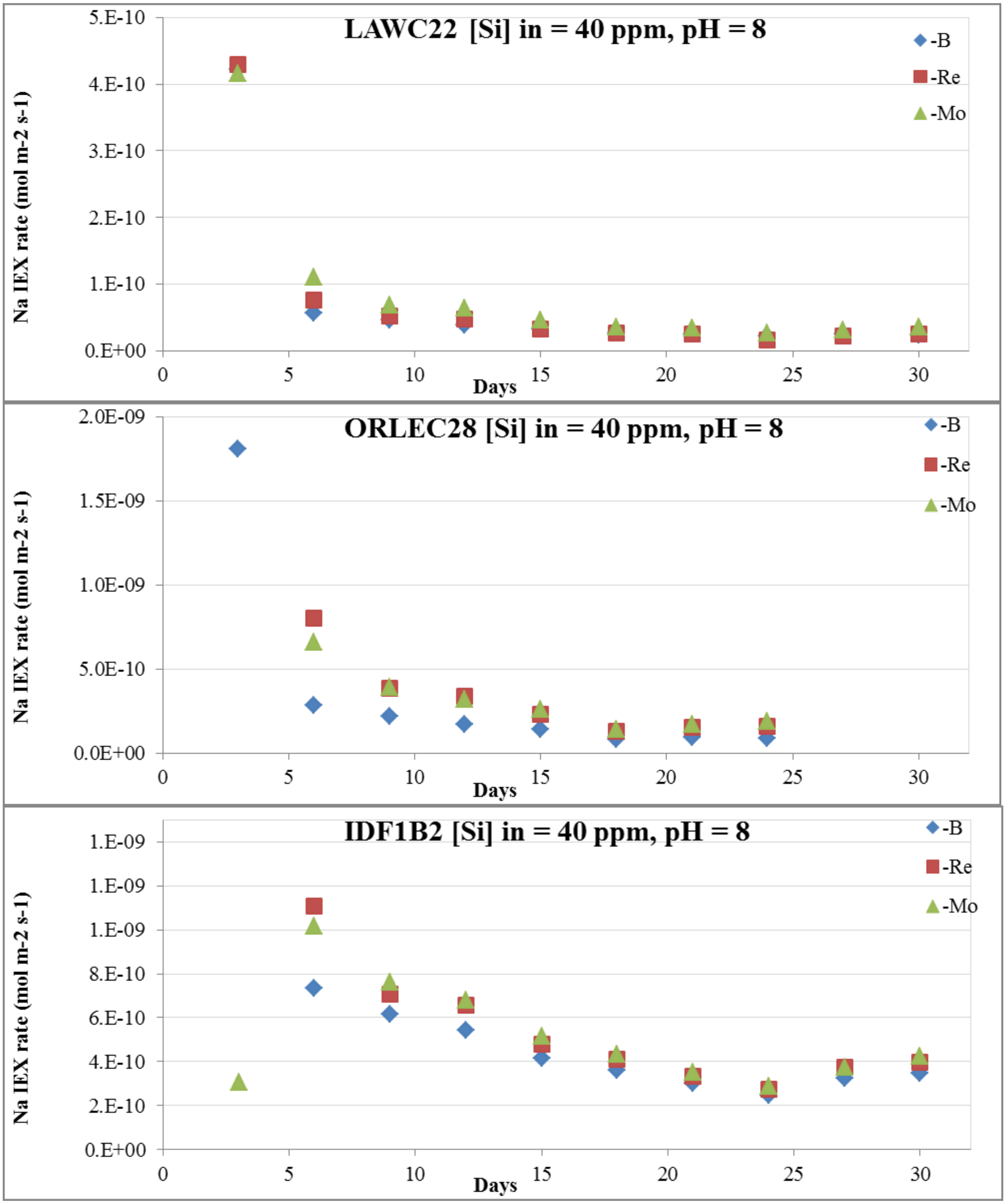

Figure F12. Plot of sodium ion exchange rate calculated from difference of respective normalized release rates to that of boron, rhenium, or molybdenum, at 23 °C, pH_{23} =8.

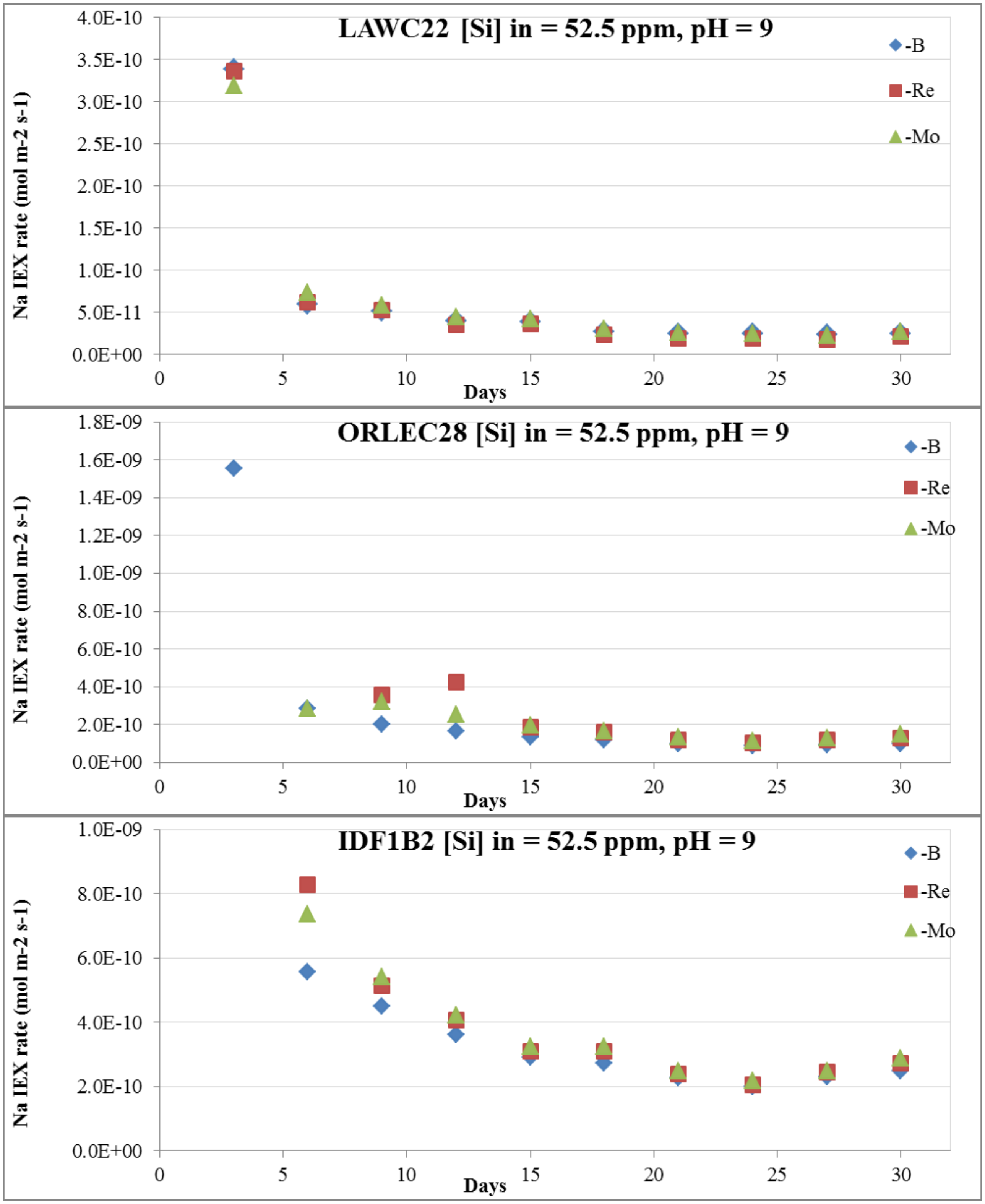

Figure F13. Plot of sodium ion exchange rates calculated from difference of respective normalized release rates to that of boron, rhenium, or molybdenum, at 23 °C, pH23 =9.

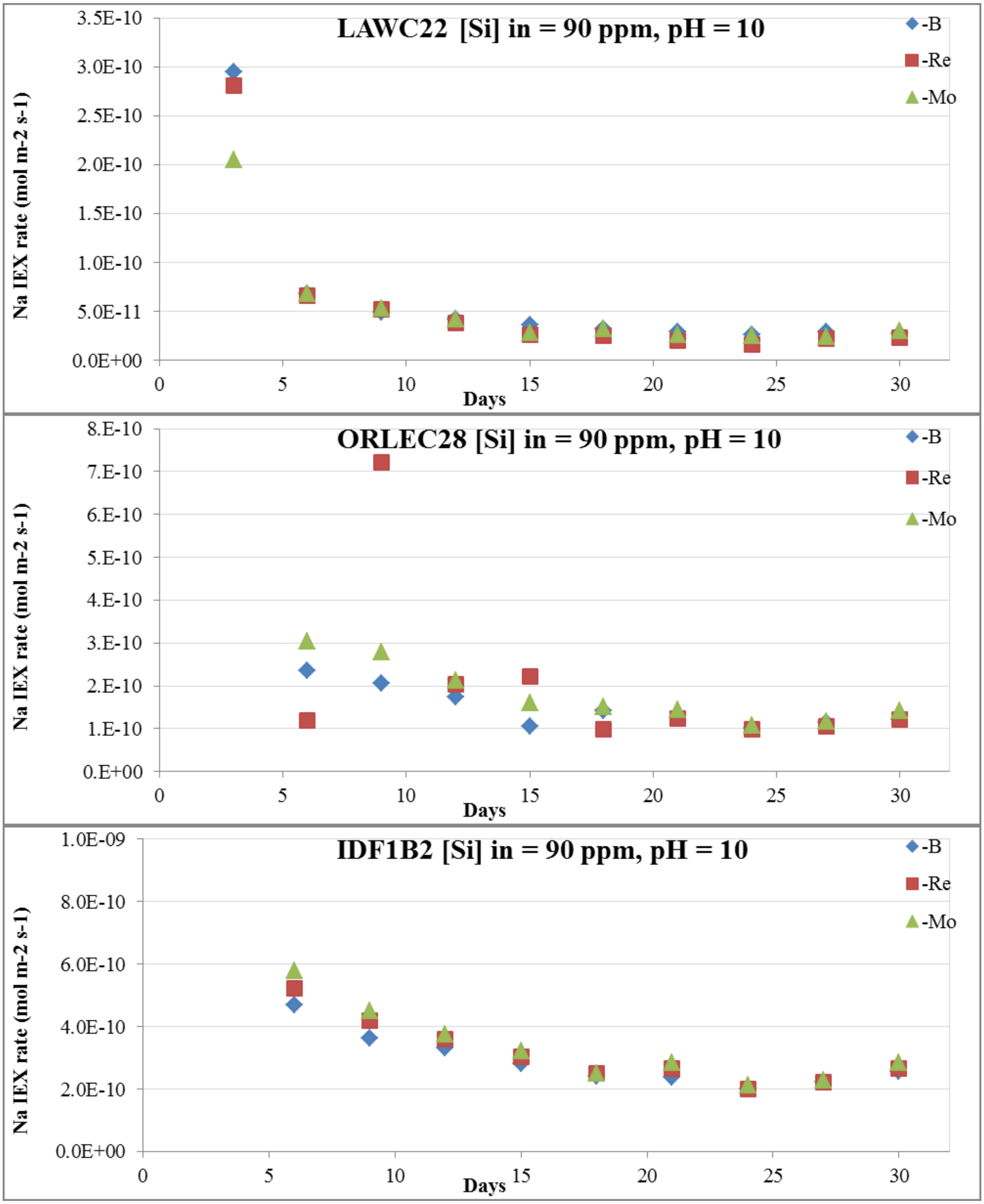

Figure F14. Plot of sodium ion exchange rates calculated from difference of respective normalized release rates to that of boron, rhenium, or molybdenum, at 23 °C, pH_{23} =10.

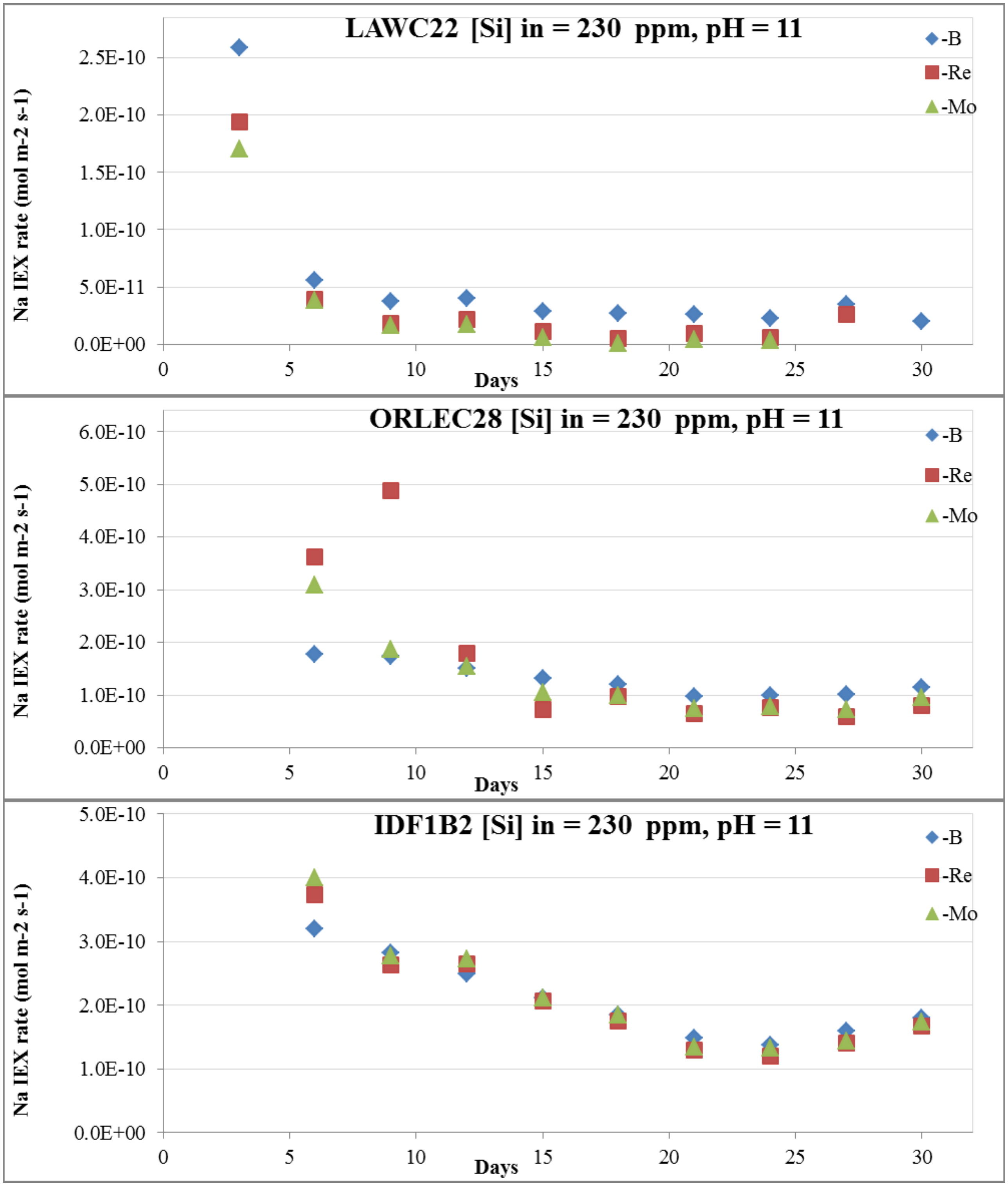

Figure F15. Plot of sodium ion exchange rates calculated from difference of respective normalized release rates to that of boron, rhenium, or molybdenum, at 23 °C, pH_{23} =11.